SECOND-ORDER ANALYSIS OF IMPERFECT LIGHT-WEIGHT AND COMPOSITE STRUCTURES

MAN FONG

Ph.D

The Hong Kong Polytechnic University

2012

THE HONG KONG POLYTECHNIC UNIVERSITY

DEPARTMENT OF CIVIL AND STRUCTURAL ENGINEERING

SECOND-ORDER ANALYSIS OF IMPERFECT LIGHT-WEIGHT AND COMPOSITE STRUCTURES

Man FONG

A Thesis Submitted in Partial Fulfillment of the Requirements for the Degree of Doctor of Philosophy

August 2011

CERTIFICATE OF ORIGINALITY

I hereby declare that this thesis is my own work and that, to the best of my knowledge and belief, it reproduces no material previously published or written, nor material that has been accepted for the award of any other degree or diploma, except where due acknowledgement has been made in the text.

_____ (Signed)

Man FONG (Name of student)

ABSTRACT

Recently published and popular national design codes such as the AISC (2010), Eurocode 3 (2005) and CoPHK (2005) recommend the use of second-order analysis and design method as an advanced tool in place of the first-order analysis and design method such that the unreliable estimation of effective length and determination of buckling reduction factors can be eliminated. The use of this simple and accurate advanced design tool for typical steel structures has been proposed by many researchers. However, research with aim for practical application of the method for steel-concrete composite structures receives relatively few discussions and verifications against test and code results. The aim of this thesis is to propose and develop a practical advanced design method for light-weight and composite structures.

The light-weight structures such as the transmission towers and tower cranes which collapse quite commonly in different parts of the world. The collapse of these structures is mainly due to the structural instability rather than material yielding. Therefore, the inclusion and consideration of the nonlinear effects such as P-Δ and P-δ moments, member initial imperfection and global structural imperfection in analysis are important so as to reflect the actual structural behaviors. However, the way to consider these effects in design by estimation of effective length in the first-order analysis and design method is not only inconvenient, but also inaccurate and

unreliable. Incorrect estimation of the effective length may lead to under-design of the structures which may eventually cause the collapse of the structures.

Convenience and reliability in design of steel structures, especially for angle members are another attraction for second-order analysis and design method. The monosymmetric or asymmetric section property and eccentric connection in angle members further complicates its design process, and many design codes provide different complex equations to consider these effects which can be simulated automatically in analysis model in the proposed method so that the design process can be much simplified.

Steel members have been popularly used in different structural forms. Due to the increase of building height and structural span, the use of steel-concrete composite members becomes more popular because of its advantages over bare steel and reinforced concrete members. Most nonlinear finite element packages are complicated and unsuitable for practical design because of the requirement of huge computational time. Therefore, an efficient and accurate analysis and design method, which includes the nonlinear effects and fulfills code requirement, is proposed for steel-concrete composite members with verification examples to confirm its validity for practical applications.

Consideration of material nonlinearity in study of inelastic behavior of composite members is obviously important and the second-order inelastic analysis is proposed in the final part of the thesis to include both the geometric and material nonlinearities in analysis. Refined plastic hinge method in conjunction with initial and full yield

surfaces is used to trace material yield for guaranteeing both efficiency and accuracy. In this thesis, extensive numerical examples are provided for verification.

LIST OF PUBLICATIONS

JOURNAL PAPERS:

1 Fong, M., Cho, S.H. and Chan, S.L. (2009). "Design of angle trusses by codes and second-order analysis with experimental verification." Journal of Constructional Steel Research **65**(12): 2140-2147.

2 Fong, M., Liu, Y.P. and Chan, S.L. (2010). "Second-order analysis and design of imperfect composite beam-columns." Engineering Structures **32**(6):1681-1690.

3 Chan, S.L. and Fong, M. (2011). "Experimental and analytical investigations of steel and composite truss." Advanced Steel Construction **7**(1): 17-26.

4 Fong, M., Chan, S.T. and Chan, S.L. (2011). "Capacities of concrete-filled steel beams of unequal double spans by testing and code." The Hong Kong Institution of Engineers Transactions **18**(1): 1-5. (This paper was selected for the Best Paper Award in year 2011)

5 Fong, M., Liu, Y.P. and Chan, S.L. (2009) "Second-order analysis and experiments of semi-rigid and imperfect domes." Advances in Structural Engineering (Accepted for publication).

6. Fong, M., Chan, S.L. and Uy, B. (2011) "Advanced design for trusses of steel and concrete-filled tubular sections." Engineering Structures **33** (12): pp. 3162-3171.

7. Fong, M. and Chan, S.L. (2011) "Advanced analysis of steel-concrete composite beam-columns by the refined plastic hinge method." International Journal of Structural Stability and Dynamics (Accepted for publication).

CONFERENCE PAPERS:

1. Chan, S.L., Fong, M. and Cho, S.H. (2008). "Design of Angle Trusses Linear and Second-Order Analysis." Proceedings of the 5th European Conference on Steel and Composite Structures. Graz, Austria :1647-1652

2. Chan, S.L., Fong, M. and Liu, Y.P. (2009). "Advanced and Second-order Analysis of Composite Columns." Proceedings of the Steel Concrete Composite and Hybrid Structures, Leeds, UK: 66-73.

3. Fong, M. and Chan, S.L. (2009). "Second-order analysis and experimental tests on shallow dome." Proceedings of the Steel Concrete Composite and Hybrid Structures, Leeds, UK: 709-714.

4. Fong, M., Cho, S.H., Liu, Y.P., Chan, S.L. and Selvanathan, J. (2009). "Second-order analysis and design of transmission tower without effective

length." Proceedings of the Six International Conference of Advances in Steel Structures, Hong Kong, China: 875-882.

5. Chan, S.L. and Fong, M. (2010). "Recent advances in simulation-based of steel and steel-concrete composite structures." Proceedings of the 9th China-Japan Structural Conference, Tokyo, Japan: 240-258.

ACKNOWLEDGEMENTS

First and foremost the author sincerely thanks his supervisor, Professor Siu-Lai Chan, for his enlightening guidance, support and encouragement throughout his research study. A valuable opportunity has been provided by his supervisor to open author mind to recognize nonlinear analysis and design concept. Prof. Chan's breadth and depth of knowledge in different areas and creative and unique insight into both academic and scientific problems for research have enlightened and encouraged the author in his research life.

The author would also like to express his special thanks to Professor Brian Uy for his valuable suggestions and guidance during author's exchange period in University of Western Sydney, Australia.

The author appreciates The Hong Kong Polytechnic University for the financial support during his study.

The author would like to thank NIDA team members including Drs. Y.P. Liu, S.H. Cho, Messrs. B. Li, H.J. Mo, S.W. Liu, Y.Q. Tang for their constructive discussions and continually assistances. The author also likes to thank Mr. Sam Chan, Misses Miya Lau, Emmy Ko, Nancy Sheng and Q. Liu, Drs. Y.M. Hu and S. Weng for their great help during four years research life.

The research project involved a series of tests. The author is very thankful to the technical staffs including Messrs. M.C. Ng, Y.H. Yiu, T.T. Wai, C.S. Liu, K.H. Wong, C.F. Cheung and W.H. Kwan for their instructions and advices during the experiments.

Finally, the author would like to express his warmest appreciation to his parents and friends for their support, understanding and endurance.

CONTENTS

LIST OF FIGURES

LIST OF TABLES

LIST OF SYMBOLS

Latin upper case latter

A	Cross-sectional area
A_c, A_r, A_s	Cross-sectional areas of concrete, reinforcement and steel
$A_{ci}, A_{ri}, A_{si},$	Cross-sectional areas in the layers of concrete, reinforcement and steel
A_{eff}	Effective cross-sectional area
A_g	Gross cross-sectional area
A_{shear}	Shear area
B	Width of the flange
B_1, B_2	Factors to amply moments to include the nonlinear effects
D	Depth of the flange
D_{out}	Outer diameter of tube
E	Modulus of elasticity
E_c, E_r, E_s	Modulus of elasticities of concrete, reinforcement and steel
E_{comp}	Modulus of elasticity of composite cross-section
G	Shear modulus of elasticity
I	Second moment of area
I_c, I_r, I_s	Second moment of areas of concrete, reinforcement and steel
I_{comp}	Second moment of area of composite cross-section
K	Effective length factor

K_{ij}	Stiffness coefficients of the element
P	Applied axial force
P_{cd}	Design compressive strength
P_{cp}	Compressive strength of a composite cross-section
P_{cr}	Elastic critical strength
P_I	Total internal force
P_n	Nominal compressive strength
P_{pm}	Compressive strength of concrete cross-section
P_{Rk}	Characteristic compressive strength
L	Length of the member
L_e	Effective length of the member
M_{cx}, M_{cy}	Moment capacities about the x and y axes
$M_{cpx,}$ M_{cpy}	Moment capacities of composite cross-section about the x and y axes
M_x, M_y	Applied moments about the x and y axes
M_{Rk}	Characteristic moment resistance
M_s	External moment at two ends of a connection
M_r	Internal moment at two ends of a connection
M_1 , M_2	Moments at element end 1 and 2.
N_1, N_2	Shape functions for perfectly straight element
S	Arc-distance in arc-length method
S_c	Spring stiffness for simulation of semi-rigid connections at ends
S_h	Spring stiffness for simulation of plastic hinge
U	Strain energy

V	External work done

Latin lower case latter

a_i	Coefficients in the polynomial function
b	Inner diameter of tube
$d_{b\text{olt}}$	Distance between the centroids of the two bolts
e	Eccentricity
e_x	Member shortening
f_{cd}, f_{rd}, f_{yd}	Design strengths of concrete, reinforcement and steel
f_{cr}	Flexural buckling strength
f_{cu}	Ultimate tensile stress on steel from couple test
f_y	Yield stress on steel from couple test
$f_{y,cr}$	Reduced design strength of steel for slender sections
$f_c^{'}$	Specified minimum compressive stress of concrete
$f_r^{'}$ and $f_y^{'}$	Specified minimum yield stresses of reinforcement and steel
k_{xx}, k_{xy}, k_{yx}, k_{yy}	Interaction factors for bending moment
l_{bolt}	Length of the bolt shank
p_c	Compressive buckling strength
p_{cr}	Elastic critical buckling strength
r	Radius of gyration
r_g	Governing radius of gyration
r_i	Displacement vector
r_m	Ratio of the end moment
s_i	Force vector

t	Thickness of the tube
t_f	Thickness of the flange
u	Axial displacement due to applied loads
v	Lateral displacement due to applied loads
v_{mo}	Amplitude of initial imperfection equal to the imperfection at mid-span
v_0	Lateral initial imperfection
x	Non-dimensional distance along the element
x_{ci}, x_{ri}, x_{si}	Distances from the center of the concrete, reinforcement and steel layers to the center of the cross-section in x axis
y_{ci}, y_{ri}, y_{si}	Distances from the center of the concrete, reinforcement and steel layers to the center of the cross-section in y axis

Greek upper case latter

Δ	Storey out-of-straightness
ΔL	Incremental member length
$\Delta M_{x,Ed}$, $\Delta M_{y,Ed}$	Moments due to the shift of the centroidal axis about the x and y axes
ΔP	Increment axial force
ΔM_s	Incremental external moment at two ends of a connection
ΔM_r	Incremental Internal moment at two ends of a connection
$\Delta\theta_s$	Incremental external nodal rotation
$\Delta\theta_r$	Incremental internal nodal rotation
$\Delta\lambda$	Load corrector factor

Greek lower case latter

α	Imperfection factor
α_a	Compression member factor
α_b	Compression member section constant
γ	Parameter to control the load size
γ_{M1}	Partial factor for resistance of members to instability
δ	Member out-of-straightness
ε_c	Strain of concrete
ε_{dc}	Strain at reaching the maximum strength
ε_{ic}, ε_{is}	Initial yield strains of concrete and steel
ε_{uc}, ε_{us}	Ultimate strains of concrete and steel
η	Perry factor
η_0	Compressive member imperfection factor in AS5100
θ_s	External nodal rotation
θ_r	Internal nodal rotation
θ_1, θ_2	Rotations of the member at end 1 and 2
λ	Slenderness ratio of the member
λ_{cr}	Elastic critical load factor
λ_g	Governing radius of gyration
λ_p	Slenderness ratio of the compact element
λ_r	Slenderness ratio of the non-compact element
λ_η	Modified compression member slenderness ratio
$\overline{\lambda}$	Relative slenderness ratio

$\overline{\lambda}_{eff}$	Effective slenderness ratio
μ	Reduction factor for moment capacity
ξ	Compression factor
ρ	Curvature of the strain distribution curve
σ_c	Stress of concrete
σ_{ic}, σ_{is}	Initial yield stresses of concrete and steel
σ_{uc}, σ_{us}	Ultimate stresses of concrete and steel
ϕ_c	Resistance factor in axially loaded column
ϕ_{full}	Full yield surface
$\phi_{initial}$	Initial yield surface
ϕ_{SCF}	Section capacity factor
χ	Reduction factor for relevant buckling mode
χ_x, χ_y	Reduction factors for flexural buckling for x and y axes
χ_{LT}	Reduction factor for lateral torsional buckling

CHAPTER 1

INTRODUCTION

1.1 Background

Use of the nonlinear analysis method as an accurate tool for design of different types of structures becomes more popular because the cost of computational time is much reduced due to the rapid development of computer technology, resulting in production of low-cost and high capacity personal computers. Different types of nonlinear analysis were studied by researchers for their advantages and limitations, see Chan and Chui (2000). The results from some analysis methods such as second-order elastic and inelastic analysis methods can be used directly for design propose but some nonlinear analysis such as the elastic bifurcation analysis only provides an upper bound solution. Latest versions of national design codes such as American standard (2010), Australian standard (2004) and European standard (2005) recommend the use of second-order analysis and design method to eliminate the uncertainties in estimation of effective length and determination of moment amplification factors in traditional first-order method. The complicated design process is simplified in second-order analysis and design method by using the section capacity check as most of the nonlinear effects such as P-δ and P-Δ effects

and member local and structural global imperfects can be included in analysis directly.

Two approaches are commonly adopted including the finite element method and stability function in developing the beam-column element for second-order analysis. The details and differences in both methods were presented by Chen and Lui (1991). Because of the simplicity in finite element method, it is widely adopted to solve the engineering analysis problems. The use of cubic Hermit element is the simplest method for development the nonlinear element which, however, is unable to include the initial imperfection in element which leads to error when the axial force is large. Therefore, higher order elements including fourth-order and fifth-order were proposed by researchers. The imperfect Pointwise Equilibrium Polynomial (PEP) element proposed by Chan and Zhou (1995) can consider not only the initial member curvature, but also the interaction between the axial force and bending moments at element level. Use of only one element per member is sufficient for most engineering problems so that a consistent model for first-order and second-order analysis can be obtained. In other words, engineers do not need to divide a member into two or more elements when they construct a computer model for second-order analysis of a frame. The application of second-order analysis and design method for different typical steel structures was studied by researchers, and the accuracy was also reported. This research project aims to propose a second-order analysis and design method for angle members and to assess the accuracy of the proposed method and the traditional codes method in design of angle trusses.

The demand on steel-concrete composite structures has increased significantly due to the requirements of high strength and ductility members especially for high-rise buildings and mega trusses. The beneficial effects on composite members over the steel and reinforced concrete members were summarized by Johnson (2004). In order to understand the different behaviors of composite members, extensive experimental investigations were carried out to study the beam, beam-column and column behaviors of composite members as described by Shanmugam and Lakshmi (2001). The research areas included the confinement effect on in-filled concrete provided by steel tubes under different cross-sectional shapes, the beneficial effect on strength and ductility of the composite members under different strengths of concrete and steel, and the increase in the capacity of composite members under different slenderness ratios and loading conditions. Most of the experimental tests on composite members focused on the behaviors of isolated columns under pinned or fixed end condition. Based on the understanding on the behaviors of isolated columns, the experimental test to study the behaviors of Concrete-Filled Steel (CFS) tubes which are acted as members in the trusses are conducted in the research project for this thesis.

The commonly used methods for analysis of composite members include one dimensional beam-column analysis model and three-dimensional finite element model. The beam-columns analysis model is relatively simple while the three-dimensional finite element model is more accurate. The uses of these methods for analysis of composite members were demonstrated by researchers with its accuracy and efficiency verified. However, due to the complexity and extensive time consumption, these methods are more applicable to analysis for behaviors of single

members. Therefore, a simple, accurate and efficient second-order analysis and design method for steel-concrete composite members which can include the nonlinear effects and initial imperfection automatically in analysis and fulfill the code requirements is needed and proposed in this thesis.

The material nonlinearity should also be considered in advanced analysis to capture the load-deflection relationship and to study the inelastic behavior of members and structures. Generally speaking, distributed plasticity (Plastic zone method) and lumped plasticity (Plastic hinge method) are two methods commonly adopted for beam-column element. The accuracy of the plastic zone method was demonstrated by researchers in different examples. An exact solution can be obtained in plastic zone method to include most of the nonlinear effects. However, the huge computational effort in discretization of the cross-section and along the member length is required and therefore this method is less applicable for engineering practice. The plastic hinge method is simpler than the plastic zone method without much loss of accuracy. In plastic hinge method, the cross-section plastification is only lumped at one or two ends of the member and the remaining region is assumed to be elastic. The studies on different refined-plastic hinge methods to simulate the gradual yield were conducted by researchers such as beam-column section stiffness degradation method by Liew et al. (1993a,b), beam-column member degradation method by King and White (1992) and zero-length pseudo-spring element method by Al-Mashary and Chen (1991). The different expressions on the section spring stiffness and definition of initial yield and full yield surfaces were studied by these researchers. This thesis proposes a practical second-order inelastic analysis method for steel-concrete composite beam-columns by using the refined-plastic hinge

method. The determination of the initial and full yield surfaces of the composite cross-section based on the cross-section analysis method is described.

1.2 Research Objectives

The primary objective of this research project is to extend the accurate and efficient second-order analysis and design method to other structural forms to replace the traditional first-order analysis and design method. It also aims to explain the inaccuracy and inconvenience of using first-order analysis and design method so as to emphasize the advantages of using the proposed second-order analysis and design method and to provide the verification examples.

This research project also aims to study the behaviors of composite beam-columns experimentally and analytically. The proposal of both the second-order elastic and inelastic analysis for composite beam-columns for applications in different situations is another objective of this research project.

The objectives of this research project can be summarized as follows.

a) To apply the second-order analysis and design method to light-weight angle structures with comparison on the accuracy of the proposed method and traditional codified method against experiments.

b) To compare both the strength and ductility of steel and CFS tubular isolated columns and members in truss systems so as to study the beneficial effects due to in-filled concrete.

c) To verify and compare the accuracy of linear-analysis and design method in some common design codes for steel-concrete composite beam-columns.

d) To propose the second-order elastic analysis and design method for composite beam-columns to include the geometric nonlinearity for fulfillment code requirements with inclusion of verification examples.

e) To develop a simple and efficient second-order inelastic analysis method to include both the material and geometric nonlinearities in analysis for composite beam-columns using the refined-plastic hinge to simulate gradual material yield.

1.3 Layout of Thesis

The thesis comprises eight chapters and the layout of this thesis is presented as follows:

Chapter 1 provides the background information on the needs and objectives of the current research project. The research layout is also described.

Chapter 2 presents a review on the existing literature covering the topics in this research project. The development of finite element method for beam-columns element in second-order analysis is reviewed. The scope of application, accuracy and limitations of different nonlinear analysis methods are concluded and compared. The experimental and analytical investigations on the behavior of CHS tubular members are concluded for development of efficient and accurate second-order analysis and design method for composite members. Finally the uses of plastic hinge and plastic zone methods in second-order inelastic analysis are also examined.

Chapter 3 presents the formulation for PEP element, which is able to model one element per member with inclusion of member imperfections. The formulations of secant and tangent stiffness matrices are described. The theories of different incremental-iterative numerical techniques, which are essential in nonlinear analysis to trace the load-deflection curves, are introduced and summarized with its limitations and efficiency described. Finally, an example of shallow dome is given to demonstrate the use and verify the accuracy of PEP element in highly nonlinear analysis and to show the ability of the numerical methods in tracing the snap-through buckling.

In Chapter 4, both the first-order and second-order analysis and design methods for steel structures especially for angle members are presented. Predicted failure loads of the angle members in the trusses by different codified method are compared with test results in order to verify the accuracy of effective length methods in design codes which commonly modify the slenderness ratio or use interaction equations to consider effects due to the eccentric connection and end rigidity. To date, design

method using the second-order analysis has become popular because it captures directly the structural behavior in analysis and eliminates the error in a linear analysis and design. Therefore, a refined second-order analysis method is proposed for design of angle trusses composed of single angle members with accuracy verified by tests.

Chapter 5 describes the experimental investigations on steel and CFS tubular columns and trusses. The beneficial effects due to the in-filled concrete on both the isolated columns and constituent members in trusses are studied. The capacities and load-deflection relationships of the members in the trusses are also compared with the isolated columns to study the effects of member end conditions.

In Chapter 6, both traditional and advanced design methods for composite beam-columns are described. The traditional codified linear analysis and design methods are summarized and compared with the test results to show its inconvenience and uncertainties in design of composite beam-columns. Due to the disadvantages of the codified method concluded in this chapter, the second-order analysis and design for composite beam-columns, which fulfills the code requirement and includes initial imperfection, is proposed. The accuracy of the proposed method in design of composite beam-columns with various cross-section types is calibrated and verified with the design codes and experimental tests.

Chapter 7 proposes the second-order inelastic analysis for steel-concrete composite beam-columns with material nonlinearity included in analysis directly. The refined plastic hinge approach is used in inelastic analysis to trace gradual material yield and

simulate the full plasticity of a cross-section. The definitions of the initial and full yield surfaces, which are used to initiate the yielding and indicate the full plastic stage, for steel-concrete composite cross-sections based on the cross-section analysis are presented. The proposed method is verified in tracing the load-deflection behavior of both isolated composite columns and structural members.

The thesis ends with Chapter 8 and the significances of this research project are highlighted in this chapter. Recommendations and suggestions for future works are given.

CHAPTER 2

LITERATURE REVIEW

2.1 Introduction

This chapter presents a review on the development of finite element method for beam-column element in second-order analysis. Different types of nonlinear analysis and its limitations and accuracy are discussed. Based on the theory of finite element method, a beam-column element with imperfection will be proposed for second-order analysis of steel and steel-concrete composite structures in the following chapters. The reviews on the experimental, analytical and codified studies on Concrete-Filled Steel (CFS) tubular members are carried out to investigate the behaviors of isolated members for studying the constitutive members in the structural systems in this thesis. Last but not least, the study of inelastic behaviors of frame structures by the plastic zone and plastic hinge methods are reviewed in this chapter for proposing the second-order inelastic analysis method by using the refined plastic hinge method for composite beam-columns.

2.2 The Finite Element Method for Beam-column Element

Rapid development of technology in desk-top computing makes the second-order analysis more popular, with extensive researches focused on refining this method for practical applications. Many design codes such as AISC (2010), AS4100 (1998), Eurocode 3 (2005) and Eurocode 4 (2004) recommend the use of second-order analysis method as a more accurate computational tool for both steel and steel-concrete composite structures and should be used when the elastic critical load factor is less than the code specified limit. In the second-order analysis, the important nonlinear effects such as the P-Δ and P-δ moments as well as local and global imperfections are included in analysis process. As a result, this analysis and design method not only increases the accuracy on estimation of failure load, but also saves the time and effort for design. The advantages of using the second-order analysis and design method have been summarized by many researches such as Chen (2000) and Chan et al. (2005) as skipping of the assumption of effective length because the P-Δ and P-δ effects are considered reliably and automatically in analysis.

Generally speaking, the finite element method (Bathe and Bolourchi 1979; Connor et al. 1968; Chan and Zhou 1994; Iu and Bradford 2010) and the stability function (Oran 1973; Chen and Lui 1987; Liew et al. 1999; Chan and Gu 2000) are two common approaches in developing the beam-column element. Their merits and limitations were reported by McGuire and Ziemian (1989) and Gu and Chan (2005). The merit of the finite element method is on its simplicity, whereas the stability function is about its accuracy. The finite element method for beam-column element in second-order analysis is focused in this chapter.

The finite element method is a widely accepted method to solve engineering analysis problems. It generally based on the energy principle. The assumption of the displacement function is important for the element. By employing the principle of total potential energy, the stiffness matrix relating the nodal forces and nodal displacements can be obtained. The use of cubic Hermite element is the simplest method for developing the nonlinear element by finite element method (Connor et al. 1968; Bathe and Bolourchi 1979; Meek and Tang 1984; Teh 2001). The third-order displacement shape function is assumed in cubic element which contains four coefficients in the displacement function, requiring four boundary conditions at both ends of the element to solve the coefficients. The successful applications of the cubic element were well demonstrated through many examples. However, researchers indicated that the error for the cubic element increases significantly when the axial force is large (see So and Chan 1991; Chan 2001). Furthermore, the P-δ effect due to member imperfection cannot be included if only one element per member is used in modeling. The use of several elements to model a member not only leads to complexity in modeling, but also causes the inconsistence between the linear and nonlinear models. The higher order elements were proposed to improve the accuracy of using one element per member in analysis, which lead to much convenience in practical design. For examples, the forth-order displacement function (Izzuddin 1996; So and Chan 1991; Iu and Bradford 2010) and fifth-order polynomial displacement function (Chan and Zhou 1994) were proposed to replace the cubic element. In the fifth-order Pointwise Equilibrium Polynomial (PEP) element, two additional constraints of equilibrium were imposed at the mid-span of an element to find out two additional coefficients. Only one element per member in PEP element is

sufficient in most practical cases and its accuracy was verified in different structures (Chan and Zhou 2000).

Initial imperfection is important for engineering design because it is essential in affecting the buckling strength of a structure and unavoidable during fabrication or erection of structures, hence, the inclusion of the initial imperfection in second-order analysis is important. Srpcic and Saje (1986) and Wen and Suhendro (1991) included the initial curvature into the curved element, however, the P-δ effect due to axial force and member deflection was still not properly included in their method. Chan and Zhou (1995) included the member initial imperfection in their imperfect PEP element by using the fifth-order displacement function via the parabola shape for the initial imperfection.

Based on the accuracy and efficiency of the PEP element and its ability to include the member imperfection by using only one element per member, the PEP element is adopted in this thesis for second-order elastic and inelastic analysis.

2.3 Different Types of Nonlinear Analysis

Different types of analysis have its assumptions, scope of applications, accuracy and limitations. The aim of each analysis method is to simulate the behavior and to give a reasonable prediction on the capacity of the structural systems. Member capacities from some analysis methods can be applied for design directly while some results should be amplified with various factors according to design codes. Some typical

analysis methods used for structures are reviewed below and they include the elastic bifurcation analysis, second-order P-Δ only elastic analysis, second-order P-Δ-δ elastic and inelastic analysis, and advanced analysis. Various analysis types are graphically presented in Figure 2.1.

In elastic bifurcation analysis, the eigenvalue problem is formulated as follows.

$$\left|[K_L] + \lambda_{cr}[K_G]\right| = 0 \tag{2.3.1}$$

where $[K_L]$ is the linear stiffness matrix and $[K_G]$ is the geometric stiffness matrix, and λ_{cr} is the elastic buckling load factor. When the applied load is at this buckling load level, the structures will buckle elastically and suddenly. In this analysis, the initial imperfection, pre-buckling deformation and material nonlinearity are not considered and hence, this method can only obtain the upper bound solution which cannot be directly used for design (Chan et al. 1995). The effective length factor for a member in the structural system can be determined by using this method (Kirby 1988) and the elastic buckling load factor can also be used as an indicator for frame classification such as non-sway, sway or sway ultra-sensitive frames.

In second-order P-Δ-δ elastic analysis method, the P-δ and P-Δ effects, local and global imperfections, member bowing deflection and stiffness change, and the equilibrium in the deformed position of the structure are considered in analysis process. Therefore, the load-deflection curve of this analysis method shown in Figure 2.1 follows the path of actual behavior before yielding. Because material nonlinearity is not considered in elastic analysis, the capacity of the structural system is over-predicted and deviation of the load-deflection curve is mainly due to this reason. In second-order P-Δ only elastic analysis, only the P-Δ effect is considered in

analysis and P-δ effect is ignored. Hence, the individual member check to compensate for the P-δ effect is still required.

The difference between second-order elastic and inelastic analysis is the consideration of the material nonlinearity in analysis (Ziemian et al. 1992a,b; Yau and Chan 1994). The ways to consider the material nonlinearity including the distributed plasticity and lumped plasticity models which are reviewed in section 2.7. Theoretically, the behavior and collapse load of the structural system analyzed by second-order inelastic analysis method are very close to the real structural behavior. However, the errors in this analysis method are generally due to the discrepancies on assumption of the material constitutive model, the value of initial member and frame imperfections as well as the residual stress in the structures.

In advanced analysis, the individual member capacity check is avoided because both the material and geometric nonlinearities are taken into account in the analysis (Chen and Kim 1997; Liew et al. 1997; Chan and Zhou 1998; Trahair and Chan 2003). Any analysis methods with elimination of the specification member buckling resistance checks by capturing all nonlinear structural behaviors in analysis can be defined as the advanced analysis.

The limitations and accuracy of typical nonlinear analysis methods have been discussed above. The second-order P-Δ-δ elastic and inelastic analysis are two common methods for analysis and design of structures. Although material nonlinearity is ignored in second-order elastic analysis, the method is simpler than inelastic analysis and only the section capacity check is required so that the complex

and unreliable process in estimation of the effective length factor is eliminated. In second-order inelastic analysis, the behaviors of structures such as the load-deflection relationship can be traced more precisely so as to study the inelastic response of the structures. Therefore, both the second-order P-Δ-δ elastic and inelastic analysis methods will be investigated in this thesis.

2.4 Experimental Investigations on Concrete-filled Steel Tubes

CFS tubes are widely used in many structural systems such as the columns of high-rise buildings and long span structures, chord and web members of mega trusses in different regions such as Japan (Morino 1998), Australia (Uy 2003; Uy 2011) Europe and Hong Kong (Vesey et al. 2005). Numerous advantages of CFS tubular members over equivalent steel and reinforced concrete members enhance the use of CFS tubular members in structural systems. The major advantages were indicated by many researchers through the experimental tests and are summarized as below.

(1) The use of CFS tubular columns eliminates the use of formwork which is replaced by steel tube so that the construction time and cost are reduced (Tomii M et al. 1973; Bridge and Webb 1993).

(2) The strength and stiffness of the CFS tubular members can be increased without enlargement of the column size with the usable space maximized (Roderick and Rogers 1969; Shakir-Khalil and Zeghiche 1989; Shakir-Khalil and Mouli 1990).

(3) The in-filled concrete core prevents the inward local buckling of the steel tube so as to delay local plate buckling of the external steel tubes (Furlong 1967; Zeghiche and Chaoui 2005).

(4) The concrete core restrained by the steel tube provides the confinement effect which increases the compressive strength of concrete (Gardner and Jacobson 1967; Matsui et al. 1995; O'Shea and Bridge 1997a,b; Johansson and Gylltoft 2002).

Extensive experiments were conducted and reported on CFS tubular columns, beam-columns and beams to study its axial, flexural and their interaction between axial and flexural actions. The main parameters of the studies on the behaviors of CFS members include the cross-sectional shapes (circular, square, rectangular), the strengths of concrete and steel, the slenderness ratios and the loading conditions (pure bending, concentric or eccentric axial load). A brief review on experimental investigation of the columns, beam-columns and beams tests of CFS tubular isolated members is given in this thesis.

2.4.1 Concrete-filled steel tubular columns and beam-columns

Experimental studies on CFS tubular columns and beam-columns are generally classified into short and slender columns according to the slenderness ratio. The failure mode of short column is typically crushing of the concrete or yielding of the steel. Therefore, the material strengths of concrete and steel especially the high strength materials, depth-to-thickness ratios and diameter-to-thickness ratios which influence the local buckling of the steel plate, and confinement effect on concrete core due to different types of cross-sections including circular, square, rectangular

and elliptical (Yang et al. 2008; Zhao and Packer 2009) were focused in the tests. Due to the development of technology, the high strength materials including high strength concrete and steel are generally used in practice. Recently, Liew (2011) studied the ultra-high strength composite columns with the use of ultra high strength concrete of 200MPa and high strength steel of 700MPa, he also applied the high strength materials in practical structures in Singapore. Although the higher ultimate strength can be reached, the sudden crash and the loss the stiffness sharply are the major concerns (Ge and Usami 1992). The influence on the ultimate strength due to local buckling was studied by (Uy and Bardford 1995; Bridge et al. 1995; Uy 2000), the capacity of the columns generally decreases with increasing of the steel plate slenderness. Therefore, many design codes limit steel plate slenderness to insure that the ductile yield of the steel can generally occur prior to the local buckling of steel plate. Also, the ductility of high strength concrete may not allow the simultaneous attainment of maximum strength of steel and concrete that equations for composite columns for normal concrete may not be applicable.

Many findings reported that the confinement effect can only observed in the CFS tube with circular section, and no significant beneficial effect is noted on square and rectangular hollow sections (Tomii M et al. 1977; Tsuda et al. 1996; Schneider 1998). This confinement effect also diminishes with increase of bending moment and slenderness ratio because the mean compressive strain in the concrete is reduced due to tension induced by bending and significant lateral deflection in slender columns. Therefore, many design codes such as Eurocode 4 (2004) and AS5100 (2004) ignore the confinement effect when the relative slenderness ratio exceeds 0.5 and eccentrically to external diameter of the column ratio (e/D_{out}) exceeds 0.1.

In intermediate length or slender CFS tubular columns tests, the increase of the applied load enlarges the mid-span deflection and P-δ moment, and therefore, the flexural instability generally governs the failure mode of slender columns, and some crushing of concrete and yielding of steel prior to buckling are involved (Wang 1999). The slenderness ratio highly influences the capacity of the slender column due to significant P-δ effect. Han (2000) pointed out that the column capacity is more controlled by the flexural rigidity rather than the strengths of steel and concrete which give very little influence on the capacity of the slender columns.

2.4.2 Concrete-filled steel tubular beams

Tests on the CFS tubular members under pure bending are limited because the primary application of the CFS tubular members is taken as columns. When the CFS tubes under flexural, the steel contributes a large portion on stiffness and strength and the in-filled concrete can enhance flexural strength and ductility and energy absorption. Lu and Kennedy (1994) tested four steel and twelve CFS hollow sections and the results show that the in-filled concrete increases the ultimate flexural capacity on the specimens by 10 to 35% relative to bare steel tube. Similar conclusions can be drawn from the test results from Elchalakani et al. (2001) in their large deformation pure bending test, that the beneficial effects on CFS tubes are more significant for thinner steel sections.

Some researchers also emphasized that the yield plateau can be observed and this reflects the good ductility for CFS circular, square and rectangular tubular members

compared with bare steel tubular members, (Han 2004; Chitawadagi and Narasimhan 2009). Good ductility is also noted in CFS tubes with high strength steel or/and concrete (Prion and Boehme 1994; Uy 2001; Gho and Liu 2004). Lu et al. (2007) tested CFS tubes with rectangular section under different plate thickness, and they found that better ductility can be obtained for beam under different plate thickness compared with the beam with equal thickness walled for same overall size and materials. The initial rigidity of CFS tube in flexure is highly influenced by the degree of bonding of two materials. Lu and Kennedy (1994) concluded from the test results that the preferred bonding between two materials can be established and the slip is not observable under various shear-span-to depth ratios.

From the research review, most previous experiments focused on the behaviors of isolated members under pinned or fixed end conditions, and the tests on steel and CFS tubes acting as members of a frames or truss structures are limited. When the CFS tubes are used as the members of a structural system, its end condition cannot be simply treated as pinned or fixed end. The contribution on stiffness from the adjacent members affects the end condition as well as the buckling resistance of the member.

2.5 Codified Methods on Composite Members

The design procedures for composite members were studied and modified by a lot of researchers over the past decades. Different approaches for design of composite members are used in AISC (2010), ACI 318 (2008), Eurocode 4 (2004), AS5100

(2004), BS5400 (2005) and CoPHK (2005). Various design methods are provided for several types of commonly used composite cross-sections. Some methods consider the composite columns as a steel column with equivalent and modified cross-sectional properties whereas other methods treat the composite columns as a concrete column with modified cross-sectional properties. The design principle, accuracy and degree of conservatism of the design codes in flexural capacity, axial strengths and their interactions are reviewed below.

In AISC (2010), the design principle of composite columns is the same as the steel columns. The equivalent flexural stiffness is calculated and the reduction factors are then applied to determine the compressive strength. The second-order effects are considered in design by using the moment magnification approach when using the linear design approach. The nominal bending capacity is obtained by the plastic stress distribution in the composite section. Similar to the design of bare steel, the bilinear interaction formulae are used in composite members for calculating the interaction between axial and flexural effects, and the biaxial bending is treated as a linear combination of moments about principal axes.

The same principle as the AISC (2010) for design of composite column is used in ACI 318 (2008) and the composite column is treated as the concrete column reinforced by steel tube with reinforcing bars or structural steel. The equivalent properties of the composite columns such as the flexural stiffness and radius of gyration with a parameter of sustained load ratio are used. A similar magnification approach is used to take the second-order effects into account. The same method used for concrete for consideration of strength interaction between the axial and

flexural effects is used for composite members, and it is based on the assumption of a linear strain distribution through the composite cross-section. Both the AISC (2010) and ACI 318 (2008) ignore the confinement effect on concrete in-filled in the steel tube for calculation of strength and ductility of composite columns.

The design method of the most commonly used cross-section types of the composite columns are covered in Eurocode 4 (2004) including concrete fully and partially encased in steel sections and concrete in-filled tubular sections. The influence on flexural stiffness of composite columns due to long term effect can be considered in this code and the confinement effect is taken into account. The buckling and second-order effects are compensated by factors to reduce the cross-section strength of the composite columns with the first-order moment amplified. The interaction of axial and flexural actions should be checked with moments properly amplified to include the second-order moments.

The design method in AS5100 (2004) is applicable for CFS tubular columns with constant or varying cross-sections. The design principle in AS5100 (2004) is similar to Eurocode 4 (2004) with difference in determination of buckling reduction factor. The interaction curve same as Eurocode 4 (2004) is employed to consider the composite columns under axial and flexural effects.

The design methods for Concrete-Encased Steel (CES) sections and CFS sections are provided in BS5400 (2005). The plastic stress distribution method over the cross-section is used to determine the flexural capacity. The approximation for the interaction curve for axial load and moment is used to determine the design load.

The enhanced strength on concrete due to the steel tube is considered in BS5400 (2005).

Many researchers compared the results from experimental tests and predictions by the design codes in the axial capacity and the axial and flexural interaction effects. These studies include American standards (Weng and Yen 2002; Han et al. 2004; Ellobody and Young 2006; Ellobody et al. 2006), European standard (Wang 1999; Han 2000; Al-Rodan 2004; De Nardin and El Debs 2007), Australian standard (Tao et al. 2008) and British standard (Johnson and May 1978; Shakir-Khalil 1994; Hunaiti and Fattah 1994). Generally speaking, Eurocode 4(2004) covers most of design considerations and influences to the resistance of the columns (Saw and Liew 2000). For the short columns, Eurocode 4 (2004) gives the closest estimation on the cross-section capacity. The other design codes generally underestimate the capacity because of the conservative reduction factors on the cross-section strength in concrete and steel. And some design codes ignore the confinement effect on the concrete due to the circular hollow tube resulting in a conservative prediction. For intermediate to slender columns, the degree of conservatism highly depends on the method to include the second-order effects and the interactive effect of axial and flexural strengths. The comparisons on test results and predictions from codes indicate that the interactive equations in AISC (2010) and BS5400 (2005) are too conservative and this leads to over-design of composite columns. Generally, results from Eurocode 4 (2004), AS5100 (2004) and ACI 318 (2008) give the relatively accurate and safe predictions. However, Hunaiti and Fattah (1994) and Zeghiche and Chaoui (2005) emphasized that the code methods on predicting the capacity of columns under double curvatures is inaccurate. The comparisons on the accuracy of

design codes in predicting the flexural capacity of composite members were also studied (Elchalakani et al. 2001; Han 2004; Gho and Liu 2004; Han et al. 2006). In conclusion, the design method in Eurocode 4 (2004) gives a better estimation in flexural capacity of the composite members while the design methods in ACI 318 (2008), AISC (2010) and BS5400 (2005) give a safer but less accurate prediction.

The degree of accuracy of design codes in predicting the capacity of CFS tubular members under concentric or eccentric load with pinned or fixed end boundary condition was compared against experimental results. The method to estimate the effective length highly governs the accuracy of the codified design. For simple end conditions like pinned and fixed ends, the effective length can be easily estimated. However, for more complicated cases in practical structures like trusses or arch structures, determination on the effective length is difficult and sometime impossible. Therefore, the degree of accuracy of those design codes should be verified, if the pinned or fixed end condition is assumed for those members of which the assumption over-simplifies the end connection in practical structures.

2.6 Analysis Method on Composite Members

The commonly used methods in analysis and simulation of the behaviors of composite members are (1) one dimensional beam-column analysis models (Neogi et al. 1969; Shakir-Khalil and Zeghiche 1989; Rangan and Joyce 1992; Matsui et al. 1993; Lakshmi and Shanmugam 2002; Tikka and Mirza 2006) and (2) three-dimensional finite element models (Schneider 1998; Shams and Saadeghvaziri 1999;

Hu et al. 2003; Hu et al. 2005; Ellobody et al. 2006; Han et al. 2008; Ellobody et al. 2011). Two one dimension beam-column analysis models and the fiber model for section analysis are described below.

The beam-column analysis model is relatively simple and the critical features of the behaviors of composite members can be simulated. Generally, there are two methods used for beam-column analysis in composite structures. The first method assumes the deflected shape of pin-end columns to be in a half sin-curve (Shakir-Khalil and Zeghiche 1989; Rangan and Joyce 1992), equilibrium is only maintained at the mid-height of the column where the maximum deflection is noted. The assumption of deflection for a single member is simple and possible, however, for practical structures with a number of members, the assignment of the deflection becomes tedious and impossible. The second method is more general and accurate where the unequal end eccentricities can be considered and it is, however, more complicated than the first method. The member is divided into a number of segments along the member and the curvature can be obtained from the moment-curvature-thrust relationship for the cross-section. By integration of the curvature over the length, the member deflection can be found (Neogi et al. 1969; Matsui et al. 1993; Lakshmi and Shanmugam 2002; Tikka and Mirza 2006). The division of the member into a number of segments increases the computing time and, therefore, this method is seldom used in large structures.

The fiber model is generally used by researchers in analysis of cross-sectional strength (Eltawil et al. 1995; Uy 1996; Hajjar and Gourley 1996; Munoz and Hsu 1997; Han et al. 2004; Liang 2008). The cross-section is divided into a number of

fibers and each fiber can be assigned with different material properties such as concrete or steel. The strain in each fiber can be calculated from the neutral axis and curvature of the cross-section and the stress in fiber can be obtained from the constitutive models. The stresses are then integrated over the fibers to find the resultant force and moments and hence the moment-curvature-thrust relationship can then be determined.

Another analysis method for composite members popularly adopted by the researchers is the three-dimensional finite element model. In this model, the behaviors of composite members is simulated accurately by using adequate elements for modeling different components such as the concrete, steel, reinforcement and the interface. The accuracy of using this method was demonstrated by different examples. However, this method is not popular in practice because huge computational effort is needed.

Both efficiency and precision are important in analysis of practical structures which include hundreds of members. The use of a simple and accurate way to include the nonlinear effects such as initial imperfection is important. Therefore, a more practically applicable analysis and design method which fulfills the code requirements for second-order analysis is needed for steel-concrete composite structures.

2.7 Plastic Hinge and Plastic Zone Methods for Frame Structures

The consideration of material nonlinearity in inelastic analysis of frame structures by beam-column element is essential because material yield is an important factor affecting the capacity as well as the load-deflection relationship of the members and structures. The studies in inelastic analysis for framed structures can be broadly classified into distributed plasticity (i.e. the Plastic zone method) and lumped plasticity (i.e. the Plastic hinge method).

2.7.1 Plastic zone method

Many researchers employed the plastic zone approach to study the inelastic behaviors of steel frames (Meek and Lin 1990; Izzuddin and Elnashai 1993b; Pi and Trahair 1994; Izzuddin and Smith 1996; Teh and Clarke 1999; Jiang et al. 2002; Wang et al. 2008; Alvarenga and Silveira 2009). In the plastic zone method, member is discretized into a number of elements with its cross-section divided into fibers. Numerical integration is then applied across the discretized cross-section located at the integration points along the element and hence gradual spread of plasticity within the whole volume of the structure can be modeled. Geometrical imperfection, residual stress and hardening effect can all be taken into account by using this method and therefore solutions are deemed to be exact. The fundamental stress-strain relationship is explicitly and directly used for moments and forces computation and the result is more accurate than the plastic hinge method. However, as demonstrated by Kitipomchai et al. (1990) that the heavy computational effort is needed in discretization across the cross-section and along the member length and hence this method is only suitable for relatively simple structures and not popular for practical engineering design.

2.7.2 Plastic hinge method

The simpler and more practical way to include material nonlinearity in inelastic analysis is the use of the plastic hinge method. In this method, the spread of cross-section plasticity is simulated at the two ends of elements as two plastic hinges. The plastic hinge method can generally be applied in larger size steel structures (King and White 1992; Izzuddin and Elnashai 1993a; Liew et al. 1993a,b; King and Chen 1994; Liew et al. 2000a; Chen et al. 2001) and composite structures (Iu 2008; Iu et al. 2009; Landesmann 2010). Researchers further inserted an additional hinge at mid-span (Chen and Chan 1995) or arbitrary location along the member (Zhou and Chan 2004; Chan and Zhou 2004). However, this method to insert an additional hinge is considered to be too complicated in formulation and for practical uses.

In plastic hinge method, the cross-section plastification is only lumped at two ends of an element and the remaining region is assumed to be elastic. Several methods can be used to model the cross-section plastification. The elastic-plastic perfect hinge method is the simplest way to simulate the elastic-plastic behavior and widely used by the researchers due to its simplicity (Defreitas and Ribeiro 1992; Guralnick and He 1992; Liu et al. 2010). However, material gradual yield cannot be simulated in this method which results in over-prediction of member capacity.

Refinements on the elastic-plastic hinge method were conducted to capture the material gradual yield which included the beam-column section stiffness degradation method studied by Liew et al. (1993a); Kim and Chen (1996b); and Chen et al. (2001)

and beam-column member degradation method studied by King and White (1992). In the beam-column section stiffness degradation method, the element stiffness is reduced gradually from the ideally elastic to perfectly plastic states by introducing the scalar parameters which allow for progressive reduction of inelastic element stiffness based on the axial force and moment at the element ends. The use of the beam-column section stiffness degradation method and its accuracy in space frame structures were also demonstrated by Liew et al. (2000b); Liew and Tang (2000) and Kim et al. (2001). In beam-column member degradation method, the overall member strength is used to simulate the inelastic behavior of the element instead of considering the plasticity effect at the ends. A similar parameter, which is determined based on the element strength ratio, is used to simulate the gradually yield of element stiffness.

The plastic strength of heavily loaded column member can be modeled by column tangent modulus method to reduce the modulus of elasticity in the element stiffness calculation (Chen and Lui 1991; Liew et al. 1993a; Kim and Chen 1996a). Two expressions of column tangent modulus including the Column Research Council (CRC) and AISC (2010) methods are generally adopted by researchers.

Use of a zero-length pseudo-spring element attached to one end or two ends of the element was studied by researchers (Al-Mashary and Chen 1991; Yau and Chan 1994; Chan and Chui 1997) with different definitions of section spring stiffness. Al-Mashary and Chen (1991) modified the method for nonlinear analysis of semi-rigid jointed frames to include the lumped-plasticity material model by end-spring in the analysis. Yau and Chan (1994) further developed a simple and efficient technique for

an element with ends having a pair of springs connected in series, hence, the effect of semi-rigid connection and material nonlinearity can be simulated by different springs. The cross-section strength is modeled by the stiffness of the spring element. The partial yield of the cross-section is simulated by the gradual reduction of the spring stiffness. The method to determine the section spring stiffness used by Chan and Chui (1997) was based on the initial and full yield surfaces, which took into account the presence of axial force and residual stress. The members remained elastic when the force point was located within the initial yield surface and the gradual yield started when the force point was beyond the initial yield surface. The full plastic hinge was formed when the force point reached the full yield surface. In this zero-length pseudo-spring element method, the accuracy of analysis depends on the validity of section spring stiffness and the associated initial and full yield surfaces.

The use of the zero-length pseudo-spring element in steel-concrete composite structures in conjunction with initial and full yield surfaces to consider the material gradual yield in inelastic analysis is limited in literature. The definition of initial yield surface of composite member is important for an accurate advanced analysis of composite structures but it is not well studied. The inelastic analysis should include both geometric and material nonlinearities so as to predict the failure load and the behavior of the structures accurately. Therefore, not only the technique to consider the geometric nonlinearity is important, but also the method to include the material nonlinearity is critical for a successful inelastic analysis.

2.8 Concluding Remarks

In this chapter, the finite element method for beam-column element used in second-order analysis has been reviewed. The shortcoming of the cubic Hermite element can be overcome by using the fifth-order PEP element, and the advantages of the PEP element over the other methods have been emphasized. Therefore, the PEP element will be used for second-order analysis in this thesis. Extensive experimental, computational and codified investigations on CFS tubular members were conducted to study their behaviors. Most researchers focused on studies of isolated members. Based on the understanding on the behaviors of CFS tubular isolated members, the experimental and analytical studies can be extended to structural systems and frames. Most analysis methods require huge computational effort to obtain accurate results and hence these methods are less applicable in engineering design and analysis of large structures. Therefore, a more practical second-order P-Δ-δ elastic and inelastic analysis and design method, which includes important nonlinear effects and member initial imperfection, should be developed. The uses of plastic zone and plastic hinge methods on frame structures have been reviewed and both the efficiency and accuracy of these methods have been discussed. The complexity of plastic zone method makes it less attractive for practical design of mega structures. Therefore, the refined-plastic hinge method will be adopted and researched in this project and reported in this thesis.

Figure

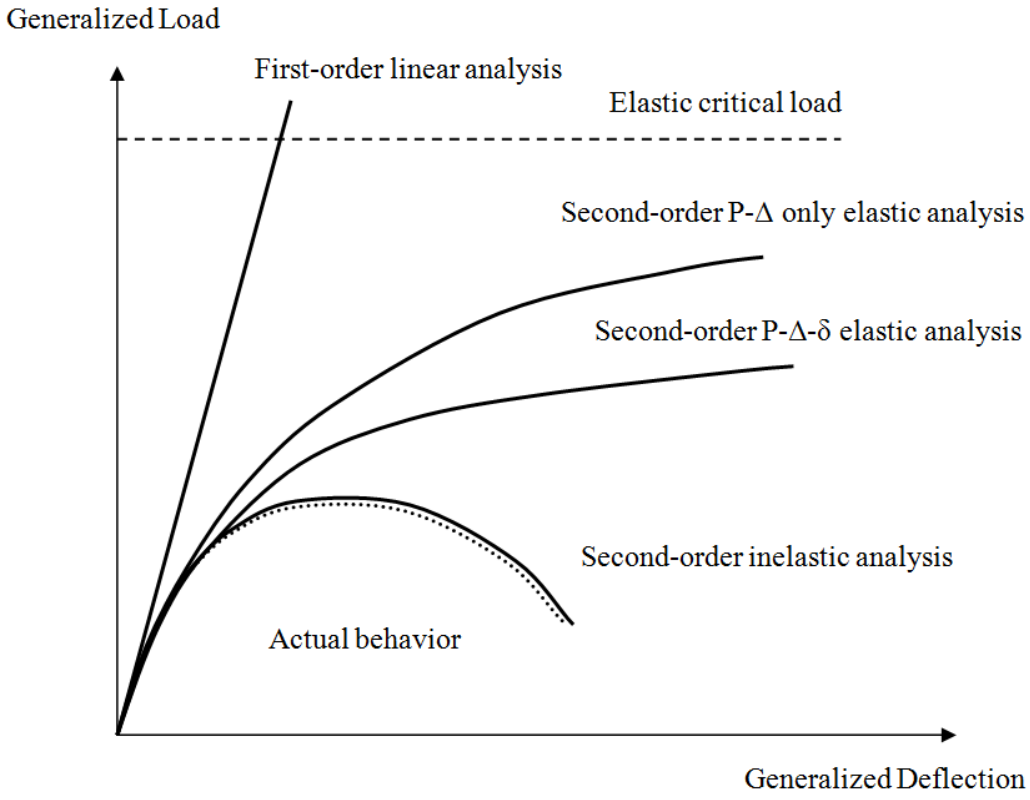

Figure 2.1 Typical Analysis Types for Frame Structures

CHAPTER 3

ELEMENT FORMULATIONS AND INCREMENTAL ITERATIVE STRATEGIES

3.1 Introduction

The finite element method and stability function are two main approaches used in beam-column element for nonlinear analysis. The details and difference between both methods have been reviewed in Chapter 2. The Pointwise Equilibrium Polynomial (PEP) element proposed by Chan and Zhou (1994) has been extensively used in analysis of different kinds of steel structures. The PEP element allowing for modeling by one element per member not only simplifies the modeling efforts, but also greatly reduces the computational time. Furthermore, the PEP element method also eliminates the need of separating the compressive and the tensile load cases with the matrix being valid for positive, negative and zero axial force of which different expressions are required in stability function. The displacement function of the PEP element is different to the cubic Hermite element in that the fifth-order polynomial function is used in the PEP element. Two additional constraints of equilibrium and its rate are imposed at the mid-span of an element together with four compatibility equations at end nodes employed in solving the coefficients of the displacement

function. The element formulation, secant stiffness matrix and tangent stiffness matrix for nonlinear analysis are given in this chapter.

Various techniques for nonlinear analysis have different limitations and efficiency in elimination of the residual or unbalanced displacement and the unbalanced forces. The commonly used techniques such as the Newton-Raphson method, displacement control method (Batoz and Dhatt 1979), the arc-length method (Crisfield 1981) and the minimum residual displacement method (Chan 1988) are introduced with their principle and limitations in this chapter.

Comparison on the behavior of a shallow dome by experimental test and prediction from proposed method is given as an example to verify the accuracy on PEP element in nonlinear analysis with allowance for member imperfection and use of the actual imperfect geometries for nodes in a structure to include the global imperfection. The cause of failure for shallow dome is not simply due to material yielding or elastic buckling of individual members, but it comes from the more complicated failure modes like snap-through buckling where the influence of nodal displacement is significant to the resistance of the dome. Therefore, an accurate prediction on the capacity of the shallow dome can only be guaranteed by use of an accurate nonlinear analysis which captures nonlinear effects, and an appropriate technique for nonlinear analysis.

3.2 Element Formulation for PEP element

The following assumptions are made in the present formulations.

(1) The element is prismatic and elastic

(2) The applied loads are conservative and nodal

(3) Small strain but arbitrarily large deflections is assumed

(4) Shear deformation and warping are ignored

(5) Rotations between the tangent at member ends and the chord joining the two ends are small

The fifth-order polynomial function with six coefficients of a_i with i =0 to 5 is given by,

$$v = a_0 + a_1 x + a_2 x^2 + a_3 x^3 + a_4 x^4 + a_5 x^5 \tag{3.2.1}$$

where x is the non-dimensional distance along the element, v is lateral displacement. The initial imperfection as shown in Figure 3.1 is assumed in the element as,

$$v_0 = v_{mo}[1 - (\frac{2x}{L})^2] \quad \text{and} \quad -L/2 \le x \le L/2 \tag{3.2.2}$$

where v_0 is the lateral initial imperfection, v_{mo} is the amplitude of initial imperfection equal to the imperfection at mid-span and L is the length of the member.

To solve the six coefficients in the polynomial function, four equations in compatibility condition and two equations in equilibrium condition are introduced as, For equilibrium,

$$EIv'' = P(v + v_0) + \frac{M_1 + M_2}{L}(x + \frac{L}{2}) - M_1 \tag{3.2.3}$$

$$EIv'''' = Pv'' + \frac{M_1 + M_2}{L} \tag{3.2.4}$$

For compatibility,

At $x = -\frac{L}{2}$; $v = 0$ and $v' = \theta_1$ (3.2.5)

At $x = \frac{L}{2}$; $v = 0$ and $v' = \theta_2$ (3.2.6)

where E is the modulus of elasticity; I is the second moment of area; v is the lateral displacement due to applied loads; P is the axial force; M_1 and M_2 are the nodal end moments. The shape function derived by PEP element is valid for positive, negative and zero value of axial force.

Considering equilibrium and compatibility conditions, the coefficients in Eq. (3.2.1) can be solved and the final displacement function about the axis passing through the two ended nodes can be expressed as,

$$v = N_1(L\theta_1) + N_2(L\theta_2) + N_0 v_{mo} \tag{3.2.7}$$

where N_1 and N_2 are the shape functions for perfectly straight element and

$$N_0 = -q\frac{(1-(\frac{2x}{L})^2)^2}{48+q} \tag{3.2.8}$$

$$q = \frac{PL^2}{EI} \tag{3.2.9}$$

3.3 Secant Stiffness Matrix

The secant stiffness matrix used to check the equilibrium convergence and to compute the equilibrium error due to change of geometry and cross-sectional strength can be found by first variation of the strain energy function.

The total potential energy function, Π, is given by,

$$\Pi = U - V \tag{3.3.1}$$

where U is the strain energy and V is the external work done expressed as,

$$V = \sum F_i u_i \tag{3.3.2}$$

and F_i is the applied forces and u_i is the displacements.

The strain energy, U, is given by,

$$U = \frac{1}{2}\int_L EAu'^2 dx + \frac{1}{2}\int_L EIv''^2 dx + \frac{1}{2}\int_L P(v'^2 + 2v'v_0')dx \tag{3.3.3}$$

where A is cross-sectional area and u is the axial displacement.

The first, second and third terms in Eq. (3.3.3) are the strain energy due to axial, bending and member bowing respectively.

The secant-stiffness relations can be obtained by the first variation of the energy functional as follows,

$$P = \frac{\partial U}{\partial e_x} + \frac{\partial U}{\partial q}\frac{\partial q}{\partial e_x}$$

$$= EA\left[\frac{e_x}{L} + b_1\left(\theta_1 + \theta_2\right)^2 + b_2\left(\theta_1 - \theta_2\right)^2 + b_{vs}\frac{v_{mo}}{L}\left(\theta_1 - \theta_2\right) + b_{vv}\left(\frac{v_{mo}}{L}\right)^2\right] \tag{3.3.4}$$

and

$$M_1 = \frac{\partial U}{\partial \theta_1} + \frac{\partial U}{\partial q}\frac{\partial q}{\partial \theta_1}$$

$$= \frac{EI}{L}\left[c_1\left(\theta_1 + \theta_2\right) + c_2\left(\theta_1 - \theta_2\right) + c_0\left(\frac{v_{mo}}{L}\right)\right] \tag{3.3.5}$$

$$M_2 = \frac{\partial U}{\partial \theta_2} + \frac{\partial U}{\partial q}\frac{\partial q}{\partial \theta_2}$$

$$= \frac{EI}{L}\left[c_1(\theta_1 + \theta_2) - c_2(\theta_1 - \theta_2) - c_0\left(\frac{v_{mo}}{L}\right)\right] \tag{3.3.6}$$

where e_x is the member shortening, θ_1 and θ_2 are the nodal rotations, and c_1, c_2, b_1, b_2, c_o, b_{vs} and b_{vv} are the coefficients and given as follows,

$$c_1 = \frac{3(80)^2 + 10(80)q + (61/7)q^2 + (23/1260)q^3}{(80+q)^2} \tag{3.3.7}$$

$$c_2 = \frac{48^2 + 6(48)q + (29/5)q^2 + (11/420)q^3}{(48+q)^2} \tag{3.3.8}$$

$$b_1 = \frac{2(80)^2 + (26/7)(80)q + (46/21)q^2 + (23/2520)q^3}{(80+q)^3} \tag{3.3.9}$$

$$b_2 = \frac{2(48)^2 + (14/5)(48)q + (66/35)q^2 + (11/840)q^3}{(48+q)^3} \tag{3.3.10}$$

$$c_o = \frac{2q\left(11q^2 + 42\times 48q + 35\times 48^2\right)}{105(48+q)^2} \tag{3.3.11}$$

$$b_{vs} = c_o'$$

$$= \frac{2\left(11q^3 + 33\times 48q^2 + 49\times 48^2 q + 35\times 48^3\right)}{105(48+q)^3} \tag{3.3.12}$$

$$b_{vv} = -\frac{64q\left(q^2 + 144q + 5376\right)}{35(48+q)^3} \tag{3.3.13}$$

A more readable form can be used to express the axial force, *P,* as shown below,

$$q = \lambda^2\left(\frac{e_x}{L} + c_b + c_{bo}\right) \tag{3.3.14}$$

and where,

$$\lambda = \sqrt{\frac{AL^2}{I}} \tag{3.3.15}$$

$$c_b = b_1\left(\theta_1 + \theta_2\right)^2 + b_2\left(\theta_1 - \theta_2\right)^2 \tag{3.3.16}$$

$$c_{bo} = b_{vs}\left(\frac{v_{mo}}{L}\right)\left(\theta_1 - \theta_2\right) + b_w\left(\frac{v_{mo}}{L}\right)^2 \tag{3.3.17}$$

The initial crookedness and end rotation are included in Eq. (3.3.14) as the last term, and which are ignored for a straight member, and the first and second terms in Eq. (3.3.14) are the linear strain and bowing due to member end rotations respectively.

3.4 Tangent Stiffness Matrix

The tangent stiffness matrix used for prediction of the displacement increment can be found by second variation of the total potential energy function as follows.

$$\delta^2 \prod = \frac{\partial^2 \prod}{\partial r_i \partial r_j} = \frac{\partial s_i}{\partial r_j} + \frac{\partial s_i}{\partial q}\frac{\partial q}{\partial r_j} \text{ ; for } i,j = 1,2,3 \tag{3.4.1}$$

where s_i and r_i are the force and displacement vectors respectively, and can be expressed as,

$$s = \left(M_1 M_2 P\right)^T \tag{3.4.2}$$

$$r = \left(\theta_1 \theta_2 e_x\right)^T \tag{3.4.3}$$

The basic matrix about a principal axis can be determined as follows,

$$k_t^e = \frac{EI}{L}\begin{bmatrix} c_1 + c_2 + \frac{G_1^2}{H} & c_1 - c_2 + \frac{G_1 G_2}{H} & \frac{G_1}{LH} \\ & c_1 + c_2 + \frac{G_2^2}{H} & \frac{G_2}{LH} \\ & & \frac{1}{L^2 H} \end{bmatrix} \tag{3.4.4}$$

where H, G_1 and G_2 can be expressed as follows,

$$H = \frac{1}{\lambda^2} - c_b' - c_{bo}' \tag{3.4.5}$$

$$G_1 = c_{b1}' = 2b_1(\theta_1 + \theta_2) + 2b_2(\theta_1 - \theta_2) + b_{vs}\left(\frac{v_{mo}}{L}\right) \tag{3.4.6}$$

$$G_2 = c_{b2}' = 2b_1(\theta_1 + \theta_2) - 2b_2(\theta_1 - \theta_2) - b_{vs}\left(\frac{v_{mo}}{L}\right) \tag{3.4.7}$$

The expression of the matrix in three-dimensional space can be obtained by repeating the process for the other principal axis. The final tangent stiffness matrix is given as,

$$[K_t] = \sum^{Nele} [L_T][k_t][L_T]^T = \sum^{Nele} [L_T]\left([T_T]^T [k_t^e][T_T] + [N]\right)[L_T]^T \tag{3.4.8}$$

where $[L_T]$ is the standard local to global transformation matrix, $[T_T]$ is the transformation matrix relating the six basic element forces and moments to the 12 forces and moments about the element ends, and $[N]$ is the geometric-stiffness matrix for translational displacement.

3.5 Techniques for Nonlinear Analysis

The response of structures under specified set of loads or displacements can be traced by nonlinear solution techniques. The divergence problem is quite common in nonlinear analysis due to the limitations of different nonlinear solution techniques which are discussed in the followings. Various numerical methods based on incremental-iterative procedure were proposed to improve rate of convergence and to prevent divergence. In this section, the numerical methods including the Newton-Raphson method, displacement control method (Batoz and Dhatt 1979), the arc-length method (Crisfield 1981) and the minimum residual displacement method (Chan 1988) are introduced and discussed. Detailed descriptions of all these techniques were given by Chan and Chui (2000).

The same approach of super-imposition of the original incremental equilibrium equation to the constraint equation can generally be used to derive those nonlinear solution methods. The incremental equilibrium equation can be written as,

$$[\Delta F] = [K_T][\Delta u] \tag{3.5.1}$$

where $[\Delta F]$ and $[\Delta u]$ are the unbalanced force and displacement respectively and $[K_T]$ is the tangent stiffness matrix.

The constraint equation with force vector parallel to the applied load vector can be expressed as follows,

$$\Delta\lambda[\Delta\overline{F}] = \Delta\lambda[K_T][\Delta\overline{u}] \tag{3.5.2}$$

where $\Delta\lambda$ is a load corrector factor for imposition of the constraint condition, $[\Delta\overline{F}]$ is the force vector parallel to the applied load vector and of arbitrary length and $[\Delta\overline{u}]$ is the conjugated displacement vector to $[\Delta\overline{F}]$.

The resulting incremental equilibrium equation can be obtained by superimposing Eqs. (3.5.1) and (3.5.2) as,

$$([\Delta F]+\Delta\lambda[\Delta\overline{F}])=[K_T]([\Delta u]+\Delta\lambda[\Delta\overline{u}]) \tag{3.5.3}$$

Therefore, both the load and displacement in each iteration can be updated as follows,

$$[F]_{i+1}=[F]_i+\Delta\lambda_{i+1}[\Delta\overline{F}] \tag{3.5.4}$$

$$[u]_{i+1}=[u]_i+[\Delta u]_{i+1}+\Delta\lambda_{i+1}[\Delta\overline{u}] \tag{3.5.5}$$

where the subscript '*i*' refers to the *i*-th iteration number within a load cycle.

Eq. (3.5.3) is used in numerical analysis for incremental-iterative nonlinear finite element analysis formulation. The different expressions of the load corrector factor $\Delta\lambda$ are used for different methods. The details of the commonly used numerical methods are described below.

3.5.1 The Newton-Raphson method

The Newton-Raphson method combines the direct iterative and pure incremental methods. The tangent stiffness is used to estimate the displacement increment due to a small but finite force, while the secant stiffness is used to check for the equilibrium

condition. The tangent stiffness is reformed in each iteration in conventional Newton-Raphson method, so that less iteration is required to achieve convergence. The tangent stiffness is reformed at the first iteration only in the modified Newton-Raphson method, hence, less computational time is needed as the formulation of tangent stiffness matrix is time consuming. The incremental-iterative schemes for both conventional and modified Newton-Raphson methods are shown in the Figures 3.2a and 3.2b respectively.

The key steps of the Newton-Raphson method procedure are given below:

1. Apply the first incremental load vector $[\Delta F]$
2. Calculate the global displacement incremental vector $[\Delta u]$

$$[\Delta u] = [K_T]^{-1}[\Delta F] \tag{3.5.6}$$

where $[K_T]$ is the global tangent stiffness matrix

3. Accumulate of displacement increment to total displacement

$$[u]_{i+1} = [u]_i + [\Delta u] \tag{3.5.7}$$

4. Update the geometry

$$[x]_{i+1} = [x]_i + [\Delta x] \tag{3.5.8}$$

5. Extract element displacement vector $[u_e]$ from global displacement vector and transform to local displacement vector $[u_l]$

$$[u_l] = [L_T][u_e] \tag{3.5.9}$$

where $[L_T]$ is the transformation matrix

6. Calculate the element resistance force vector $[F_l]$

$$[F_l] = [k][u_l] \tag{3.5.10}$$

where $[k]$ is the element stiffness matrix

7. Accumulate the element resistance force to obtain the final element force vector $[R_e]$ and transform to global axes for resistance force $[R]$

$$[R_e] = \sum [F_l] \tag{3.5.11}$$

$$[R] = [L_T]^T [R_e] \tag{3.5.12}$$

8. Compare the applied forces and resistance forces to compute the unbalanced forces

$$[\Delta R] = [F] - [R] \tag{3.5.13}$$

where $[F]$ is the external force vector

The process is repeated by revising the displacements and re-checking the equilibrium condition until the unbalanced forces are eliminated with its norm less than a pre-defined tolerance. The convergence check is carried out by using the following conditions,

$$[\Delta u]^T [\Delta u] < TOLER \cdot [u]^T [u] \tag{3.5.14}$$

$$[\Delta F]^T [\Delta F] < TOLER \cdot [F]^T [F] \tag{3.5.15}$$

The *TOLER* should be set sufficiently small so as to get an accurate analysis result and the value is normally set to be 0.1%. After the convergence, a new load cycle is applied using an updated tangent stiffness matrix and the whole previous process is repeated.

The use of Newton-Raphson method is sufficient for engineering design for most pratical structures, since the post-buckling behavior is seldom investigated in daily design. However, the inability of the load control Newton-Raphson method to converge near the limit point is a handicap for nonlinear analysis of some structures such as rafters and shallow domes which are discussed in next section. Therefore, the following solution schemes should be used in analysis of these structures to overcome the divergence problem in post-buckling analysis.

3.5.2 Displacement control method

In the displacement control method proposed by Batoz and Dhatt (1979), a single degree of freedom with a pre-defined magnitude of displacement increment is chosen to be the steering displacement degree of freedom for control of the advance of the solution for equilibrium path. This method simultaneously possesses the capacity of traversing the limit point without destroying the symmetrical property of the tangent stiffness matrix. A graphical representation of this method is shown in Figure 3.3.

In this method, the *m*-th degree of freedom is selected as the steering displacement degree of freedom. The displacement increment is set to be $\Delta_m u_1$ in the first iteration for each load increment and then substituted it into Eq. (3.5.5) to obtain the corrector factor as,

$$\Delta\lambda_1 = -\frac{\Delta_m u_1}{\Delta_m \bar{u}_1} \tag{3.5.16}$$

For second onward iteration within a load cycle, u_{i+1} will be equaled to u_i for no displacement increment in *m*-th or the steering degree of freedom, Eq. (3.5.5) can then be expressed as,

$$\Delta\lambda_i = -\frac{\Delta_m u_i}{\Delta_m \bar{u}_i} \quad \text{for } i \geq 2 \tag{3.5.17}$$

The selection of the steering degree of freedom correctly is important in this method. However, for practical large structures with many degrees of freedom, the choosing of steering displacement is difficult and inconvenient. Furthermore, the method breaks down in a snap-back problem because of the non-existence in solution for a certain displacement in a snap-back problem.

3.5.3 The arc-length method

The arc-length method was initially proposed by Riks (1979) and refined by Crisfield (1981) and Crisfield (1983) by making the original un-symmetric tangent stiffness matrix to become symmetrical. In the arc-length method, the dot product of the displacements is used to control the load increment. This arc- distance is specified and kept constant in a particular load cycle. A graphical representation of this method is shown in Figure 3.4.

The arc-distance is given in *S*, and the constraint equation in the first iteration of a load cycle from Eq. (3.5.5) can be obtained as,

$$\Delta\lambda_1 = \frac{S}{\sqrt{[\Delta\bar{u}]_1^T [\Delta\bar{u}]_1}} \tag{3.5.18}$$

For the second iteration onwards, the arc-distance S is kept constant. The following expression can be obtained,

$$([u]_{i-1}+[\Delta u]_i+\Delta\lambda_i[\Delta\bar{u}]_i)^T([u]_{i-1}+[\Delta u]_i+\Delta\lambda_i[\Delta\bar{u}]_i)=S^2 \tag{3.5.19}$$

The arc–length method is superior to both constant load method and constant displacement method, and applicable to most structural problems such us tracing the snap-through and snap-back behaviors. However, the involvement of the quadratic equation in the iterative procedure may give the imaginary root, and the selection of the root makes this method complicated.

3.5.4 The minimum residual displacement method

The minimum residual displacement method was proposed by Chan (1988) to provide a simple and fast way to eliminate the residual displacements or unbalance forces. The graphically presentation of this method is shown in Figure 3.5. A simple technique is used to search for a direction leading to the minimum value for the displacement error expressed as $\Delta\lambda_i[\Delta\bar{u}]+[\Delta u]_i$. This can be achieved by differentiating the residual displacement with respect to the parameter, $\Delta\lambda_i$, as,

$$\frac{\partial\left\{(\Delta\lambda_i[\Delta\bar{u}]+[\Delta u]_i)^T(\Delta\lambda_i[\Delta\bar{u}]+[\Delta u]_i)\right\}}{\partial\Delta\lambda_i}=0 \tag{3.5.20}$$

The following expression can be obtained by simplifying Eq. (3.5.20),

$$\Delta\lambda_i=-\frac{[\Delta u]_i^T[\Delta\bar{u}]}{[\Delta\bar{u}]^T[\Delta\bar{u}]} \tag{3.5.21}$$

For the size of load increment, the simple scaling of the load factor is used as follows:

$$\Delta\lambda_1^k = \Delta\lambda_1^1 S_p^{\gamma} \text{ and } 2 > \frac{\Delta\lambda_1^k}{\Delta\lambda_1^1} > 0.1 \tag{3.5.22}$$

where γ is a parameter to control the load size, and the second condition ensures a proper incremental load size.

The minimum residual displacement method can deal with the most problems with simplicity and efficiency and its performance is comparable and sometimes superior to the arc-length method.

3.6 Investigation on the Snap-through Behavior of Shallow Dome

Cause of failure for space structures like shallow dome is not simply due to material yielding or individual member buckling, but it comes from the more complicated failure mode of snap-through buckling where the influence on the capacity due to nodal displacement is significant (Rothert et al. 1981; Shibata et al. 1993). The comparison on the failure loads of a shallow dome between the laboratory test and nonlinear analysis is carried out here to verify the use of PEP element in nonlinear analysis and the capability of the nonlinear solution techniques to trace the snap-through buckling of the shallow dome. There have been quite a few collapses of domes in different countries such as Poland, Germany, China and others even under a snow load less than the normal design load in some cases. Although engineers need not consider snow load in some regions, wind pressure can be upward on one side and downward on the other side that can lead to asymmetric snap-through buckling.

Therefore, the use of an accurate nonlinear analysis method, which includes both the local and global imperfections correctly, and an appropriate technique is important.

3.6.1 Experimental setup

A single layer shallow dome of spherical geometry with depth of 0.27m and span of 4.76m was fabricated for test. The shallow dome consisted of 90 members and 37 nodes as shown in Figure 3.6. The stainless circular hollow section steel tube with 19mm diameter and 0.8mm thick was used as the members of the dome. The length of each member was basically the same and equal to 0.8m approximately. The mean value of Young's modulus of elasticity was 201.9N/mm^2, and yield and ultimate strengths were 394.2N/mm^2 and 691.4N/mm^2 respectively.

The hexagonal stainless steel plates were used to connect the members of the dome and its dimensions are given in Figure 3.7. The side length of the plates was 106.9mm. There were 12 holes in the plates with 9mm diameter and the spacing between holes was 22.5mm. The distance between the center of the outer hole and the edge was 20mm. Six members were jointed together through the plates with an intercepting angle of approximately 60 degrees spaced evenly and connected to the plates by 8mm bolts.

The dome was supported at six nodes (nodes 1, 4, 16, 22, 34 and 37) and the other nodes were free. The supports were fixed to the ground as shown in Figure 3.8. Each support consisted of two hexagonal plates, two I channels and one base plate which was fixed to the ground, and one 6mm iron plate was placed together with two

additonal hexagonal paltes as protection during the test. The overall picture of the setup of the dome is given in Figure 3.9.

A high precision surveying procedure was adopted to measure the coordinates of each node before test. The coordinates of all nodes are listed in Table 3.1 and the set up of the shallow dome is shown in Figure 3.6. The dome was not perfectly symmetric but with local asymmetry present and surrounding the nodes, and the actual imperfect shape of the dome and the designed perfect dome are represented by the dot line and the solid line respectively in Figure 3.6. The maximum geometrical imperfections were 40mm at node 7 in lateral direction and 56mm at node 9 in vertical direction comparing with the perfect dome.

Load cell was placed at the centre of the dome to record the corresponding load under the change of displacement, and the vertical movement was applied by using a rigid bar which connected to the load cell directly. A thick plate was bolted together with the hexagonal plate to prevent the failure of central node during the test. The vertical movements of the nodes of the dome were measured by transducers. The deflection of the central node was recorded at 0.1kN interval before the snap-through buckling and 0.05kN interval after snap-through buckling.

3.6.2 Test results

The load-deflection relationship of node 19 (central node of the dome) from the test is plotted in Figure 3.10. The central node moved downward linearly with increase of applied load at the initial stage. When the applied load reached around 0.2kN, the

relationship became nonlinear. As the load increased to 0.51kN, the dome snapped suddenly at the centre as shown in Figure 3.11 and the deflection increased with a decreasing load. Due to the geometric imperfection, the deformed shape of dome was unsymmetrical with the maximum deflection at the center of the dome. The final deformed shape of the dome is given in Figure 3.12

3.6.3 Nonlinear analysis method

The analysis model of the shallow dome is shown in Figure 3.13. The mean Young's modulus of elasticity and yield strength from material test are assigned for all members of the dome in the analysis model and the measured coordinates of each node are adopted in the analysis model and two groups of solid plates with the total of 12 elements are used in modeling the connection of the dome as shown in Figure 3.14. The first group including 6 solid plates connects the members side by side. The width of the solid plates is taken as 22.5mm by assuming only the center distance of two holes in the member is effective to provide stiffness. The depth of the solid plates is equal to the thickness of the hexagonal plate by assuming only one plate provides stiffness effectively. The second group consists of another 6 solid plates to connect the members to the center of the connection. The width of the solid plates is taken as the diameter of the hollow tube, and the depth is the same as the first group. Using two groups of solid plates, the properties of the connection in the dome could be simulated directly in analysis model.

For a practical nonlinear analysis, both the local member and global structure imperfections, which will be discussed in next chapter, should be taken into account.

The actual imperfect coordinates of each node are used in the analysis model for consideration of global imperfection. The local member imperfection for all members is set to be $L/500$, in which L is the member length.

The load-deflection relationships of some failure types like snap-through buckling cannot be traced by load-control method due to the divergence problem at limit point. Hence, the combined arc-length method and the minimum residual displacement method are used for incremental-iterative procedure to trace the path up to and beyond the limit point.

The computed load-deflection curve of node 19 is compared with test result in Figure 3.10. The snap-through buckling load in nonlinear analysis is 0.47kN. After reaching the snap-through buckling load, the deflection increases continuously with the decrease of applied load. After the deflection of node 19 reaches 50mm, the dome regains stiffness and thus stability and the applied load increases continually.

3.6.4 Discussions of the results

The load-deflection relationship of dome predicted by the nonlinear analysis with PEP element is close to the test result. The predicted snap-through buckling load from nonlinear analysis is slightly lower than the test result and the post-buckling behavior of the dome can be modeled well. The comparison on the results implies the accuracy of using the PEP element in nonlinear analysis to simulate the behaviors of the shallow dome, and only one element per member is required in analysis with inclusion of member imperfection. The example has also verified the

capability of tracing the load-deflection relationship before and after the limit point as well as the snap-through buckling by using the combined arc-length and the minimum residual displacement methods.

The major reason for the discrepancies on the test and analysis results is due to the assumptions of the effective width and depth to contribute the stiffness in modeling the connection which may be varied from reality. Furthermore, the initial imperfection of all members is set to be $L/500$ in the nonlinear analysis but the actual imperfection of each individual member may be different from this value. Therefore, the difference in member imperfection between the test and analysis model also leads to the discrepancy on the results.

3.6.5 Study on the dome connections

The influences on the buckling load and behavior of the shallow dome by using the rigid connection between the members are examined for comparison. In the analysis model, all members are connected rigidly instead of simulating the actual condition of the connection. The load-deflection curve for node 19 presented by dot line is compared with the test result and plotted in Figure 3.10. The buckling load of the dome is found to be 1.47kN which is nearly 3 times higher than the test result. Therefore, it shows that the different properties of the connection greatly influence the capacity of the dome and should not be overlooked.

3.7 Concluding Remarks

The use of nonlinear analysis for structures is preferable and becomes more popular nowadays. An efficient and simple element in nonlinear analysis is important and essential to obtain an accurate result with high efficiency that engineers would accept it as a better alternative to the effective length method. The use of PEP element only requires one element per member with the ability to include imperfections at local member and global frame levels. The detailed element formulation and the secant and tangent stiffness matrices have been presented in this chapter, and the properties of commonly used numerical methods in tracing the behaviors of structures have been summarized and discussed. The comparison on the load-deflection behavior of shallow dome between the test and analysis method has been carried out to verify the accuracy of PEP element in nonlinear analysis and to demonstrate the capability to trace the snap-through behavior by using the combined arc-length and the minimum residual displacement methods where the arc-length method controls the first iteration and the minimum residual displacement method iterates for a solution.

In the following chapters, the PEP element will be used for second-order analysis for both steel and steel-concrete composite members. The different nonlinear analysis techniques will be used in incremental-iterative process to find the ultimate capacity and load-deflection curve of the members and structures.

Figures

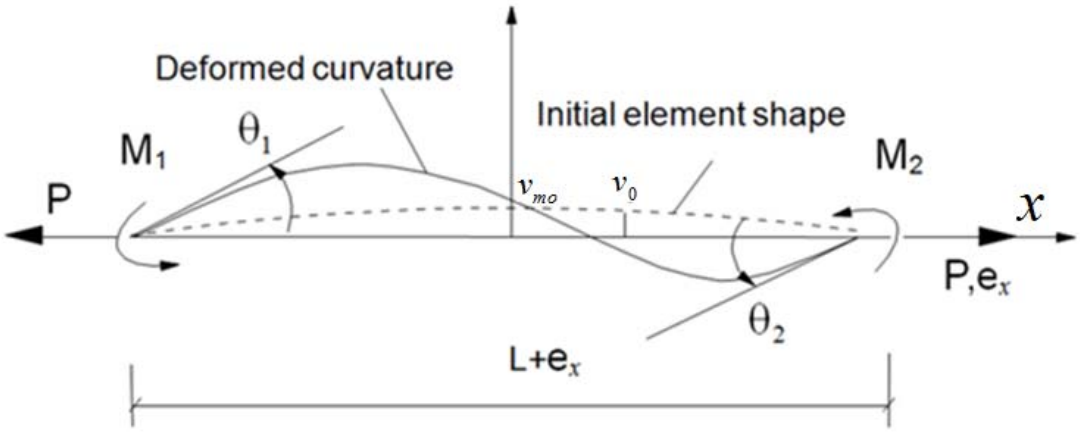

Figure 3.1 Basic Forces versus Displacements Relations in PEP Element

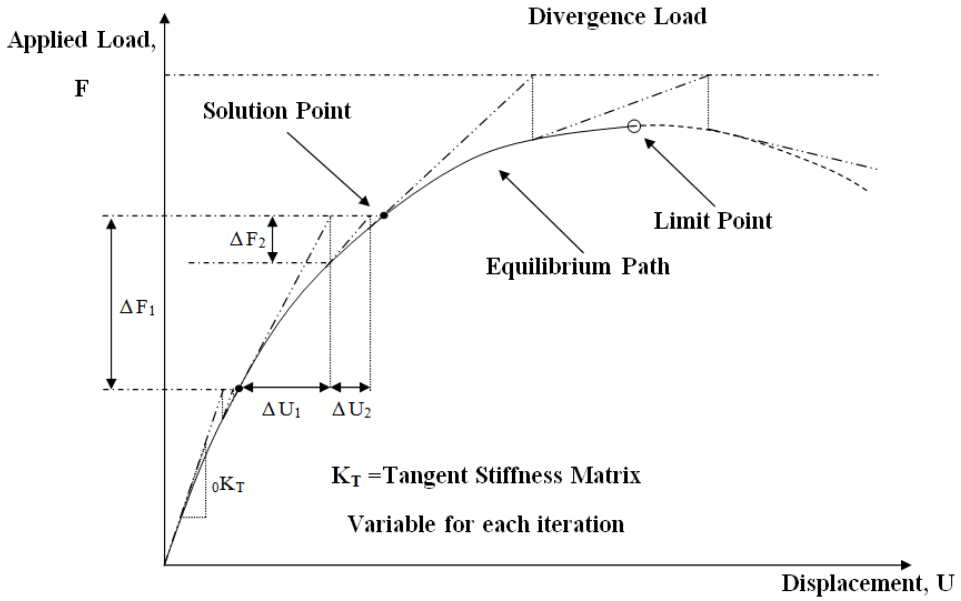

(a) Conventional Newton-Raphson Method

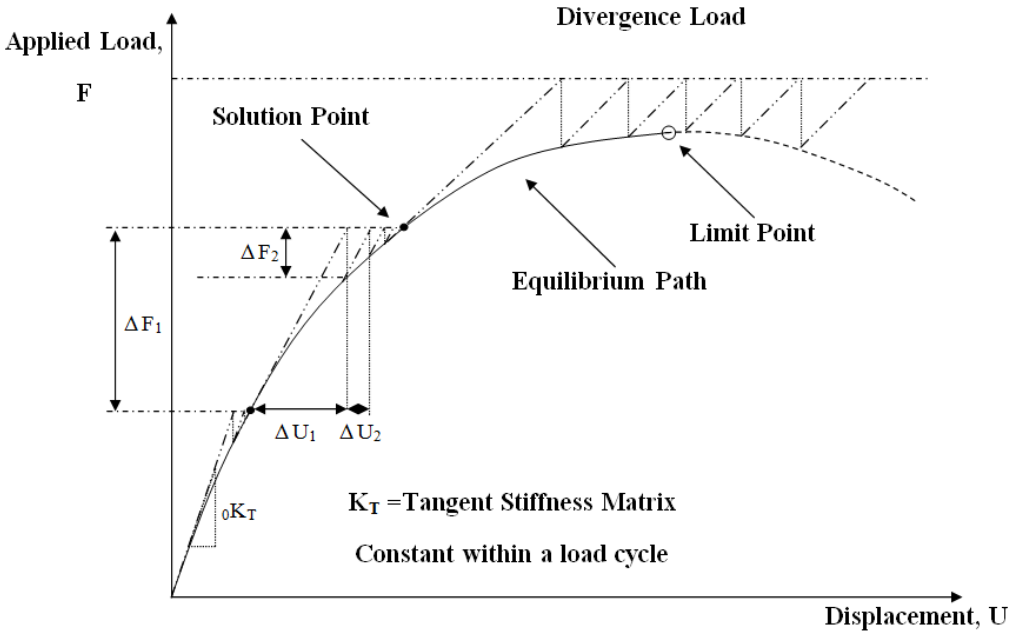

(b) Modified Newton-Raphson Method

Figure 3.2 The Newton-Raphson Method

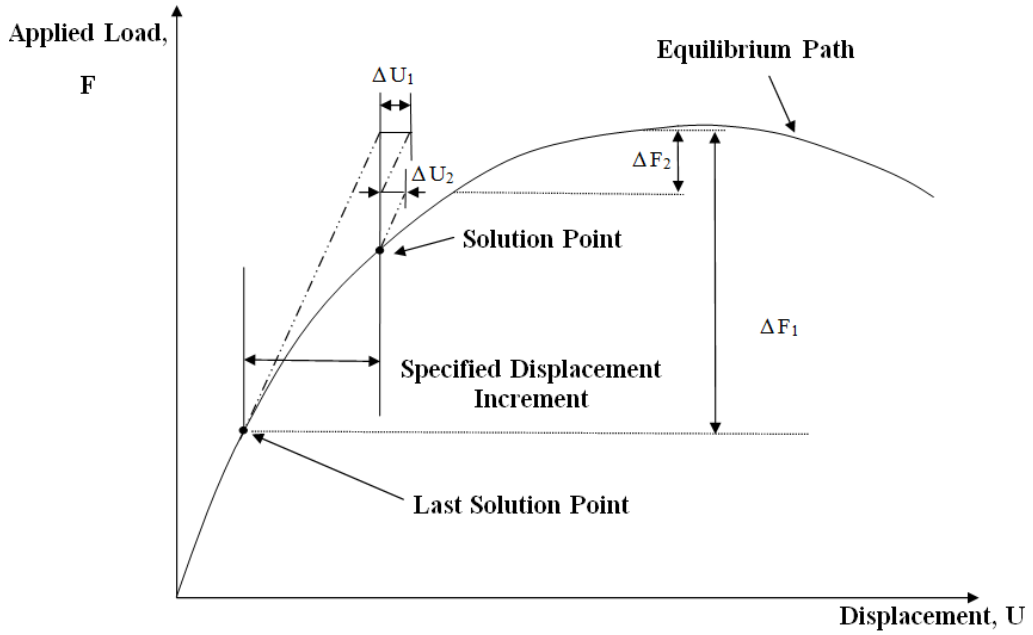

Figure 3.3 The Displacement Control Method

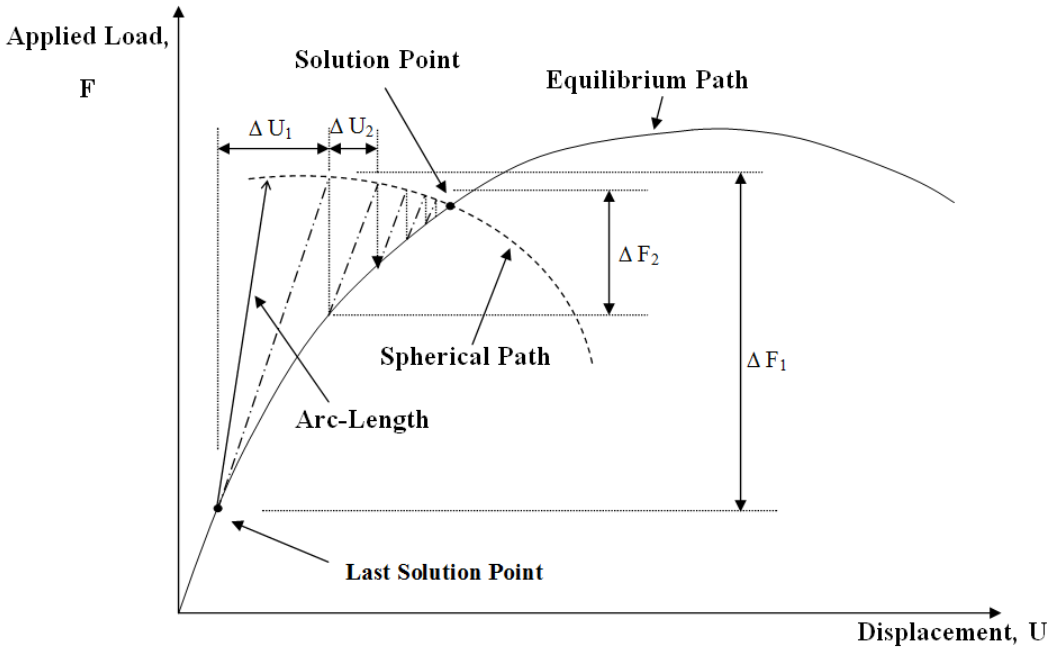

Figure 3.4 The Arc-length Method

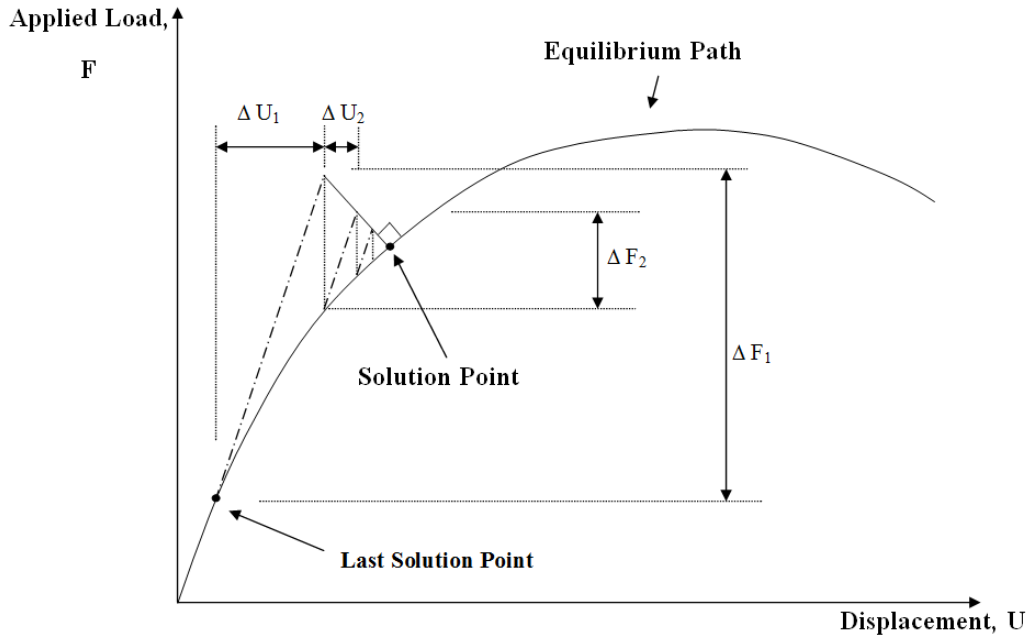

Figure 3.5 The Minimum Residual Displacement Method

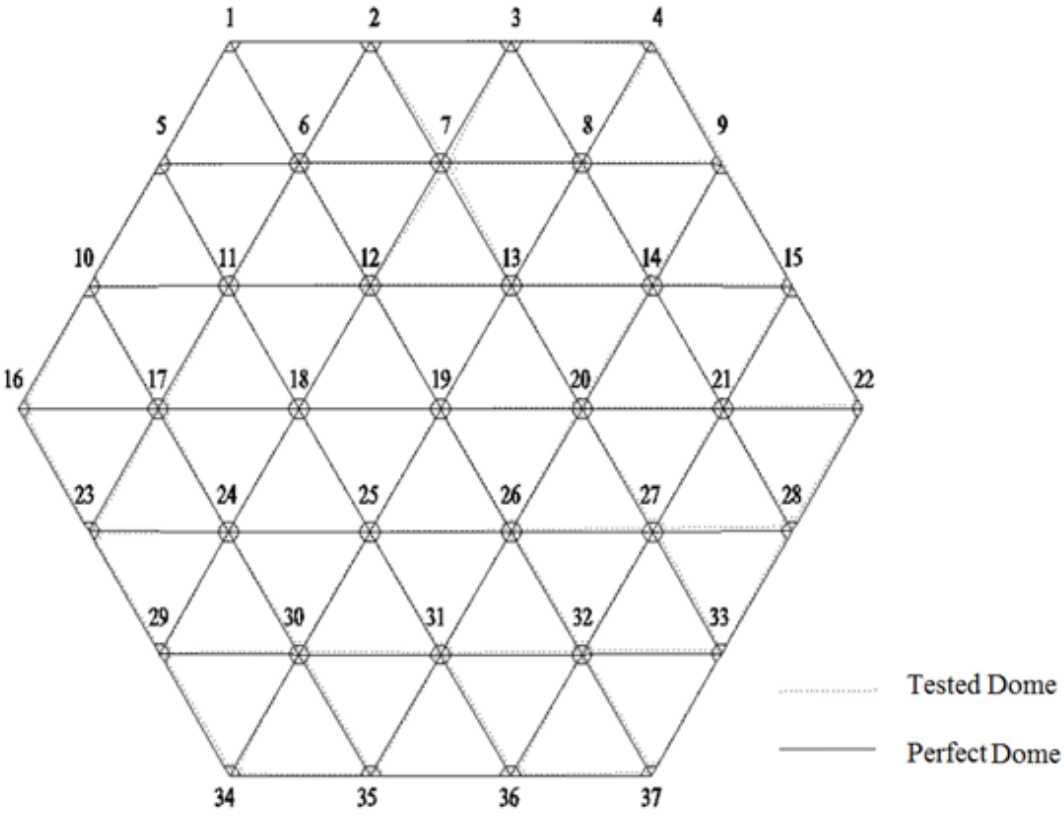

Figure 3.6 Layout of the Tested and Perfect Domes

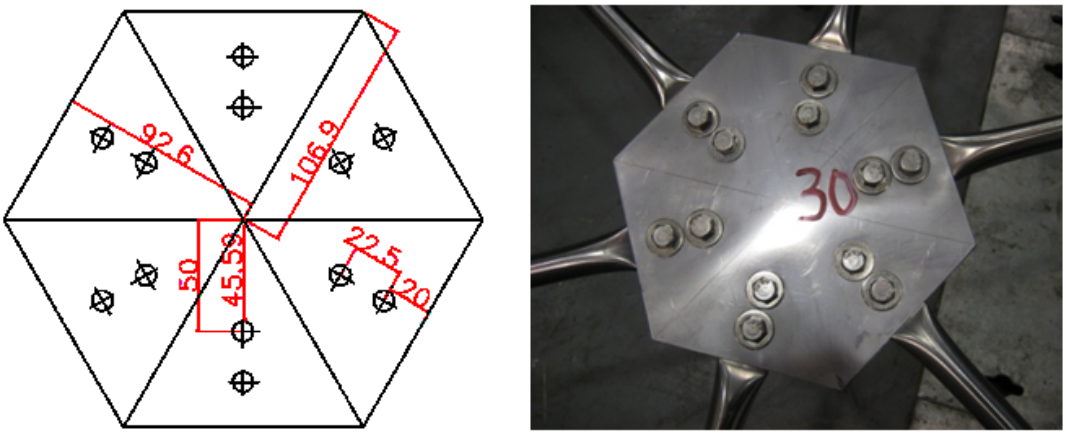

Figure 3.7 Connection Detail of the Dome

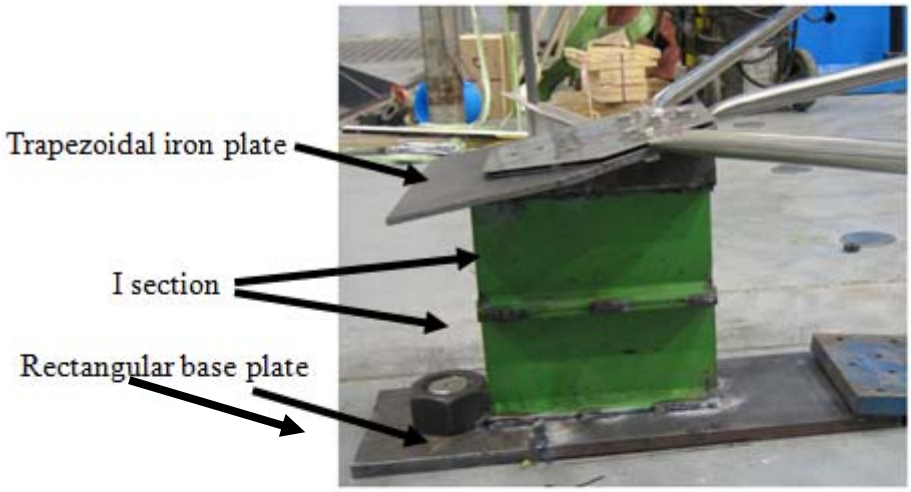

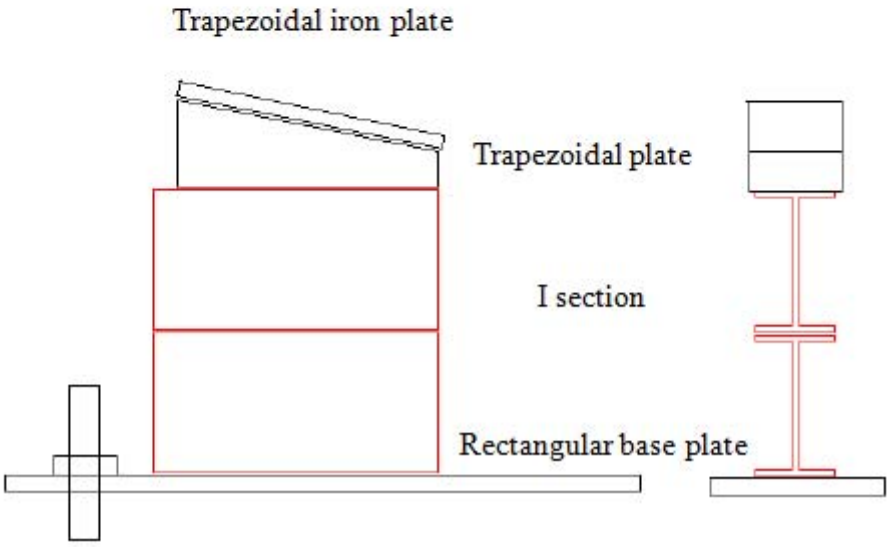

Figure 3.8 Support of the Dome

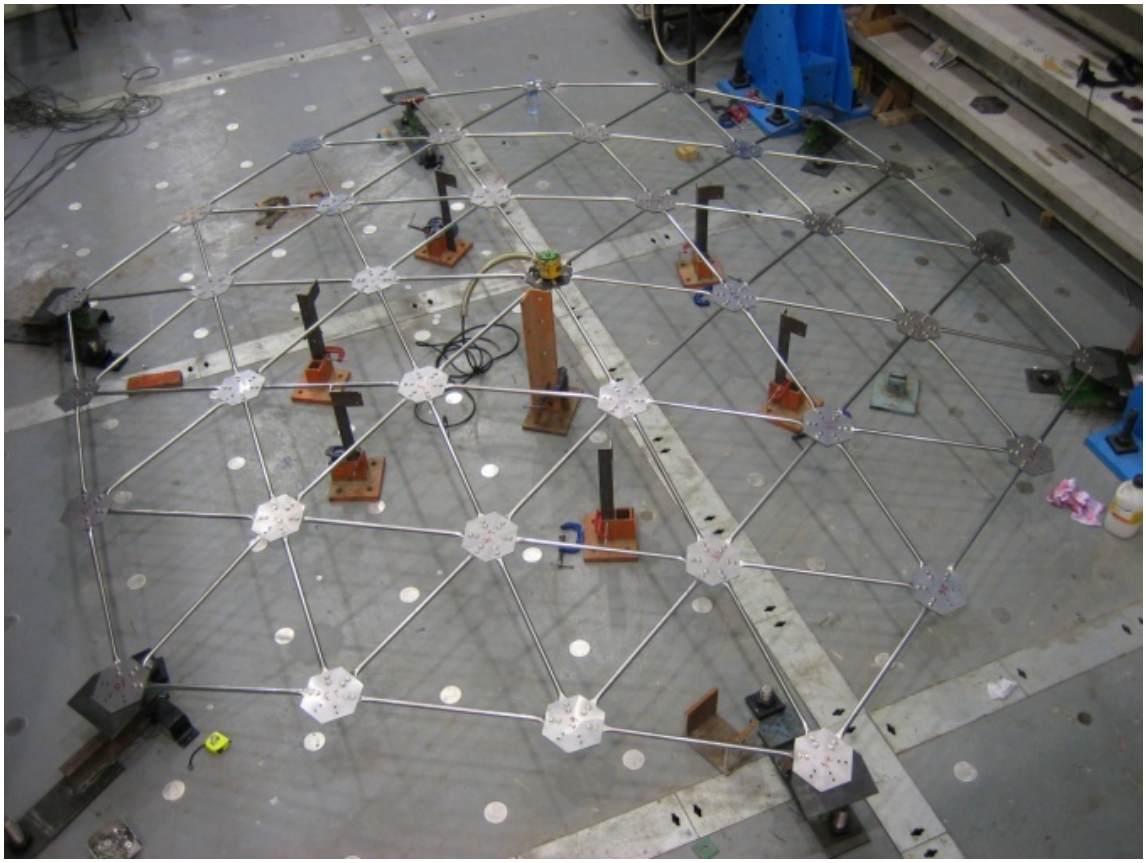

Figure 3.9 Experimental Setup of the Dome

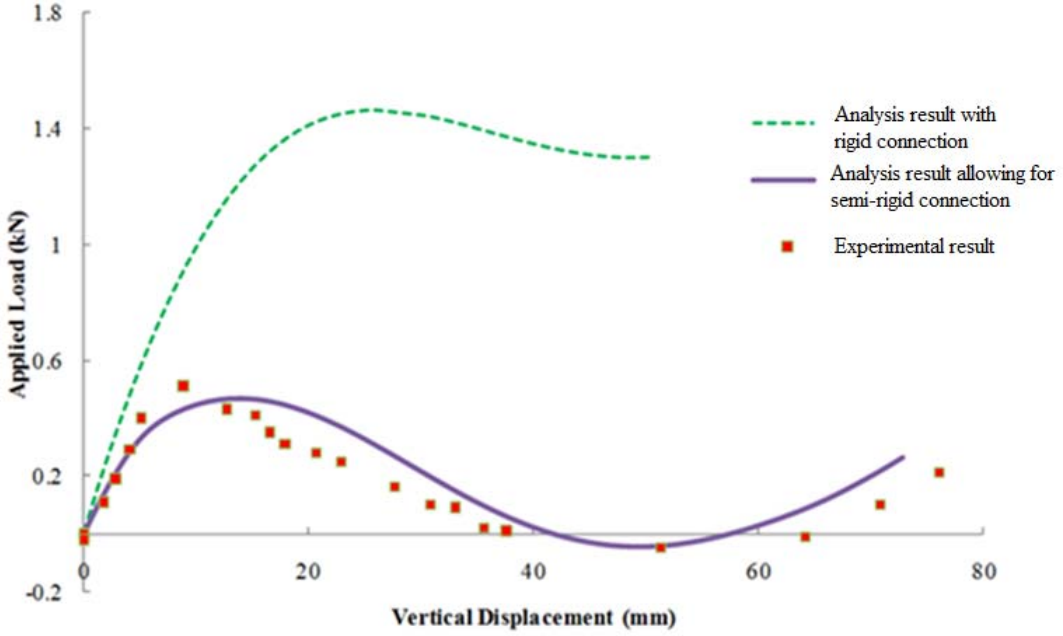

Figure 3.10 Load against Deflection Curves of Node 19

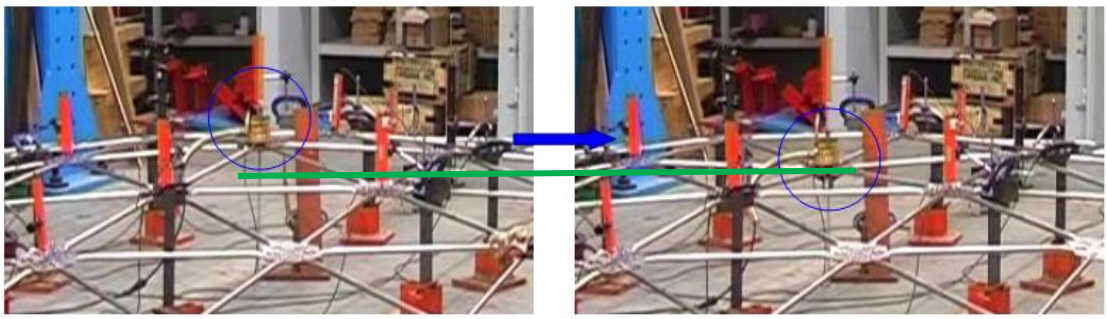

Figure 3.11 Snap-through Buckling at Node 19

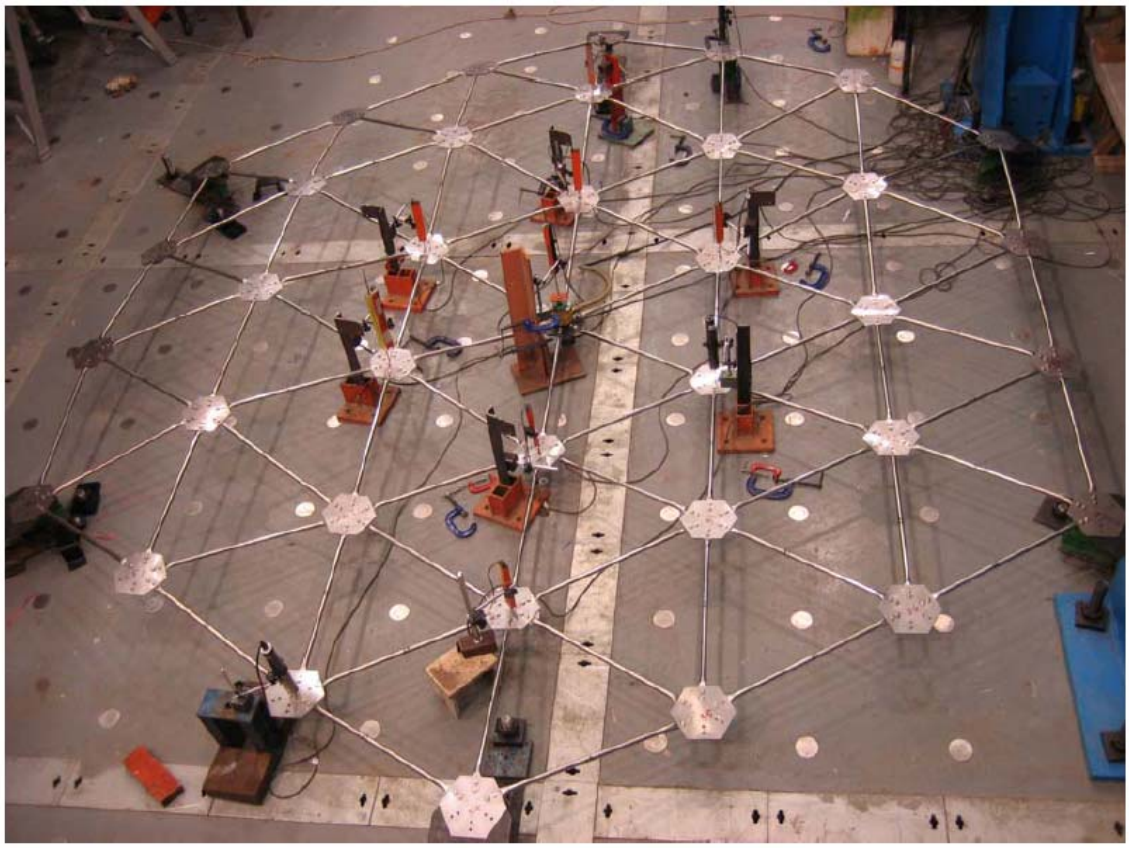

Figure 3.12 Final Deformed Shape of the Dome

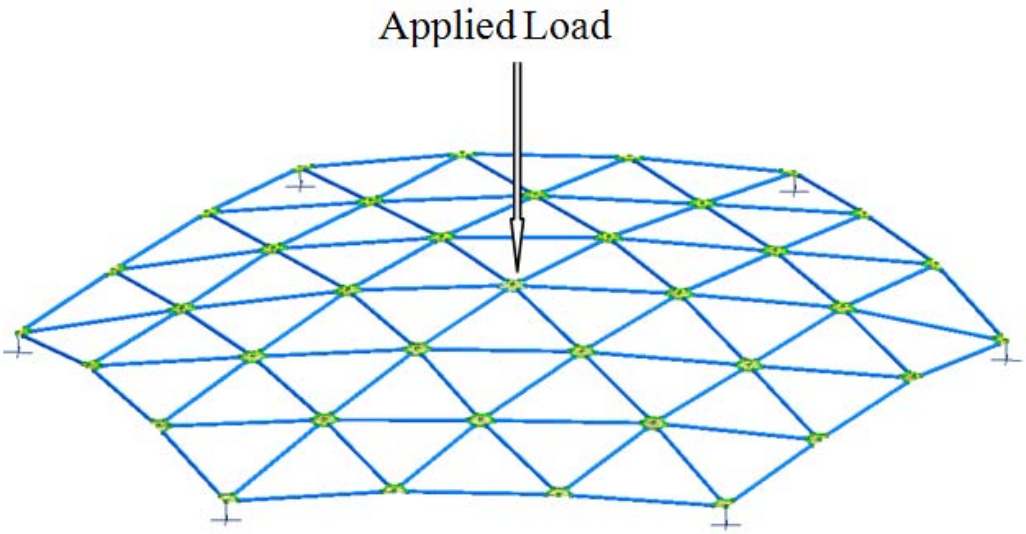

Figure 3.13 Analysis Model of the Dome

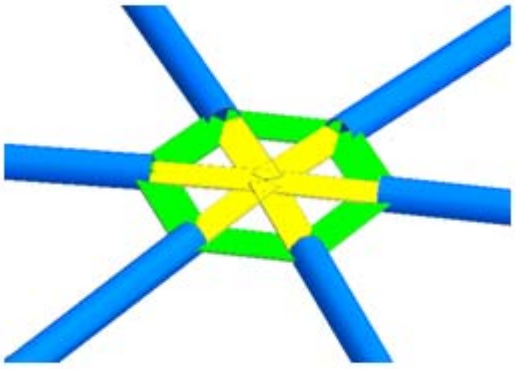

Figure 3.14 Modeling of the Connection

Table

Table 3.1 Nodal Coordinates of the Tested Shallow Dome

Node No.	X (mm)	Y (mm)	Z (mm)	Node No.	X (mm)	Y (mm)	Z (mm)
1	-1190	2060	250	20	790	10	490
2	-390	2060	302	21	1590	10	385
3	400	2070	316	22	2380	20	256
4	1210	2050	248	23	-1970	-700	354
5	-1580	1370	307	24	-1200	-690	418
6	-790	1380	391	25	-400	-690	482
7	40	1380	398	26	400	-680	479
8	790	1380	393	27	1210	-670	416
9	1590	1390	356	28	1980	-660	301
10	-1980	690	347	29	-1570	-1370	330
11	-1190	690	405	30	-790	-1360	378
12	-390	700	473	31	10	-1370	411
13	400	700	479	32	800	-1360	375
14	1190	700	432	33	1590	-1360	311
15	1980	700	375	34	-1170	-2050	256
16	-2360	0	253	35	-380	-2060	324
17	-1580	0	419	36	420	-2060	334
18	-800	0	484	37	1200	-2040	263
19	0	0	520				

CHAPTER 4

FIRST-ORDER AND SECOND-ORDER ANALYSIS FOR DESIGN OF ANGLE TRUSSES

4.1 Introduction

As discussed in the introduction of this thesis, the objective of this research project is to investigate the application of second-order analysis to design of unconventional structures not comfortably designed by the traditional effective length method of design. This chapter is about a new application of the second-order analysis to design of trusses made of angle sections.

The first-order analysis and design method provided in design codes with different design formulae for design of steel structures has been used for many decades. In this traditional design method, the member forces and moments are calculated first by the linear analysis which ignores the nonlinear effects such as the initial imperfection, P-Δ and P-δ effects, and then some factors are used to amplify the linear moments and reduce the section capacity. For some light weight steel members like angles, it is normally used as the web members of trusses and bracing members or main legs of tower cranes and transmission towers. The design process

of these angle members is more complicated due to the monosymmetric or asymmetric property when compared with design of members of doubly symmetric section. Inaccurate estimation on the capacity of angle members would result in inconsistent factors of safety among its members and finally to an unsafe and uneconomical design with some members over-designed and others under-designed. Several steel codes such as AISC (2010), BS5950 (2000), CoPHK (2005) and Eurocode 3 (2005) are applicable to design of the single angle members with different end conditions by using either the simplification method modifying the slenderness ratio or interaction equations to take the effect of eccentricity and different end conditions into account. The detailed design methods in these design codes used for steel structures and particularly for angle members are given in this chapter.

First-order analysis and design method includes nonlinear effects in design, this method is not only inconvenient to determine these factors but also inaccurate as the true behaviors of structures cannot be reflected in analysis. The use of first-order analysis and design method also becomes inappropriate in some scenarios including the case when loads are along the member length affecting the buckling strength but not the effective length factor, and the effect of eccentric connections affecting the buckling resistance in a nonlinear analysis but not the effective length factor in the linear analysis. As an alternative, the second-order analysis and design method is proposed in this chapter as an advanced tool for design of steel structures to include nonlinear effects such as the P-δ and P-Δ moments in analysis directly. As these nonlinear effects are included in analysis, the complicated and sometimes irrational design process using the effective length can be eliminated. The inclusions of the

local and global imperfections precisely and in a simple manner are essential and important for the success of the second-order analysis used in the industry. The resistance of the structures may be overestimated with dangerous design resulted, if the imperfections are ignored in analysis and this is demonstrated in section 4.3.3. It must be emphasized that imperfections are essential for the validity of the proposed second-order analysis otherwise the code results cannot be reproduced by the second-order analysis for some benchmark examples such as the one by Machowski and Tylek (2008). In this chapter, the use of second-order analysis and design method for single angle members is proposed, and the effects due to different end conditions and eccentricity can also be considered directly in analysis instead of using the irrational and complicated slenderness modification equation. Furthermore, the effect of connecting the angle members on the same side or on the alternate sides of truss can be simulated and considered directly in the analysis which is beyond the scope of many design codes. In order to verify the accuracy of the proposed method, the predicted resistances of single angle columns by proposed method are compared with the test results.

The failure loads of angle members used as web members of truss with single and doubled bolted connections connected on the same side and opposite sides are predicted according to the design methods in AISC (2010), BS5950 (2000), CoPHK (2005) and Eurocode 3 (2005) and the proposed method. The results from different design methods are also compared with test results so as to scrutinize their reliability and accuracy in prediction of failure loads of angle members under different end conditions.

4.2 First-order Linear Analysis and Design Method for Angle Members

The conventional design method is based on the first-order linear theory with the use of effective length to consider buckling effect. The member forces and moments are first calculated by the linear analysis, and the design formulae in codes are then employed to check the buckling strength of each member individually by applying the effective length factor (i.e. the K-factor). The member would be considered safe if the resistance of every member is larger than its external force. The reliability of this design method depends highly on the accuracy of the estimated effective length factor. However, the ideal and simple end conditions like pin and rigid ends are unrealistic in practical structures and therefore the determination of the effective length depends heavily on the experience of the engineer. Discrepancies and controversy among designers will appear when different assumed effective length factors are used.

The first-order linear analysis ignores the nonlinear effects such as P-Δ and P-δ effects in analysis process, and uses factors to amplify the linear moments and reduce the axial capacity to compensate these effects. For example, AISC (2010) uses the factor B_1 which is employed to include the moment due to the P-δ effect, and B_2 which is used to consider the moment due to the P-Δ effect. BS5950 (2000) and CoPHK (2005) use the factor of $\frac{\lambda_{cr}}{\lambda_{cr}-1}$, in which λ_{cr} is the elastic critical load factor, to amplify the moment so as to include the sway effect. For analysis and

design of light-weight steel members like angles, the cross-sectional property is monosymmetric or asymmetric instead of doubly symmetric, which further complicates the design process. In many design codes, the effects due to end fixity and end eccentricity are implicitly included by modifying the slenderness ratio and thus the compressive strength, and the effective length factors under different conditions are calculated from the slenderness modification equations. The design codes like AISC (2010) and Eurocode 3 (2005) do not provide the simplified method for design of angle members with single bolted connection, hence the interaction equations should be used to consider the combined effect due to axial force and bending moments arise from end fixity and eccentricity of the angle members. These interaction equations are mostly derived on the basis of doubly symmetric sections, and the moment ratios in these formulae are evaluated for the case of maximum stresses about each principal axis. For doubly symmetric sections, the most critical location for maximum moments about two principal axes occurs at one of the four corners. However, for monosymmetric and asymmetric angle sections, the points having maximum bending stress about the two principal x- and y-axes may not be coincident and it depends on the load location. Hence, the interaction equations may underestimate considerably the loading resistance of angle sections.

The first-order analysis and design methods in some commonly used design codes such as AISC (2010), BS5950 (2000), CoPHK (2005) and Eurocode 3 (2005) for angle sections under different end conditions are introduced below. The difference on the web members connected at the same side and alternate sides cannot be reflected in these design codes.

4.2.1 AISC

AISC (2010) provides a simplified method to determine the compressive strength of single angle members by using the slenderness modification formulae when the members are evaluated as axially compressed members. The following conditions should be fulfilled for using this simplified method.

(1) Members are loaded at their ends in compression through the same leg;

(2) Members are connected by welding or by minimum two-bolt connections; and

(3) There are no intermediate transverse loads.

For different length to radius of gyration ratio ($\frac{L}{r_x}$), there are two formulae provided to modify the slenderness ratio as,

For $0 \le \frac{L}{r_x} \le 80$ $\qquad \frac{KL}{r_g} = 72 + 0.75\frac{L}{r_x}$ (4.2.1)

For $\frac{L}{r_x} > 80$ $\qquad \frac{KL}{r_g} = 32 + 1.25\frac{L}{r_x} \le 200$ (4.2.2)

where L is the length of member between centre of intersection lines at chord of truss, K is the effective length factor, r_x is the radius of gyration about geometric axis parallel to the connected leg and r_g is the governing radius of gyration.

The flexural buckling stress, f_{cr}, can then be determined as,

For $\frac{KL}{r_g} \le 4.71\sqrt{\frac{E_s}{f_y}}$ $\quad f_{cr} = \left[0.658^{\frac{f_y}{p_{cr}}} \right] f_y$ (4.2.3)

For $\frac{KL}{r_g} > 4.71\sqrt{\frac{E_s}{f_y}}$ $\quad f_{cr} = 0.877 p_{cr}$ (4.2.4)

where E_s is the Modulus of elasticity of steel, f_{yd} is the design strength of steel and and p_{cr} is the elastic critical buckling stress as,

$$p_{cr} = \frac{\pi^2 E_s}{\left(\frac{KL}{r_g} \right)^2} \tag{4.2.5}$$

The nominal compressive strength can be obtained from the flexural buckling stress and section area as,

$$P_n = f_{cr} A_g \tag{4.2.6}$$

where A_g is the gross cross-sectional area.

The design compressive strength can then be determined by multiplying the resistance factor, ϕ_c, to the nominal compressive strength as,

$$P_{cd} = \phi_c P_n \tag{4.2.7}$$

For single bolted connection angle sections, this simplified method is not applicable. The appropriate interaction equations of Eqs. (4.2.8) and (4.2.9) from the code are used and they combine the effect due to the axial force and bending moments.

For $\frac{P}{P_{cd}} \ge 0.2$ $\quad \frac{P}{P_{cd}} + \frac{8}{9}\left(\frac{M_x}{M_{cx}} + \frac{M_y}{M_{cy}}\right) \le 1.0$ (4.2.8)

For $\frac{P}{P_{cd}} < 0.2$ $\qquad \frac{P}{2P_{cd}} + (\frac{M_x}{M_{cx}} + \frac{M_y}{M_{cy}}) \le 1.0$ (4.2.9)

where P is the applied axial compressive strength, M_x, M_y, M_{cx} and M_{cy} are the applied and available flexural strength for major and minor axes respectively.

4.2.2 BS5950

In BS5950 (2000), a simplified method is given to compute the compressive strength of single angle members. The members can be treated as axially loaded members with reduced compressive strength and ignorance of eccentricity at end connections, provided that the following conditions are satisfied.

a) For connections composed of two or more bolts in standard clearance holes in line along the angle, or by an equivalent welded connection, the slenderness ratio λ is taken as the greater of:

1) $0.85\lambda_v$ but $\ge 0.7\lambda_v + 15$ (4.2.10)

2) $1.0\lambda_{x,y}$ but $\ge 0.7\lambda_{x,y} + 30$ (4.2.11)

b) For single bolted connection, the compressive resistance is taken as 80 % of the compressive resistance of an axially loaded member and the slenderness ratio λ is taken as the greater of:

1) $1.0\lambda_v$ but $\ge 0.7\lambda_v + 15$ (4.2.12)

2) $1.0\lambda_{x,y}$ but $\ge 0.7\lambda_{x,y} + 30$ (4.2.13)

where λ_v and $\lambda_{x,y}$ are the slenderness ratios of the segment about the v axis and x,y axes respectively.

The compressive strength of the angle can then be obtained as follows:

$$p_c = \frac{p_{cr} f_y}{\phi + \left(\phi^2 - p_E f_y\right)^{0.5}} \tag{4.2.14}$$

where

$$\phi = \frac{f_{yd} + (\eta + 1) p_{cr}}{2} \tag{4.2.15}$$

$$p_{cr} = \left(\frac{\pi^2 E_s}{\lambda^2} \right) \tag{4.2.16}$$

where λ is the slenderness ratio determined in Eqs. (4.2.10) to (4.2.13) under different conditions. η is the Perry factor which can be obtained according to different Robertson constants.

The compressive resistance of angle members can be calculated as,

$$P_{cd} = A_g p_c \tag{4.2.17}$$

4.2.3 CoPHK

The design method in CoPHK (2005) is based on the design principle in both Eurocode 3 (2005) and BS5950 (2000), and can be used for design of angle sections which are connected eccentrically with different degrees of connection stiffness. For angle sections connected by two or more bolts, the slenderness ratio is calculated

from the larger of the actual member length, and the effective slenderness ratio $\overline{\lambda}_{eff}$ is taken as follows.

For buckling about minor v axis,

$$\overline{\lambda}_{eff,v} = 0.35 + \frac{0.7\lambda_v}{93.9\varepsilon} \tag{4.2.18}$$

For buckling about x axis,

$$\overline{\lambda}_{eff,x} = 0.5 + \frac{0.7\lambda_x}{93.9\varepsilon} \tag{4.2.19}$$

And the slenderness ratio λ is

$$\lambda = \overline{\lambda}_{eff}\sqrt{\frac{\pi^2 E}{f_y}} \tag{4.2.20}$$

and

$$\varepsilon = \sqrt{\frac{275}{f_{yd}}} \tag{4.2.21}$$

where λ_v and λ_x are respectively the slenderness ratios about minor v axis and the x axis parallel to the two legs.

The compressive resistance of single angle members can be determined by using the same formulae in Eqs. (4.2.14) to (4.2.17) with different slenderness ratio computed in Eqs. (4.2.18) and (4.2.19).

For a single bolted connection, 80% of the compressive resistance of the double bolted connection is used as the resistance of angle members with single bolted connection.

4.2.4 Eurocode 3

For design of the angles as web members in compression, Eurocode 3 (2005) also provides simplified formulae to calculate the effective slenderness ratio. The end fixity can be allowed for in the design of angle and the eccentricity can be neglected under the condition that the appropriate end restrained is supplied by chords to web member with appropriate end fixity as welded connections or connected by at least 2 bolts. The effective slenderness ratio is taken as the greater of:

a) For buckling about minor v axis

$$\overline{\lambda}_{eff,v} = 0.35 + 0.7\overline{\lambda_v} \tag{4.2.22}$$

b) For buckling about x axis

$$\overline{\lambda}_{eff,x} = 0.50 + 0.7\overline{\lambda}_x \tag{4.2.23}$$

where

$$\overline{\lambda} = \sqrt{\frac{A_g f_{yd}}{P_{cr}}} = \frac{L}{r}\frac{1}{\lambda_1} \qquad \text{for class 1, 2 and 3 cross-sections} \tag{4.2.24}$$

$$\overline{\lambda} = \sqrt{\frac{A_{eff} f_{yd}}{P_{cr}}} = \frac{L}{r}\frac{\sqrt{\frac{A_{eff}}{A_g}}}{\lambda_1} \qquad \text{for class 4 cross-sections} \tag{4.2.25}$$

and

$$\lambda_1 = \pi\sqrt{\frac{E}{f_{yd}}} = 93.9\varepsilon \tag{4.2.26}$$

$$\varepsilon = \sqrt{\frac{235}{f_{yd}}} \tag{4.2.27}$$

where P_{cr} is the elastic critical force, L is the member length, r is the radius of gyration about the relevant axis, A_{eff} is the effective area of a cross-section.

The buckling reduction factor is calculated as,

$$\chi = \frac{1}{\phi + \sqrt{\phi^2 - \overline{\lambda}_{eff}^{\ 2}}} \tag{4.2.28}$$

where

$$\phi = 0.5\left[1 + \alpha\left(\overline{\lambda}_{eff} - 0.2\right) + \overline{\lambda}_{eff}^{\ 2}\right] \tag{4.2.29}$$

and α is the imperfection factor.

The design buckling resistance of the compressive members is given as follow.

$$P_{cd} = \frac{\chi A_g f_{yd}}{\gamma_{M1}} \qquad \text{for class 1, 2 and 3 cross-sections} \tag{4.2.30}$$

$$P_{cd} = \frac{\chi A_{eff} f_{yd}}{\gamma_{M1}} \qquad \text{for class 4 cross-sections} \tag{4.2.31}$$

where γ_{M1} is the partial factor for resistance of members to instability assessed by member check.

The simplified formulae are not applicable to single bolted connection of angle web members. For single bolted connection, the effect of eccentricity should be included by using interaction equations as shown below.

$$\frac{P}{\frac{\chi_x P_{Rk}}{\gamma_{M1}}} + k_{xx}\frac{M_{x,Ed} + \Delta M_{x,Ed}}{\chi_{LT}\frac{M_{x,Rk}}{\gamma_{M1}}} + k_{xy}\frac{M_{y,Ed} + \Delta M_{y,Ed}}{\frac{M_{y,Rk}}{\gamma_{M1}}} \le 1 \tag{4.2.32}$$

$$\frac{P}{\frac{\chi_y P_{Rk}}{\gamma_{M1}}} + k_{yx}\frac{M_{x,Ed} + \Delta M_{x,Ed}}{\chi_{LT}\frac{M_{x,Rk}}{\gamma_{M1}}} + k_{yy}\frac{M_{y,Ed} + \Delta M_{y,Ed}}{\frac{M_{y,Rk}}{\gamma_{M1}}} \le 1 \tag{4.2.33}$$

where P_{Rk} is characteristic value of resistance to compression and $M_{x,Rk}$, $M_{y,Rk}$ are the characteristic values of resistance to bending moments , χ_x, χ_y and χ_{LT} are the reduction factors for flexural buckling and lateral torsional buckling respectively. $\Delta M_{x,Ed}$ and $\Delta M_{y,Ed}$ are the moments due to the shift of the centroidal axes. k_{xx}, k_{yy}, k_{xy}, k_{yx} are the interaction factors.

4.3 Second-order Analysis and Design Method for Angle Members

Second-order analysis and design method has been recommended in many design codes such as AISC (2010), Eurocode 3 (2005) and CoPHK (2005) as an advanced tool for design of steel structures because the interactive effect between the structural members and structural system can be considered. Hence, the actual structural behaviors can be reflected in analysis. In this design method, the nonlinear effects such as the member imperfection and frame imperfection are included in analysis. These nonlinear effects change critically the ultimate load when a member is slender or when the deflection or end rotation is large that the nonlinear effects are significant. The consideration of these nonlinear effects in analysis is important and essential for structures with the estimation of effective length factor (K-factor) no longer required and the complicated process in determination of many factors to compensate for the nonlinear effects is eliminated. And the use of first-order analysis could be non-conservative if these effects are not carefully considered. The idea of local member and global structure imperfections, the importance on inclusion of

these imperfections in analysis, and the use of section capacity check for steel structures are described in the followings.

4.3.1 P-δ and P-Δ effects

The P-δ effect is due to the member bowing in the presence of axial force and the deflection along the member length as instructed in Figure 4.1. It affects the state of stress and the stiffness of the member. As a result, the second-order moment named P-δ moment is induced due to this effect. The importance of this effect increases for buckling analysis and design of slender skeletal structures.

The P-Δ effect is due to the nodal geometrical change of the structure as shown in Figure 4.1. When a structure deforms, the original geometry can no longer be employed for the formulation of the transformation matrix simply because the coordinates of the structures have been changed. When the deflection and/or the conjugate force are large such as the case of a building under a heavy mass at the roof and a lateral wind load, this P-Δ effect becomes important. Hence, the second-order moment named P-Δ moment is induced due to this P-Δ effect.

Both P-δ and P-Δ effects generate the additional nonlinear moments which should be included correctly and rationally in an analysis. This thesis considers both effects in the analysis such that separated member design is not needed.

4.3.2 Local and global imperfections

Perfectly straight members or structures are non-existent and therefore both the local and global imperfections should be included in second-order analysis.

Generally speaking, local imperfection means imperfection for individual members or so-called the member imperfection which is due to combined effects of the initial geometric imperfection and residual stress. For practical design, local imperfection can be considered as an equivalent initial bow imperfection in member. Based on different cross-section types, the different values of initial bow imperfections are specified in different design codes. The method of calculating the imperfection values under various column buckling curves was demonstrated by Chan and Cho (2002) and the imperfection values for different cross-sections for nonlinear analysis of steel structures in CoPHK (2005) are given in Table 4.1 for illustration.

The global imperfection is the imperfection of the whole structures which is resulted from the out of plumbness of frame in the construction. The imperfection in the structures may increase the sway effect and induce the P-Δ moment. In second-order analysis, the global imperfection can be included by a reliable and convenient method of using the elastic buckling mode as the imperfection mode with an amplitude set equal to the out-of-plumbness normally taken as height/200 or other justified values. The inclusion of global imperfection is important in second-order analysis as its ignorance may overestimate the resistance of the structures and leads to dangerous design as demonstrated below.

4.3.3 The importance of consideration the global imperfection in second-order analysis

Failure load of dome is especially sensitive to the global imperfections (See and McConnel 1986; Morris 1991; Zhao et al. 1993; Kim et al. 1997). Therefore, the behavior and snap-through buckling load of two shallow domes are studied by using second-order analysis with one dome ignores the global imperfection as a case of perfect dome while another dome includes the global imperfection as imperfect dome in the analysis to demonstrate the influence of the resistance of the dome against global imperfection. The domes consist of 1024 members of rectangular hollow section with 40mm in width, 60mm in depth and 4mm in thickness as shown in Figure 4.2. The domes are assumed to be pin-supported at all corner nodes and the loads are applied to all nodes. The local member initial imperfection of *L*/500 is assigned to all members in both domes.

The deformed shapes of the perfect and imperfect domes are given in Figures 4.3a and 4.3b respectively. For the perfect dome, when the applied load increases gradually, the dome deforms symmetrically with the largest vertical deflection occurs at the centre. The snap-through buckling load is 39.5kN. When the global imperfection is considered as the first elastic buckling mode, the dome deforms asymmetrically as shown in Figure 4.3b. The node with maximum vertical movement shifts away from the centre to node 284 as shown in Figure 4.3b. Because the symmetrical geometric property of the dome no longer exists, the resistance of the dome against snap-through buckling is greatly reduced. The snap-through buckling load drops to 15.5kN which is 60.8% lower than the prefer dome. The load-

deflection curves of the largest vertical movement nodes for perfect dome (node 513) and imperfect dome (node 284) are compared in Figure 4.4. The discrepancy in capacity of the prefect and imperfect domes indicates the necessary of considering global imperfection in second-order analysis in dome as well as the other structures for a reliable and safe design.

4.3.4 Section capacity check

Second-order analysis and design method considers the change of the geometry and member stiffness due to the present of force and load in analysis, so that the effective length is not required to be assumed. In second-order analysis, the individual member check is replaced by the section capacity check as follows.

$$\frac{P}{A_g p_{yd}} + \frac{M_x + P(\delta_x + \Delta_x)}{M_{cx}} + \frac{M_y + P(\delta_y + \Delta_y)}{M_{cy}} = \phi_{SCF} \leq 1 \tag{4.3.1}$$

in which p_{yd} is the design strength of the member, P is the axial force in the member, A_g is the cross-sectional area, M_x and M_y are the first-order moments about the x and y axes, M_{cx} and M_{cy} are the moment capacities about the x and y axes, and ϕ_{SCF} is the section capacity factor. $P(\delta_x+\Delta_x)$ and $P(\delta_y+\Delta_y)$ are the second-order moments about the x and y axes of which the consideration allows one to include automatically the bending effect due to axial force and second-order deflections. Therefore, the use of effective length is not required as the P-Δ and P-δ effects have been included in the Eq. (4.3.1) for section capacity check. Moreover, the initial imperfection is also included in analysis so that the Perry-Robertson formula for imperfect columns can be directly applied in this integrated analysis and design procedure.

4.3.5 Simulation of the end conditions for angle members

Different end conditions for angle such as single bolted and double bolted connections as shown in Figure 4.5 provide various rotation spring stiffness. The end conditions of the angle members can be simulated by inserting rotational spring elements to the two ends of the members as demonstrated by Cho and Chan (2005). The properties of gusset plate are used to determine the rotation spring stiffness of double bolted connection. For single bolted connection, the spring stiffness is zero as the connection joints are allowed to rotate freely. The magnitude and direction of end moments due to the load eccentricities can be modeled by a rigid arm joining the centroid of gusset plate and the point of load application.

4.3.5.1 Connection spring

The stiffness of a rotational spring in a double bolted connection can be calculated as,

$$S_c = \frac{GA_{shear}d_{bolt}^2}{l_{bolt}} \tag{4.3.2}$$

where d_{bolt} is the distance between the centroids of the two bolts; l_{bolt} is the length of the bolt shank; G is the shear modulus of elasticity. A_{shear} is the shear area which can be taken as 0.9 of the cross-sectional area recommended in design codes like the CoPHK (2005). As the connections are dominantly under axial force with small moment, only the linear portion of the nonlinear moment-rotation curve of connections can be used that the connection stiffness is assumed linear in Eq. (4.3.2).

To account for the rotational stiffness of the spring element in the analysis, the tangent stiffness matrix is used to determine the incremental displacement. Consider the equilibrium of moment at internal and external nodes as shown in Figure 4.6, the equilibrium condition at two ends of a joint is given by,

$$M_s + M_r = 0 \tag{4.3.3}$$

and

$$M_s = S_c(\theta_s - \theta_r) \tag{4.3.4}$$

$$M_r = S_c(\theta_r - \theta_s) \tag{4.3.5}$$

where S_c is the stiffness of the connection, M_s and M_r are the external and internal moments at two ends of a connection, θ_s and θ_r are the conjugate rotations for the moments M_s and M_r.

Re-arranging Eqs. (4.3.4) and (4.3.5) to an incremental form, the following expression can be obtained,

$$\begin{pmatrix} \Delta M_s \\ \Delta M_r \end{pmatrix} = \begin{bmatrix} S_c & -S_c \\ -S_c & S_c \end{bmatrix} \begin{pmatrix} \Delta\theta_s \\ \Delta\theta_r \end{pmatrix} \tag{4.3.6}$$

where ΔM_s and ΔM_r are the incremental external and internal moments at two ends of a connection. The external node refers to the one connected to the global node and the internal node is joined to the angle element, $\Delta\theta_s$ and $\Delta\theta_r$ are the conjugate incremental nodal rotations to these moments.

The basic equations for incorporating the end connection stiffness are considered both in the tangent and the secant stiffness matrix equations.

4.3.5.2 Tangent stiffness matrix with combination of connection spring

The incremental displacements corresponding to the incremental forces are solved and the basic element stiffness is modified by addition of the element stiffness to the connection spring, which is modeled as a dimensionless spring element in analysis as,

$$\begin{pmatrix} \Delta M_{s1} \\ \Delta M_{r1} \\ \Delta M_{r2} \\ \Delta M_{s2} \end{pmatrix} = \begin{bmatrix} S_{c1} & -S_{c1} & 0 & 0 \\ -S_{c1} & K_{11}+S_{c1} & K_{12} & 0 \\ 0 & K_{21} & K_{22}+S_{c2} & -S_{c2} \\ 0 & 0 & -S_{c2} & S_{c2} \end{bmatrix} \begin{pmatrix} \Delta\theta_{s1} \\ \Delta\theta_{r1} \\ \Delta\theta_{r2} \\ \Delta\theta_{s2} \end{pmatrix} \tag{4.3.7}$$

External load is applied or transformed to the global nodes only, and both the ΔM_{s1} and ΔM_{r1} are therefore equal to zero. Hence, the incremental rotations at the internal nodes can be expressed as,

$$\begin{pmatrix} \Delta\theta_{r1} \\ \Delta\theta_{r2} \end{pmatrix} = \begin{bmatrix} S_{c1}+k_{11} & K_{12} \\ K_{21} & S_{c2}+K_{22} \end{bmatrix}^{-1} \begin{bmatrix} S_{c1} & 0 \\ 0 & S_{c2} \end{bmatrix} \begin{pmatrix} \Delta\theta_{s1} \\ \Delta\theta_{s2} \end{pmatrix} \tag{4.3.8}$$

Substituting Eq. (4.3.8) into Eq. (4.3.7) to eliminate $\Delta\theta_i$ in Eq. (4.3.7), the following expression can be obtained,

$$\begin{pmatrix} \Delta M_{s1} \\ \Delta M_{s2} \end{pmatrix} = \left(\begin{bmatrix} S_{c1} & 0 \\ 0 & S_{c2} \end{bmatrix} - \frac{\begin{bmatrix} S_{c1} & 0 \\ 0 & S_{c2} \end{bmatrix} \begin{bmatrix} S_{c2}+K_{22} & -K_{12} \\ -K_{21} & S_{c1}+K_{11} \end{bmatrix} \begin{bmatrix} S_{c1} & 0 \\ 0 & S_{c2} \end{bmatrix}}{(S_{c1}+K_{11})(S_{c2}+K_{22})-K_{12}K_{21}} \right) \times \begin{pmatrix} \Delta\theta_{1s} \\ \Delta\theta_{2s} \end{pmatrix} \tag{4.3.9}$$

where S_{c1} and S_{c2} are the spring stiffness for simulation of semi-rigid connections at ends; K_{ij} are the stiffness coefficients of the element; $\Delta\theta_{s1}$, $\Delta\theta_{r1}$, $\Delta\theta_{s2}$ and $\Delta\theta_{r2}$ are respectively the incremental rotations at the two ends of an element.

Assembling the element matrix, the global stiffness matrix for the angle frame and truss is formed. The incremental displacement vector is solved and added to the last displacement for determination of member resistance which is then assembled to obtain the frame resistance by a standard finite element procedure.

4.3.6 Verification of second-order analysis and design method on single angle struts

To verify the accuracy of the proposed second-order analysis and design method on single angle members, a comparison on the resistances of the members between the laboratory test results and proposed method is conducted. Trahair et al. (1969) tested single angle columns under eccentric load with the slenderness ratios from 60 to 200 which cover the common range of angle struts in practice. The legs of the test specimens were welded to the stem of the structure tee to simulate the chord of the truss. The load was applied through the centre of the stem of the structural tee to induce an eccentricity. The specimens were tested under three different end conditions. In end condition (a), a fixed end was assumed that the testing machine head and base connected to the outside face of the flange of the structural tees directly. In end condition (b), only the rotation along the direction of the outstanding leg was allowed. Similar to condition (b), the plane in end condition (c) was allowed to rotate along the connected leg of the angle.

In the test, equal angles with section 50.8 × 50.8 × 6.35 mm with ASTM A242 steel were used. The test results from Series A are compared with the predicted results by the proposed method with the inclusion of the member initial imperfection according

to the code requirement so as to verify the accuracy of the proposed method. A good agreement between the test and the predicted results can be obtained as shown Table 4.2 with the second-order analysis method being more conservative generally. The average ratios of the test to predicted results are 1.04, 1.05 and 1.02 with standard deviations of 0.05, 0.09 and 0.06 for End condition A, End condition B and End condition C respectively. The comparison on the capacities of angle members implies the accuracy and efficiency of the proposed method in analysis and design of angle member and the discrepancy between the predicted results of stocky columns and the test results are still considered as well acceptable for engineering applications.

4.4 Experimental Investigation on Angle Trusses

The accuracy of the second-order analysis and design method in single angle members has been verified above. However, the use of isolated member is uncommon in practice and hence, the verification on the accuracy of first-order analysis and design method according to the design codes and the proposed second-order analysis and design method on angle trusses is further carried out below.

4.4.1 Test setup

Four single angle struts were tested as web members of two plane trusses by Chan and Cho (2008) and shown with dimensions and support condition in Figure 4.7. The members with length of two meters were used and the material properties of the

specimens are given in Table 4.3. Four tested single angle members were divided into two sets (Trusses 1 and 2) with two variables including web arrangements and end conditions. In Truss 1, the web members were connected to the chords on the same side, while in Truss 2 the web members were connected to the chord members on the alternative sides. The different end conditions of each specimen and the dimensions of gusset plate, which were used to connect the members at each end, are summarized in Table 4.4. Point load was applied to the upper joint of the target failure member and the out-of-plane bucking at connecting node between chords and webs was fully restrained. The target member, chosen as the compression web under applied point load and closer to the left end support, was purposely designed to fail first.

4.4.2 Test result

The failure loads of all specimens are presented in Table 4.5. The design strength of the angle members was controlled by the resistance to the flexural buckling about the principal minor axis. The single and double bolted connections were most likely to be treated as perfectly pinned and partially restrained at ends. The results represent that the failure loads of specimens with double bolted end connection are 17% to 25% higher than corresponding specimens with single bolted end connection. The load resistances of the specimens with web members on the same side are 9% to 17% higher than the specimens with web members on alternate sides under the same end conditions. Therefore, the test results indicate that double bolted connection can provide greater end fixity, which gives a more beneficial effect to the compressive resistance of the angle members than single bolted connection. Moreover, the test

results also show that the web members connected on the same side are able to take a considerably greater load than the web members connected on alternate sides, since the trusses with web members connected on alternate sides contain a larger eccentric moment at ends of the webs which reduces considerably the buckling strength.

4.5 Comparisons on Different Design Methods

The predicted results based on the codified method including AISC (2010), BS5950 (2000), CoPHK (2005) and Eurocode 4 (2004) and second-order analysis and design method are compared with the test results of the angle trusses to verify the accuracy of different design methods.

4.5.1 First-order analysis and design method

The predicted results according to different design codes are compared with test results and given in Table 4.6. The findings show that AISC (2010) gives an over-conservative estimation on failure loads with the differences of 49% and 68%, 52% and 58% for single and double bolted connections respectively. BS5950 (2000) gives an over-conservative prediction on failure loads of single bolted connection with the differences of 46% and 62%, and a more reasonable conservative prediction is obtained on double bolted connection with the differences of 10% and 14%. CoPHK (2005) gives an economical design in the angle sections as the predicted failure loads are close to the actual failure loads, and the differences are 3% and 21% for single bolted connection with the same and alternate sides arrangement of web, and the

differences become 2% and 13% for double bolted connection with web members on the same and opposite sides. The predicted capacities from Eurocode 3 (2005) are only about half of the test results in single bolt connection, and it shows that the highly conservative interaction equations have been used for single bolted connection in Eurocode 3 (2005). However, a reasonably safe prediction for double bolted connection is provided in Eurocode 3 (2005) with nearly 20% difference between two sets of results.

4.5.2 Second-order analysis and design method

The analysis model of the trusses is shown in Figure 4.8, and the failure loads predicted by second-order analysis and design method with three imperfection values are compared in Table 4.7. In present method, both the end moments and end rotational restraints can be considered and included in analysis. The rotational stiffness "*k*" is assumed as 100kNm/radian by taking 10% of the flexural stiffness of the bolts. For angle members connected by single bolt, the members are released at the end; for angle members connected by double bolts, the rotational stiffness is inserted into two ends of members. The capacities of the angle members based on three initial imperfection values are calculated. The first initial imperfection is taken as *L*/360, in which *L* is the length of the member, and the imperfection of *L*/360 is based on a calibration exercise between the second-order analysis and the buckling curve used in the CoPHK (2005). The second initial imperfection is assumed to be *L*/300 which is provided in CoPHK (2005) as shown in Table 4.1. The third initial imperfection is conservatively taken as *L*/200 as given in Eurocode 3 (2005). However, a more precise value of initial imperfection can be back-calculated from

the formulae for the buckling curves given in Eurocode 3 (2005) using the appropriate section modulus. The same and alternate side arrangements of web members are simulated in the analysis model as shown in Figure 4.9. For same side arrangement, the web members are first connected to a rigid bar to simulate the eccentricity and then the rigid bar is connected to the chord member. For alternate side arrangement, the web members are connected to the rigid bars in different sides. The effect due to different arrangements of web members can be reflected in the predicted members capacities that the first set of specimens are higher than the second set for both single and double bolted connections. The differences between the test and predicted results in single bolted connection are 6% and 12% for imperfection equal to L/360, 8% and 15% for imperfection equal to L/300, and 14% and 25% for imperfection equal to L/200. The differences in double bolted connection are 1% for imperfection equal to L/360, 3% and 4% for imperfection equal to L/300, and 7% and 13% for imperfection equal to L/200. The results indicate that both the CoPHK (2005) and Eurocode 3 (2005) recommended initial imperfection values are conservative for single angle members in second-order analysis. The use of imperfection of L/360 gives a close prediction on the failure loads for both single and double bolted connections compared with the other design methods.

4.5.3 Comments on studied design methods

All design codes give a safe design on single angle members, and the differences on the failure loads between the test and design methods are summarized in Tables 4.8 and 4.9. The discrepancy between the same and alternate side arrangements of the

web members cannot be reflected in all studied design codes. For angle members with single bolted connection, the ratios of the predicted and tested failure loads in descending order are Eurocode 3 (2005), AISC (2010), BS5950 (2000), CoPHK (2005) and second-order analysis method. It appears that the interaction equations for single bolted angle members in Eurocode 3 (2005) and AISC (2010) are too conservative as the difference is nearly 70%. A large difference in BS5950 (2000) also means that the slenderness modification equations are too conservative for slender angle members. CoPHK (2005) gives the closest results when compared with the other codes and this implies taking 80% of the axial force compressive resistance of the double bolted connection as the compressive resistance of single bolt connection seems to be more reasonable.

For double bolted connection, the differences between the tested and predicted results arranged in descending order are AISC (2010), Eurocode 3 (2005), BS5950 (2000), CoPHK (2005) and second-order analysis method. The results show that the modification equations for slenderness ratio in AISC (2010) are over-conservative for double bolted compressive members. CoPHK (2005), BS5950 (2000) and Eurocode 3 (2005) give a closer prediction on failure loads. This is due to their provided simplified formulae for slenderness modification and estimation of the effective length being close to the actually buckling length.

The results predicted by the proposed second-order analysis with imperfection of $L/360$ are close to the test results for both single and double bolted connections, since the true behavior of the members is simulated and reflected. This analysis method can include the nonlinear large deflection and buckling effect, imperfections

of the members and structures, and the arrangement details of webs and joints in analysis. With the consideration of the rotational stiffness due to the gusset plates, the accuracy of the second-order analysis and design method could be further increased. Furthermore, only one element is used to model a single member which makes the proposed method efficient and simple to use, and the advantage of using only one element per member becomes more significant for mega structures.

4.6 Concluding Remarks

The different codified first-order analysis and design methods including AISC (2010), BS5950 (2000), CoPHK (2005) and Eurocode 3 (2005) for design of steel structures have been discussed in this chapter. The specific design requirements for angle members have been emphasized due to its monosymmetric or asymmetric cross-section property which further complicates the design process. Some codes greatly underestimate the failure loads of the angle members by using the over-simplified and conservative interaction equations which are mostly based on doubly symmetric section. As a result, when used in monosymmetric or asymmetric cross-section like angle section, these interaction equations may underestimate the loading resistance of angle sections. Some codes give a less conservative estimation on the failure loads of angle sections, not only due to the error in effective length method itself which ignores P-δ deflection due to member loads, but the code methods also sensibly rely on the judgment by the designer on the value of the effective length factor for some non-typical structural forms and connections. Moreover, the method

cannot rationally consider the effect of end moments on members connected on the same and on the alternate sides of webs of a truss.

Due to the complicity and inaccuracy on using the first-order analysis and design method, the second-order analysis and design method has been proposed in this chapter for design of the steel angle members. Both the local and global imperfections and residual stresses are included automatically in the analysis to reflect the structural behaviors. Therefore, the estimation of the effective length and factors to compensate for the nonlinear effects are eliminated. The different behaviors due to the same side and alternate side arrangements of web members and the moments due to the end eccentricity are also included directly in analysis in the proposed method. The comparisons between the test and the analysis results further confirm the validity of the proposed method for practical applications.

Figures

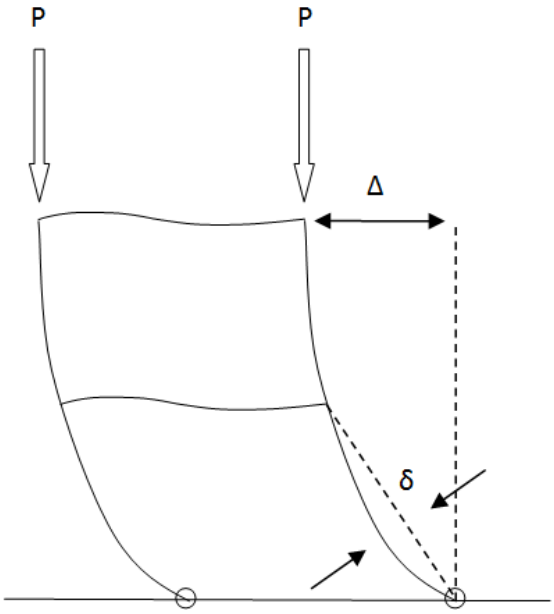

Figure 4.1 P-Δ and P-δ Effects in the Frames

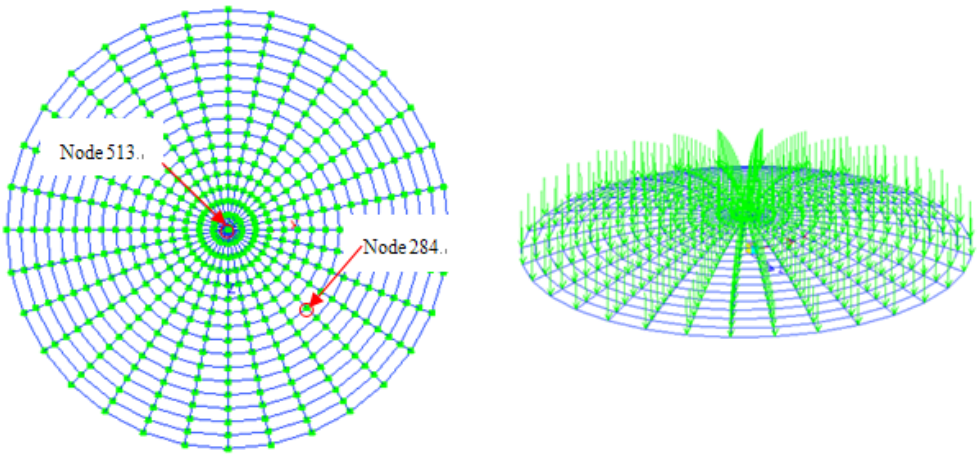

Figure 4.2 Layout of 1024-members Dome

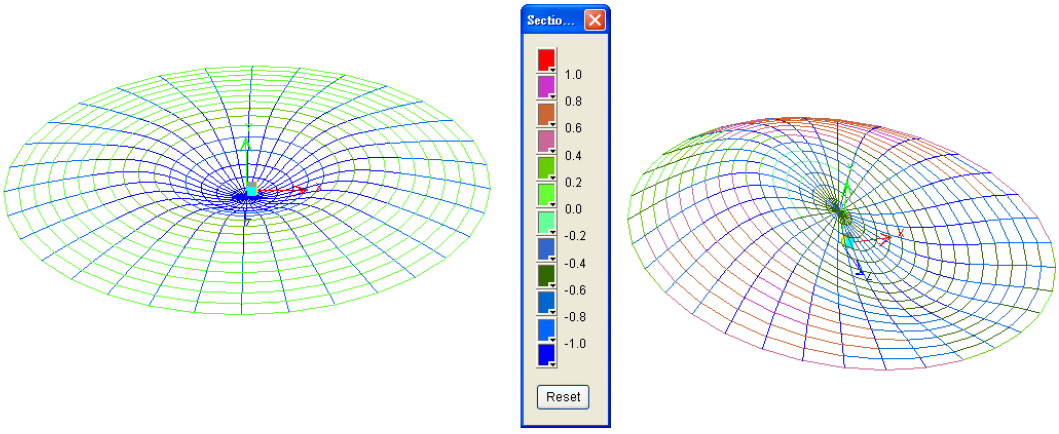

(a) Excluding Global Imperfection (b) Including Global Imperfection

Figure 4.3 Analysis Failure Modes of Perfect and Imperfect Domes

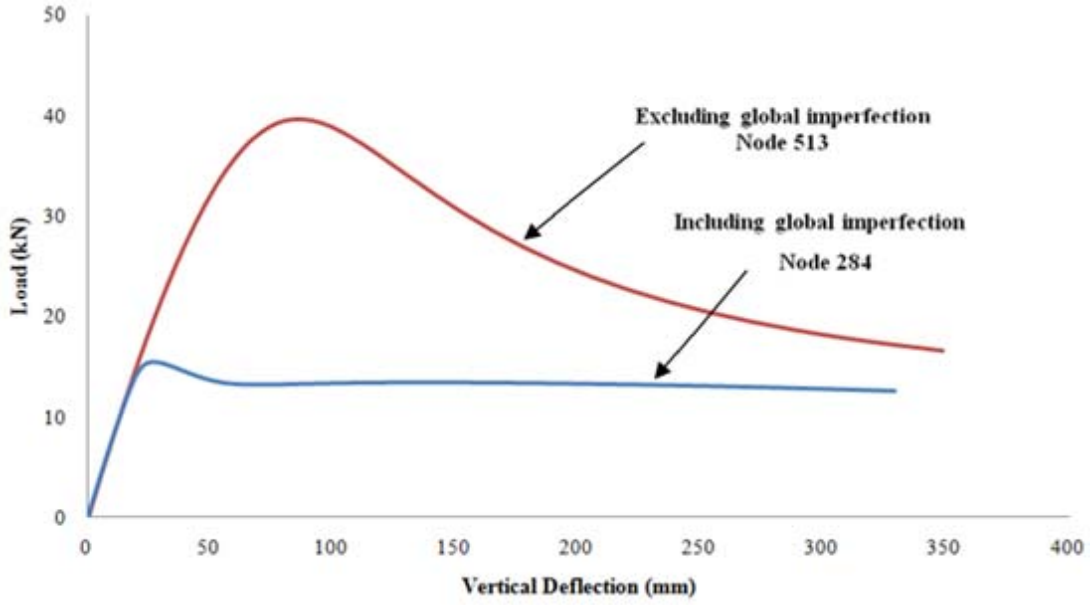

Figure 4.4 Load against Deflection Curves of Perfect and Imperfect Domes

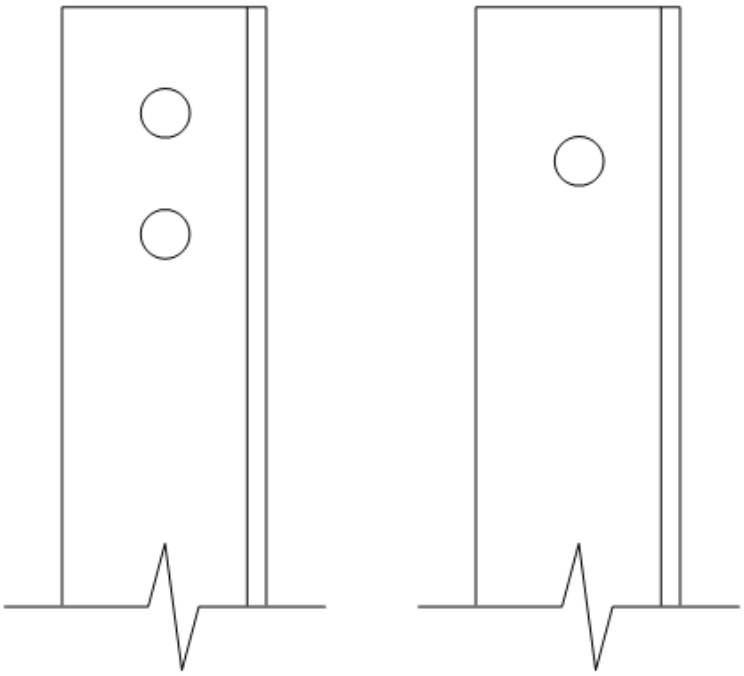

Figure 4.5 Angle with Single and Double Bolted Connections

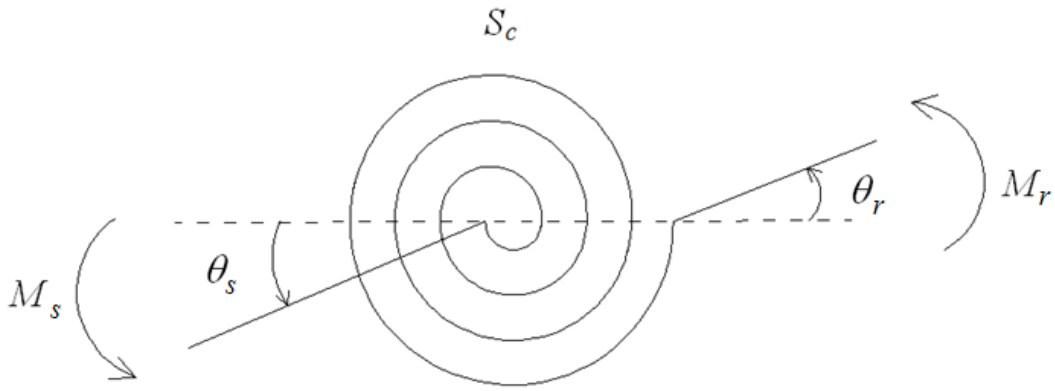

Figure 4.6 Connection Spring Element

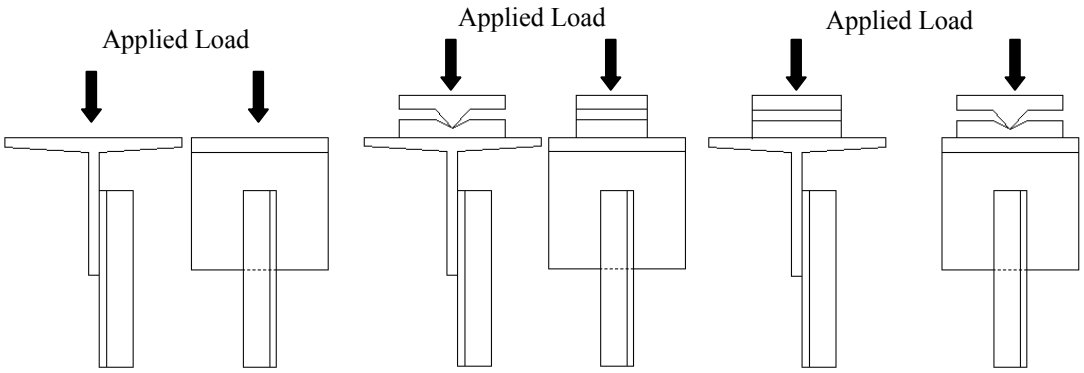

End condition (a) End condition (b) End condition (c)

Figure 4.7 End Conditions on Single Angle Member Tests

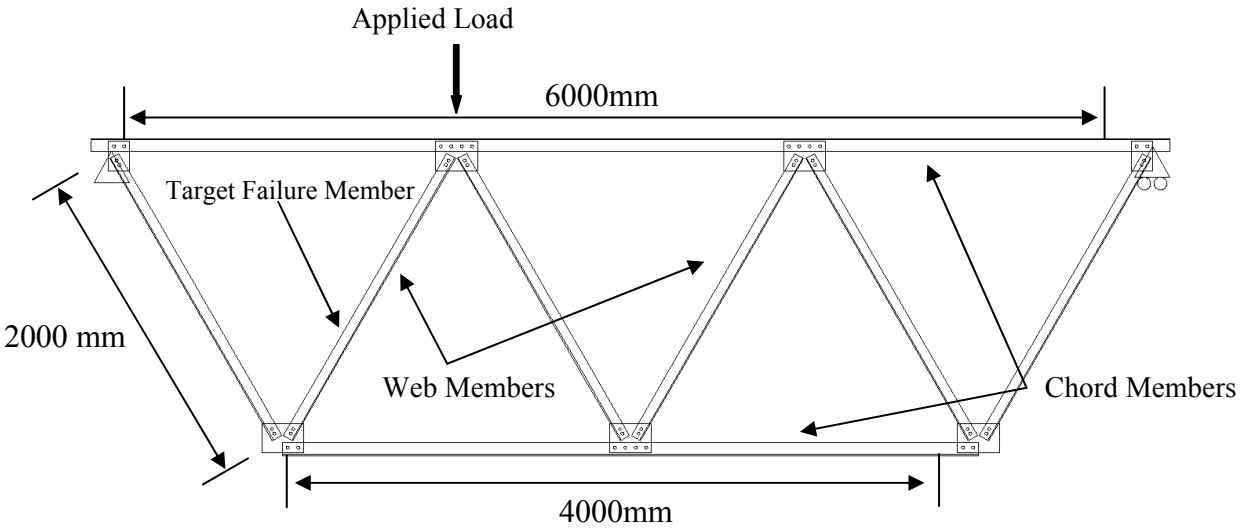

Figure 4.8 Layout of the Angle Trusses

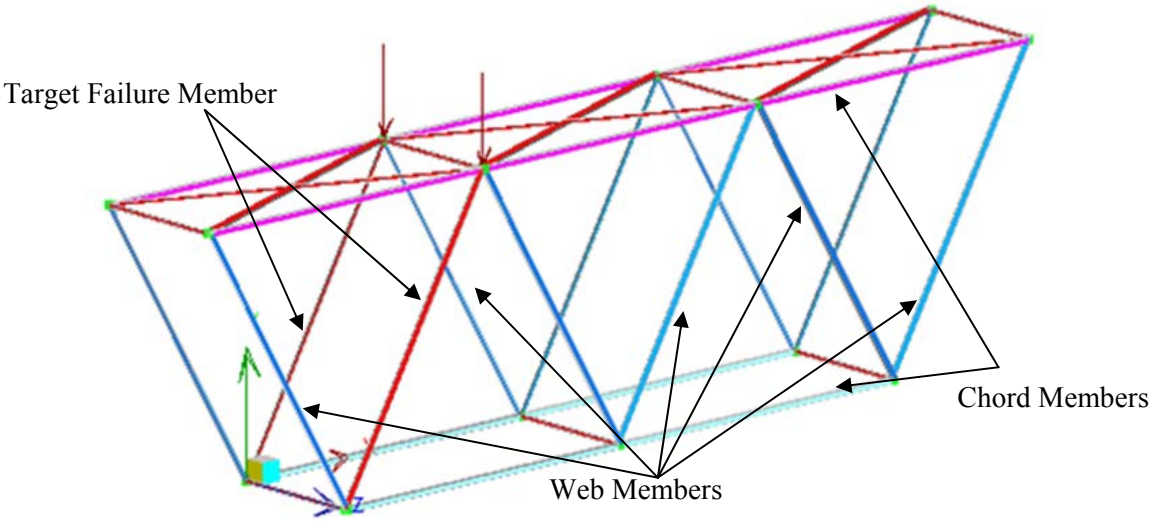

Figure 4.9 Analysis Model of the Angle Trusses

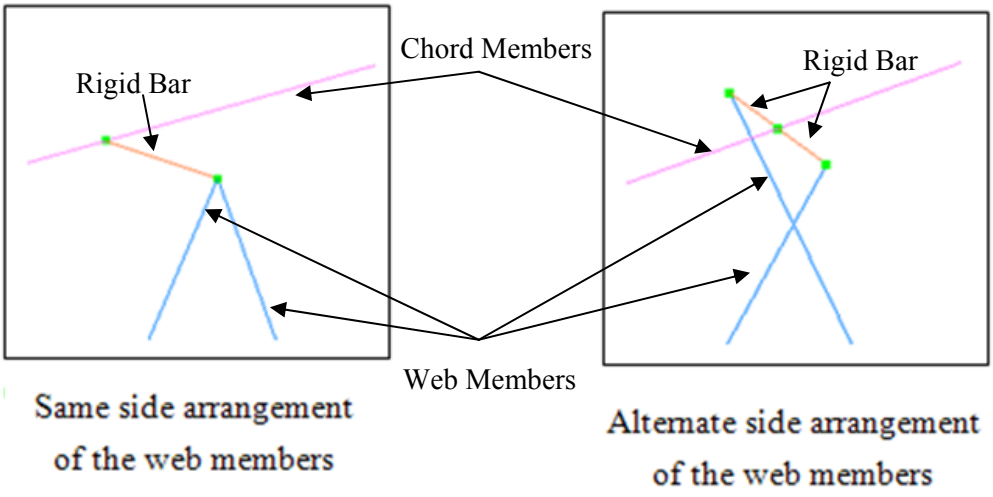

Figure 4.10 Modeling of Different Sides Arrangement of Web Members

Tables

Table 4.1 The Values of Steel Member Initial Bow Imperfection in CoPHK (2005)

Buckling curve	Member initial bow imperfection for second-order analysis
a	$L/500$
b	$L/400$
c	$L/300$
d	$L/200$

Table 4.2 Test and Analysis Results of Angle Members

Specimen	Length (mm)	Test result P_{test} (kN)	Analysis result P_{prop} (kN)	P_{test}/P_{prop}
End condition A				
A1	2009.1	66.7	68.6	0.97
A2	1574.8	101.0	97.0	1.04
A3	1371.6	110.3	105.6	1.04
A4	1295.4	108.5	108.6	1.00
A5	1168.4	112.1	113.2	0.99
A6	1064.3	120.5	116.5	1.03
A7	962.7	122.8	119.1	1.03
A8	861.1	129.0	121.0	1.07
A9	762.0	118.8	122.2	0.97
A10	683.3	135.7	122.4	1.11
A11	553.7	137.5	121.4	1.13
			Mean	1.04
			SD	0.05
End condition B				
B1	2034.5	31.6	34.5	0.92
B2	1397.0	50.3	52.4	0.96
B3	1193.8	63.2	60.3	1.05
B4	1005.8	72.1	68.5	1.05
B5	886.5	75.2	74.1	1.01
B6	787.4	90.3	79.0	1.14
B7	708.7	95.2	82.9	1.15
B8	584.2	100.5	89.0	1.13
			Mean	1.05
			SD	0.09
End condition C				
C1	1600.2	57.8	59.0	0.98
C2	1320.8	74.3	72.6	1.02
C3	1092.2	80.1	83.9	0.95
C4	889.0	94.3	92.1	1.02
C5	711.2	106.8	96.1	1.11
			Mean	1.02
			SD	0.06

* SD=Standard Deviation

Table 4.3 Coupon Test Results and Experimental Failure Loads of Angle Trusses

Set	Specimen	Young's modulus (kN/mm^2)	Yield stress (N/mm^2)	Failure load (kN)	Failure load/ Squash load
1	1a	216.9	347.0	67.2	0.26
	1b	211.8	347.6	78.4	0.30
2	2a	194.5	348.6	57.5	0.22
	2b	185.6	344.9	72.1	0.28

Table 4.4 Details of Specimens and Gusset Plates

Set	Specimen	Specimen size	Web arrangement	End condition	Gusset plate dimension
1	1a	65×65×6	Same side	Single bolt	240×180×8
	1b	65×65×6	Same side	Double bolt	240×180×8
2	2a	66×66×6	Alternate sides	Single bolt	240×180×10
	2b	66×66×6	Alternate sides	Double bolt	240×180×10

Table 4.5 Test Results of Angle Trusses

Set	Specimen	Test result (kN)	Ratio	
			Double bolt/ Single bolt	Same side/ Alternate sides
1	1a	67.2	/	1.17
	1b	78.4	1.17	1.09
2	2a	57.5	/	/
	2b	72.1	1.25	/

Table 4.6 Predicted Capacities by Design Codes

Set	Specimen	Test result (kN)	Predicted capacity (kN)			
			Design code			
			AISC	BS5950	CoPHK	Eurocode 3
1	1a	67.2	39.9	41.5	55.5	33.8
	1b	78.4	51.5	68.5	69.5	65.1
2	2a	57.5	38.5	39.4	55.9	33.1
	2b	72.1	45.8	65.3	70.8	61.2

Table 4.7 Predicted Capacities by Second-order Analysis and Design Method

Set	Specimen	Test result (kN)	Predicted capacity (kN)		
			Imperfection value 1	Imperfection value 2	Imperfection value 3
			L/360	*L*/300	*L*/200
1	1a	67.2	60.1	58.4	53.6
	1b	78.4	77.4	75.4	69.4
2	2a	57.5	54.3	53.2	50.5
	2b	72.1	71.4	70.3	67.6

Table 4.8 Ratios of Test to Predicted Results by Design Codes

Set	Specimen	Ratio of test to predicted results			
		Design codes			
		AISC	BS5950	CoPHK	Eurocode 3
1	1a	1.68	1.62	1.21	1.99
	1b	1.52	1.14	1.13	1.20
2	2a	1.49	1.46	1.03	1.74
	2b	1.58	1.10	1.02	1.18

Table 4.9 Ratios of Test to Predicted Results by Second-order Analysis and Design Method

Set	Specimen	Ratio of test to predicted results		
		Second-order analysis and design method (Imperfections)		
		L/360	*L*/300	*L*/200
1	1a	1.12	1.15	1.25
	1b	1.01	1.04	1.13
2	2a	1.06	1.08	1.14
	2b	1.01	1.03	1.07

CHAPTER 5

EXPERIMENTAL STUDIES OF STEEL AND CONCRETE-FILEED STEEL TUBULAR COLUMNS AND TRUSSES

5.1 Introduction

Owing to the rapid development of world economies, the requirement of high-rise buildings and long span structures has been ever increasing. Traditional steel and reinforced concrete structures are no longer able to fulfill the demands and requirements of the society, and steel-concrete composite structures have become popular in modern structural systems. Generally speaking, the Concrete-Filled Steel (CFS) tubular composite members are favorably used as columns of high-rise buildings and long span structures, and chord and web members of mega trusses such as the recently constructed Tamar Government Headquarters in Hong Kong. There exist numerous advantages on using composite members over the conventional steel and reinforced concrete members such as the enhancement of strength and stiffness of columns without enlargement of their size which then maximizes the usable space. The construction time and cost can be reduced as the steel tubes can be used as the formwork for fresh concrete. The concrete inside the

sections can also delay the local buckling of circumstancing steel walls. In order to understand the behaviors of composite members, extensive experiments were conducted and reported to study the beam, column and beam-column behaviors of various types of composite members such as CFS tubular members and concrete-encased steel members reviewed in Chapter 2.

From the review on the composite column and beam-column tests, most previous experiments focused on the behavior of isolated columns under pinned or fixed end condition, and tests on steel and CFS tubes acting as members of a frame or truss structure are limited. When the CFS tubes used as the members of a structure, its boundary condition cannot be simply treated as pinned or fixed end. The contributions to overall stiffness at connection from connecting members affect the end conditions as well as the member capacity. Therefore, tests on trusses composed of the bare steel and CFS tubes as chords and webs were carried out together with tests on the isolated columns with same section and material properties in order to investigate the actual behaviors of CFS tubes in a structure. The test program was divided into two parts including tests on the columns and trusses. In the first part, the four columns under pinned and fixed end conditions were tested and their capacities were compared. The second part of test included two sets of trusses with different member sections and concrete strengths. The behaviors of trusses under point loads were monitored and the beneficial effects due to in-filled concrete on trusses members were investigated.

Furthermore, the capacities of these isolated columns and members in the trusses will be predicted by the traditional codified design methods and proposed second-

order elastic analysis and design method in next chapter and compared with the test results from this chapter. The load-deflection responses of composite trusses members from the test will also be compared against the proposed second-order inelastic analysis method for composite members in Chapter 7.

5.2 Behaviors of Steel and Concrete-filled Steel Tubular Columns

In the first part of the experimental program, the behavior of isolated columns was studied. The tests on steel and CFS tubular columns were aimed to compare the increase in the capacity of CFS tubular columns under different end conditions including pinned and fixed ends. The buckling resistances of the isolated struts were also compared with the resistances of the constituting members in the trusses so as to investigate the behaviors of these members under the idealized design condition and actual condition.

5.2.1 General

The conducted column test included two bare steel and two CFS tubes. Square hollow steel tubes with cross-section of 60x60x3mm were used in the test and the average width, depth and thickness are listed in Table 5.1. Two boundary conditions were set up in the test as indicated in Figure 5.1 for pinned end and Figure 5.2 for fixed end cases. The specimen length for the pinned end condition and fixed end condition were 1.74m and 2m respectively. The failure loads as well as load-deflection behavior were studied.

5.2.2 Material properties

The steel plate slenderness ratio was selected according to the guidelines provided in Eurocode 3 (2005) and Eurocode 4 (2004) so that the effect of the local buckling on the steel plate can be neglected. Four steel tensile coupon tests were carried out in accordance with British Standard BS EN 10002-1:1990 to determine the stress-strain curve of the steel material. Properties including the average yield stress, ultimate tensile stress and Young's modulus of elasticity of the steel tube used in the isolated column test are listed in Table 5.1.

Normal strength concrete was used in filling the steel tubes. The concrete mix included 200kg/m^3 water, 408kg/m^3 Ordinary Portland Cement, 1074kg/m^3 coarse aggregate and 716kg/m^3 fine aggregate. A series of standard concrete cylinders, 100mm in diameter and 200mm in height, were cast and cured under the same conditions as the specimens until the day of test. The average compressive cylinder strength and modulus of elasticity of the concrete used in the CFS tubes are given in Table 5.1.

5.2.3 Test setup

The setups of steel and CFS tubular columns with pinned and fixed boundary conditions are given in Figures 5.3 and 5.4. The columns were 2 meters in length, measured between the centre of rotation at both ends. The test specimens were cast on the surface of flat steel plates at both ends to ensure smooth surface for producing

uniform load. For pinned end case, the specimens were welded to the steel plates and bolted to the pinned ends and fixed by four bolts, and rotation was only allowed in the in-plane direction. For the fixed end condition, the specimens were welded to the steel plates at both ends and bolted to the ground at the bottom and rigid connected to the load cell at top, and no rotation was allowed in both the in-plane and out-of-plane directions. During the test, point load was applied to the top of the column via the loading jack with maximum capacity of 400kN. The load interval was taken as 0.5kN throughout the whole test and the load cell was located at the top of the column to record the applied load.

5.2.4 Instrumentation

Totally 12 and 10 displacement transducers were used for pinned and fixed end conditions respectively to measure the displacements of the specimens. Four transducers were used to measure the downward and lateral displacements at the top of the specimens. The deflections at the middle and quarter points for both the in-plane and out-of-plane directions of the specimens were monitored by other six transducers. The displacements at the bottom of the pinned end specimens were measured by other two transducers with their locations shown in Figure 5.5. Strains on each face of the steel tubes at the middle and quarter points were monitored by 12 strain gauges at each point as indicated in Figure 5.5.

5.2.5 Discussion of test results

5.2.5.1 Failure modes

All the specimens failed in flexural buckling mode with the maximum deflection at the middle of the specimens as shown in Figures 5.6 and 5.7 for pinned end and fixed end conditions respectively. Local buckling was not observed before reaching the maximum applied load for all columns. For pinned end columns, owing to the friction in the pinned ends, the degree of end restraint may be varied and the maximum applied load could be higher than the theoretically perfect pinned end case.

5.2.5.2 Lateral load-deflection curves in the in-plane direction

The axial load versus mid-length in-plane deflection curves for both steel and CFS tubular columns are plotted in Figure 5.8. Generally speaking, the load versus in-plane deflection relationships were expectedly similar for all tested specimens that the deflection increased linearly with applied load at the initial stage, and the relationship became nonlinear when the load approached failure load. After attaining the maximum load, the deflection of the members increased significantly with decreasing load.

5.2.5.3 Lateral deflection-load curves in the out-of-plane direction

The load against out-of-plane deflection curves are presented in Figure 5.9. The results show that the deflections were small before reaching the maximum load when compared with the deflections in the in-plane direction for pinned end columns. However, for fixed end columns, the mid-length deflections along the out-of-plane direction were similar to the deflections along the in-plane direction, which indicates

that the columns deflected in both directions with similar initial imperfections in these directions. After the peak load, the out-of-plane deflection increased significantly due to the lost of stability.

5.2.5.4 Resistance of the isolated columns

The maximum loads in test for all specimens are listed in Table 5.2. The load resistances of steel tubular columns were 152.5kN and 249.4kN for pinned and fixed end conditions and larger resistance were obtained for CFS tubular columns with loads of 186.9kN and 249.4kN for pinned and fixed ends respectively. The load resistance ratios of CFS to bare steel tubular columns were 1.23 and 1.33 for pinned end and fixed end conditions respectively, and the load ratios of fixed to pinned end conditions were 1.64 and 1.77 respectively for steel and CFS tubular columns. The results show that the beneficial effect due to the in-filled concrete on the columns under fixed end condition is more significant than under pinned end condition.

5.2.5.5 Axial strain-load curves

The load against strain curves at the mid-length of the columns are plotted in Figures 5.10 and 5.11 for pinned end columns, and Figures 5.12 and 5.13 for fixed end columns. These curves were noted to possess a typical and consistent pattern similar to load-deflection curves. Sign of local buckling on the steel plate was not observed from these curves.

5.3 Behaviors of Steel and Concrete-filled Steel Tubular Trusses

The behaviors of steel and CFS tubular isolated columns have been studied in last section. However, the behavior of the CFS tubular members used in structural systems instead of an isolated column is more interesting because the use of single and isolated column in practice is rare. Hence, in the second part of the experimental program, test was carried out on two pairs of trusses to study the behaviors of steel and CFS tubular members in the trusses. The results of the first set of trusses were also compared with the results of the column test to identify the effects of end condition on a constituting member in a truss system.

5.3.1 General

Two sets of trusses with members composed of bare steel tubes (named as steel truss) and CFS tubes together with steel tubes (named as composite truss) were tested with the dimensions of trusses members shown in Figure 5.14. Each pair of tested trusses included one steel truss and one composite truss. Steel trusses were composed of steel tubes for all members and the composite trusses consisted of CFS tubes in the compressive members and bare steel tubes in the tensile members. The steel tubes with the same section and material strength as the tested columns were used in the first set of trusses so that the results can be compared directly with the column test results. In truss set 1, the steel tubes with section of 60x60x3mm were used for all members. In truss set 2, the two target failure members were 50x30x3mm rectangular hollow section tubes and the remaining members were 60x60x3mm square hollow section tubes. Each of these three-dimensional trusses consisted of 19

members including 14 main members of 2m length and 5 tie members of 0.8m length connecting the two plane trusses. All members were connected as moment joints by 8mm fillet welds.

5.3.2 Material properties

The same materials used in columns test were adopted for truss set 1 which further used normal concrete while the high strength concrete was chosen in the steel tubes for truss set 2. The composition of concrete mix used in the CFS tube in truss set 2 were water (238.1kg/m^3), Ordinary Portland Cement (479.5kg/m^3), coarse aggregate (862.5kg/m^3), fine aggregate (709kg/m^3) and Pulverized Fly Ash (205.5kg/m^3). The material properties of steel tube, and the average compressive cylinder strength and the modulus of elasticity of the concrete on the same day of trusses tested are given in Table 5.3 for both sets of trusses.

5.3.3 Test setup

Trusses were simply and pin supported at two ends and roller supported at another two ends, and they were loaded vertically at their top at one side by hydraulic jacks with a maximum capacity of 400kN as shown in Figure 5.15 The loads were applied gradually in the test at a rate of 2kN/minute and the loads increment was taken as 0.5kN during the test. Two load cells were located under point loads to record the load during the test. Sufficient lateral restraints were provided to ensure out-of-plane buckling at connecting nodes between members was prevented.

5.3.4 Instrumentation

In the test, the displacement transducers were set to monitor deformation of the trusses including the overall movements of the trusses at the top and bottom of the target failure members, in-plane movements of the target failure members at mid-length and quarter-lengths, and out-of-plane displacement of the target failure members at mid-length. The exact locations of displacement transducers are shown in Figure 5.16. The strain gauges were mounted on four faces of steel plate at the mid-length and quarter points of the target failure members to trace the strain during the test. The detailed locations of strain gauges for both trusses are shown in Figure 5.16.

5.3.5 Discussion of test results

5.3.5.1 Failure modes

The deformation of the trusses was most obvious in the members near the point loads. The failure of the trusses was due to the member flexural buckling at the in-plane direction on the target failure member, and the maximum deflection was noted at the middle of the member for all tested trusses. During the test, the surfaces of the tubes were examined continuously and the local plate buckling was not observed in all members of the tested trusses before reaching the maximum applied load. The final deformed shapes are shown in Figures 5.17 and 5.18 for truss set 1 and Figures 5.19 and 5.20 for truss set 2.

5.3.5.2 Lateral load-deflection curves in the in-plane direction

The applied load against mid-length in-plane deflection curves of the failed members are plotted in Figures 5.21 and 5.22 for truss sets 1 and 2. Similar load versus deflection curves were observed for both the steel and CFS tubular members that, when the load was small, a linear relationship between the load and deflection was noted and the relationship became nonlinear when the maximum load was approached. The load was applied continuously after reaching the maximum load in order to study the post-buckling behavior of the trusses.

5.3.5.3 Lateral load-deflection curves in the out-of-plane deflection

The applied load against the out-of-plane deflection curves at mid-length of the failure members are plotted in Figures 5.23 and 5.24 for truss sets 1 and 2 respectively. The curves show that the out-of-plane deflections were small compared with the in-plane deflections and remained constant with increasing load before reaching the maximum load for all tested trusses, and the out-of-plane deflections were mainly due to the initial member and truss global imperfections. After reaching the maximum load, the member buckled and the trusses deformed globally with the lateral out-of-plane deflections increased drastically.

5.3.5.4 Resistance of the trusses

The test results are given in Table 5.4 and the maximum applied loads were 250.4kN and 323.1kN for steel and CFS tubular members respectively in truss set 1, and

76.6kN and 90.0kN for steel and CFS tubular members respectively in truss set 2. The maximum loads resisted by the members in the composite trusses were respectively 29% and 17% higher than the trusses for sets 1 and 2. The normal concrete was used for truss set 1 and high strength concrete was filled for truss set 2 which also used a smaller steel section. The increase in the capacity of the failure member due to in-filled concrete was more significant in truss set 1 than set 2. The results indicate that the capacity of the member is more controlled by the second moment of area instead of strength of concrete for slender members. The increase on the member stiffness is more effective than the increase of material strength to obtain a larger member resistance for slender members.

5.3.5.5 Axial strain-load curves

The applied load against the strain curves at the mid-length of the failure members are shown in Figures 5.25 and 5.26 for truss set 1, and Figures 5.27 and 5.28 for truss set 2. The nonlinear relationship and post failure behaviour were observed in the figures. Large compressive strains were developed at the bottom fibres which gave a consistent result with displacement transducers. The strains recorded on both sides of the member were nearly identical for both steel and CFS tubular members and the slight difference was mainly due to the out-of-straightness imperfections. The results also imply that the out-of-plane deflection was insignificant before reaching the failure load, after which the out-of-plane deflection increased significantly with decreasing load.

5.3.5.6 Post buckling behaviors

After reaching the maximum load, the deflection and strain on the steel plates increased continuously with decreasing load and the local buckling on the steel plate was detected. For steel tubular members, the inward buckling of the steel plate was observed first at the mid-span of the members and then at top and bottom of the same member. For CFS tubular members, the concrete core prevented the inward buckling and therefore the steel plate local buckled outward as shown in Figure 5.29.

5.4 Comparisons on the Results of Columns and Trusses

The results on isolated columns and truss set 1 have been presented above. The same materials and section were used for both tests with different end conditions. The pinned and fixed end conditions were set for isolated columns while the end condition of the members in the trusses was more complicated because the movement was restricted by the other members. The member force against deflection curves of columns under pinned and fixed end conditions and the failure members in the trusses are plotted in the same figures (Figures 5.30 and 5.31) for comparison of the capacities and behavior. The comparison results show that the resistances of both the steel and CFS tubular members in the trusses were somewhere between members with pinned and fixed end conditions which implies that the boundary condition of the trusses members was between these extremes and semi-rigid.

5.5 Concluding Remarks

Experimental investigation on the behaviors of steel and CFS tubes used as isolated columns and members in the trusses has been presented in this chapter. Four columns including two steel and two CFS tubes were tested under pinned and fixed end conditions. The beneficial effects in strength and ductility due to the in-filled concrete were compared and the load ratios on pinned and fixed end columns were studied.

Extending the studies on the behaviors of isolated columns, tests were extended to study the structural systems. Trusses consisted of steel and CFS tubular members were tested. The end condition of the members in the trusses was not simply the idealized pinned or fixed end and they were complicated with the realistic end condition that the end movement and rotation were restricted by the other members. From the comparison, the actual buckling length of the member cannot be arbitrarily estimated and used for determination of the buckling resistance of the members.

The comparisons on the behaviors of isolated columns and members in the trusses verified that the end condition of the members was in-between the pinned and fixed ends. Therefore, assuming pinned or fixed end condition for those members will give an inaccurate and even dangerous design which will be demonstrated in the next chapter. Furthermore, the accuracy of first-order analysis and second-order analysis design method in design of isolated columns and members in the trusses will also be verified in the next chapter through the comparisons on the predicted and test results. The load-deflection behavior of the members in the trusses for both loading and

unloading stages will also be compared with the analysis results by using the proposed second-order inelastic analysis method for composite members in Chapter 7 for verification.

Figures

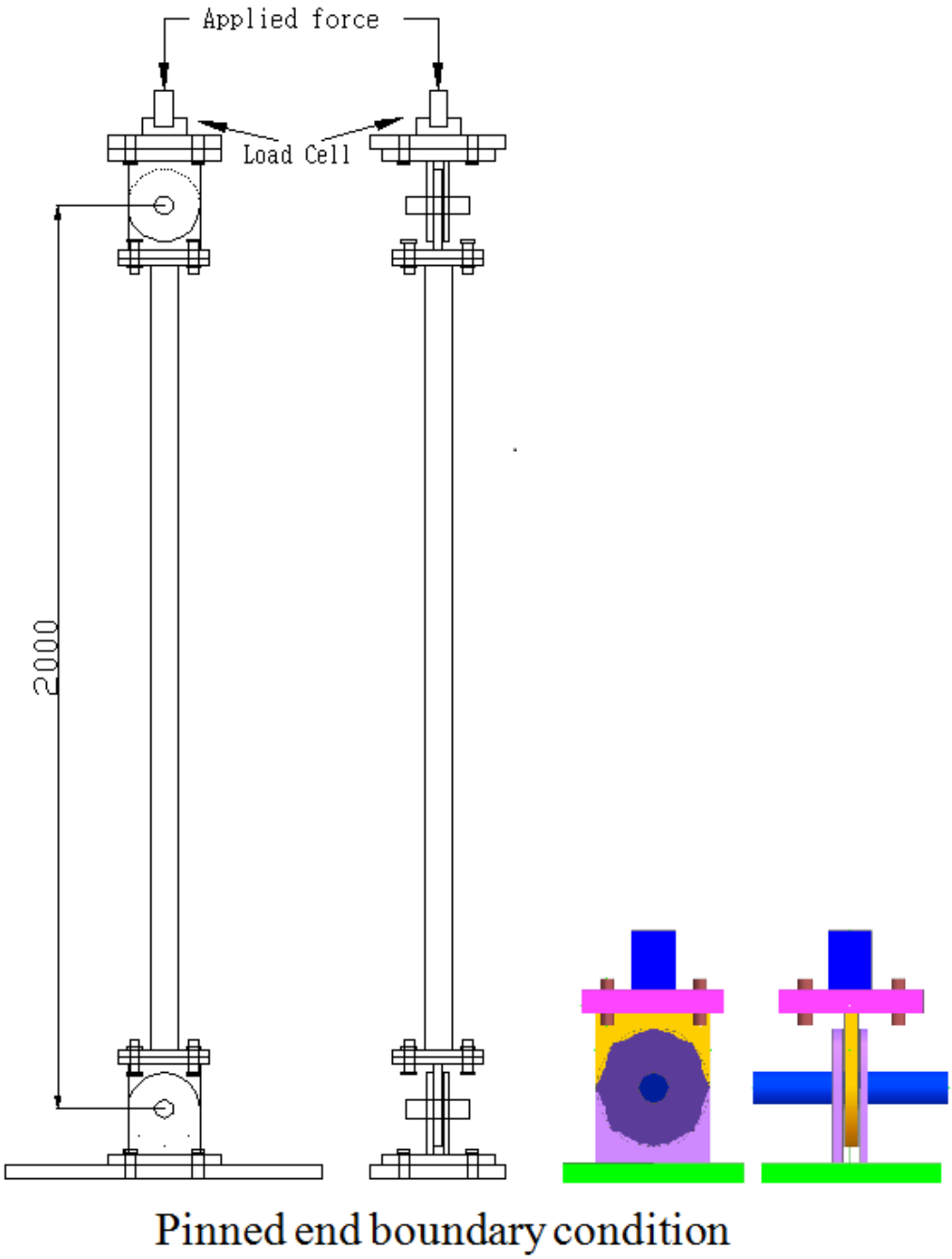

Figure 5.1 Layout of Pinned End Columns

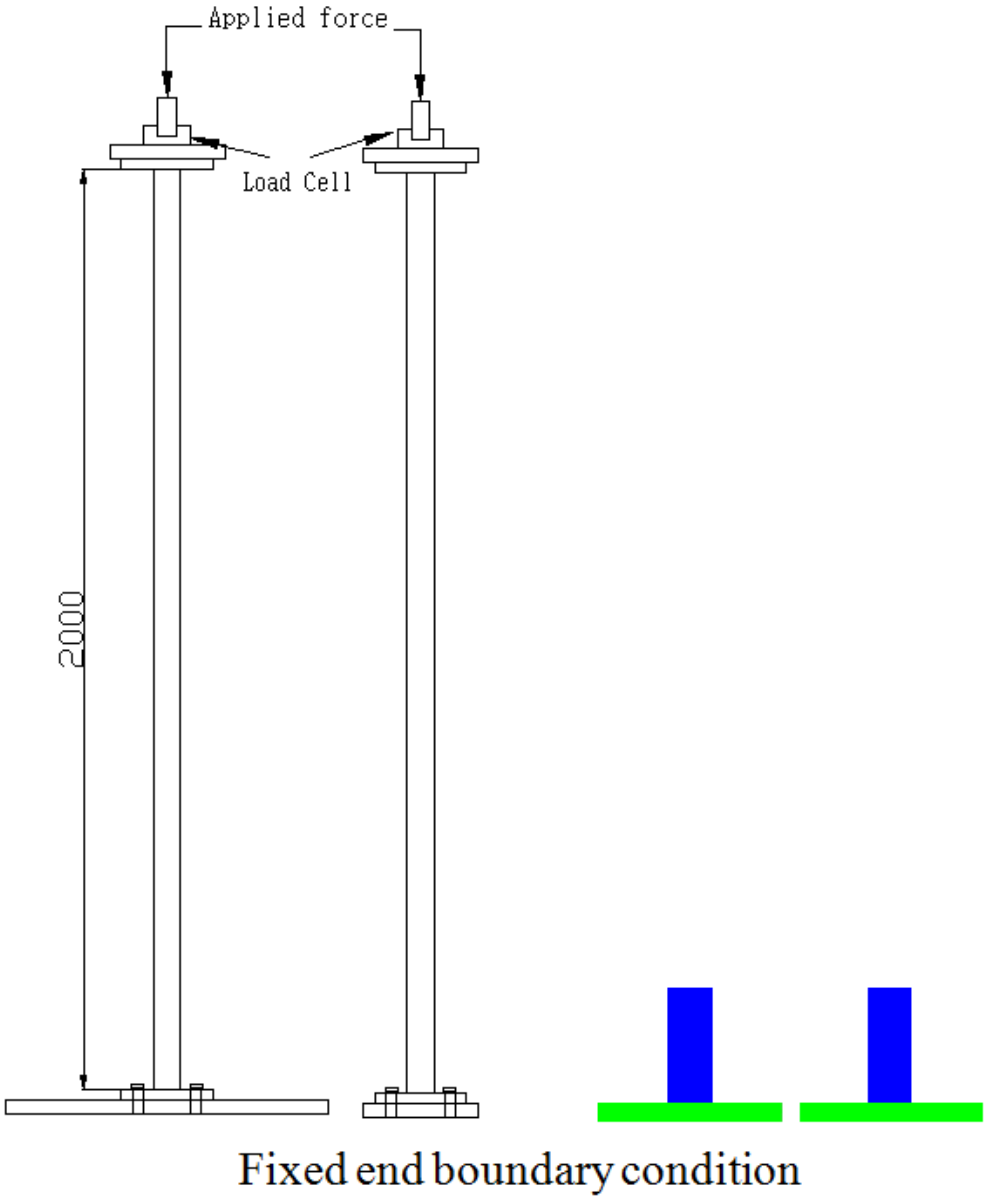

Figure 5.2 Layout of Fixed End Columns

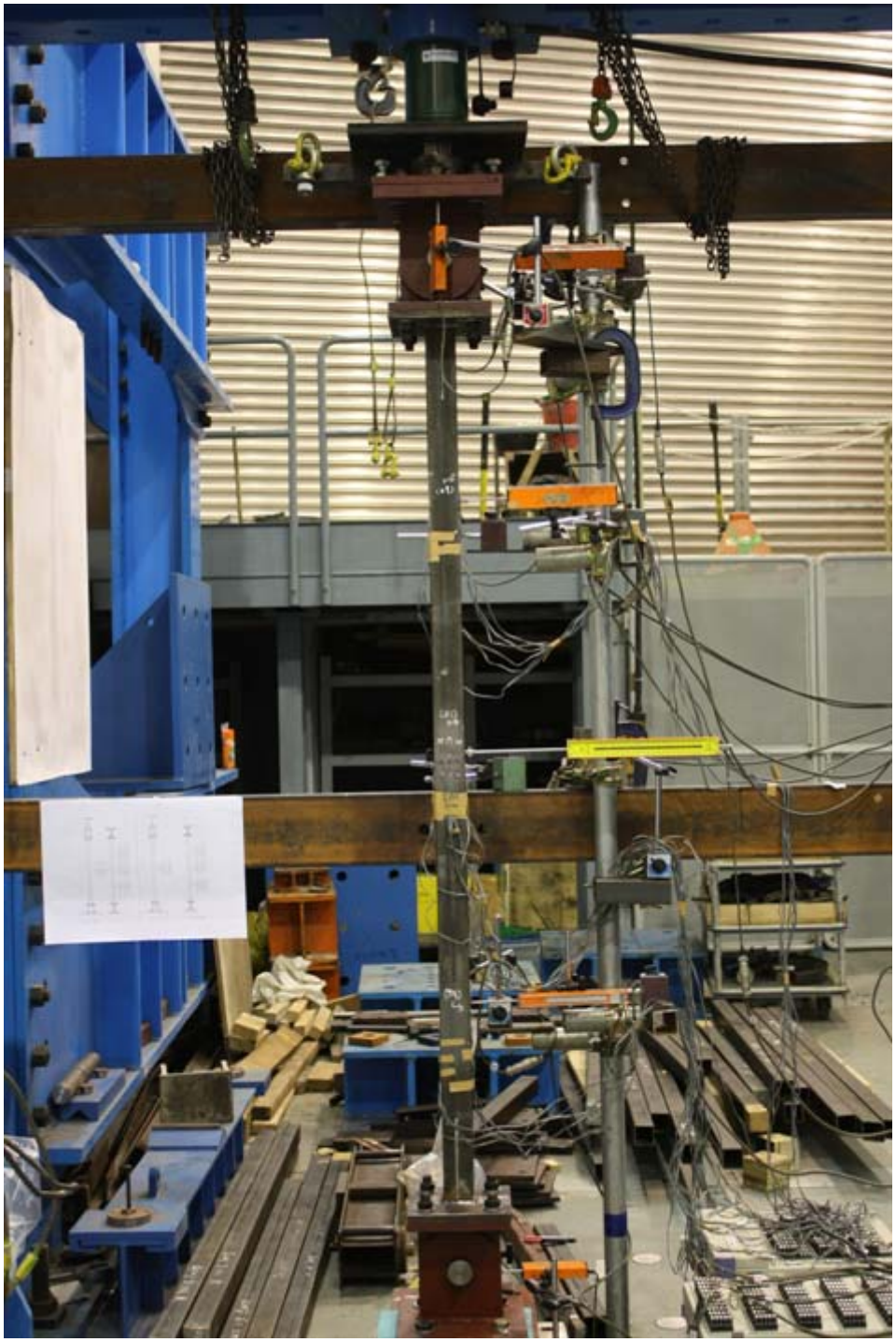

Figure 5.3 Experimental Setup of Pinned End Columns

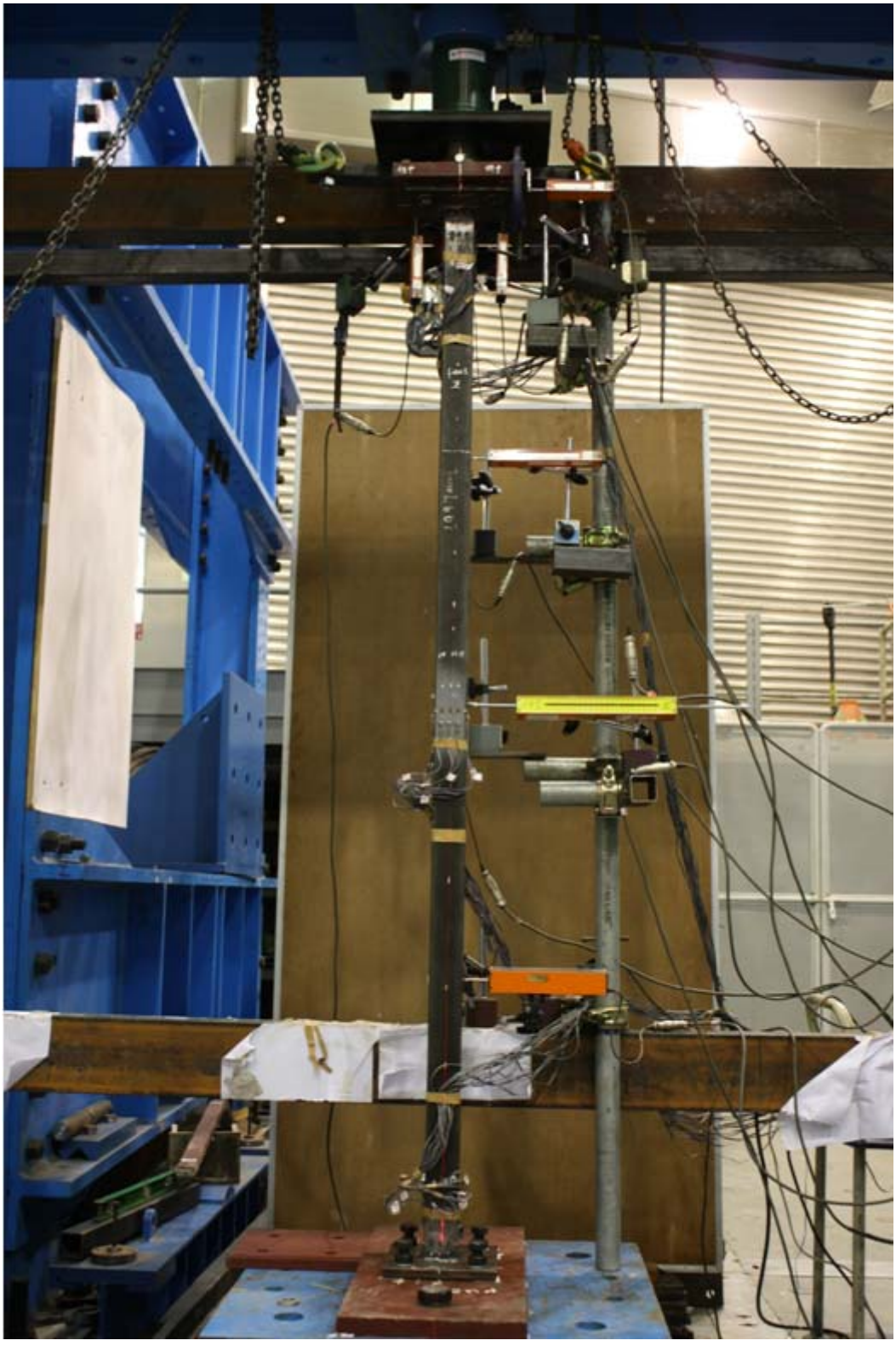

Figure 5.4 Experimental Setup of Fixed End Columns

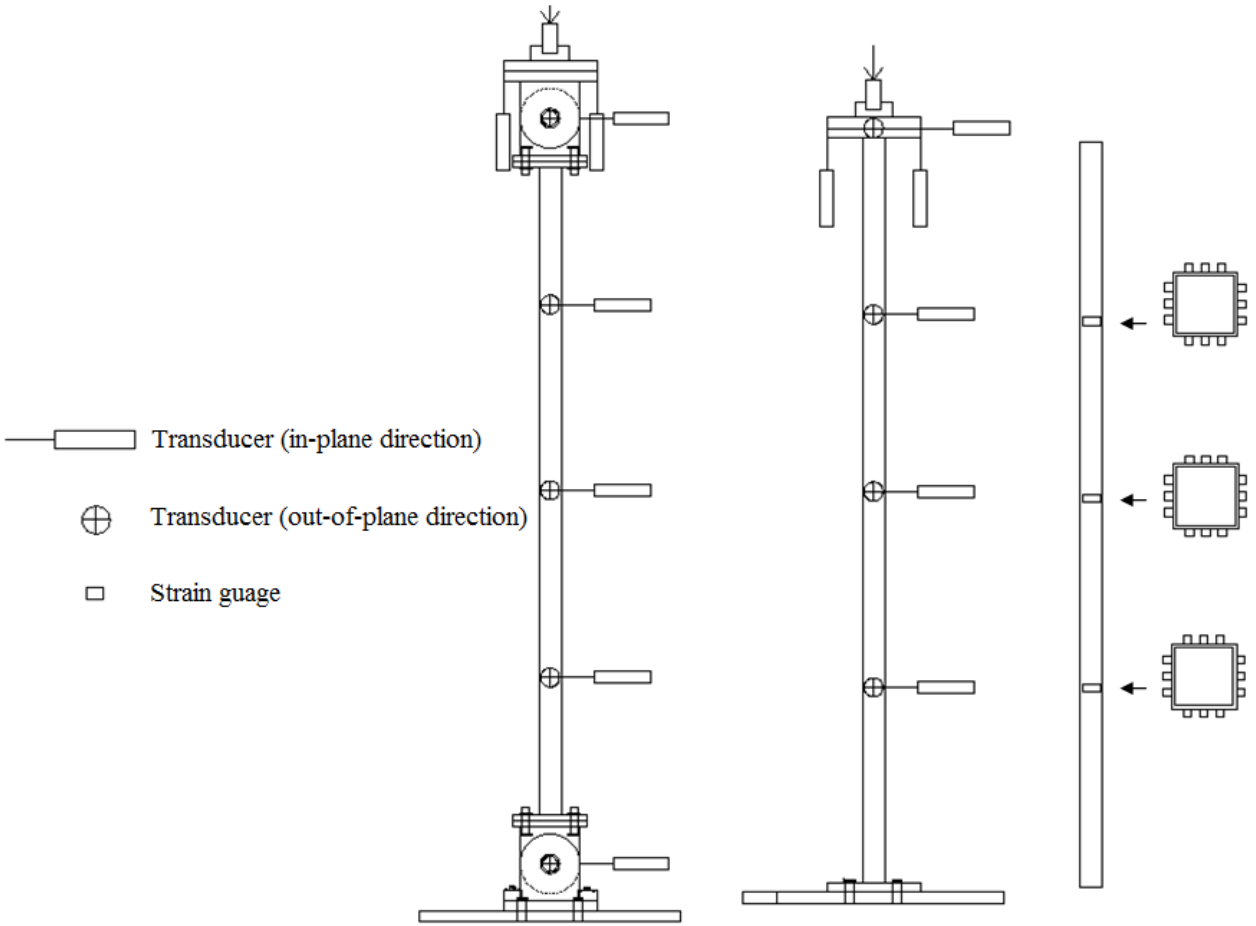

Figure 5.5 Locations of Strain Gauges and Displacement Transducers on the Columns

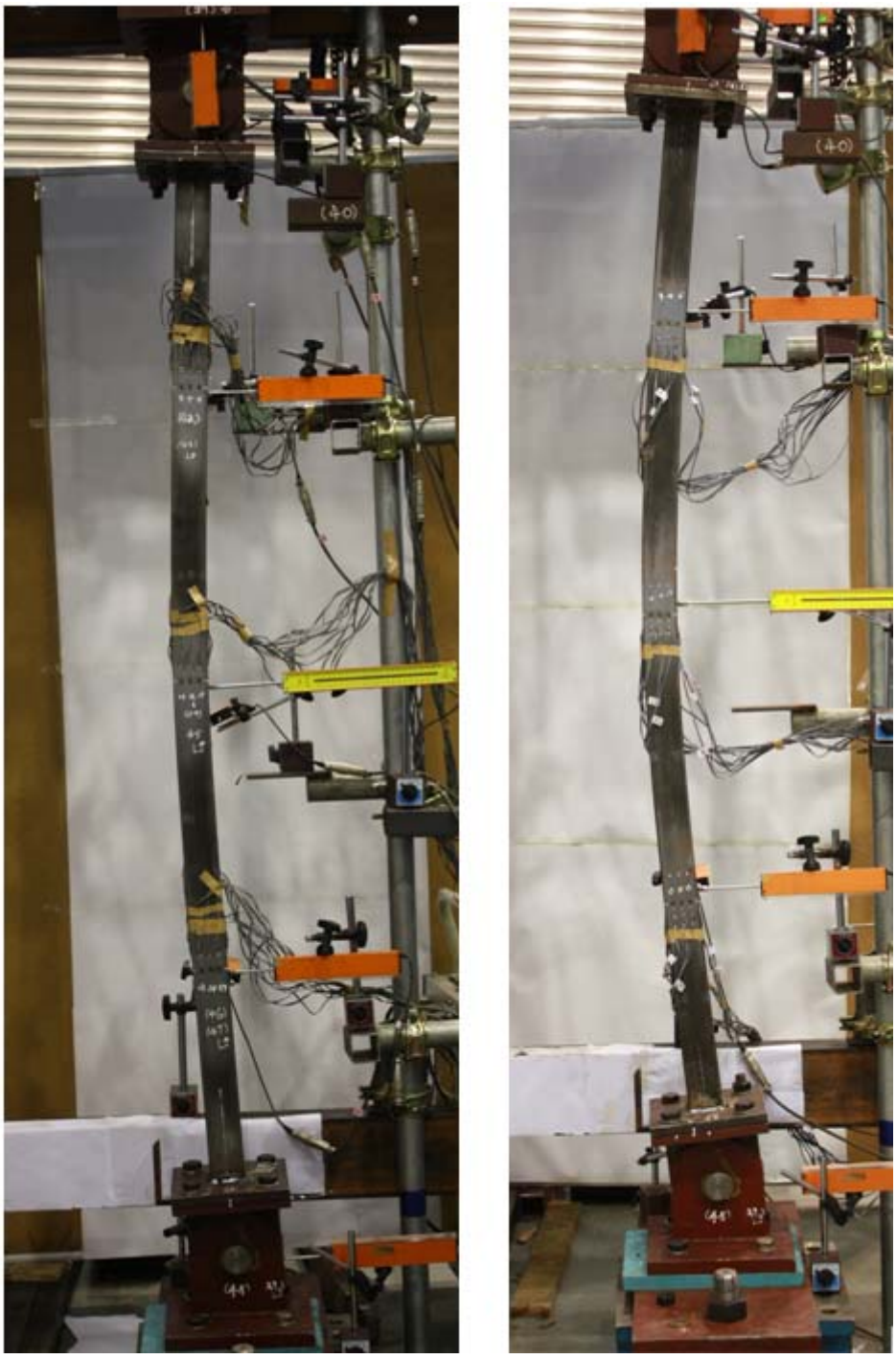

Steel tubular column CFS tubular column

Figure 5.6 Failure Mode of Pinned End Columns

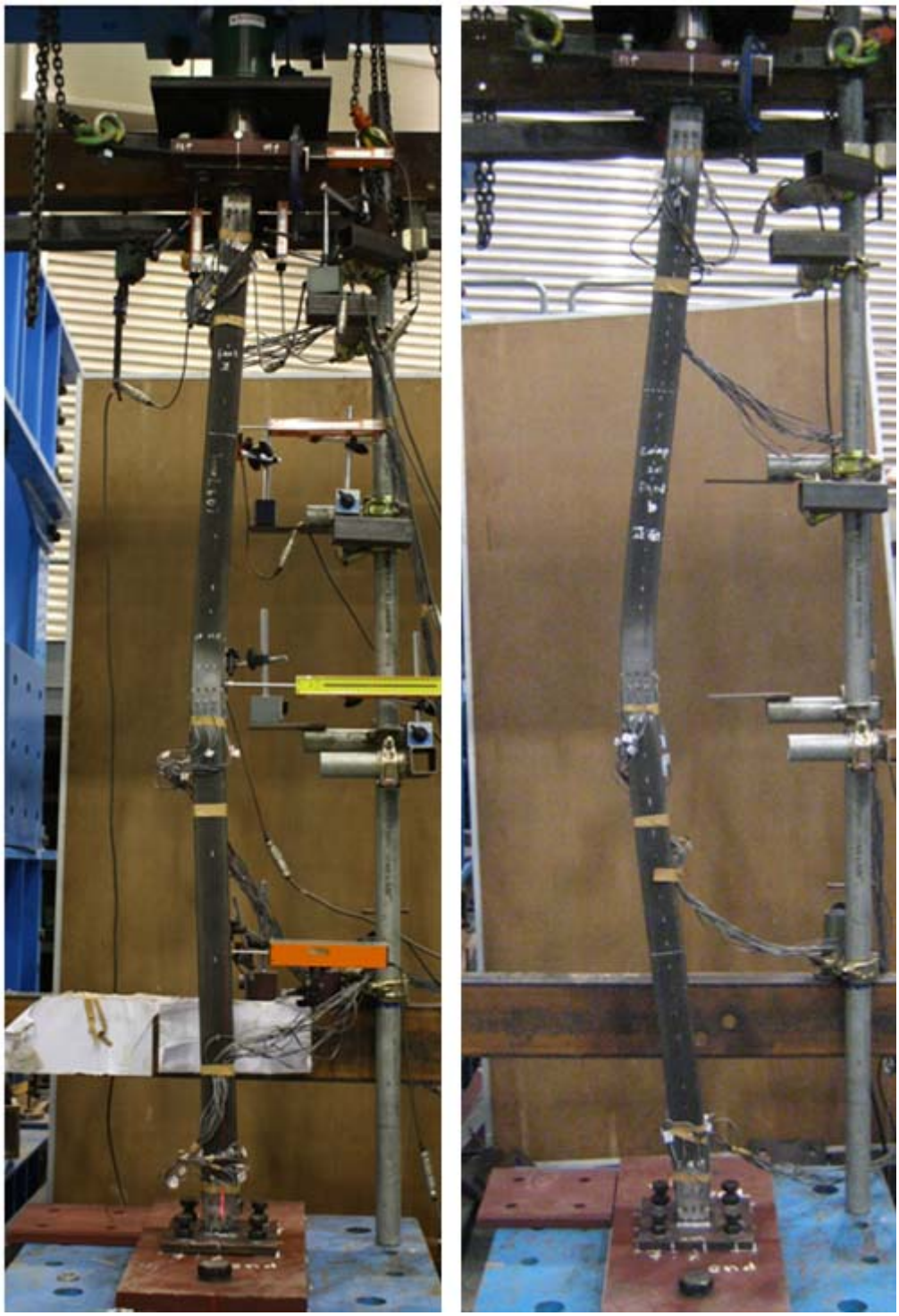

Steel tubular column CFS tubular column

Figure 5.7 Failure Mode of Fixed End Columns

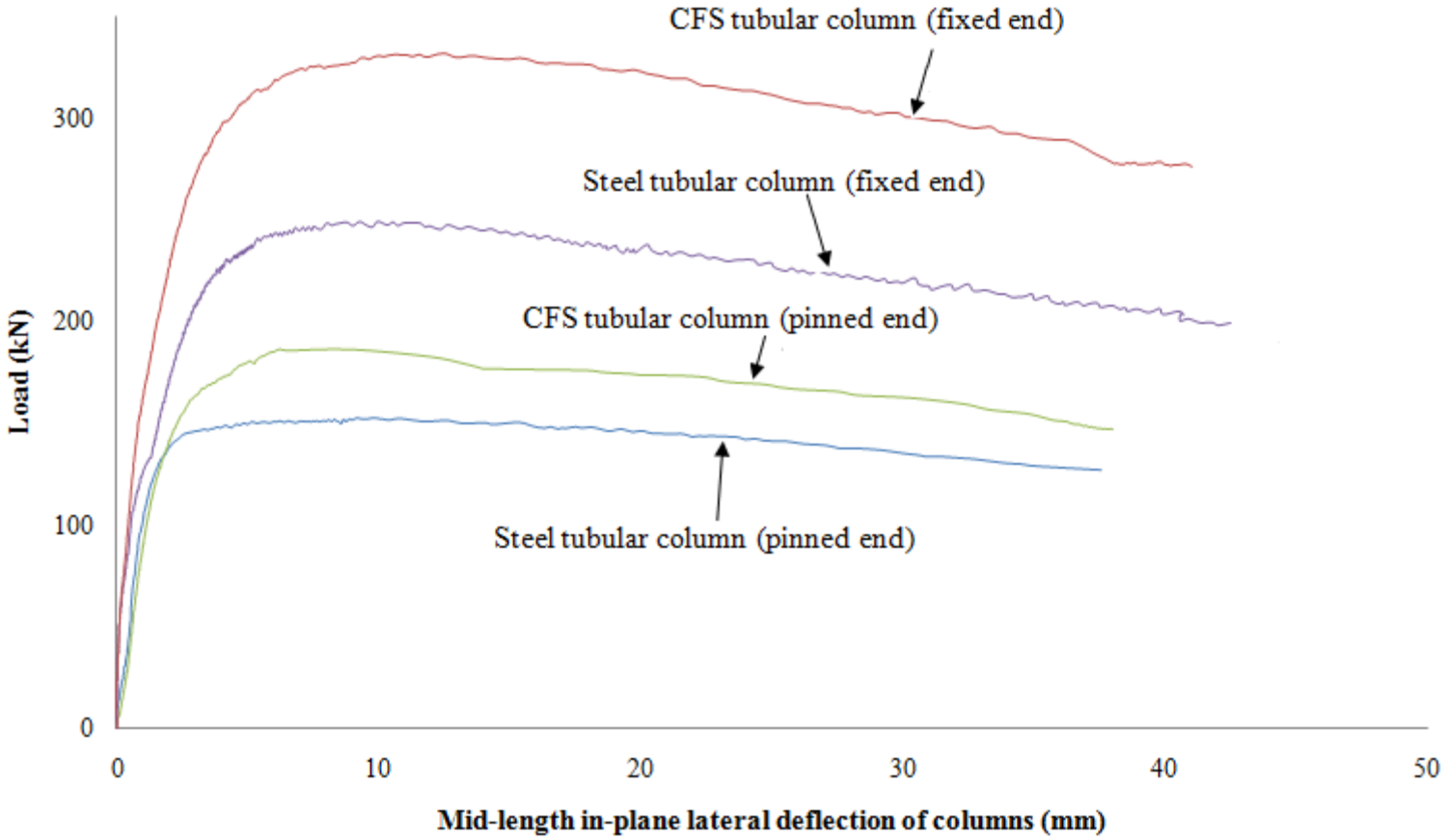

Figure 5.8 Load against In-plane Lateral Deflection Curves of Columns

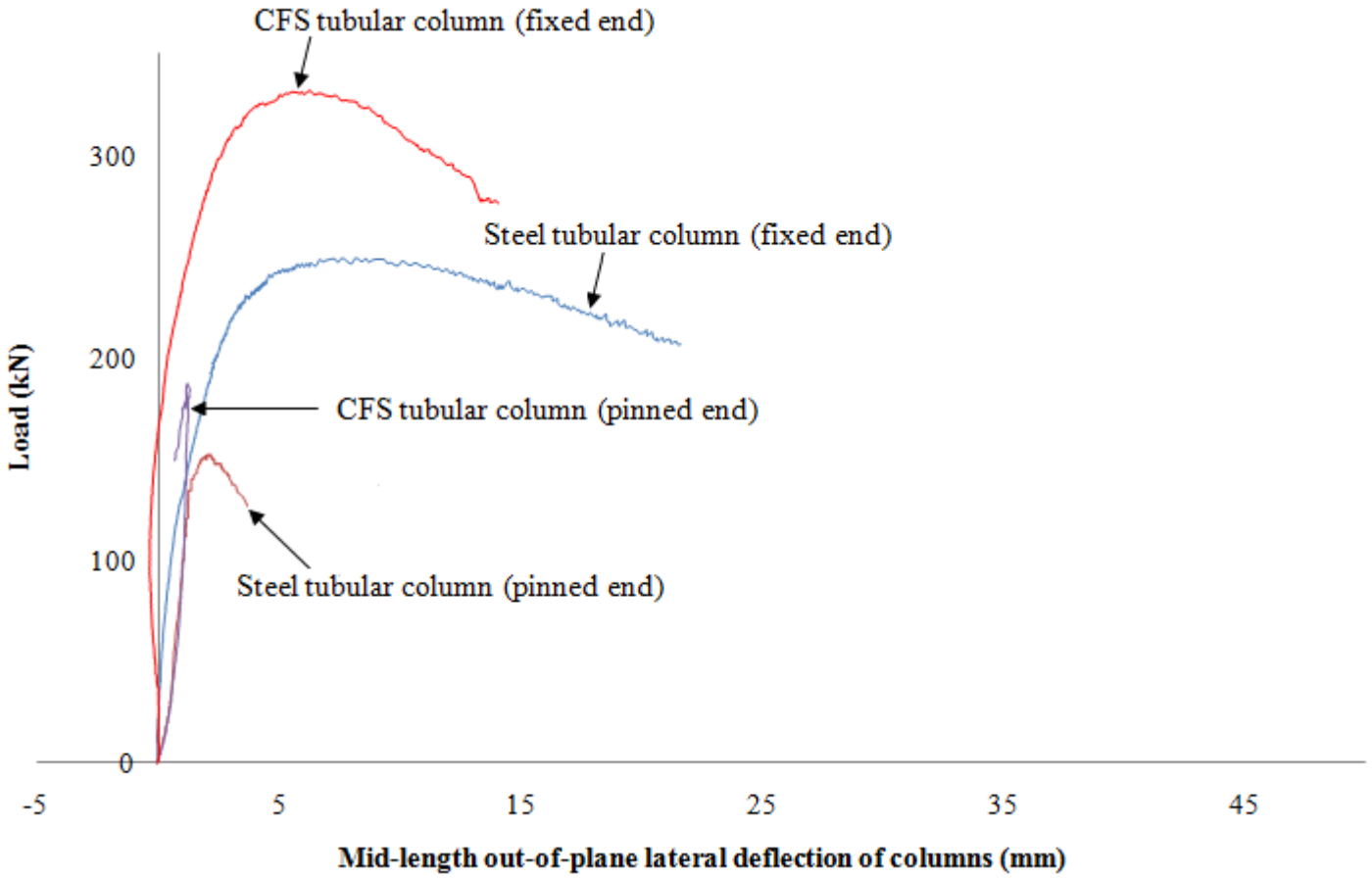

Figure 5.9 Load against Out-of-plane Lateral Deflection Curves of Columns

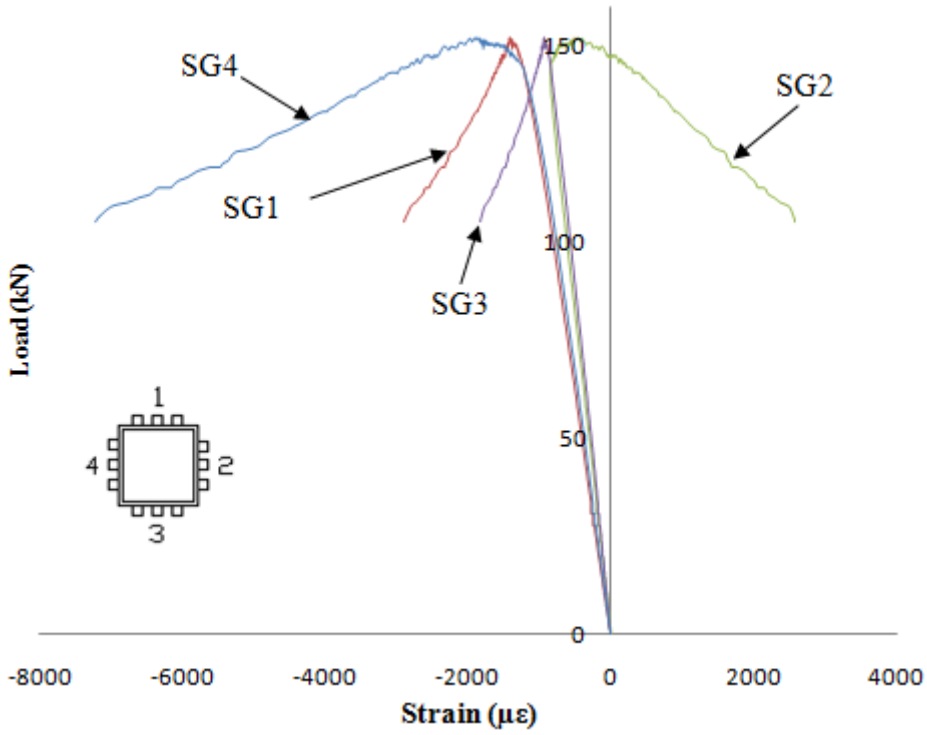

Figure 5.10 Load against Strain of Pinned End Steel Tubular Columns

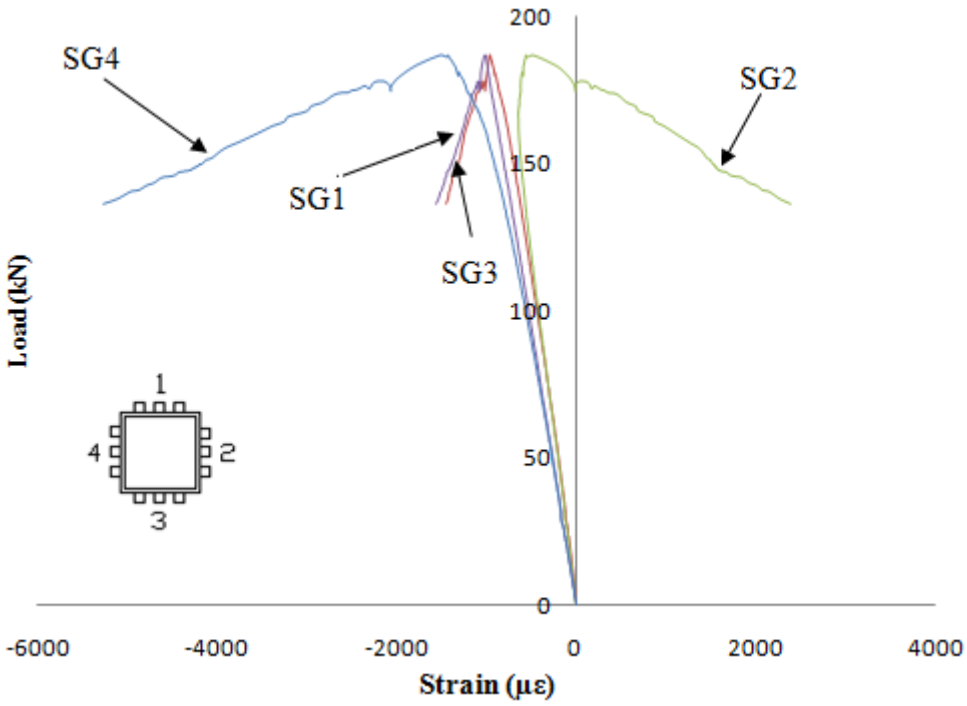

Figure 5.11 Load against Strain of Pinned End CFS Tubular Columns

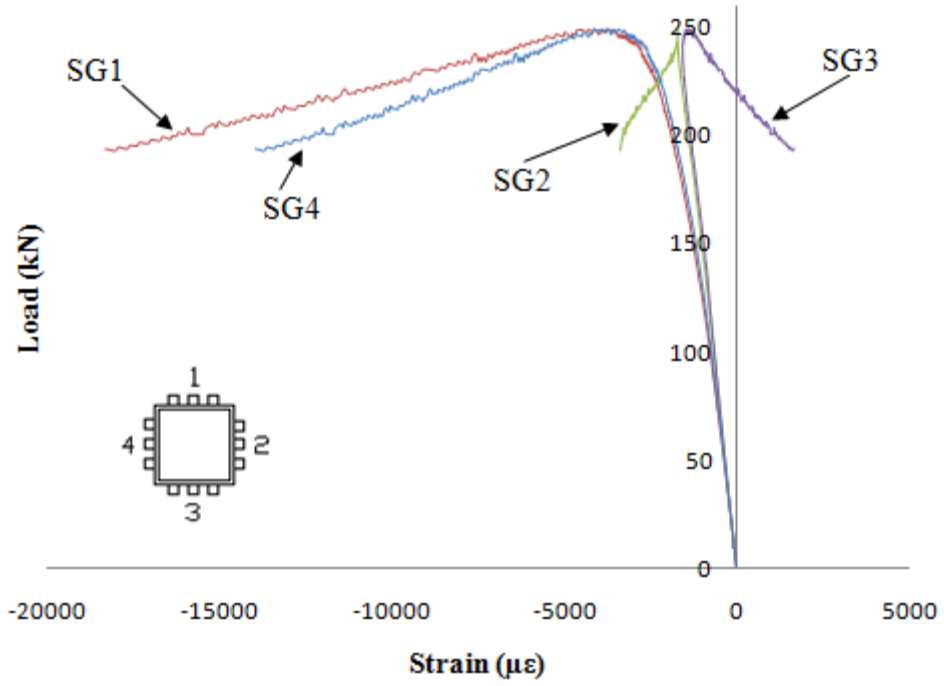

Figure 5.12 Load against Strain of Fixed End Steel Tubular Columns

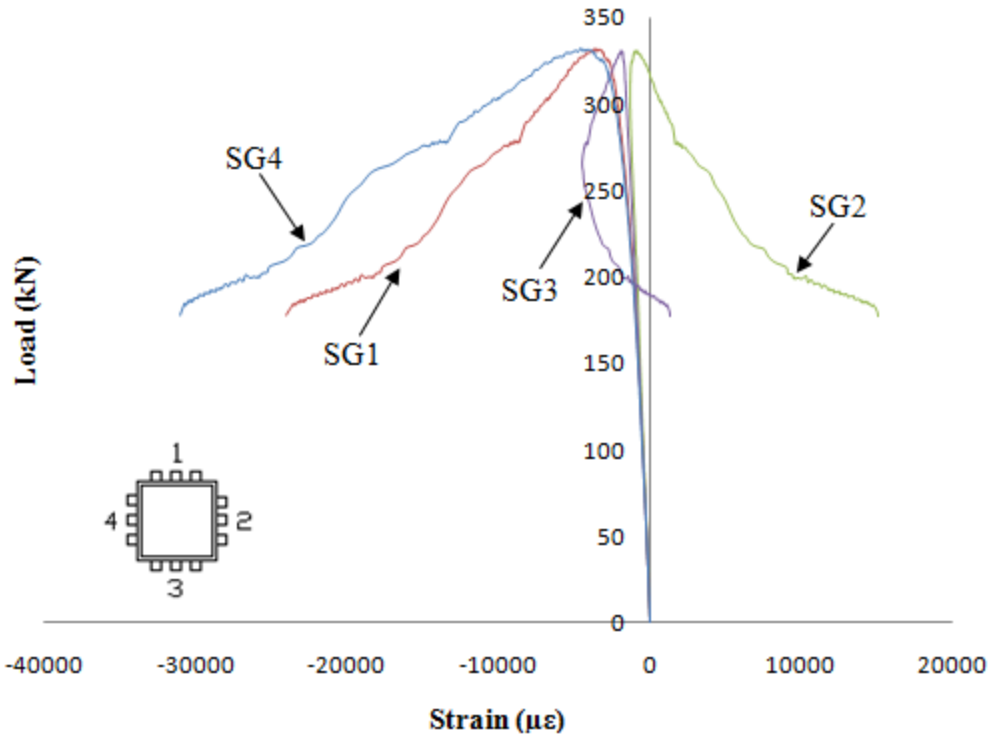

Figure 5.13 Load against Strain of Fixed End CFS Tubular Columns

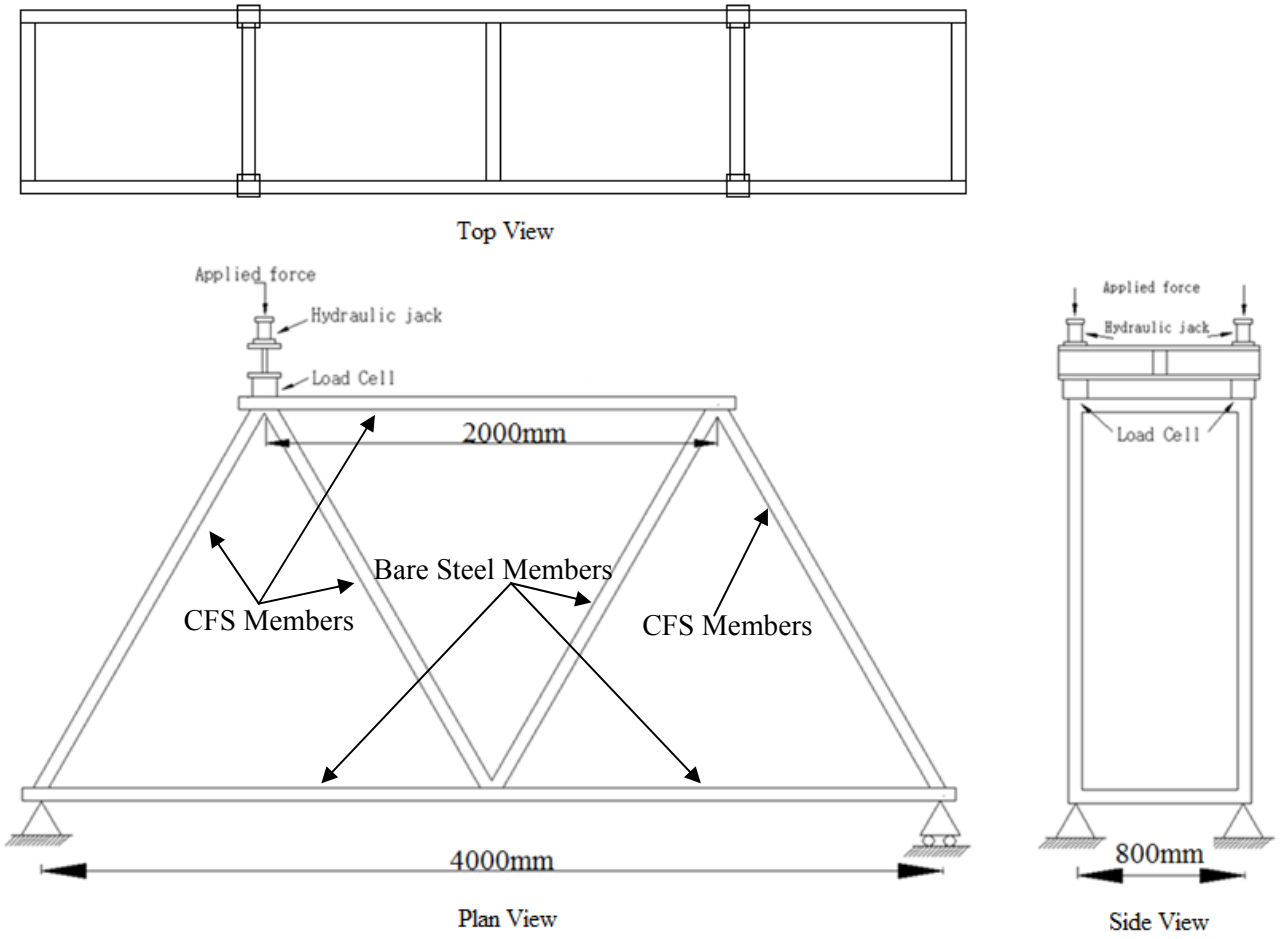

Figure 5.14 Layout of the Steel and Composite Trusses

Figure 5.15 Experimental Setup of the Steel and Composite Trusses

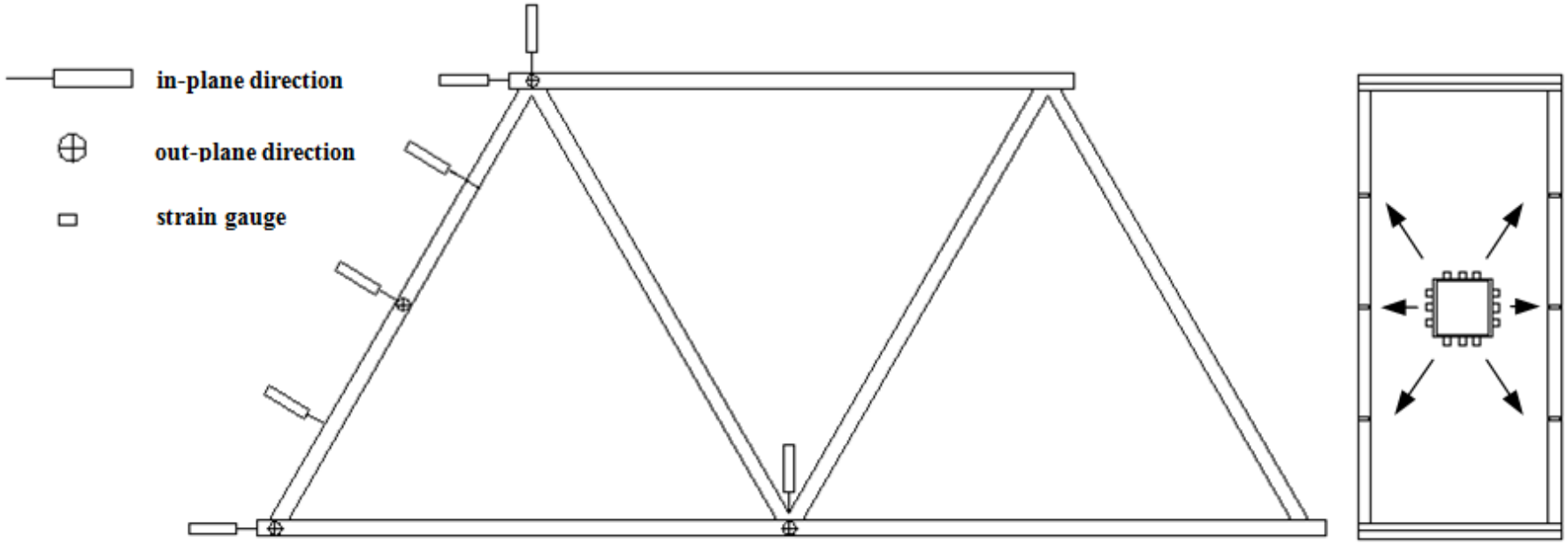

Figure 5.16 Locations of Strain Gauges and Displacement Transducers on the Trusses

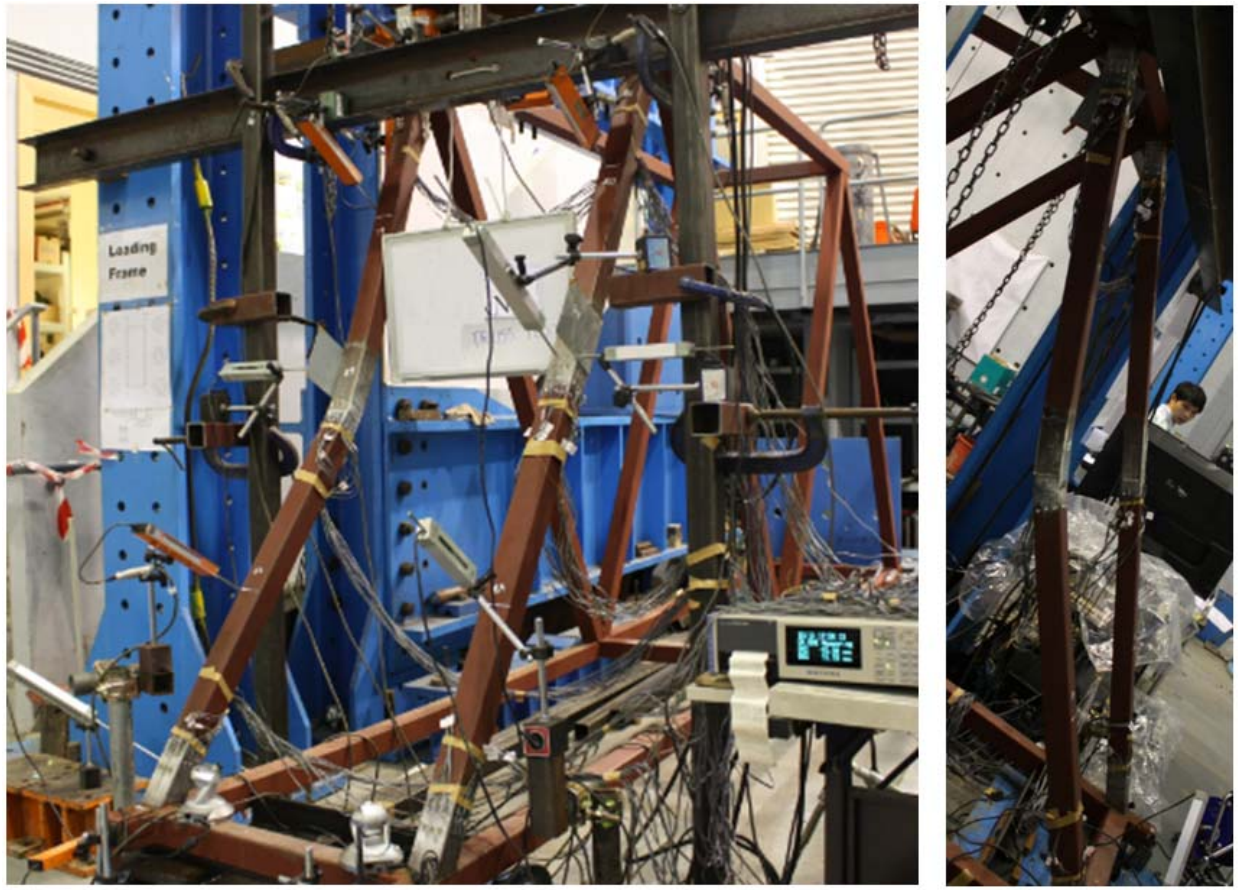

Figure 5.17 Buckling Mode of Set-1 Steel Truss

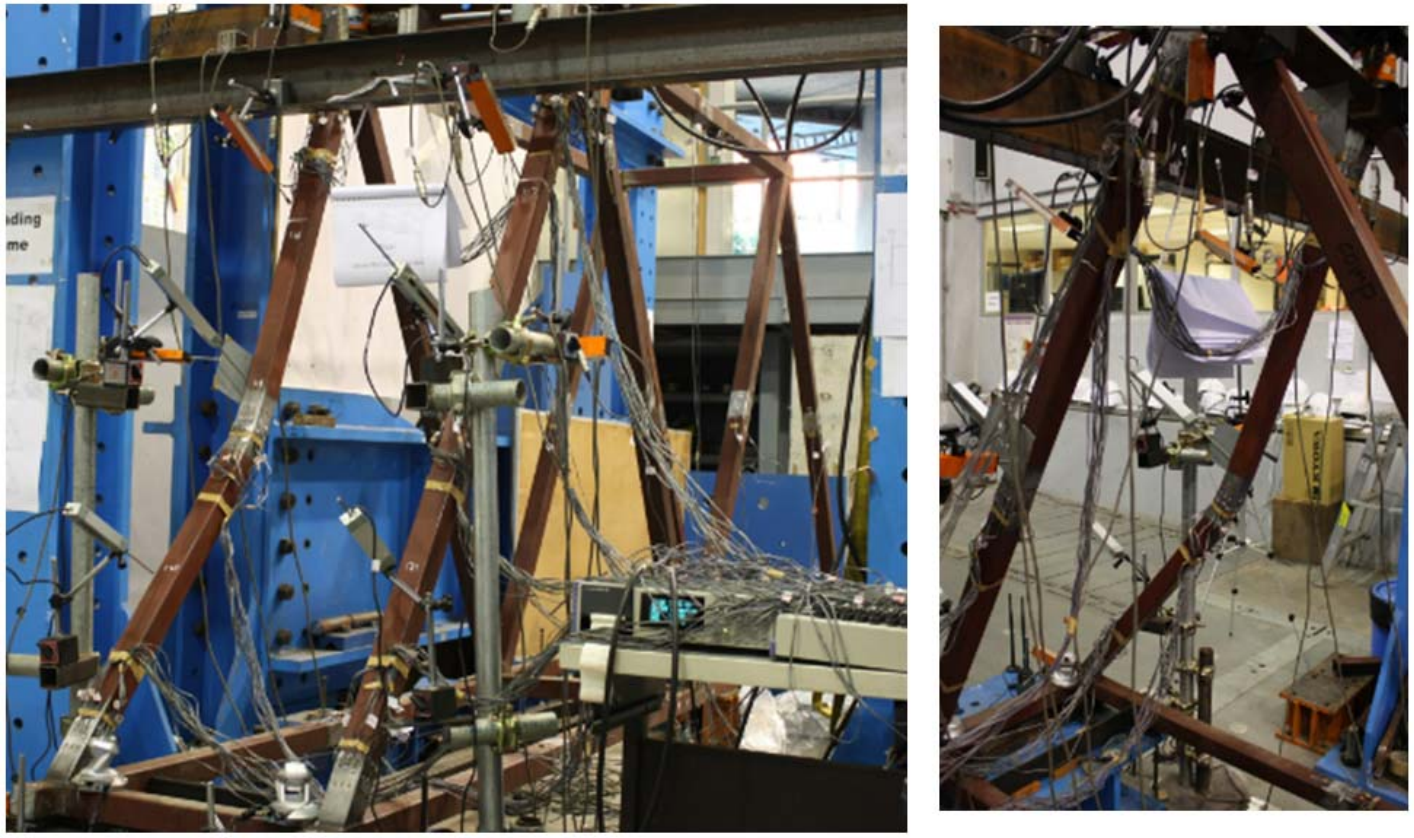

Figure 5.18 Buckling Mode of Set-1 Composite Truss

Figure 5.19 Buckling Mode of Set-2 Steel Truss

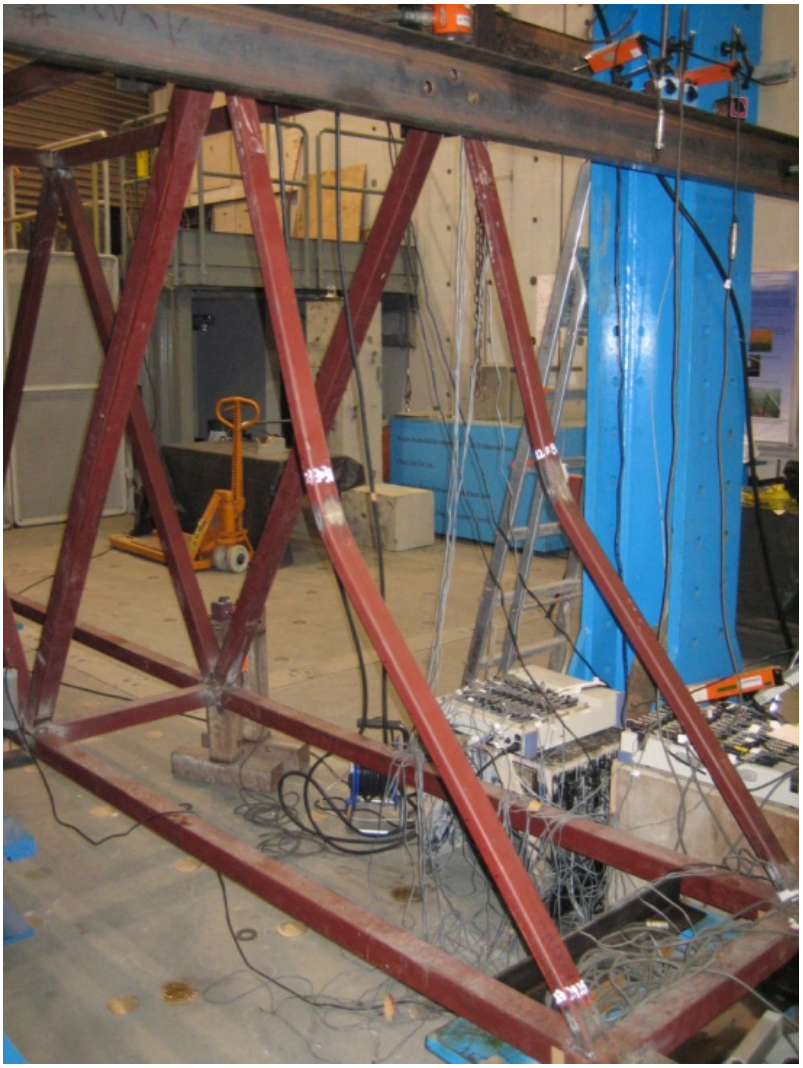

Figure 5.20 Buckling Mode of Set-2 Composite Truss

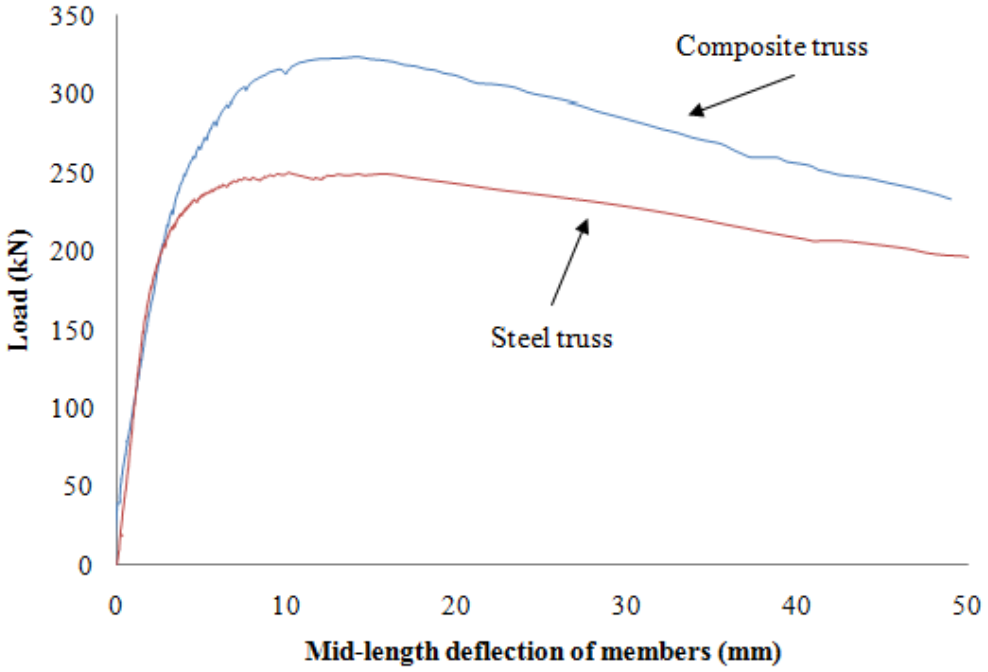

Figure 5.21 Load against In-plane Lateral Deflection Curves of Set-1 Truss

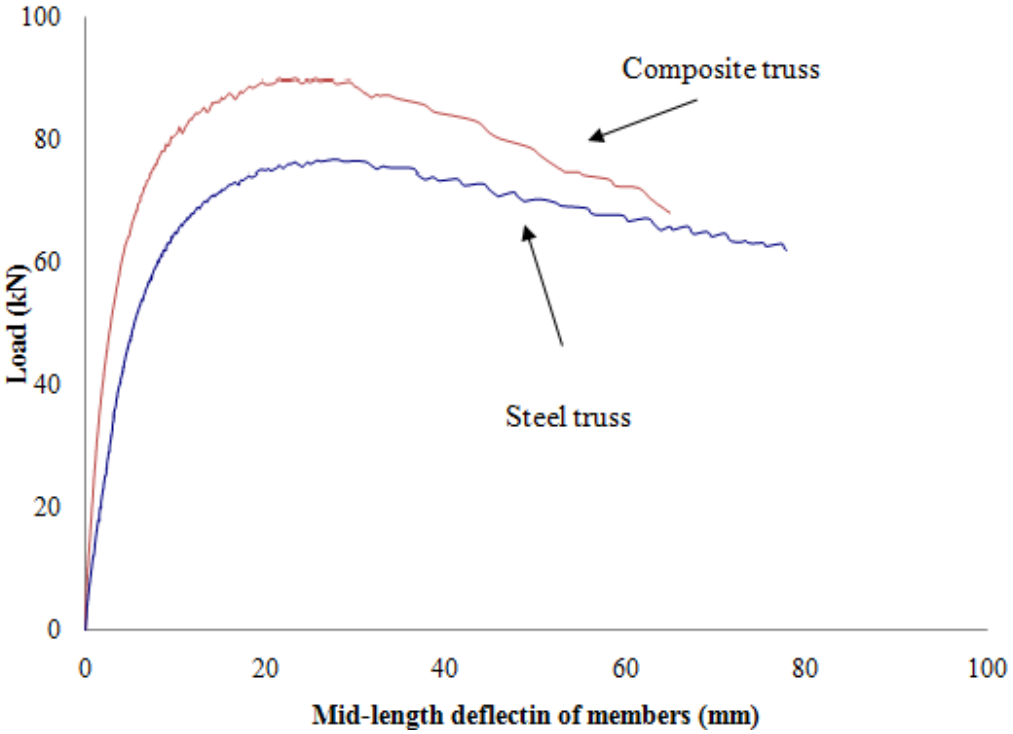

Figure 5.22 Load against In-plane Lateral Deflection Curves of Set-2 Truss

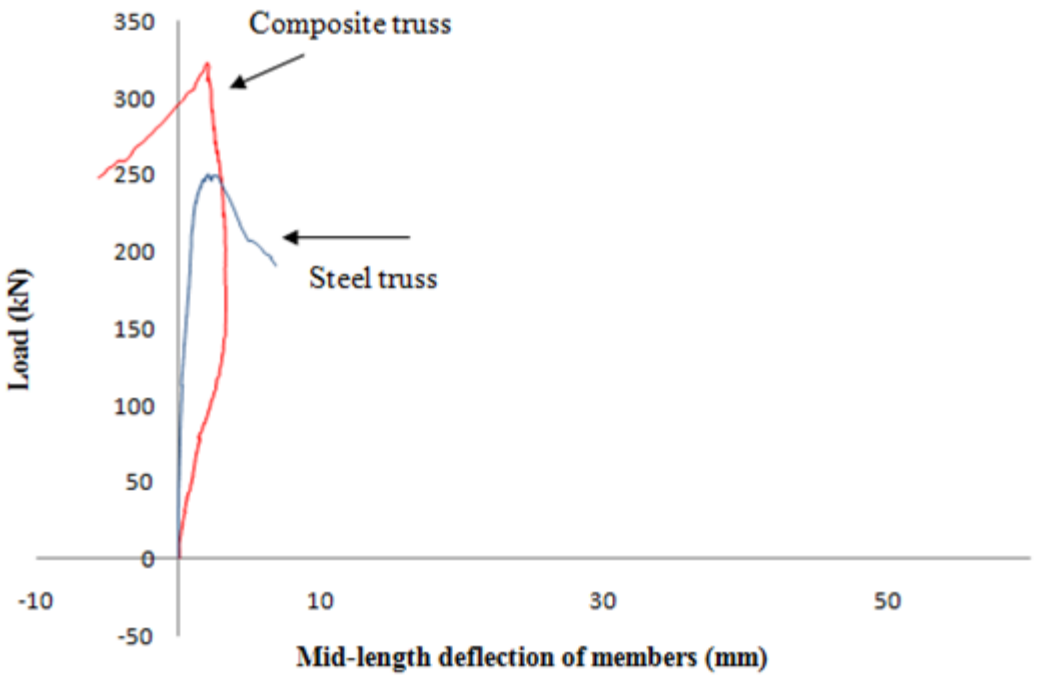

Figure 5.23 Load against Out-of-plane Lateral Deflection Curves of Set-1 Truss

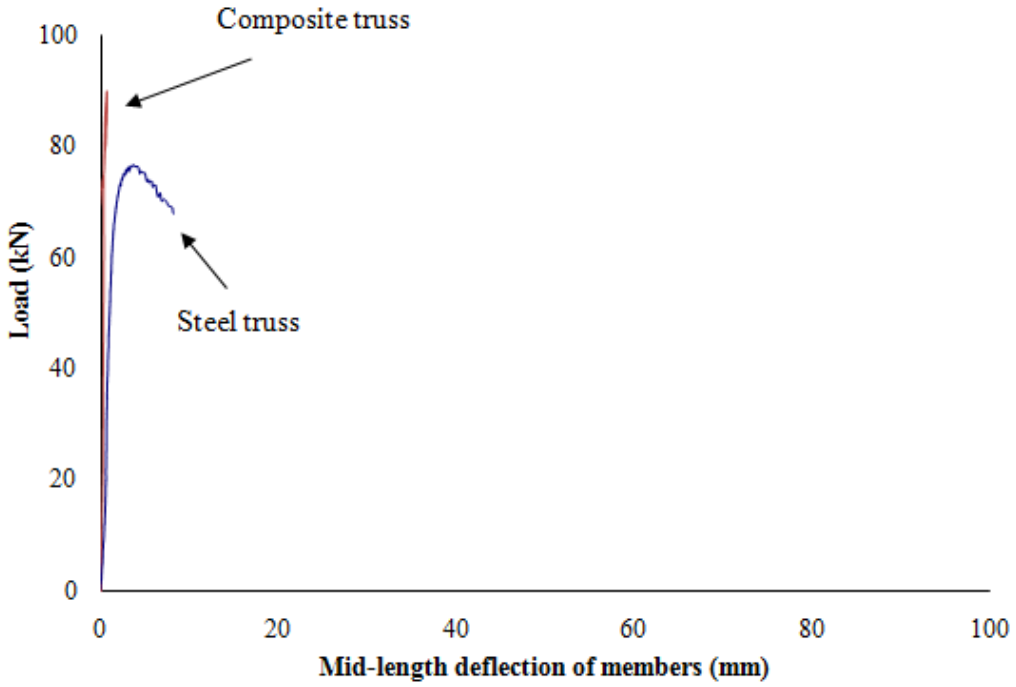

Figure 5.24 Load against Out-of-plane Lateral Deflection Curves of Set-2 Truss

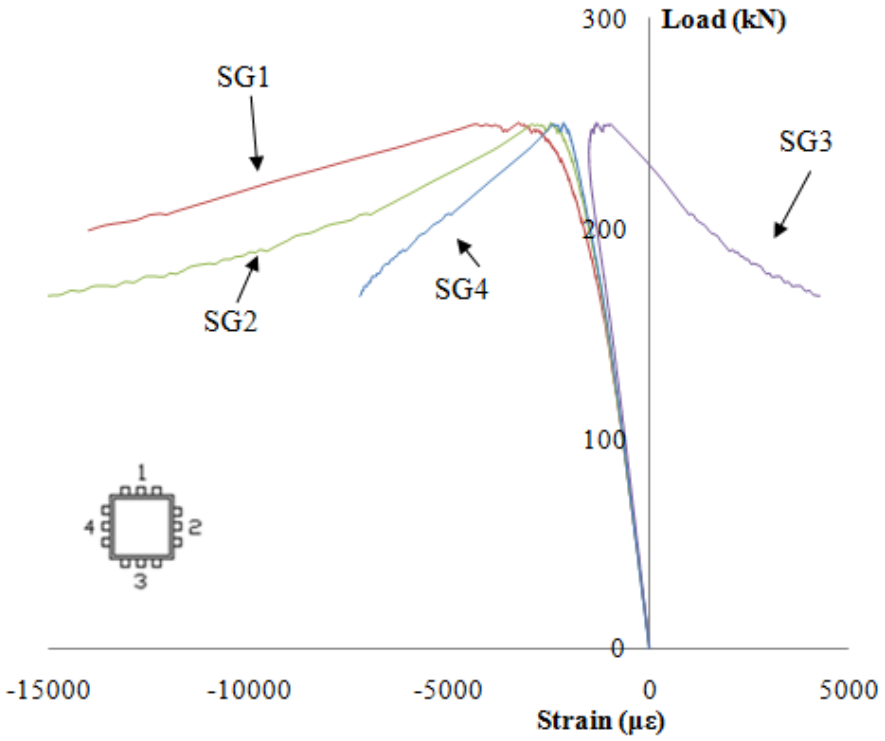

Figure 5.25 Load against Strain of Steel Truss 1

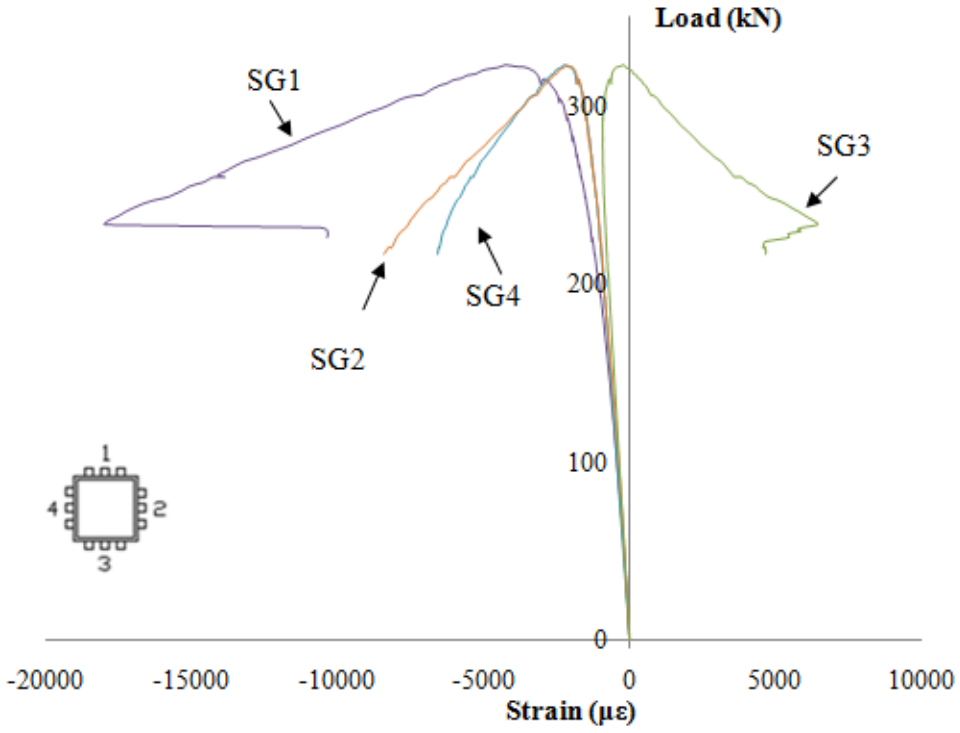

Figure 5.26 Load against Strain of Composite Truss 1

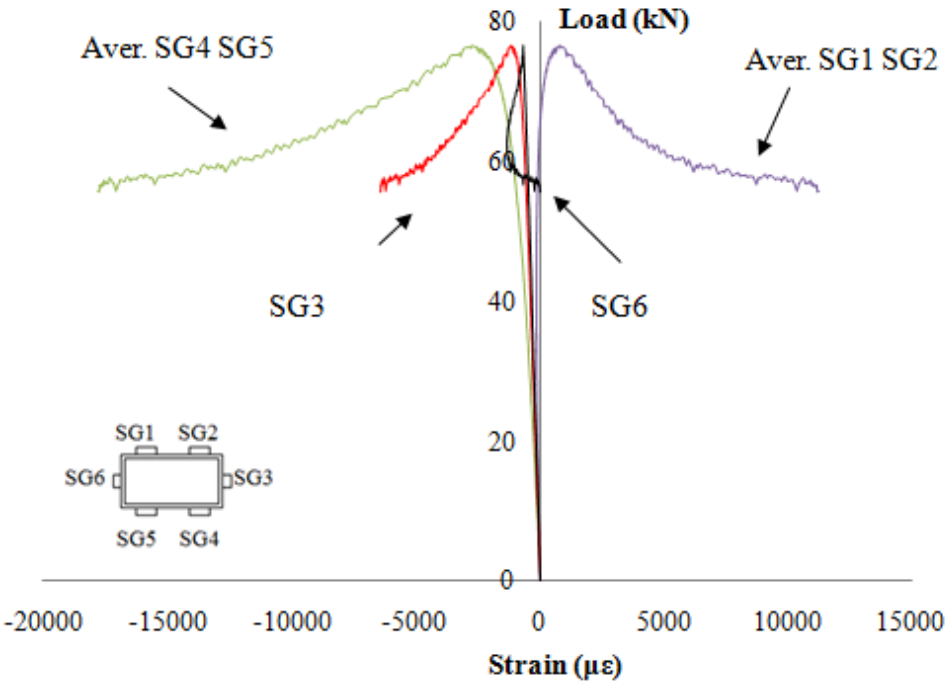

Figure 5.27 Load against Strain of Steel Truss 2

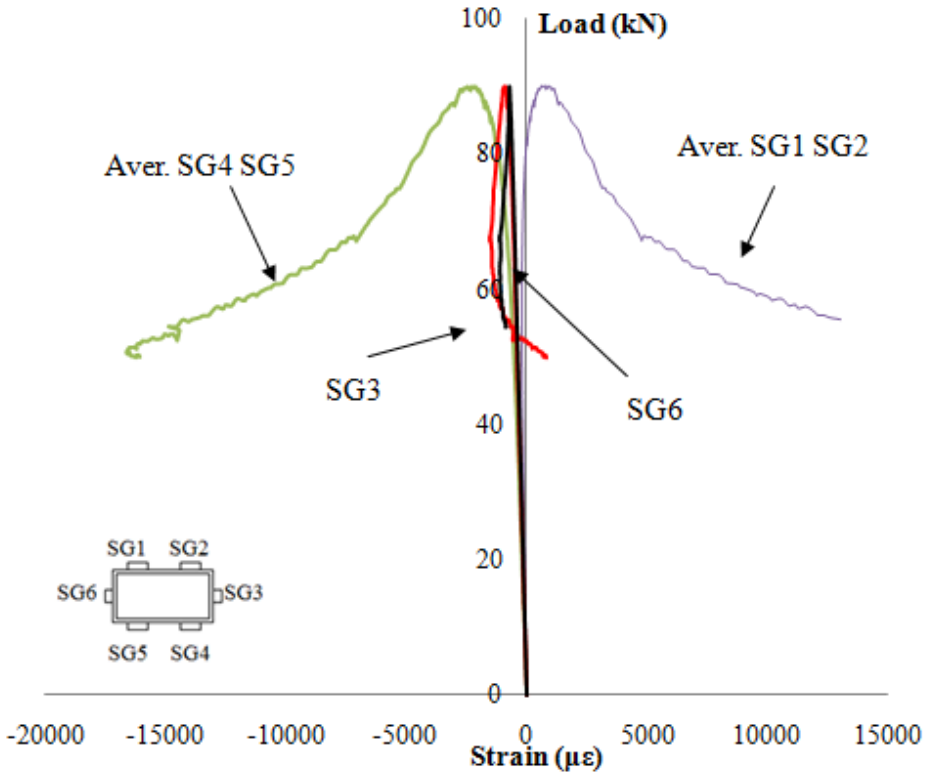

Figure 5.28 Load against Strain of Composite Truss 2

Inward buckling in steel tubular member

Outward buckling in CFS tubular member

Figure 5.29 Local Buckling in Steel and Composite Members

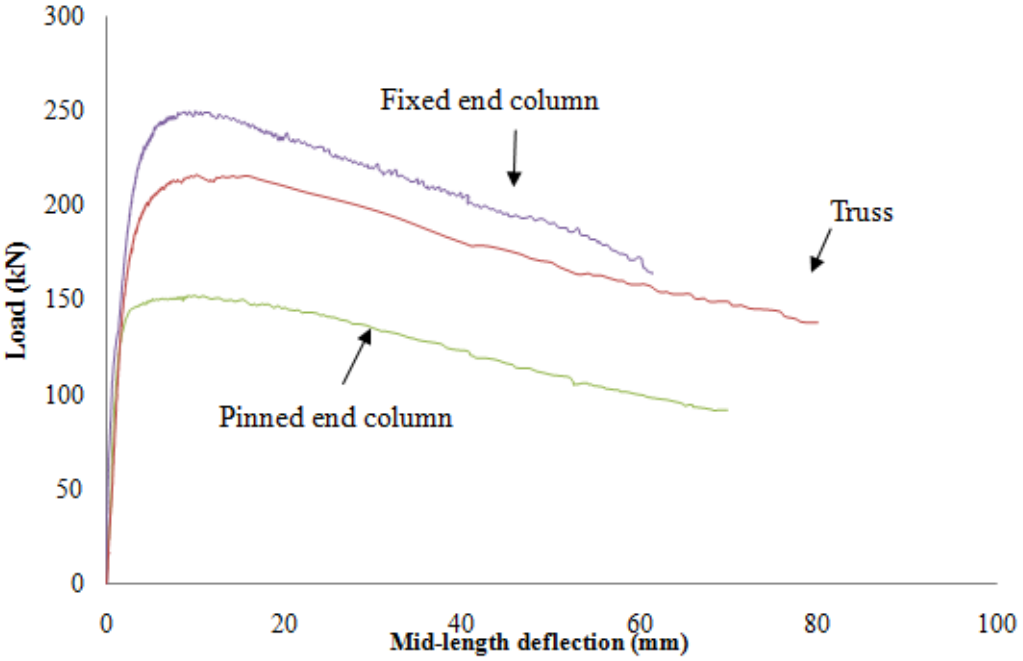

Figure 5.30 Member Force against In-plane Lateral Deflection of Steel Columns and Truss Member

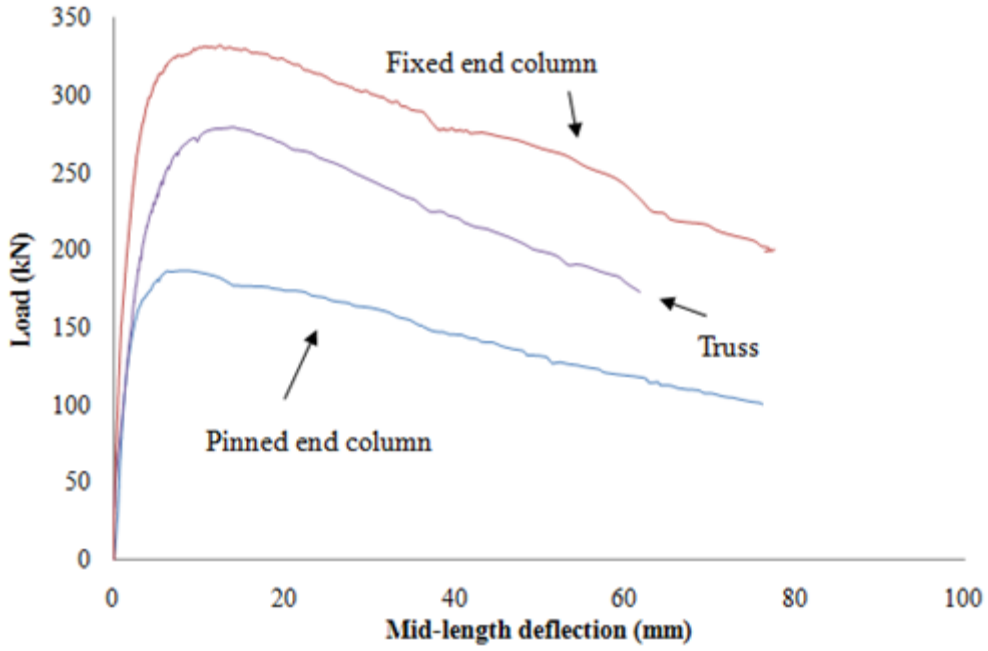

Figure 5.31 Member Force against In-plane Lateral Deflection of Composite Columns and Truss Member

Tables

Table 5.1 Material Properties on the Columns

Steel section	Width B (mm)	Depth D (mm)	Thickness t (mm)	Steel: Yield stress f_y (N/mm^2)	Steel: Ultimate tensile stress f_u (N/mm^2)	Steel: Young's modulus E_s (kN/mm^2)	f_u/f_y	Concrete: Age at testing (days)	Concrete: Compressive Stress f_c (N/mm^2)	Concrete: Young's modulus E_c (kN/mm^2)
60x60x3	60.40	60.30	3.10	407.98	480.22	206.36	1.18	34	40.96	22.17

Table 5.2 Test Results of Columns

Specimen	End condition	Applied load (kN)	Ratio: CFS column/ Steel column	Ratio: Fix/Pin
Steel tubular column	Pin	152.45	/	/
CFS tubular column	Pin	186.88	1.23	/
Steel tubular column	Fix	249.40	/	1.64
CFS tubular column	Fix	331.60	1.33	1.77

Table 5.3 Material Properties of the Members in the Steel and Composite Trusses

Truss	Steel section	Width B (mm)	Depth D (mm)	Thickness t (mm)	Steel: Yield stress f_y (N/mm^2)	Steel: Ultimate tensile stress f_u (N/mm^2)	Steel: Young's modulus E_s (kN/mm^2)	f_u/f_y	Concrete: Age at testing (days)	Concrete: Compressive Stress f_c (N/mm^2)	Concrete: Young's modulus E_c (kN/mm^2)
Set 1	60x60x3	60.20	60.20	3.10	404.11	473.55	205.72	1.17	56	41.16	22.73
Set 2	50x30x3	50.00	30.08	2.96	399.17	448.30	203.87	1.12	51	89.87	37.45

Table 5.4 Test Results of Steel and Composite Trusses

Set	Specimen	Applied load on truss (kN)	Failure member force (kN)	Ratio Composite/Steel
1	Steel truss	250.37	216.57	/
	Composite truss	323.09	279.47	1.29
2	Steel truss	76.61	66.27	/
	Composite truss	90.00	77.85	1.17

CHAPTER 6

FIRST-ORDER AND SECOND-ORDER ANALYSIS FOR DESIGN OF COMPOSITE BEAM-COLUMNS

6.1 Introduction

Steel-concrete composite beam-columns are widely used due to its advantages over the bare steel and reinforced concrete beam-columns as mentioned in Chapter 5. Many design codes such as Eurocode 4 (2004), AISC (2010) and AS5100 (2004) and CoPHK (2005) generally recommend the use of two design approaches as the first-order linear and second-order nonlinear analysis and design for steel-concrete composite members. For the linear analysis method, it simplifies the analysis process and complicates the design process which needs to allow for buckling and the second-order effects. The accuracy of this design method for predicting the capacity of isolated composite members under pinned and fixed end boundary conditions was reported by many researchers. However, the behavior of composite members under more realistic boundary conditions such as constitutive members in a truss has not been widely considered in previous research. The traditional linear analysis method of design assumes an effective length factor for different boundary conditions of a chord or a web member in a truss and assesses various factors to compensate for

buckling and second-order effects in the determination of buckling strength of individual members. Unfortunately, the accuracy on determination of the effective length highly affects the reliability of these methods. For some complicated and practical structures like trusses and curved structures, the accurate determination of effective length is difficult and sometime impossible. This chapter describes and compares the accuracy of the codified linear analysis and design methods in Eurocode 4 (2004), AISC (2010), AS5100 (2004) and CoPHK (2005) in predicting the resistances of composite columns, and steel and Concrete-Filled Steel (CFS) tubes acting as isolated columns with pinned and fixed end conditions and as constituent members in the trusses.

Similar to the tendency in design of steel structures, many design codes tend to recommend the use of second-order analysis and design method so as to obtain a more accurate result in an efficient manner. In current practice, the design of composite columns such as CFS and Concrete-Encased Steel (CES) columns is a member-based procedure which is based on the linear analysis in conjunction with effective length method, rather than a system-based approach utilizing the concept of advanced analysis. In principle, the second-order analysis can be used for any structural form when imperfections are considered and plastic functions for cross-sections are used. Both efficiency and precision are critical in analysis for practical structures made of many members and the use of a simple and reliable way to include nonlinear effects is important. Therefore, a more practical analysis and design method fulfilling the code requirements for second-order analysis is proposed in this chapter for design of steel-concrete composite beam-columns. The accuracy of the proposed method is verified by comparing the predicted results of columns

with results calculated according to the design method in Eurocode 4 (2004) as well as experimental test. The degree of conservatism of the initial imperfection provided from Eurocode 4 (2004) is also studied.

Furthermore, the capacities of the tested columns and members in the trusses in chapter 5 are compared with the predicted results by using the proposed method. With the verification and calibration carried out in this chapter and, without loss of generality, the proposed method can be applied to the design of practical composite beam-columns beyond the scope of the conventional design method and without the assumption of uncertain effective length factor which implies a significant improvement in accuracy and convenience as frame classification for use of effective length or alignment charts is no longer needed. Finally, recognizing stiffness of a member and a frame varied by presence of forces on them such as brace in tension is stiffer than in compression, an important error for the linear analysis of using the stiffness under unloaded condition can be eliminated.

6.2 Codified Design Methods for Composite Columns

Many design codes such as Eurocode 4 (2004), AS5100 (2004) and CoPHK (2005) provide conventional design method for composite columns, which allows engineers to use the first-order linear analysis and effective length method to check the strength and stability of each member separately. The codified methods including Eurocode 4 (2004), CoPHK (2005), AISC (2010) and AS5100 (2004) in checking the axial capacity of composite columns are briefly introduced in this section. In the linear

analysis method below, the second-order effects are only included in design process, such that many factors are required to be determined for consideration of buckling and second-order effects. In other words, the analysis process is simplified but the design process is much complicated and unreliable.

6.2.1 Eurocode 4 and CoHPK

The design methods in Eurocode 4 (2004) and CoPHK (2005) are similar for composite columns, the section capacity of the composite columns is determined by summation of the resistances of the concrete, steel and reinforcement as follows.

$$P_{cp} = A_s f_{yd} + 0.85 A_c f_{cd} + A_r f_{rd} \tag{6.2.1}$$

where P_{cp} is the compressive strength of a composite cross-section, A_s, A_c and A_r, and f_{yd}, f_{cd} and f_{rd} are the cross-sectional areas and the design strengths of the steel, concrete and reinforcement respectively.

For concrete filled rectangular and square hollow section, the coefficient of 0.85 in the second term of Eq. (6.2.1) is replaced by 1.0. For concrete filled circular hollow section, the strength of concrete would be further increased under specific conditions by considering the confinement effect due to the external steel tube surrounding the in-filled concrete.

To allow for the buckling effect, a reduction factor χ, which is based on the effective slenderness ratio and section type, is multiplied to the section capacity of the columns, and then the compressive resistance is given as follows.

$$P_{cd} = \chi(A_s f_{yd} + 0.85 A_c f_{cd} + A_r f_{rd}) \tag{6.2.2}$$

The reduction factor χ can be determined by,

$$\chi = \frac{1}{\phi + \sqrt{\phi^2 - \overline{\lambda}^2}} \tag{6.2.3}$$

and

$$\phi = \frac{1}{2}\left[1 + \alpha(\overline{\lambda} - 0.2) + \overline{\lambda}^2\right] \tag{6.2.4}$$

where α is the imperfection factor and $\overline{\lambda}$ is the relative slenderness ratio and can be expressed as,

$$\overline{\lambda} = \sqrt{\frac{P_{Rk}}{P_{cr}}} \tag{6.2.5}$$

where P_{Rk} is the characteristic value of the compressive capacity and P_{cr} is the elastic critical buckling load for the relevant buckling mode.

6.2.2 AISC

Design methods for composite columns with encased and in-filled sections are provided in AISC (2010) and the compressive strength of the composite columns is calculated under two conditions as follows.

For $P_{cr} \geq 0.44 P_{cp}$

$$P_n = P_{cp}[0.658^{(\frac{P_{cp}}{P_{cr}})}] \tag{6.2.6}$$

For $P_{cr} < 0.44P_{cp}$

$$P_n = 0.877P_{cr} \tag{6.2.7}$$

where $P_{cr} = \pi^2(EI_{eff})/(KL)^2$, and P_{cp} is the nominal axial compressive strength without consideration of length effects. The expression for P_{cp} for encased and in-filled sections are given below,

For encased composite members

$$P_{cp} = A_s f_y^{'} + A_r f_r^{'} + 0.85A_c f_c^{'} \tag{6.2.8}$$

where $f_y^{'}$, $f_r^{'}$ and $f_c^{'}$ are the specified minimum yield stress of steel, reinforcement and specified minimum compressive strength of concrete respectively.

For in-filled composite members, different expressions for compact, non-compact and slender sections are given.

A1. For compact sections

$$P_{cp} = P_p \tag{6.2.9}$$

where $P_p = A_s f_y^{'} + (A_c + A_r \frac{E_s}{E_c})0.85 f_c^{'}$, and the coefficient of 0.85 is replaced by 0.95 for circular sections, and E_s and E_c are modulus of elasticity of steel and concrete.

A2.For non-compact sections

$$P_{cp} = P_p - \frac{P_p - P_y}{(\lambda_r - \lambda_p)^2}(\lambda - \lambda_p)^2 \tag{6.2.10}$$

where $P_y = A_s f_y^{'} + (A_c + A_r \frac{E_s}{E_c})0.7 f_c^{'}$, and λ, λ_p and λ_r are the slenderness ratios of the member, compact and non-compact element

A3.For slender sections

$$P_{cp} = A_s f_{y,cr} + (A_c + A_r \frac{E_s}{E_c})0.7 f_c^{'} \tag{6.2.11}$$

and $f_{y,cr}$ is the reduced steel strength for slender steel section and it is equal to $f_{y,cr} = 9E_s / (b/t)^2$ for rectangular concrete-filled hollow sections, and $f_{y,cr} = 0.72 f_y^{'} / \left[(D_{out}/t) f_y^{'} / E_s \right]^{0.2}$ for round concrete-filled hollow sections, where b, D_{out} and t are the inner and outer diameters and thickness of the tube.

Finally, the design compressive resistance of composite columns can be obtained by multiplying the resistance factor of 0.75 as,

$$P_{cd} = 0.75 P_n \tag{6.2.12}$$

6.2.3 AS5100

The ultimate section capacity of concrete-filled rectangular and circular steel tubular columns can be determined by summing the axial capacity of the steel tube and concrete and reinforcement as follows.

$$P_{cp} = 0.9A_s f_y + 0.6A_c f_c + 0.9A_r f_r \tag{6.2.13}$$

where f_c is characteristic compressive strength of concrete. The value of 0.9 is the capacity factor for steel and reinforcement, and 0.6 is the capacity factor for concrete. The stability of CFS tubular members is considered by multiplying a buckling reduction factor χ in calculating the member resistance as,

$$P_{cd} = \chi P_{cp} \tag{6.2.14}$$

and

$$\chi = \xi\left[1 - \sqrt{1 - \left[\frac{90}{\xi\lambda}\right]^2}\right] \tag{6.2.15}$$

$$\xi = \frac{\left(\frac{\lambda}{90}\right)^2 + 1 + \eta_0}{2\left(\frac{\lambda}{90}\right)^2} \tag{6.2.16}$$

$$\lambda = \lambda_\eta + \alpha_a \alpha_b \tag{6.2.17}$$

$$\eta_0 = 0.00326(\lambda - 13.5) \geq 0 \tag{6.2.18}$$

$$\lambda_\eta = 90\overline{\lambda} \tag{6.2.19}$$

$$\alpha_a = \frac{2100(\lambda_\eta - 13.5)}{\lambda_\eta{}^2 - 15.3\lambda_\eta + 2050} \tag{6.2.20}$$

where α_b is the section constant.

Similar to Eurocode 4 (2004) and CoPHK (2005), the beneficial effect due to the confinement on concrete core by the circular hollow steel tube can be taken into account in AS5100 (2004) when the relative slenderness and eccentricity are within the limitation.

The accuracy on the codified methods in prediction the capacity of CFS tubular columns and members in the truss system is given in Section 6.5.

6.3 Second-order Analysis and Design Method for Composite Members

Due to the disadvantages and inconvenience of the traditional design method, the second-order analysis and design method for composite beam-columns is proposed in this chapter. In second-order analysis, the nonlinear effects are directly included in the analysis so that the estimation of effective length is no longer required, and member section capacity can directly be used for design. The individual member check is replaced by the section capacity check in a single equation in place of the approach requiring the use of several parameters embedded in several checking equations such as the section capacity and the member buckling checks. This section presents the section capacity check equations for composite beam-columns so that the method can be used by engineers and researchers in second-order and advanced analysis of composite columns and frames.

6.3.1 Section capacity check

The finite element method is used for beam-column element formulation and the fifth-order imperfect PEP element is adopted for second-order analysis of composite structures to include the geometric nonlinearity in analysis. The element formulation

of the fifth-order PEP element for steel structure has been described in Chapter 3. For steel-concrete composite structures, the equivalent flexural stiffness of the composite column $E_{comp}I_{comp}$ should be used in formulation of element and stiffness matrices and the section capacity check equations should be modified by using the properties of composite columns so that the second-order analysis method can be applied for composite members. The equivalent flexural stiffness of the composite columns can be taken according to each design code, in this study, the flexural stiffness equation from Eurocode 4 (2004) is used and expressed as $E_{comp}I_{comp} = 0.9(E_sI_s + E_rI_r + 0.5E_cI_c)$, where E_s, E_r and E_c are the modulus of elasticities of steel, reinforcement and concrete and I_s, I_r and I_c are the second moment of areas of steel, reinforcement and concrete.

In second-order analysis and design method, the section capacity check under two conditions is carried out for composite columns. When the applied force is larger than the section capacity of concrete section (i.e. $P>P_{pm}$), Eq. (6.3.1) will be used and it allows for the effects of axial force and moment in the section capacity equation. The first term of Eq. (6.3.1) is the section capacity factor due to the axial force and the second and third terms are the factors due to the moments in two principal directions. When the applied force is less than the capacity of concrete section (i.e. $P\leq P_{pm}$), only the applied moments are considered since the axial force does not reduce the failure load and Eq. (6.3.2) is then used for section capacity check. These two sets of section capacity check equations are given below.

$$\frac{P-P_{pm}}{P_{cp}-P_{pm}}+\frac{M_x+P(\delta_x+\Delta_x)}{M_{cpx}}+\frac{M_y+P(\delta_y+\Delta_y)}{M_{cpy}}=\phi_{SCF}\leq 1 \text{ , when } P>P_{pm} \qquad (6.3.1)$$

$$\frac{M_x + P(\delta_x + \Delta_x)}{M_{cpx}} + \frac{M_y + P(\delta_y + \Delta_y)}{M_{cpy}} = \phi_{SCF} \le 1, \qquad \text{when } P \le P_{pm} \qquad (6.3.2)$$

where P is the axial force, P_{pm} is compressive capacity of concrete cross-section, P_{cp} is compressive capacity of a composite cross-section, M_x and M_y are the external moments about the x and y axes, $P(\delta_x+\Delta_x)$ and $P(\delta_y+\Delta_y)$ are the P-δ and P-Δ moments about the x and y axes, M_{cpx} and M_{cpy} are the moment capacities of composite cross-section about the x and y axes.

In every load cycle, a small load increment of, say 5 to 10% of expected design load, is applied to the structure by an incremental-iterative procedure until the design load is achieved in which the section capacity factor ϕ_{SCF} in Eq. (6.3.1) or Eq. (6.3.2) should not be greater than unity for second-order elastic design.

6.3.2 Member initial imperfection for composite cross-sections

In second-order analysis and design method, the member initial imperfection should be assigned to the members. The importance of both the member and global imperfections has been discussed in Chapters 3 and 4. Ignoring or assigning the imperfections improperly is dangerous. Many design codes provide the member initial imperfection values for different composite cross-section types. Reviewing different design codes, the member initial imperfection provided by Eurocode 4 (2004) covers most common composite cross-section types and the values are summarized in Table 6.1. For the verification examples in the next section, the member initial imperfection values according to Eurocode 4 (2004) are assigned to

the members for different composite cross-sections.

6.3.3 Numerical procedure

The load control Newton-Raphson method combined with the arc-length or the minimum residual displacement method as described in Chapter 3 is capable of tracing the path up to and beyond the limit point without numerical divergence. And the minimum residual displacement guarantees a minimum equilibrium error in each iteration, therefore, it is used in the present analysis.

6.4 Numerical Examples

6.4.1 Composite columns under axial load

A parametric study of composite columns is conducted here. Two CFS tubular sections including one rectangular and one square hollow section, and one CES section are studied. The dimensions of the specimens are shown in Figure 6.1. The capacities of the specimens are predicted according to the proposed second-order analysis method and first-order linear method in Eurocode 4 (2004). The columns are assumed to be pinned at both ends. The modulus of elasticities of steel and reinforcement are assumed to be 205kN/mm^2 and the steel strength, concrete cylinder compressive strength are tabulated in Table 6.2. The plates slenderness ratio are chosen to be less than the value of $D_{out}/t \le 52\sqrt{235/f_y}$ for concrete filled

hollow section and $B/T_f \le 44\sqrt{235/f_y}$ for concrete-encased section, in which D_{out} is the outer diameter of the tube and B is the width of the flange, and t and T_f are the thickness of tube and flange, so that the effect due to local buckling can be neglected. The capacities of the columns with relative slenderness ratios $\overline{\lambda}$ from around 0.05 to 2 are calculated, in which, the limit of 2 is the maximum permissible relative slenderness ratio for the simplified design method in Eurocode 4 (2004).

The predicted capacities by proposed method for specimens 1, 2 and 3 are tabulated in Tables 6.3, 6.4 and 6.5 respectively. The first column of the tables lists the lengths of the specimens and the second column represents the relative slenderness ratios of the columns in the axis of buckling. The capacities with two imperfections of L/300 and L/400 for CFS tubular columns and two imperfections of L/150 and L/250 for CES columns are included in the tables, where L is the length of the columns. The larger imperfections of L/300 and L/150 are the recommended imperfections in Eurocode 4 (2004) for CFS tubular columns and CES columns respectively. The predicted capacities of specimen 3 with imperfection of L/1000 for the relative slenderness ratio less than 0.22 are also included for completeness. Finally, the predicted results according to the linear design method in Eurocode 4 (2004) are included and compared with the results predicted by the proposed method in the tables. The reduction in capacity due to the increase of member length for both proposed method and code method are graphically presented in Figures 6.2, 6.3 and 6.4 for specimens 1, 2 and 3 respectively.

The results in the tables show a good agreement on the predicted capacities between the proposed method and code method. For CFS tubular columns (specimen 1 and 2), the average ratios of the loads predicted by proposed method and by the code method are both 0.95 for specimen 1 and 2 for imperfection equal to $L/300$ with a standard deviation of 0.02, and average load ratios are 0.99 (specimen 1) and 0.98 (specimen 2) for imperfection equal to $L/400$ with a standard deviation of 0.02 (specimen 1) and 0.01 (specimen 2). For CES columns, the average ratio of the proposed method to the code method is 0.87 for imperfection equal to $L/150$ with a standard deviation of 0.04, and average ratio is 0.97 for imperfection equal to $L/250$ with a standard deviation of 0.02 respectively.

The results indicate that the imperfections of $L/300$ and $L/150$, which are the suggested imperfections in the code for CFS tubular columns and CES columns, are conservatively appropriate for use with second-order analysis. For columns with relative slenderness ratios between 0 and 0.2, the differences in predictions by both methods increase and the proposed method gives a lower capacity, because the buckling reduction factor in code is exactly equal to 1 when the relative slenderness ratio is smaller than 0.2 which has no reduction in the compressive strength of the columns due to the buckling effect. However, in the present method, second-order moments due to initial member imperfection still exist and this make the proposed method to have lower predicted results. The consideration of imperfection for stocky members leads to the difference between two sets of results. Therefore, for specimen 3, a very small imperfection equal to $L/1000$ is chosen for proposed method and the results are compared with code results for slenderness ratio less than 0.22. The differences in results between these two methods are less than 1%. Thus, it is

recommended to adopt a lower imperfection when the slenderness ratio is small otherwise the second-order analysis may give an over-conservative prediction for stocky columns.

6.4.2 Composite columns under axial load and end moments

When the column is under an axial load with equal end moments causing the single curvature with r_m=1, where r_m is the ratio of the end moments, the moment diagram is given as Figure 6.5a. Under such a load application, the most critical section of the member is located at the mid-height of the column. However, when the end moment ratio is not equal to unity, the critical location of the member shifts away from the mid-height of the column. Figures 6.5b and 6.5c show the shift of critical location at the column under axial together with smaller and larger end moments respectively. However, this effect cannot be reflected in Eurocode 4 (2004) as the reduction factor μ for moment capacity is not related to the magnitude of end moments. In this section, the capacities of the columns under axial load and equal end moments are studied and the predicted capacities by the proposed method with two imperfections are compared. The stress block reduction factor is taken as unity for both methods in prediction of capacities for consistency and simplicity.

The columns with lengths equal to 3, 4 and 5 meters and end moments ranged from 100 to 400 kNm with 100 kNm increment for CFS tubular columns and end moments of 100, 200 and 300 kNm for CES columns are studied. Tables 6.6, 6.7 and 6.8 list the predicted capacities by the code method and the proposed method with different imperfections.

Predicted results of CFS tubular columns by proposed method for both imperfections of $L/300$ and $L/400$ are close to the code method. The average load ratios of the proposed method to the code method are 0.96 to 0.97 for imperfection of $L/300$ with a standard deviation of 0.01 to 0.02, and average ratio is 0.99 for imperfection of $L/400$ with a standard deviation of 0.01 to 0.02. For CES columns, the average ratio of the proposed method to the code method is 0.89 for imperfection equal to $L/150$ with a standard deviation of 0.02, and the average ratio is 0.98 for imperfection equal to $L/250$ with a standard deviation of 0.02.

6.4.3 Comparisons with test results

The predictions on the resistances of composite columns based on proposed method are compared with experimental results conducted by De Nardin and El Debs (2007), Bridge (1976), and Neogi et al. (1969). All specimens were pinned end CFS tubular columns under concentric or eccentric load with equal end eccentricity and bent in single curvature. Totally 20 slender composite columns are studied here. The main variables in these specimens are the eccentricities, steel shapes and slenderness ratios, and the details of each column are provided in Tables 6.9 and 6.10 for clarity.

De Nardin and El Debs (2007) tested six numbers of 1.2 meter long CFS tubular columns which included two rectangular, two square and two circular columns under concentric load. The results from Bridge (1976) included four square CFS tubular columns under axial load with same end eccentricity ratios equal to 0, 0.187, 0.25

and 0.417. The test results from Neogi et al. (1969) included 12 circular CFS tubular columns under eccentric load with eccentricity ratios equal to 0.23 and 0.28.

Comparisons between the results from experimental tests and second-order analysis and design method are listed in Tables 6.9 and 6.10 for verification. The average ratios of the test to analysis results for three tests are 1.09, 0.99 and 1.02 with respective standard deviation equal to 0.04, 0.04 and 0.03. Thus, the second-order analysis gives close and slightly conservative predictions in general.

6.4.4 Portal frame with composite columns and steel beam

A portal frame made of composite columns and steel beam with dimensions and members sizes shown in Figure 6.6 is studied here. The beam connects to the columns rigidly and the columns are fixed to the ground. The capacities of the composite columns are computed by using the design method in Eurocode 4 (2004) and the proposed second-order analysis and design method. In linear analysis, the effective length of the columns is assumed by using the K-factor method specified in design code and the K-factor for column is 1.08 in this example. The results by both design methods are given in Table 6.11. Only one element per member is used for modeling, and the rigid connection is assumed for beam and column. The design moment obtained from the proposed second-order analysis includes both first-order linear and second-order moments, whereas the linear design method considers only the second-order effects via code formulae.

The results from this example show that similar capacities of the composite columns can be obtained for this portal frame by using both methods. However, in most practical cases the effective length cannot be determined easily and accurately, and therefore the traditional linear design method cannot give a reasonable result while the high accuracy of the proposed second-order analysis is not limited to the degree of complexity of the structure. Thus, the proposed method is considered as a more reliable and robust design method than the first-order linear analysis used with the effective length assumption.

6.5 Comparisons of Codified and Second-order Analysis Methods on Isolated Columns and Members in the Trusses

The test results of CFS tubular columns and composite trusses given in Chapter 5 are used to compare with the predicted results from design codes and proposed second-order analysis and design method to verify the accuracy of design code methods including Eurocode 4 (2004), CoPHK (2005), AISC (2010) and AS5100 (2004) and second-order analysis method in design of composite isolated members and structural systems.

For completing the comparisons of the test results in Chapter 5, the test results on the steel isolated columns and steel truss are also compared with the codified methods including Eurocode 3 (2005), CoPHK (2005), AISC (2010) and AS5100 (2004) and

second-order analysis and design method for steel structures as described in Chapter 4.

6.5.1 Comparisons on isolated columns

6.5.1.1 Codified method

The material factors reducing the strengths and modulus of elasticities of steel and concrete are taken as unity when compared with the test and predicted results. The effective length factors equal to 1.0 (L_e=2000) and 0.5 (L_e=1000) are assumed for the pinned and fixed end conditions respectively. Predicted capacity according to the different design methods are summarized and compared in Table 6.12.

Generally speaking, for steel columns under pinned and fixed end conditions, conservative predictions are obtained from Eurocode 3 (2005), AISC (2010) and CoPHK (2005) with an under-estimation around 5% to 23%, and close estimations are made by AS5100 (2004) (under-design by 1%-3%). For CFS tubular columns under pinned and fixed end conditions, highly conservative predictions are obtained from AISC (2010) (over-design by 29%-35%) due to the conservative resistance factor, and the reasonable predictions are made by the other codes with the differences less than 7%. Although the design codes such as the AS5100 (2004), among others, overestimate the columns capacities. Material factors have been adopted in these codes but not considered here for consistency, and therefore the final design in these codes should still warrant a design with adequate factor of safety.

6.5.1.2 Second-order analysis and design method

Similar to the comparisons in section 6.4, two initial imperfections equal to $L/300$ and $L/400$ are used for both steel and composite members in prediction the columns resistances to demonstrate the degree of conservatism of the recommended magnitude of imperfections. The load increment factor 0.01kN is used in analysis until the section capacity factor is equal to 1.0.

The predicted results for both columns and members in the trusses are shown in Table 6.13. For the columns under pinned and fixed end conditions, the ratios of test to predicted results are 1.09 and 1.08 for steel tubular columns, and 1.14 and 1.03 for CFS tubular columns with the initial imperfection equal to $L/300$, and closer predictions are made with the imperfection of $L/400$ that the ratios are 1.02 and 1.03 for steel tubular columns, and 1.08 and 0.98 for CFS tubular columns.

6.5.2 Comparisons on members in the trusses

6.5.2.1 Codified method

In the tested trusses, end movements of the members were allowed but their connections to other members provided partial restraints. Hence, the boundary condition of the truss members was between the extreme pinned and fixed end conditions. The predicted resistances of the members according to those design codes by assuming the pinned and fixed end conditions are compared with

experimental results and reported in Table 6.12. As expected, very conservative predictions are made with the differences from 40% to 74% for steel tubular member and 44% to 92% for CFS tubular members if the pinned end condition is assumed which implies an uneconomical design. If the fixed end boundary condition is assumed, the capacity of the member is overestimated for steel tubular member in the range of 3% to 16%, and CFS tubular member with 21%, with the exception for AISC (2010) which gives a load below the tested load.

6.5.2.2 Second-order analysis and design method

The analysis model of the trusses is given in Figure 6.7. The center-to-center length of the members is used in the model and rigid connection between members is assumed. The analysis results with two imperfection values are presented together with test results in Table 6.13. The predicted failure loads of the members in the trusses are between the failure loads of isolated steel and CFS tubular columns, this indicates that the interactive effect between the members can be simulated in the analysis model with actual member end condition modeled. A close and conservative prediction is made with the discrepancy within 5% for both steel and CFS tubular trusses members when using the imperfection of $L/400$.

6.5.3 Comments on studied design methods

The comparisons show that the conservative predictions are obtained for steel columns by the design codes with the exception of AS5100 (2004) which gives aggressive ultimate load predictions, and close predictions for composite columns

are made except with AISC (2010) which underestimates considerably the resistances of the CFS tubular columns. The comparisons on the test and predicted results of trusses members according to the design codes by assuming the effective length as member length for pinned and half of member length for fixed end conditions indicate that the pinned end assumption underestimates the resistances of the members which led to an uneconomic design, while the fixed end assumption overestimates the capacities of the members and the design becomes non-conservative. The main disadvantage of using the effective length method was demonstrated that the idealized pinned and fixed end conditions do not exist in practice and the results by either assumption are inaccurate, and the effect due to bracing members cannot be taken into account directly and accurately. The comparisons on the results by the proposed method also indicate that the second-order analysis and design method not only provides an accurate design solution, but also avoids uncertain approximation of effective lengths which involves complications in sway or non-sway frame classification or determination from inspection of buckling mode shape. Lastly, the change of members and frame stiffness in the presence of loads is considered in the second-order analysis but not in the linear analysis and this consideration makes the linear analysis method unsuitable for uses in design of structures susceptible to buckling and second-order effects.

6.6 Concluding Remarks

This chapter has reviewed the first-order linear analysis and design method in several international design codes for predicting the capacity of steel-concrete

composite beam-columns. The accuracy of these design codes in predicting the resistances of isolated columns and members of trusses has been given. The uncertainties in estimation of effective length in structural systems have been emphasized and the second-order analysis and design method has been proposed for design of composite beam-columns. The advantages of the proposed method, which include avoidance of complicate and uncertain processes like estimation of effective length factor and use of amplified first-order moment for consideration of the second-order effects, have been described in this chapter. As the second-order moments are directly considered in the section capacity check, the proposed method is more rational with a more accurate reflection of the true behavior of the members and a considerable simplification on design of composite beam-columns. The failure loads of columns with two CFS tubular sections and one CES section under axial load with and without end moments and the composite columns in a portal frame have been analyzed by the proposed method with the results compared well against the design method in Eurocode 4 (2004). This indicates that the proposed method is consistent with the design output by the established code and can be used for practical structural design. Further, the good agreement of the failure loads between the proposed method and laboratory tests including isolated columns and members in the structures verifies the accuracy of this second-order analysis and design method for composite beam-columns design. Without loss of generality, the proposed method can be applied to the design of complex and large composite structures of which the reliability of the effective length method is in doubt. Further, the present method considers change of stiffness in the presence of loads on structures.

Figures

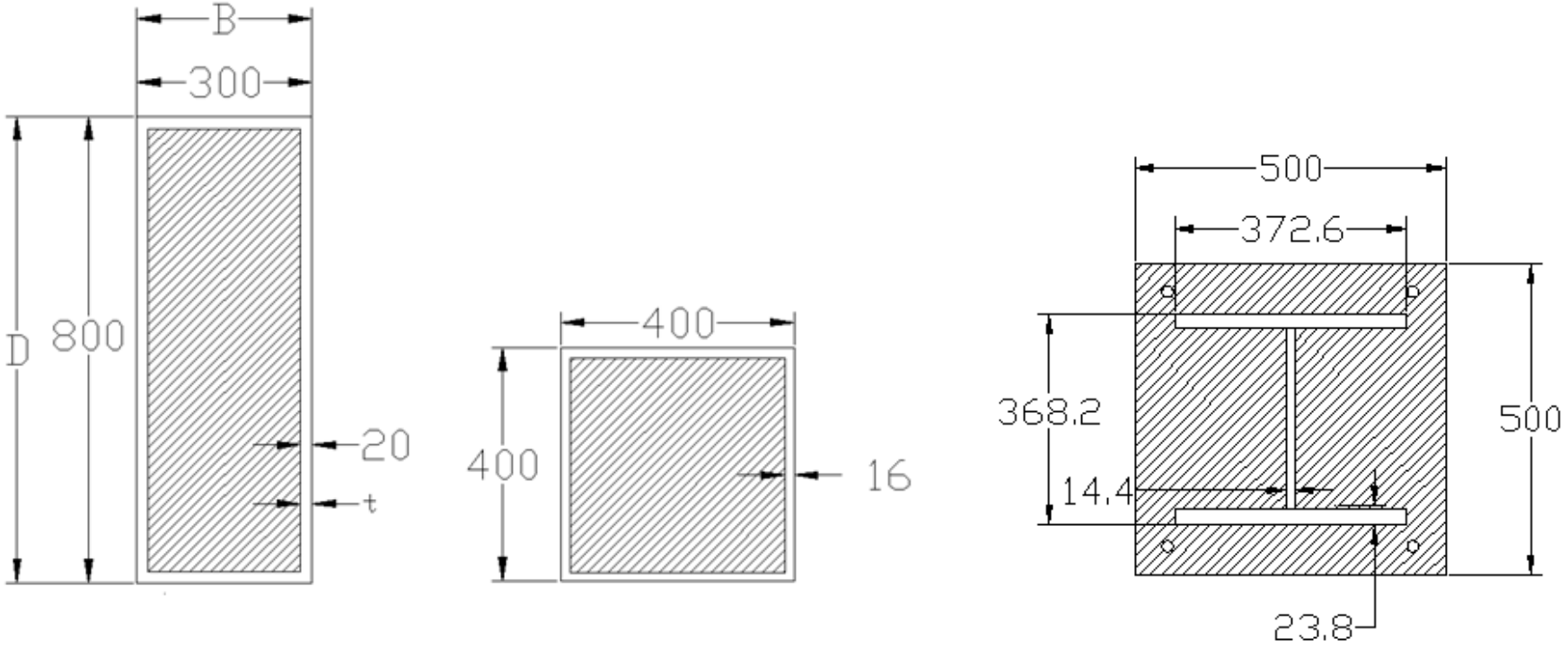

Figure 6.1 Dimensions of the Specimens

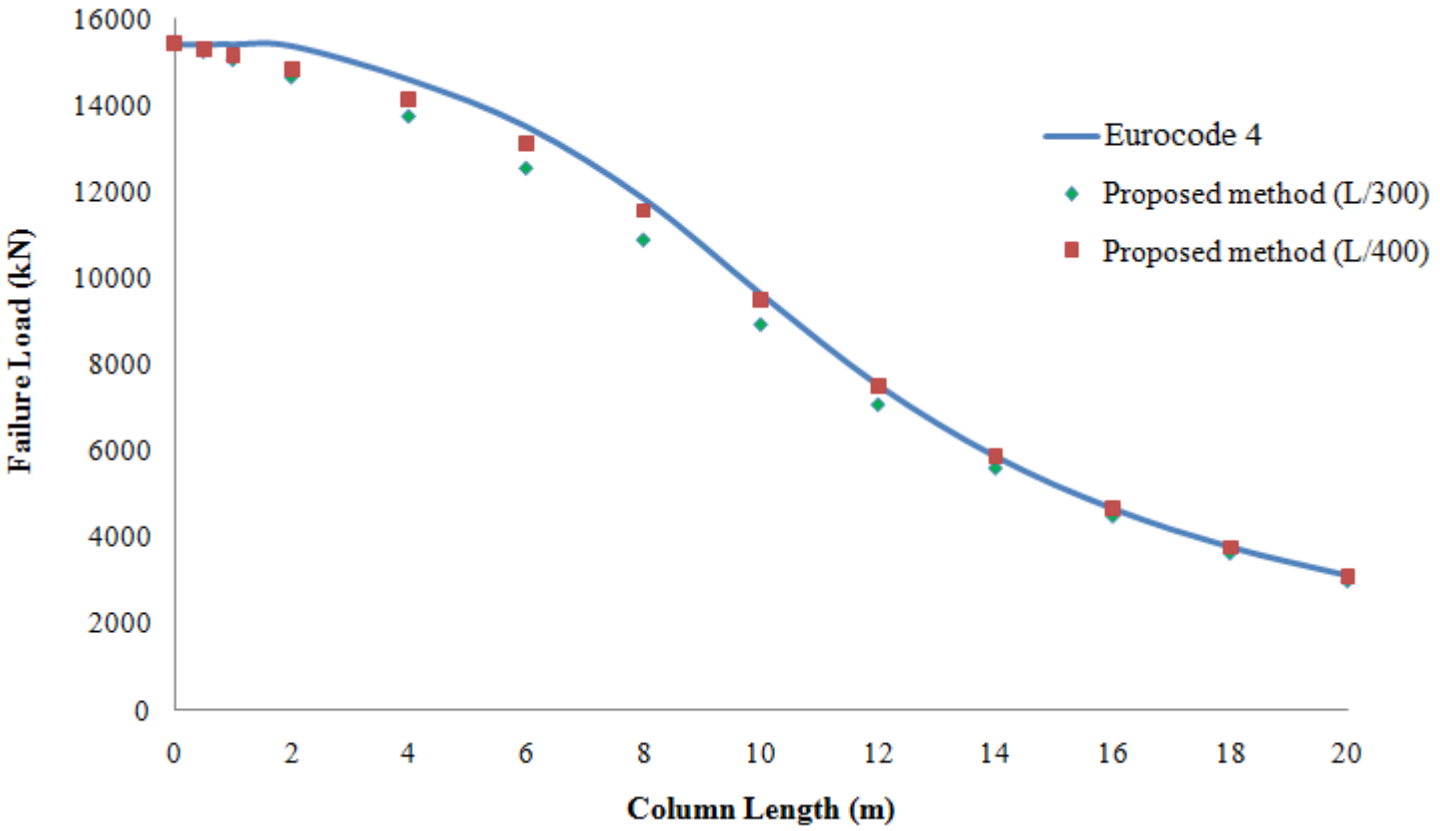

Figure 6.2 Reduction in Capacity with Increasing Member Length for Specimen 1

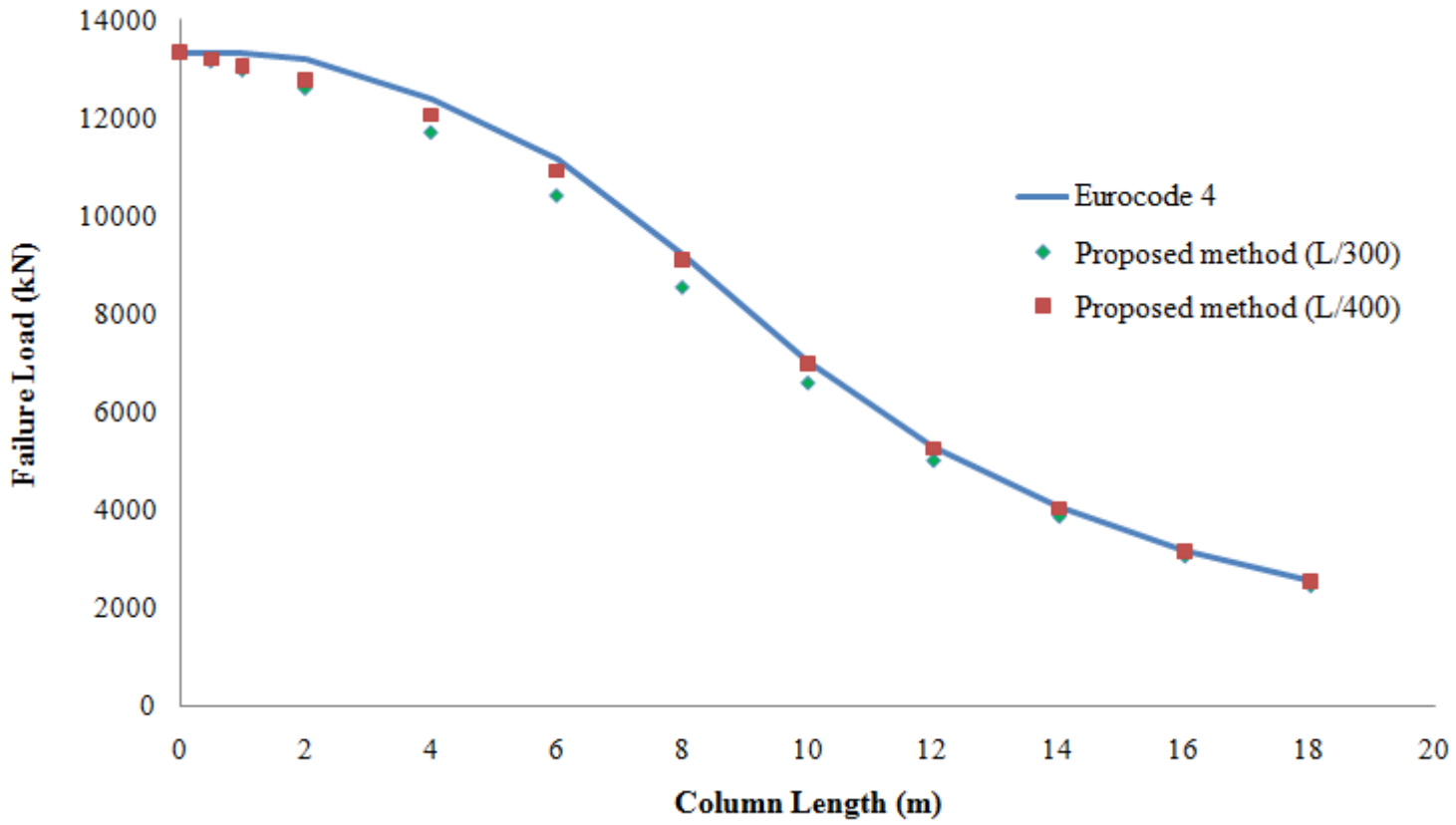

Figure 6.3 Reduction in Capacity with Increasing Member Length for Specimen 2

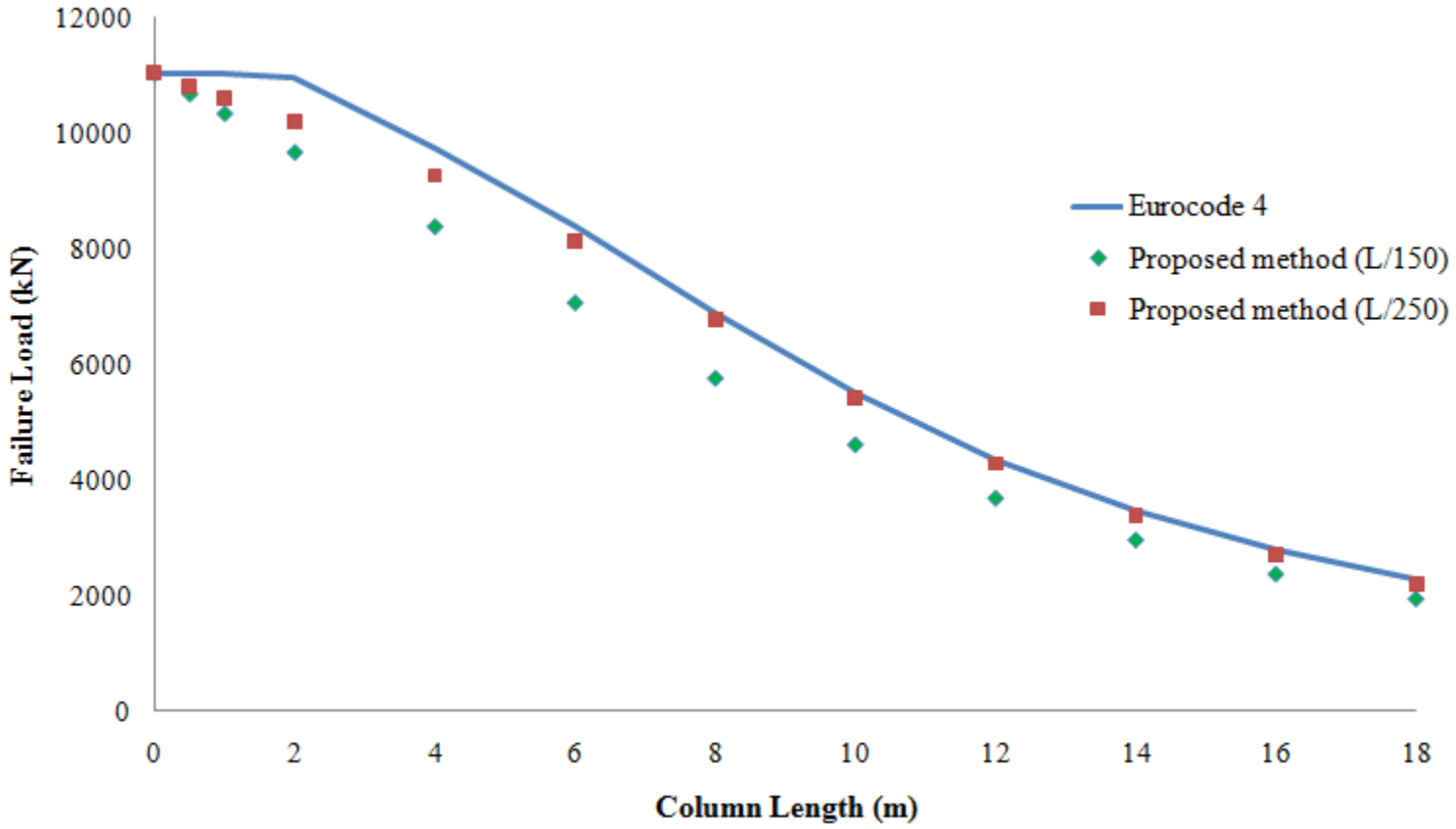

Figure 6.4 Reduction in Capacity with Increasing Member Length for Specimen 3

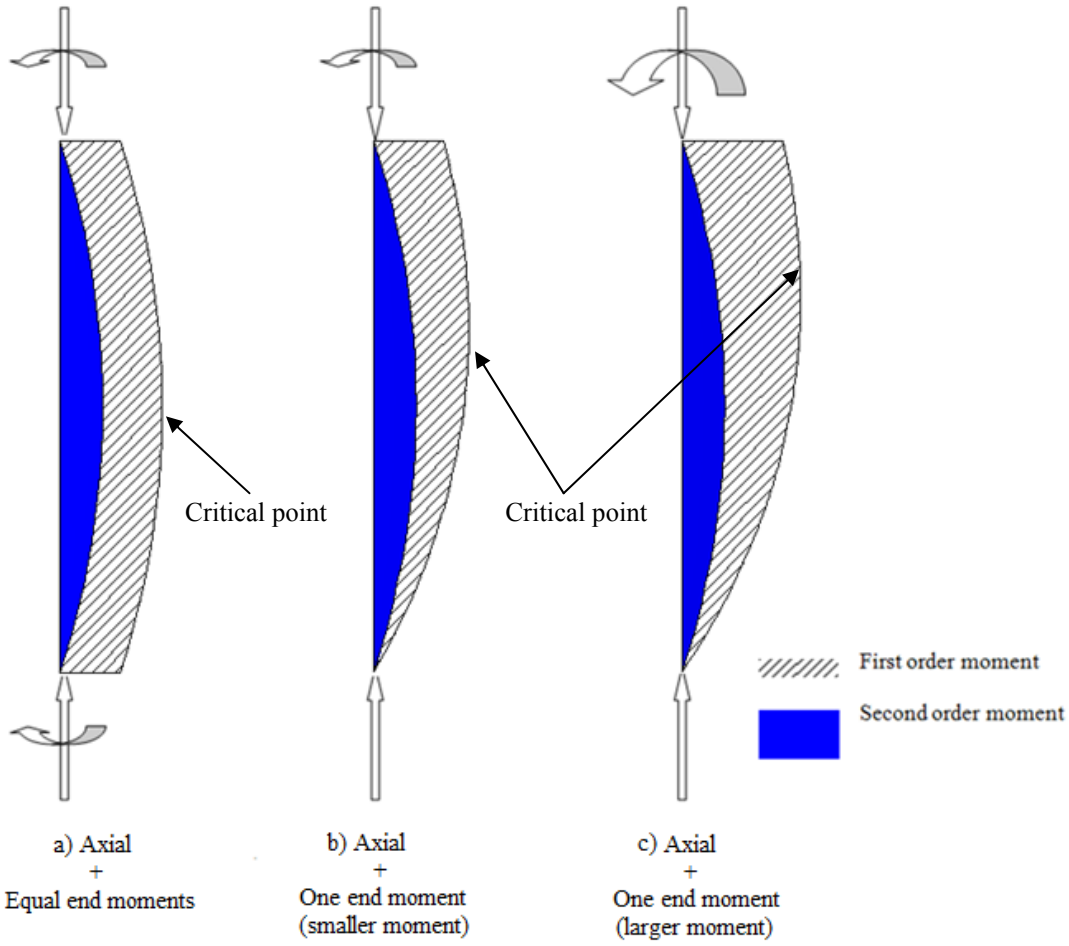

Figure 6.5 Locations of Critical Moment of the Columns under Different Conditions

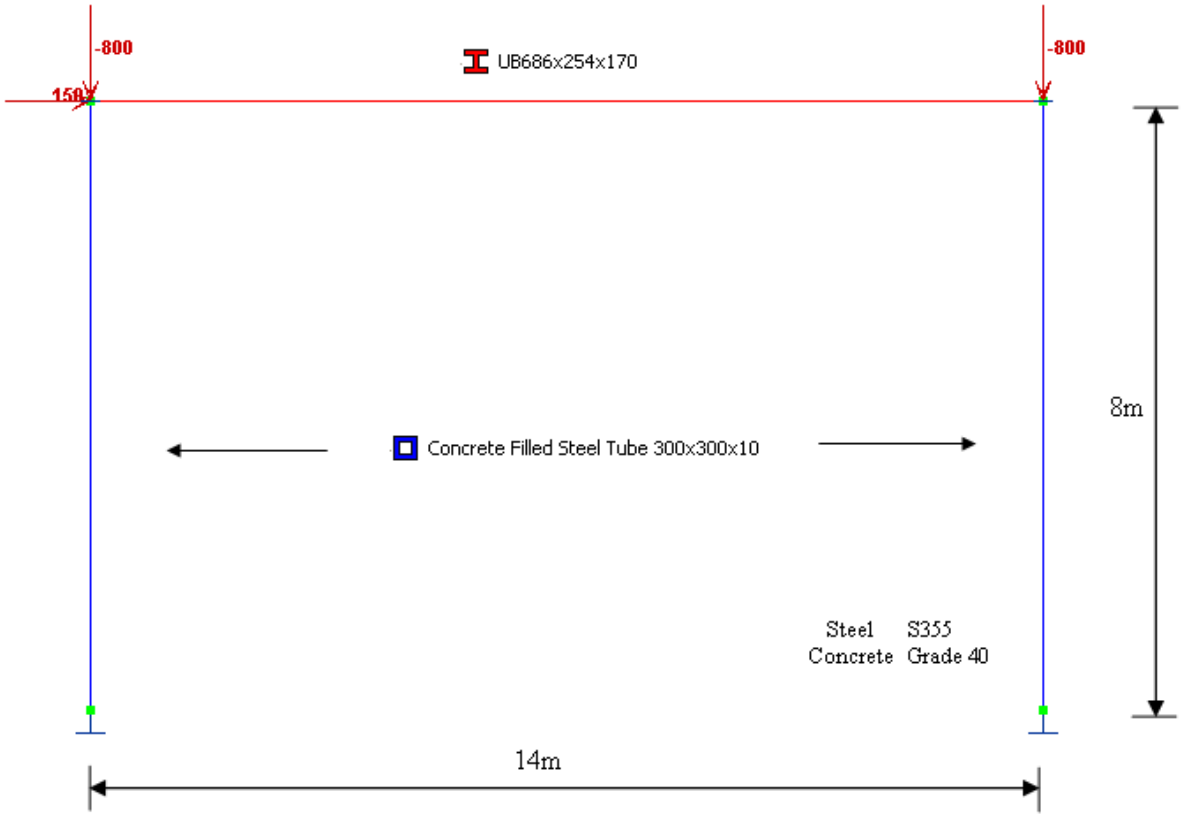

Figure 6.6 Layout of the Portal Frame with Composite Columns and Steel Beam

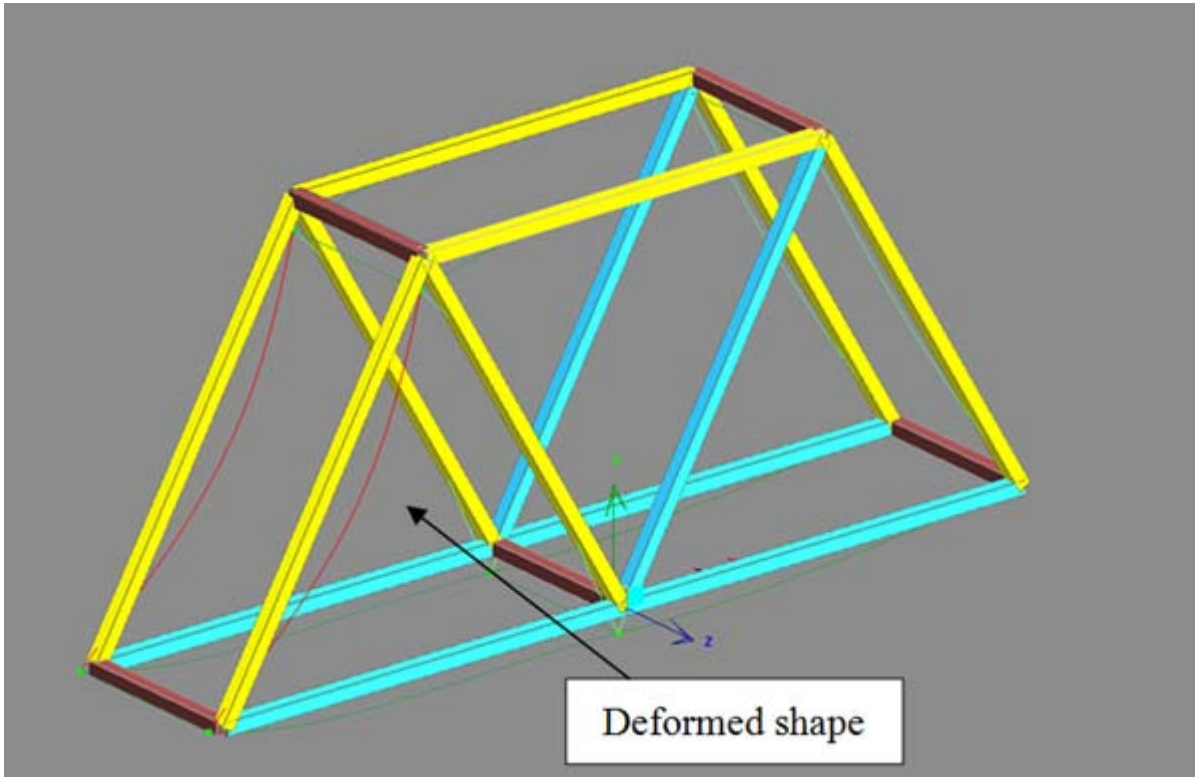

Figure 6.7 Analysis Model of the Trusses

Tables

Table 6.1 Member Imperfections for Composite Cross-sections in Eurocode 4 (2004)

Cross-section type	Reinforcement ratio limit (ρ_s)	Axis of buckling	Member imperfection
Concrete-encased section	/	Major	L/200
		Minor	L/150
Partially concrete-encased section	/	Major	L/200
		Minor	L/150
Hollow steel sections (Circular, Square and rectangular)	$\rho_s \leq 3\%$	Any	L/300
	$3\% < \rho_s \leq 6\%$	Any	L/200
Circular hollow steel section with additional I-section	/	Major	L/200
		Minor	L/200
Partially concrete-encased section with crossed I-sections	/	Any	L/200

Table 6.2 Dimensions and Material Properties of the Specimens

Specimen	Cross-section	Steel section						Reinforcement		Concrete	
		D	B	T_f	t_w	A_s	f_s	A_r	f_r	A_c	f_c
No.	mm	mm	mm	mm	mm	mm^2	N/mm^2	mm^2	N/mm^2	mm^2	N/mm^2
1	300x800	800	300	20	20	42400	275	/	/	197600	32
2	400x400	400	400	16	16	24576	355	/	/	135424	32
3	500x500	368	373	24	14	22600	355	452	460	226948	24

Table 6.3 Comparison of Results for Specimen 1 under Axial Force

Length (m)	$\bar{\lambda}$	Predicted capacity (kN)			Analysis /Eurocode 4	
		Analysis (*L*/300)	Analysis (*L*/400)	Eurocode 4	*L*/300	*L*/400
Specimen 1						
0.5	0.05	15230	15280	15425	0.99	0.99
1	0.11	15040	15140	15425	0.98	0.98
2	0.21	14640	14830	15385	0.95	0.96
4	0.42	13730	14120	14600	0.94	0.97
6	0.64	12530	13110	13510	0.93	0.97
8	0.85	10870	11550	11830	0.92	0.98
10	1.06	8912	9501	9615	0.93	0.99
12	1.27	7060	7485	7495	0.94	1.00
14	1.48	5590	5866	5845	0.96	1.00
16	1.7	4476	4660	4635	0.97	1.01
18	1.91	3620	3760	3745	0.97	1.00
20	2.12	2978	3080	3085	0.97	1.00
				Mean	0.95	0.99
				SD	0.02	0.02

* SD=Standard Deviation

Table 6.4 Comparison of Results for Specimen 2 under Axial Force

Length (m)	$\bar{\lambda}$	Predicted capacity (kN)			Analysis /Eurocode 4	
		Analysis (L/300)	Analysis (L/400)	Eurocode 4	L/300	L/400
Specimen 2						
0.5	0.06	13150	13200	13340	0.99	0.99
1	0.12	12970	13060	13340	0.97	0.98
2	0.24	12600	12760	13220	0.95	0.97
4	0.48	11700	12060	12403	0.94	0.97
6	0.72	10410	10920	11160	0.93	0.98
8	0.96	8540	9090	9210	0.93	0.99
10	1.21	6590	6970	7025	0.94	0.99
12	1.45	5010	5250	5280	0.95	0.99
14	1.69	3870	4020	4050	0.96	0.99
16	1.93	3060	3150	3180	0.96	0.99
18	2.17	2457	2530	2560	0.96	0.99
20	2.41	2020	2070	2100	0.96	0.99
				Mean	0.95	0.98
				SD	0.02	0.01

Table 6.5 Comparison of Results for Specimen 3 under Axial Force

Length (m)	$\bar{\lambda}$	Predicted capacity (kN)				Analysis /Eurocode 4		
		Analysis			Eurocode 4	*L*/150	*L*/250	*L*/1000
		(*L*/150)	(*L*/250)	(*L*/1000)				
Specimen 3								
0.5	0.05	10690	10820	10980	11042	0.97	0.98	0.99
1	0.11	10350	10610	10920	11042	0.94	0.96	0.99
2	0.22	9680	10190	10810	10955	0.88	0.93	0.99
4	0.43	8390	9262		9730	0.86	0.95	
6	0.65	7070	8130		8370	0.84	0.97	
8	0.86	5760	6785		6892	0.84	0.98	
10	1.08	4610	5425	N.A.	5490	0.84	0.99	
12	1.29	3680	4280		4335	0.85	0.99	N.A.
14	1.51	2955	3390		3451	0.86	0.98	
16	1.71	2365	2705		2790	0.85	0.97	
18	1.94	1935	2190		2290	0.85	0.97	
					Mean	0.87	0.97	
					SD	0.04	0.02	

Table 6.6 Comparison of Results for Specimen 1 under Axial Force and End Moments

Length (m)	Moment (kNm)	Predicted capacity (kN)			Analysis/Eurocode 4	
		Analysis (*L*/300)	Analysis (*L*/400)	Eurocode 4	*L*/300	*L*/400
Specimen 1						
3	100	13410	13660	14094	0.95	0.97
3	200	12620	12870	13188	0.96	0.98
3	300	11850	12090	12294	0.96	0.98
3	400	11070	11290	11411	0.97	0.99
4	100	12890	13240	13635	0.95	0.97
4	200	12090	12410	12696	0.95	0.98
4	300	11290	11590	11781	0.96	0.98
4	400	10530	10800	10886	0.97	0.99
5	100	12310	12740	13082	0.94	0.97
5	200	11470	11870	12100	0.95	0.98
5	300	10680	11020	11165	0.96	0.99
5	400	9904	10220	10260	0.97	1.00
				Mean	0.96	0.99
				SD	0.02	0.02

Table 6.7 Comparison of Results for Specimen 2 under Axial Force and End Moments

Length (m)	Moment (kNm)	Predicted capacity (kN)			Analysis /Eurocode 4	
		Analysis (*L*/300)	Analysis (*L*/400)	Eurocode 4	*L*/300	*L*/400
Specimen 2						
3	100	11310	11560	11846	0.95	0.98
3	200	10470	10690	10872	0.96	0.98
3	300	9629	9833	9918	0.97	0.99
3	400	8814	8998	8985	0.98	1.00
4	100	10800	11100	11342	0.95	0.98
4	200	9912	10200	10327	0.96	0.99
4	300	9055	9310	9353	0.97	1.00
4	400	8255	8475	8417	0.98	1.01
5	100	10140	10540	10705	0.95	0.98
5	200	9250	9580	9645	0.96	0.99
5	300	8406	8703	8660	0.97	1.00
5	400	7608	7840	7730	0.98	1.01
				Mean	0.97	0.99
				SD	0.01	0.01

Table 6.8 Comparison of Results for Specimen 3 under Axial Force and End Moments

Length (m)	Moment (kNm)	Predicted capacity (kN)			Analysis /Eurocode 4	
		Analysis (L/150)	Analysis (L/250)	Eurocode 4	L/150	L/250
Specimen 3						
3	100	8144	8765	9213	0.88	0.95
3	200	7256	7819	8102	0.90	0.97
3	300	6403	6869	7015	0.91	0.98
4	100	7519	8262	8580	0.88	0.96
4	200	6667	7315	7485	0.89	0.98
4	300	5850	6385	6435	0.91	0.99
5	100	6879	7718	7906	0.87	0.98
5	200	6079	6768	6827	0.89	0.99
5	300	5298	5884	5824	0.91	1.01
				Mean	0.89	0.98
				SD	0.02	0.02

Table 6.9 Comparison of Test and Analysis Results -De Nardin and El Debs (2007) and Bridge (1976)

Specimen information								Failure load	Analysis	Ratio
Specimen	B mm	D mm	t mm	L mm	e mm	f_y N/mm^2	f_c N/mm^2	P_{test} kN	P_{prop} kN	P_{test}/P_{prop}
De Nardin and El Debs (2007)										
S4	100	200	3.0	1200	0	251.2	45.8	1296.0	1170.0	1.11
S5	100	200	6.3	1200	0	247.1	51.6	1710.0	1596.0	1.07
S6	150	150	3.0	1200	0	357.5	43.4	1534.6	1446.0	1.06
S7	150	150	6.3	1200	0	262.1	48.1	1836.0	1754.0	1.05
S8	127	127	3.2	1200	0	355.0	47.7	1051.5	920.0	1.14
S9	127	127	3.2	1200	0	329.1	59.3	1292.1	1167.0	1.11
									Average	1.09
									SD	0.04
Bridge (1976)										
S10	203.7	203.9	9.96	2130	38	291	30.2	1956.0	2001.0	1.00
S11	204.0	203.3	10.01	3050	0	290	30.6	2869.0	2880.0	1.04
S12	152.5	152.3	6.48	3050	38	254	35.0	680.0	718.0	0.98
S13	152.5	152.3	6.48	3050	64	254	35.0	513.0	583.0	0.93
									Average	0.99
									SD	0.04

Table 6.10 Comparison of Test and Analysis Results - Negoi et. al. (1969)

Specimen information								Failure load	Analysis	Ratio
Specimen	B mm	D mm	t mm	L mm	e mm	f_y N/mm^2	f_c N/mm^2	P_{test} kN	P_{prop} kN	P_{test}/P_{prop}
Negoi et. al. (1969)										
S14	169.5	169.5	5.1	3327	47.6	308.9	47.2	621.8	577.0	1.08
S15	169.2	169.2	5.3	3327	38.1	308.9	45.9	701.5	665.0	1.05
S16	168.9	168.9	5.7	3327	47.6	295.0	36.1	599.8	597.0	1.00
S17	168.4	168.4	6.6	3327	47.6	298.1	32.3	624.7	635.0	0.98
S18	169.2	169.2	7.2	3327	47.6	312.0	27.2	652.6	653.0	1.00
S19	169.2	169.2	7.3	3327	38.1	312.0	28.2	738.3	723.0	1.02
S20	168.9	168.9	8.8	3302	47.6	322.8	28.1	757.3	753.0	1.01
S21	140.2	140.2	9.6	3327	31.8	273.4	35.3	548.0	566.0	0.97
S22	140.2	140.2	9.8	3327	31.8	273.4	23.0	548.0	532.0	1.03
S23	141.0	141.0	5.0	3327	31.8	293.4	36.2	416.5	412.0	1.01
									Average	1.02
									SD	0.03

Table 6.11 Comparison on the Results Calculated by Two Design Methods

	Design moment (kNm)	Design axial load (kN)	Capacity factor
Linear design method of Eurocode 4	309.7	841.4	0.72
Proposed second-order analysis and design method	361.5	850.0	0.74

Table 6.12 Predicted Results from Different Design Codes

Specimen	End condition	Member force (kN)	Predicted capacity from design code				Ratio			
			Eurocode 3 Eurocode 4	AISC	CoPHK	AS 5100	Test/ Eurocode 3 Eurocode 4	Test / AISC	Test/ CoPHK	Test/ AS 5100
Steel tubular column	Pin	152.45	124.23	141.21	132.54	154.61	1.23	1.08	1.15	0.99
Steel tubular column	Fix	249.40	226.59	223.63	236.64	256.75	1.10	1.12	1.05	0.97
Member in steel truss	/	216.57	Pinned end assumed				1.74	1.53	1.63	1.40
			Fixed end assumed				0.96	0.97	0.92	0.84
CFS tubular column	Pin	186.88	184.33	145.35	184.33	193.96	1.01	1.29	1.01	0.96
CFS tubular column	Fix	331.60	353.21	246.39	353.21	354.81	0.94	1.35	0.94	0.93
Member in composite truss	/	279.47	Pinned end assumed				1.52	1.92	1.52	1.44
			Fixed end assumed				0.79	1.13	0.79	0.79

Table 6.13 Predicted Results from Second-order Analysis and Design Method

Specimen	End condition	Member force (kN)	Predicted capacity from second-order analysis and design method			
			Load (kN)		Ratio	
			L/300	*L*/400	*L*/300	*L*/400
Steel tubular column	Pin	152.45	140.43	149.28	1.09	1.02
Steel tubular column	Fix	249.40	229.96	241.92	1.08	1.03
Member in steel truss	/	216.57	190.20	205.70	1.14	1.05
CFS tubular column	Pin	186.88	164.11	172.30	1.14	1.08
CFS tubular column	Fix	331.60	322.50	340.10	1.03	0.98
Member in composite truss	/	279.47	254.36	272.94	1.10	1.02

CHAPTER 7

SECOND-ORDER INELASTIC ANALYSIS OF STEEL-CONCRETE COMPOSITE BEAM-COLUMNS

7.1 Introduction

The consideration of material nonlinearity directly in inelastic analysis of steel-concrete composite beam-columns is important in predicting the failure load and tracing the load-deflection relationship accurately. The way to include geometric nonlinearity in analysis for composite members has been detailed in Chapter 6. In this chapter, the procedure to take the material nonlinearity into account for second-order inelastic analysis and design of steel-concrete composite beam-columns is given. Research works on the inelastic analysis can be broadly categorized into distributed plasticity (plastic zone) method and lumped plasticity (plastic hinge) method. Details of these two methods have been reviewed in Chapter 2. Generally, an exact solution can be obtained by using the plastic zone method which, however, requires extensive computer time in the discretization process across the cross-section and along the member length, so that this method is seldom used in practical engineering design.

The more practical, easy and accurate way to include the material nonlinearity in inelastic analysis is the use of the plastic hinge method. In this method, cross-section plastification is only lumped at the two ends of a member and the remaining region is assumed to be elastic. The different methods to simulate the cross-section plastification have been summarized in Chapter 2. The refined-plastic hinge method by using the zero-length pseudo-spring element in conjunction with initial and full yield surfaces is proposed in this chapter to simulate gradual yield of composite cross-section in inelastic analysis. The studies on the different expressions of initial and full yield surfaces were carried out by Duan and Chen (1989), Orbison et al. (1982), Liew et al. (1993a,b) and Chan and Chui (1997) for steel cross-sections and Iu et al. (2009) for steel-concrete composite cross-sections. In this chapter, the determination of the initial and full yield surfaces, which are used to indicate the initiation of yield by reducing the spring stiffness and full plasticity state, based on the cross-section analysis method are described with its application demonstrated. The constitutive laws of steel and concrete, and the procedure to calculate the cross-section properties are given below. Numerical examples for various types of isolated composite columns, beam-columns and constitutive structural members in trusses and portal frame are given to confirm the accuracy of the proposed method.

7.2 Constitutive Laws of Steel and Concrete

The stress-strain relationships are given in Figure 7.1 for structure steel and reinforcement and in Figure 7.2 for concrete material. An elastic-plastic bi-linear

stress-strain curve is assumed for steels. Isotropic and ductile behavior for steel material in the direction of longitudinal normal stress is assumed for elastic range, and this assumption is made for both tension and compression zones. Strain hardening is not considered in the present study. The stress-strain relationship for concrete in uni-axial compression is represented by the parabola-rectangle diagram given in Eurocode 2 (2004), the stress of concrete σ_c can be obtained as follows.

$$\sigma_c = \sigma_{uc}\left[1-\left(1-\frac{\varepsilon_c}{\varepsilon_{dc}}\right)^n\right] \qquad \text{for } 0 \le \varepsilon_c \le \varepsilon_{dc} \tag{7.2.1}$$

$$\sigma_c = \sigma_{uc} \qquad \text{for } \varepsilon_{dc} \le \varepsilon_c \le \varepsilon_{uc} \tag{7.2.2}$$

where σ_{uc} is the compressive stress of concrete, n is the exponent, ε_c is the strain of concrete, ε_{dc} is the strain of concrete at maximum strength and ε_{uc} is the ultimate strain of concrete. The tension capacity of concrete is ignored for conservative design. ε_{is} and ε_{ic} are the initial yield strains of steel and concrete which are taken as the strain at the intersection point of the tangents of the initial slope and of the ultimate stress in the stress-strain curves. When the strains are beyond the limit of initial yield strain, the materials are assumed to become inelastic. σ_{is} and σ_{ic} are the corresponding initial yield stresses for steel and concrete respectively. σ_{us} and σ_{uc} are the ultimate stresses of the steel and concrete, and ε_{us} and ε_{uc} are the ultimate strains of steel and concrete.

7.3 Cross-section Properties

Concrete-Filled Steel (CFS) tubular sections and Concrete-Encased Steel (CES) sections are two typical cross-sections of composite columns as shown in Figure 7.3. The internal force and bending moments in both axes of the composite cross-sections can be determined by the cross-section analysis method.

The following assumptions are made in cross-section analysis method.

(1) The plane section remains plane after deformation

(2) Shear deformation is ignored

(3) No slippage exists between concrete and steel elements, and the complete interaction is assumed

(4) Strain hardening of steel and tensile stress of concrete are ignored

The composite cross-section is sub-divided into a number of layers (n) as indicated in Figure 7.3. The areas of steel, reinforcement and concrete in each layer are represented by $A_{si,}$, A_{ri} and A_{ci} respectively. The distances from the center of the layer to the center of the cross-section are represented by x_{si}, x_{ri}, x_{ci} and y_{si}, y_{ri}, y_{ci} for steel, reinforcement and concrete respectively in both x and y axes. The corresponding stresses and strains can be obtained from the stress-strain relationship of steel and concrete materials as shown in Figures 7.1 and 7.2. The linear strain distribution at each layer can be determined by the distance from the neural axis to the center of each layer and the curvature (ρ) as indicated in Figure 7.3. From the stress-strain curves of the constitutive materials, the corresponding stresses can be obtained. The total internal force (P_I) in the composite cross-section is equal to the sum of the forces in individual steel, reinforcement and concrete layers as shown in Eq. (7.3.1).

$$P_I = \int_A \sigma dA = \sum_{i=1}^{n} \left(A_{si}\sigma_{si} + A_{ri}\sigma_{ri} + A_{ci}\sigma_{ci} \right) \tag{7.3.1}$$

The neutral axis of the cross-section can be found by an iterative process. Force is first applied to the section and, with the value of neutral axis is assumed, the curvature of the section at initial yield and full yield states can be found according to the pre-defined initial yield strain and full yield strain. The corresponding internal force can then be obtained and compared with the applied force. If the difference is below a pre-defined tolerance, convergence is assumed and the corresponding solution is obtained. Otherwise, a new value of neural axis is assumed using the same iterative process. After convergence, the bending moments (M_{cx} and M_{cy}) of the composite cross-section under various values of axial forces at initial yield and full yield states can be calculated by summing individual bending moments of each steel, reinforcement and concrete layer by Eqs. (7.3.2) and (7.3.3).

$$M_{cx} = \int_A \sigma x dA = \sum_{i=1}^{n} \left(A_{si}\sigma_{si}x_{si} + A_{ri}\sigma_{ri}x_{ri} + A_{ci}\sigma_{ci}x_{ci} \right) \tag{7.3.2}$$

$$M_{cy} = \int_A \sigma y dA = \sum_{i=1}^{n} \left(A_{si}\sigma_{si}y_{si} + A_{ri}\sigma_{ri}y_{ri} + A_{ci}\sigma_{ci}y_{ci} \right) \tag{7.3.3}$$

7.4 Initial Yield and Full Yield Surfaces

The initial and full yield surfaces of composite cross-sections under biaxial bendings are given in Figure 7.4. The initial yield state of the cross-section is assumed when either the strain of steel or concrete in the outmost layer reaches the corresponding

initial yield strain of steel (ε_{is}) or concrete (ε_{ic}). The full yield state of the cross-section is achieved when the strain of steel or concrete in the outmost layer equal to either the ultimate strain of steel (ε_{us}) or concrete (ε_{uc}). The curved initial and full yield surfaces can be simplified into tri-linear line for full yield surface (see curve ABCD) and bi-linear line for initial yield surface (see curve EFG).

Points A and D in Figure 7.4 represent the axial and moment capacities of the composite cross-section at full yield state. The moment capacities when the axial force equal to the full and half axial capacities of the concrete cross-section are represented by points B and C. The full yield surface $\phi_{full}\left(P, M_x, M_y\right)$ is a function of applied force and moments represented by Eqs. (7.4.1) - (7.4.3) under different axial load conditions.

In the initial yield surface, points E and G represent the axial and moment capacities of the composite cross-section at initial yield state. The point with the axial force at the maximum moment capacity is represented by the point F. The initial yield surface $\phi_{initial}\left(P, M_x, M_y\right)$ is a function of applied force and moments and expressed by Eqs. (7.4.4) - (7.4.5) under different axial load conditions.

$$\phi_{full} = \frac{P - P_B}{P_A - P_B} + \frac{M_x + P\left(\delta_x + \Delta_x\right)}{M_{Bx}} + \frac{M_y + P\left(\delta_y + \Delta_y\right)}{M_{By}} = 1 \quad \text{For } P_A \geq P \geq P_B \qquad (7.4.1)$$

$$\phi_{full} = \frac{M_x + P\left(\delta_x + \Delta_x\right)}{M_{Bx}\alpha_{x1}} + \frac{M_y + P\left(\delta_y + \Delta_y\right)}{M_{By}\alpha_{y1}} = 1 \qquad \text{For } P_B \geq P \geq P_C \qquad (7.4.2)$$

$$\phi_{full} = \frac{M_x + P(\delta_x + \Delta_x)}{M_{Dx}\alpha_{x2}} + \frac{M_y + P(\delta_y + \Delta_y)}{M_{Dy}\alpha_{y2}} = 1 \qquad \text{For } P_C \geq P \geq P_D \qquad (7.4.3)$$

$$\phi_{initial} = \frac{P - P_E}{P_F - P_E} + \frac{M_x + P(\delta_x + \Delta_x)}{M_{Fx}} + \frac{M_y + P(\delta_y + \Delta_y)}{M_{Fy}} = 1 \qquad \text{For } P_E \geq P \geq P_F \qquad (7.4.4)$$

$$\phi_{initial} = \frac{M_x + P(\delta_x + \Delta_x)}{M_{Gx}\alpha_{x3}} + \frac{M_y + P(\delta_y + \Delta_y)}{M_{Gy}\alpha_{y3}} = 1 \qquad \text{For } P_F \geq P \geq P_G \qquad (7.4.5)$$

and

$$\alpha_{x1} = \frac{P_B - P}{P_B - P_C}\left(\frac{M_{Cx}}{M_{Bx}} - 1\right) + 1 \qquad (7.4.6)$$

$$\alpha_{y1} = \frac{P_B - P}{P_B - P_C}\left(\frac{M_{Cy}}{M_{By}} - 1\right) + 1 \qquad (7.4.7)$$

$$\alpha_{x2} = \frac{P}{P_C}\left(\frac{M_{Cx}}{M_{Dx}} - 1\right) + 1 \qquad (7.4.8)$$

$$\alpha_{y2} = \frac{P}{P_C}\left(\frac{M_{Cy}}{M_{Dy}} - 1\right) + 1 \qquad (7.4.9)$$

$$\alpha_{x3} = \frac{P}{P_G}\left(\frac{M_{Fx}}{M_{Gx}} - 1\right) + 1 \qquad (7.4.10)$$

$$\alpha_{y3} = \frac{P}{P_G}\left(\frac{M_{Fy}}{M_{Gy}} - 1\right) + 1 \qquad (7.4.11)$$

where P is the applied force, M_x and M_y are the linear moments about the x and y axes, $P(\delta_x+\Delta_x)$ and $P(\delta_y+\Delta_y)$ are the P-δ and P-Δ moments about the x and y axes, P_A to P_G are the axial capacities of the composite cross-section at different points, and

M_{Ax} to M_{Gx} and M_{Ay} to M_{Gy} are moment capacities of composite cross-section at different points about the x and y axes respectively.

When the force-moment interaction point lies inside the initial yield surface ($\phi_{initial} < 1$), the composite cross-section remains elastic. When the force point reaches the initial yield surface ($\phi_{initial} \geq 1$), gradual yield on the composite cross-section activates before the full yield surface ($\phi_{full} = 1$) is reached. The full plastic state is achieved when the force point reaches the full yield surface. If the force point is located outside the full yield surface ($\phi_{full} > 1$), the force point should be shifted back onto the surface to avoid the violation of yield function.

7.5 Refined-plastic Hinge Formulation

A smooth transition from the elastic to the plastic states can be achieved by using the proposed refined-plastic hinge approach. The plastic hinge is modeled by the zero-length pseudo-spring of degradable stiffness formed at one end or both ends of the member to simulate the spread of cross-section plastification. The complicated integration procedure is not required in the proposed refined-plastic hinge method and thus this method is preferable in practical structures. The detailed section spring stiffness and the element stiffness formulation are given below.

7.5.1 Section spring stiffness

The section spring stiffness S_h is defined below,

$$S_h = \frac{E_{comp} I_{comp}}{L} \frac{\left| M_{pr}^* - M \right|}{\left| M - M_{er}^* \right|} \tag{7.5.1}$$

where E_{comp} and I_{comp} are the Young Modulus and the stiffness of the composite section. L is the length of the member. M_{pr}^* and M_{er}^* are the initial yield and full yield moments which take the effect due to axial force into account.

The section spring stiffness S_h defined in Eq. (7.5.1) is inserted at the element ends when the force point is located between the initial yield and the full yield surfaces ($\phi_{initial} \geq 1$ and $\phi_{full} < 1$). If the force point is located within the initial yield surface ($\phi_{initial} < 1$), the section spring with a very large value of $S_h = 10^{+10} \frac{E_{comp} I_{comp}}{L}$ is assigned. If the full yield surface is reached ($\phi_{full} \geq 1$), a very small value of $S_h = 10^{-10} \frac{E_{comp} I_{comp}}{L}$ is assumed in analysis to avoid numerical over-flow.

7.5.2 Element stiffness formulation

With the inclusion of the section spring stiffness to the element stiffness matrix, the element stiffness can be used for second-order inelastic analysis to trace load-deformation relationship of the composite beam-columns. The modified element stiffness matrix is expressed in incremental form as,

$$\begin{pmatrix} \Delta M_{s1} \\ \Delta M_{r1} \\ \Delta M_{r2} \\ \Delta M_{s2} \end{pmatrix} = \begin{bmatrix} S_{h1} & -S_{h1} & 0 & 0 \\ -S_{h1} & K_{11}+S_{h1} & K_{12} & 0 \\ 0 & K_{21} & K_{22}+S_{h2} & -S_{h2} \\ 0 & 0 & -S_{h2} & S_{h2} \end{bmatrix} \begin{pmatrix} \Delta\theta_{s1} \\ \Delta\theta_{r1} \\ \Delta\theta_{r2} \\ \Delta\theta_{s2} \end{pmatrix} \tag{7.5.2}$$

where ΔM_{si} is the incremental nodal moments connecting the beam and the global node and ΔM_{ri} is the incremental nodal moments connecting the beam and the section spring. $\Delta\theta_{si}$ and $\Delta\theta_{ri}$ are the corresponding incremental nodal rotations. The subscript '1' and '2' represent nodes 1 and 2 respectively as indicated in Figure 7.5.

By assuming both the internal moments equal to zero that ΔM_{r1}=0 and ΔM_{r2}=0, the incremental nodal rotations of $\Delta\theta_{r1}$ and $\Delta\theta_{r2}$ can be represented by $\Delta\theta_{s1}$ and $\Delta\theta_{s2}$ as follows.

$$\begin{pmatrix} 0 \\ 0 \end{pmatrix} = \begin{bmatrix} -S_{h1} & 0 \\ 0 & -S_{h2} \end{bmatrix} \begin{pmatrix} \Delta\theta_{s1} \\ \Delta\theta_{s2} \end{pmatrix} + \begin{bmatrix} K_{11}+S_{h1} & K_{12} \\ K_{21} & K_{22}+S_{h2} \end{bmatrix} \begin{pmatrix} \Delta\theta_{r1} \\ \Delta\theta_{r2} \end{pmatrix} \tag{7.5.3}$$

and,

$$\begin{pmatrix} \Delta\theta_{r1} \\ \Delta\theta_{r2} \end{pmatrix} = \begin{bmatrix} K_{11}+S_{h1} & K_{12} \\ K_{21} & K_{22}+S_{h2} \end{bmatrix}^{-1} \begin{bmatrix} S_{h1} & 0 \\ 0 & S_{h2} \end{bmatrix} \begin{pmatrix} \Delta\theta_{s1} \\ \Delta\theta_{s2} \end{pmatrix} \tag{7.5.4}$$

Substituting the Eq. (7.5.4) into Eq. (7.5.2), the incremental stiffness relationships can be re-written as,

$$\begin{pmatrix} \Delta P \\ \Delta M_{s1} \\ \Delta M_{s2} \end{pmatrix} = \begin{bmatrix} \dfrac{EA}{L} & 0 & 0 \\ 0 & S_{h1} - S_{h1}^2(K_{22}+S_{h2})/\beta & S_{h1}S_{h2}K_{12}/\beta \\ 0 & S_{h1}S_{h2}K_{21}/\beta & S_{h2} - S_{h2}^2(K_{11}+S_{h1})/\beta \end{bmatrix} \begin{pmatrix} \Delta L \\ \Delta\theta_{s1} \\ \Delta\theta_{s2} \end{pmatrix} \tag{7.5.5}$$

and

$$\beta = (K_{11}+S_{h1})(K_{22}+S_{h2}) - K_{12}K_{21} > 0 \tag{7.5.6}$$

where ΔP is the increment axial force and ΔL is the incremental axial deformation.

The use of this refined-plastic hinge together with PEP element in second-order inelastic analysis includes both the geometric and material nonlinearities. This method avoids the complicated integration procedure, which is required in the computer time-extensive plastic zone method, and gives accurate results. The load-deflection relationship at both elastic and inelastic stages can be traced and the member ultimate capacity can be predicted by the proposed method. Several examples including the isolated composite columns and structural members are presented in the next section to demonstrate the accuracy of the proposed method for inelastic analysis.

7.6 Numerical Procedure

The combined arc-length method and the minimum residual displacement method is used for incremental-iterative scheme and it is capable of tracing the elastic, plastic and unloading paths efficiently and accurately without numerical divergence. Details of the arc-length method and the minimum residual displacement method have been discussed in Chapter 3.

7.7 Numerical Examples

The proposed second-order inelastic analysis method for steel-concrete composite beam-columns with the used of refined plastic hinge is verified in isolated members

including the CFS tubular columns and CES columns. The ultimate capacities and load-deflection curves of the tested columns are compared with proposed method. Further, the precision of the proposed method used in the structural systems such as trusses and portal frame is presented.

7.7.1 Isolated columns

The comparisons on results from experimental tests and proposed method for the isolated columns including four CFS square and circular sections and three CES sections are given below.

7.7.1.1 Concrete-filled steel square hollow section

Eight slender CFS tubular columns under uniaxial bending were tested by Bridge (1976). The results of three columns with the lengths of 2.13 and 3.05m and the eccentricities of 38 and 64mm were compared with proposed method. The geometric and material properties of the compared columns are given in Table 7.1 and graphically presented in Figure 7.6. The predicted results are given in Table 7.1, and the variations of deflection under applied load at the mid-height of the columns are plotted in Figure 7.7. Both geometric and material nonlinearities are included in analysis, and the assumption of effective length of the columns is unnecessary. The comparisons show that the experimental results can be well replicated by the proposed method with the peak loads predicted by proposed method 4% higher than the experiment loads on average.

7.7.1.2 Concrete-filled steel circular hollow section

Elasto-plastic behavior of CFS circular tubular columns was studied by Neogi et al. (1969). 18 specimens with pinned end were loaded concentrically and eccentrically and all specimens behaved in a ductile manner with no local buckling of the tubes occurred. The result of column (M5) is used in comparison and its section and material properties are given in Table 7.1. The lateral deflection at the mid-height of the column (M5) under applied load is traced by the proposed method and compared against the experimental results in Figure 7.8. The axial response from the analysis model is reasonably consistent with the test result and close prediction on the behavior of the columns in both elastic and plastic stages is obtained. The difference on the maximum loads between the test and predicted results is about 3%.

7.7.1.3 Concrete-encased steel section

Three groups of CES columns with pin ended condition were tested by Roderick and Rogers (1969). Totally 15 columns were loaded concentrically and eccentrically with different steel sections, concrete strengths, eccentricities and member lengths. Three columns (SE1, SE2 and SE3) from group 1 loaded axially with eccentricities equal to 0, 10 and 20mm are used in comparisons for the ultimate capacities and load-deflection curves with the proposed method. The material properties of the columns are given in Table 7.2 and the central deflection against load curves of the columns by test and predicted results are presented in Figure 7.9. The results from proposed method give close predictions on the maximum loads with the difference within 6%.

7.7.2 Structural members

Comparisons on the isolated columns have been demonstrated above. The comparisons on the CFS tubes used as constituting members in the trusses and columns of portal frame are given here. The isolated columns are seldom used in practice and hence the applicability and accuracy of the proposed method in analysis of structural members are important and demonstrated below.

7.7.2.1 Composite trusses

The failure loads and load-deflection curves of members in two composite trusses are compared with the proposed second-order inelastic analysis method. The test procedures and results of both trusses have been detailed in Chapter 5. The dimensions of the members are given in Table 7.3. The trusses were simply supported at four points and loaded in pairs by hydraulic jacks.

In the test, flexural buckling took place in the in-plane direction, the local buckling on the steel plate was not observed before reaching the maximum load, and the deflection in the out-of-plane direction was insignificant when compared with the deflection in the in-plane direction. The load-deflection curves of both trusses 1 and 2 in the in-plane direction are compared with the analysis results. The computer models of the trusses are shown in Figure 7.10 and the target failure member is divided equally into two elements so that the plastic hinge can be formed at the middle of the member. This division of a member to two elements is not needed if we are only interested to detect member failure. However, if one wants to plot the

post-yield load-deflection curve of the member, this member division is needed to insert a plastic hinge to the mid-span of a member. A load increment of 1kN is used in analysis and the behavior of the members before and after yield is traced by the proposed method. The force point at the middle of the member reaches the initial yield surface first, and the springs are inserted to the mid-height of the member to initiate the gradual yield on the composite cross-section. Subsequently, the section springs are inserted to the ends of the member as the force points at the ends of the member reach the initial yield and the stiffness of the springs start to reduce as load increases. The applied load against mid-height in-plane deflection curves of the failed members in truss 1 and truss 2 are plotted and compared with the analysis results in Figure 7.11. The results show that the consistency load-deflection paths between the tests and analysis models can be obtained with sufficient accuracy.

7.7.2.2 Portal frame

The portal frame consists of CFS tubular columns and steel beam is shown in Figure 7.12, together with its geometric properties. The vertical loads of 1000kN are applied to the top of the columns, and the vertical loads are kept constant with increasing horizontal load. The initial yield and full yield surfaces for the CFS tubular column under uniaxial bending are given in Figure 7.13 for illustration. The horizontal load versus lateral displacement (Δ) curves under constant vertical load traced by the proposed second-order inelastic analysis method and second-order elastic analysis method are shown in Figure 7.14 for comparison. The elastic, plastic and unloading stages can be traced by using the proposed method. Both the geometric and material nonlinearities are considered and included directly in analysis.

7.8 Concluding Remarks

Second-order inelastic analysis of steel-concrete composite beam-columns has been proposed in this chapter. Both geometric and material nonlinearities are included in analysis so that the actual behavior of the structures is captured. Inclusion of geometric nonlinear effects, member imperfection and frame imperfection in analysis avoids the uncertainty in assuming an effective length with accuracy of predictions improved. Material nonlinearity for advanced analysis is taken into account in analysis so that the elasto-plastic collapse load is determined. The refined-plastic hinge has been proposed herein to give an efficient and accurate procedure to simulate gradual material yield whereas the traditional elastic-perfectly plastic analysis over-predicts the resistance of the structures because gradual yield is not modeled. The plastic hinges simulated by the zero-length pseudo-spring can be formed at one or both ends of the element, and the plasticity of the cross-section is lumped at the ends of an element. The determination of the initial and full yield surfaces, which are used to initiate the reduction of spring stiffness and indicate full plasticity, of the composite cross-sections based on the cross-section analysis has been described. Numerical examples are given for predictions of both the ultimate capacities and load-deflection relationships of isolated columns and members in a structural system. Close correlations with experiments confirm the validity of the proposed method.

Figures

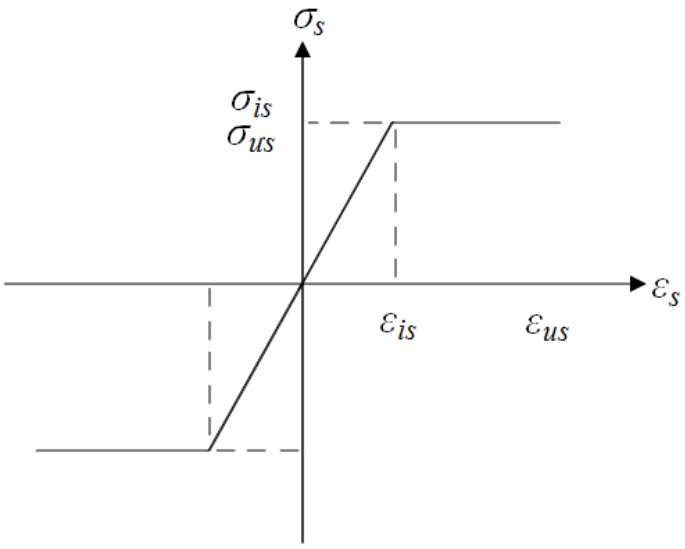

Figure 7.1 The Stress-strain Relation for Steel and Reinforcement

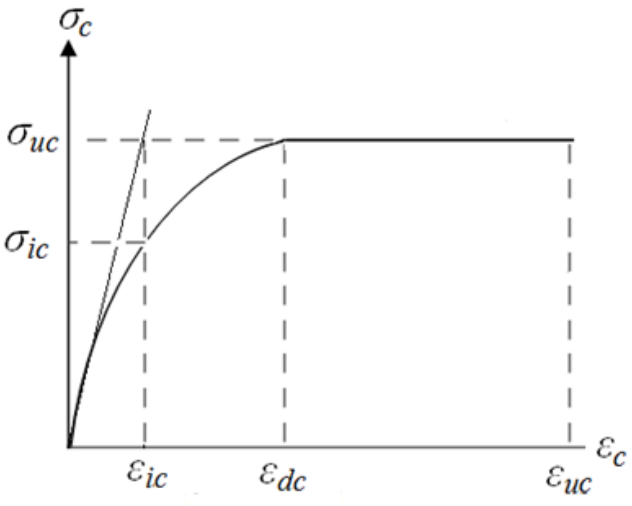

Figure 7.2 The Stress-strain Relation for Concrete

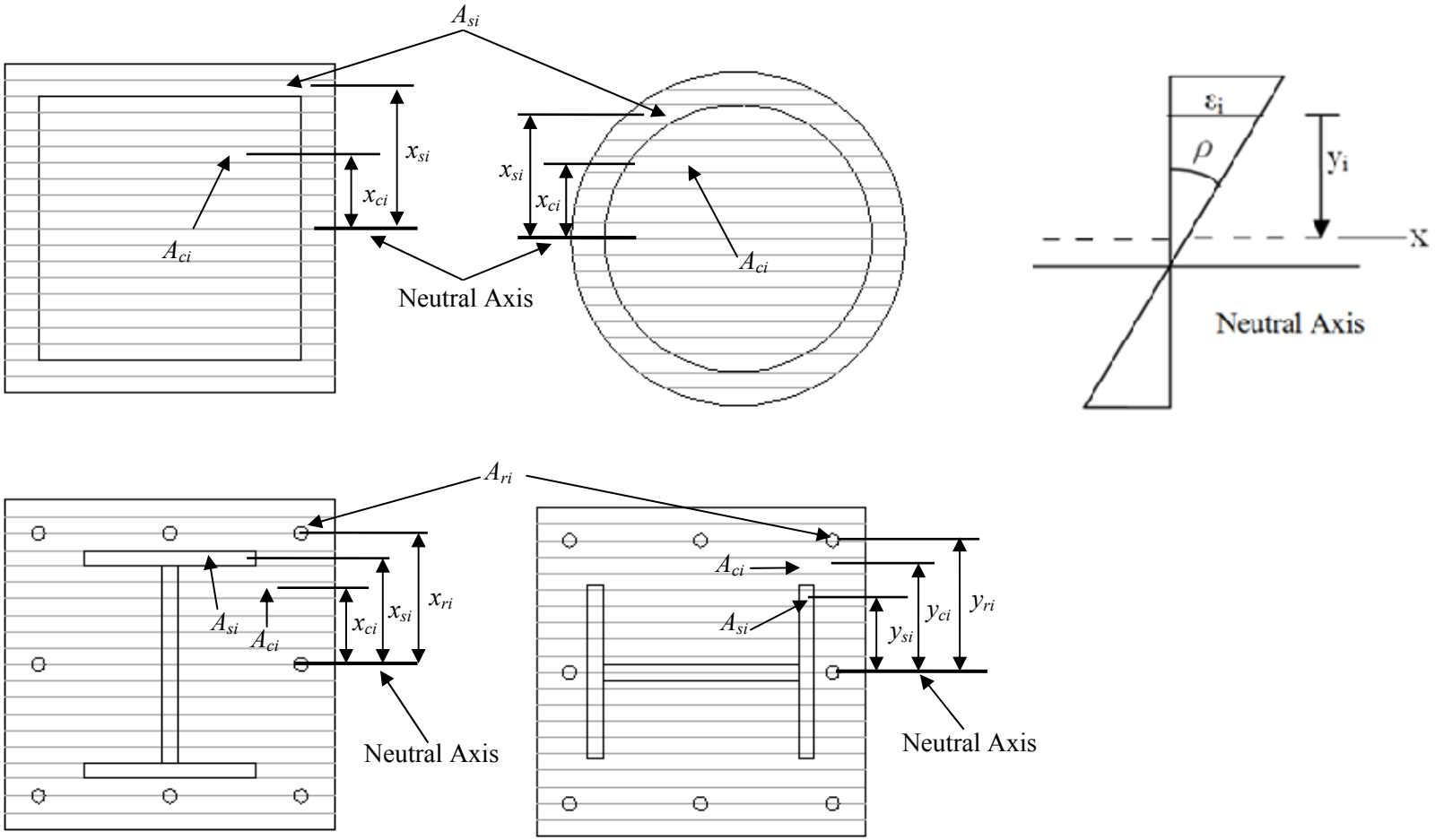

Figure 7.3 Segmentation of Composite Cross-sections

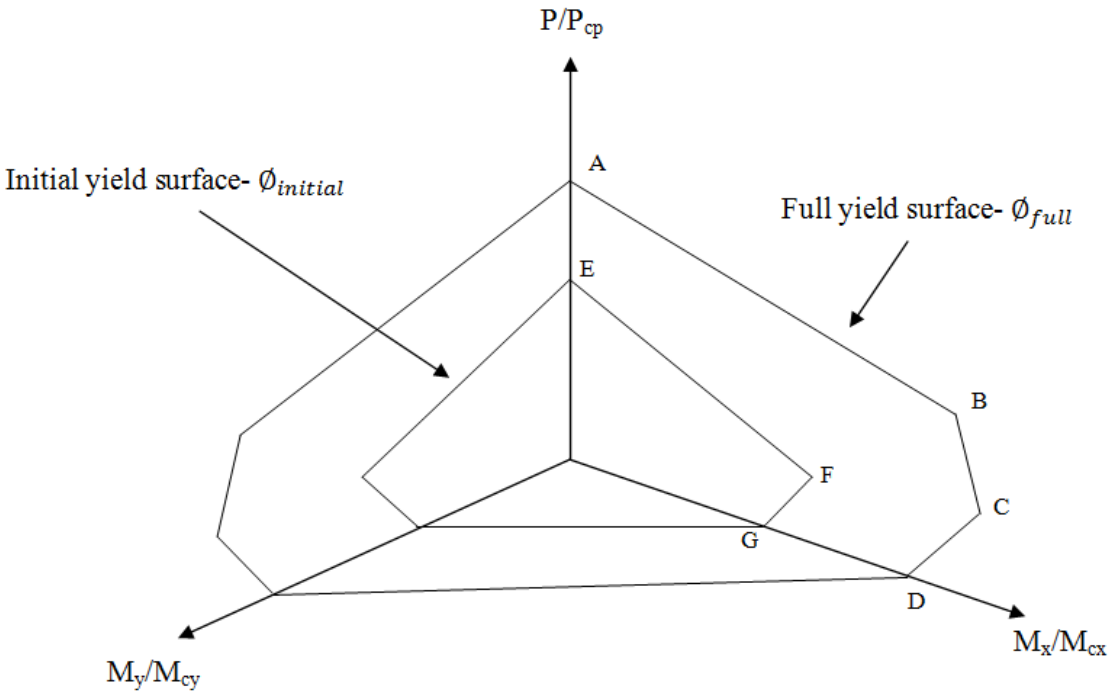

Figure 7.4 Initial and Full Yield Surfaces

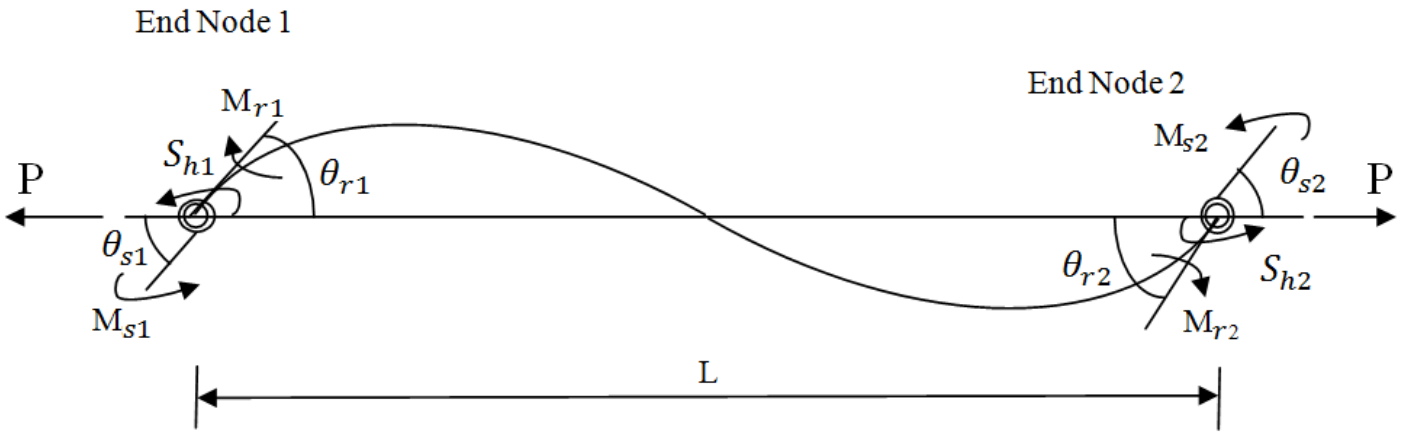

Figure 7.5 The Plastic Hinge Simulated by Section Spring Model

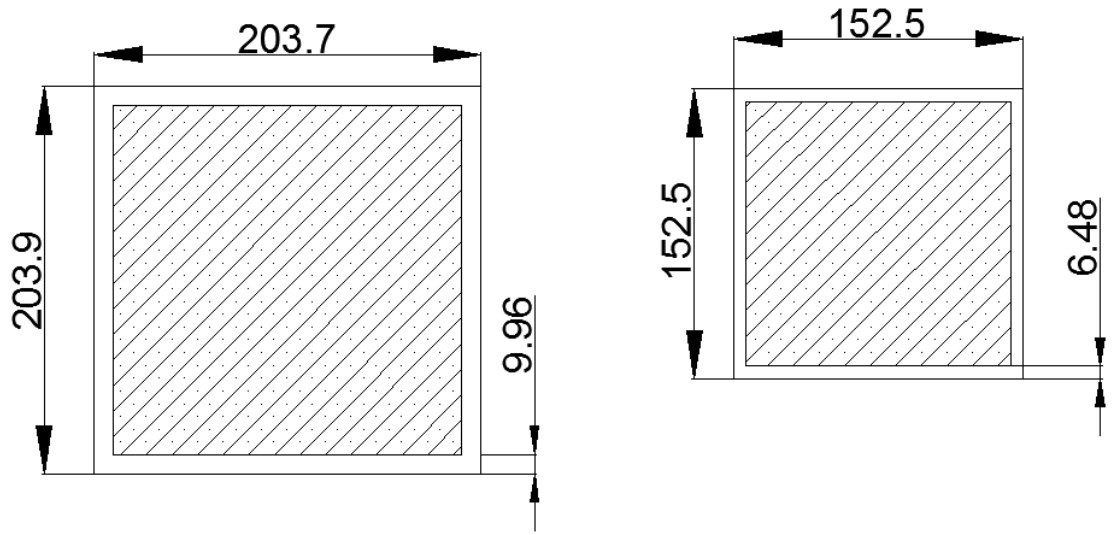

Figure 7.6 Cross-sections of the Columns from Bridge (1976)

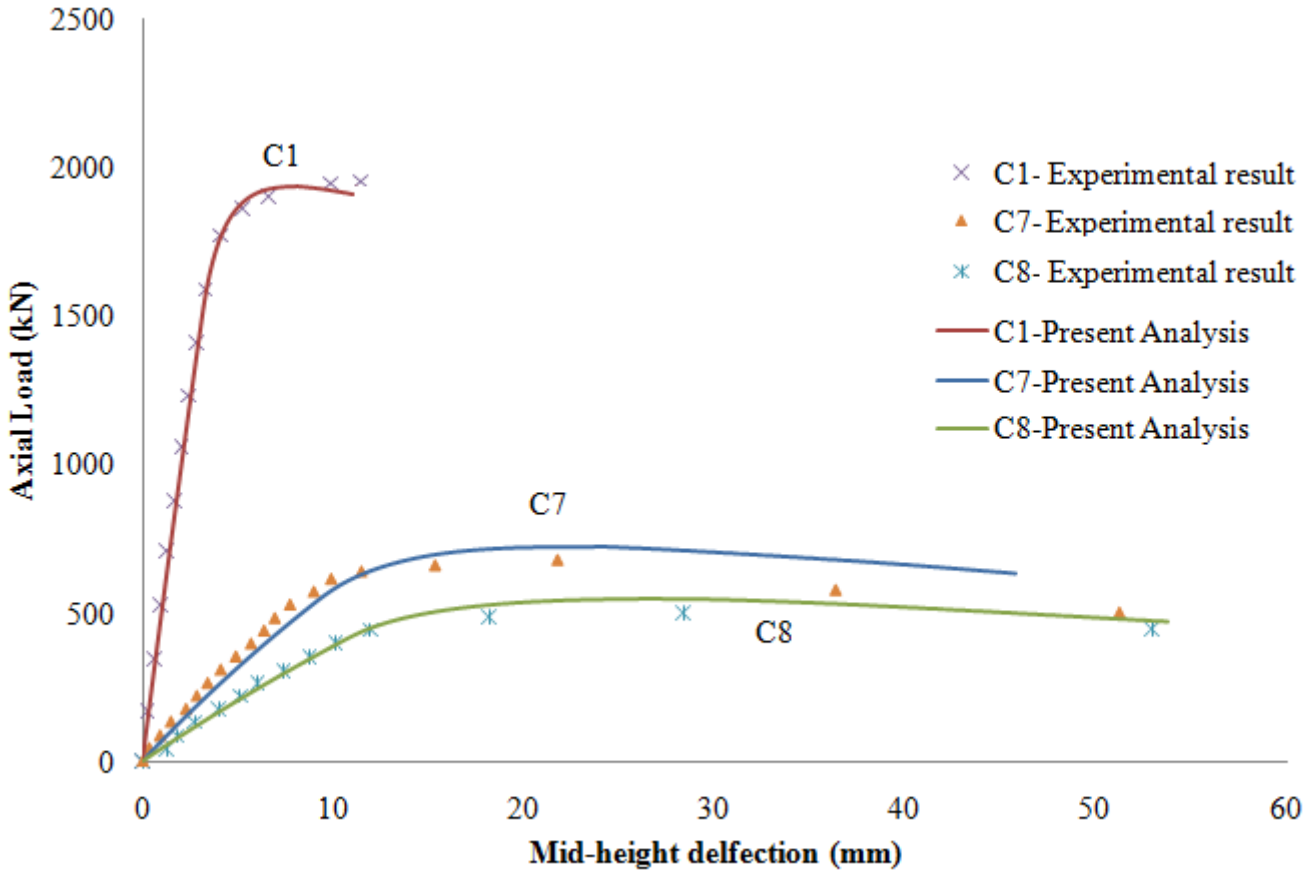

Figure 7.7 Comparison with the Test Results from Bridge (1976)

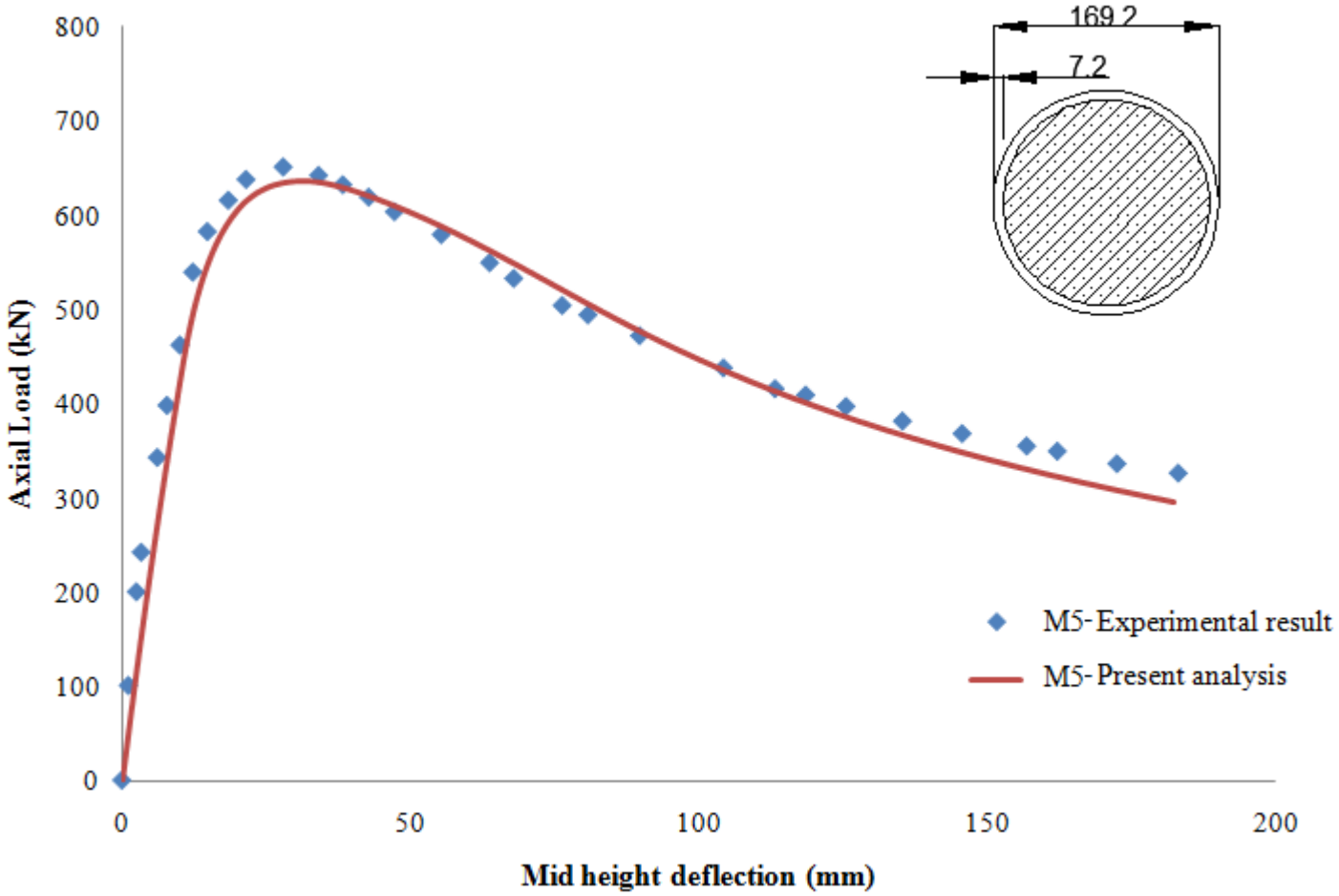

Figure 7.8 Comparison with the Test Result from Neogi et al. (1969)

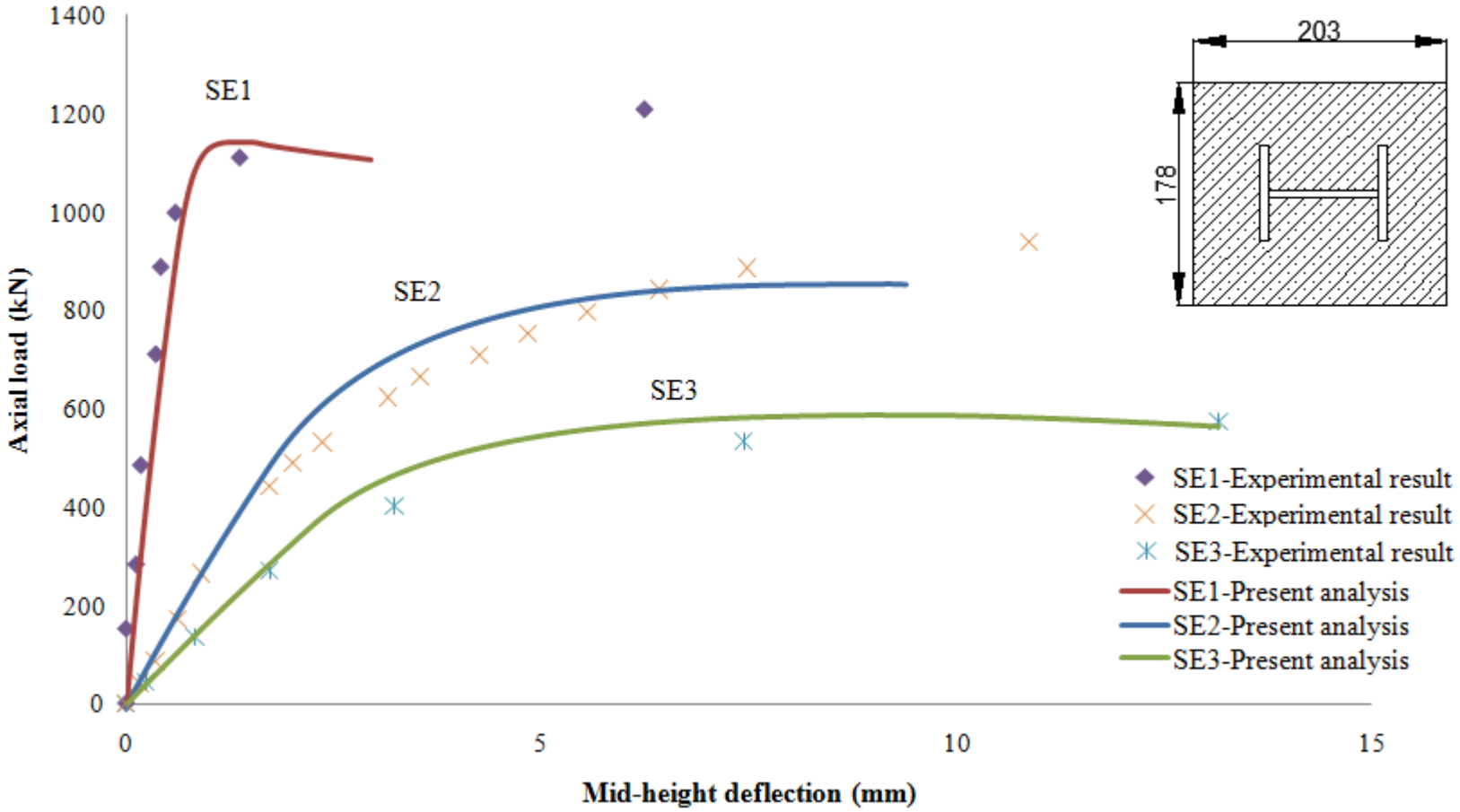

Figure 7.9 Comparison with the Test Results from Roderick and Rogers (1969)

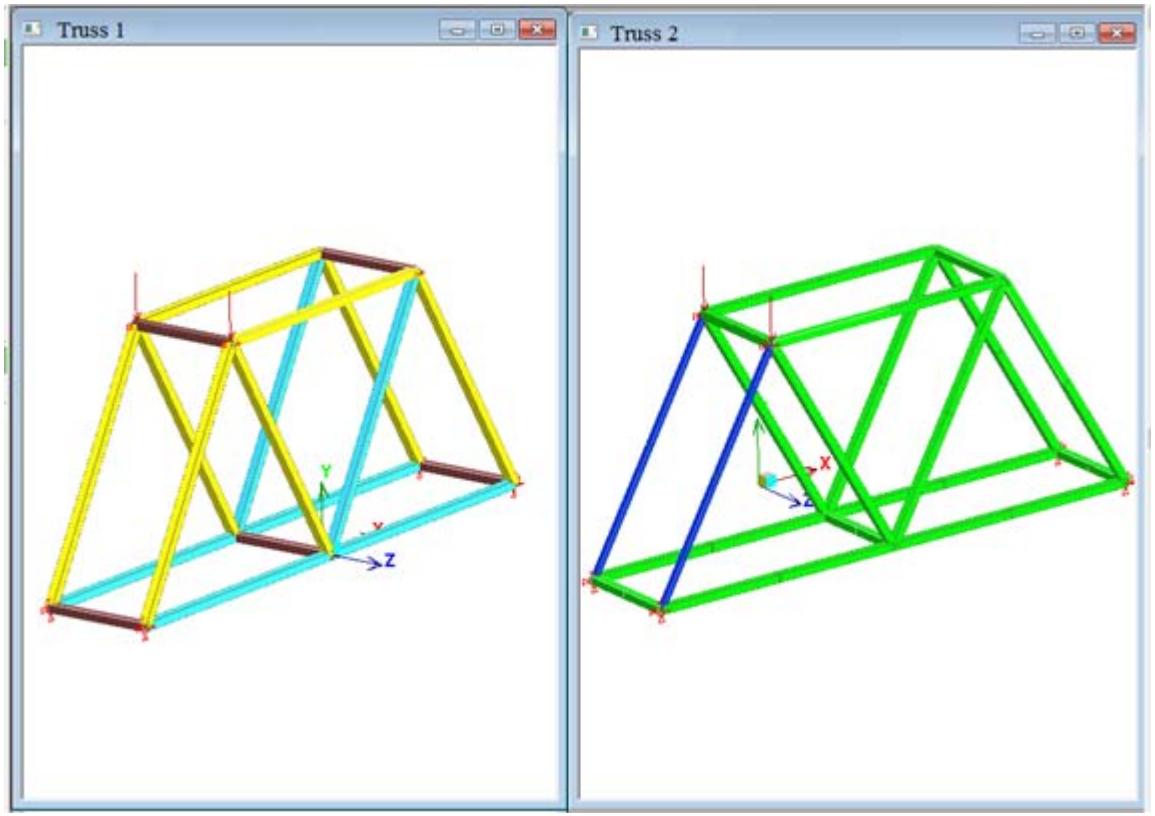

Figure 7.10 Analysis Models of the Composite Trusses1 and 2

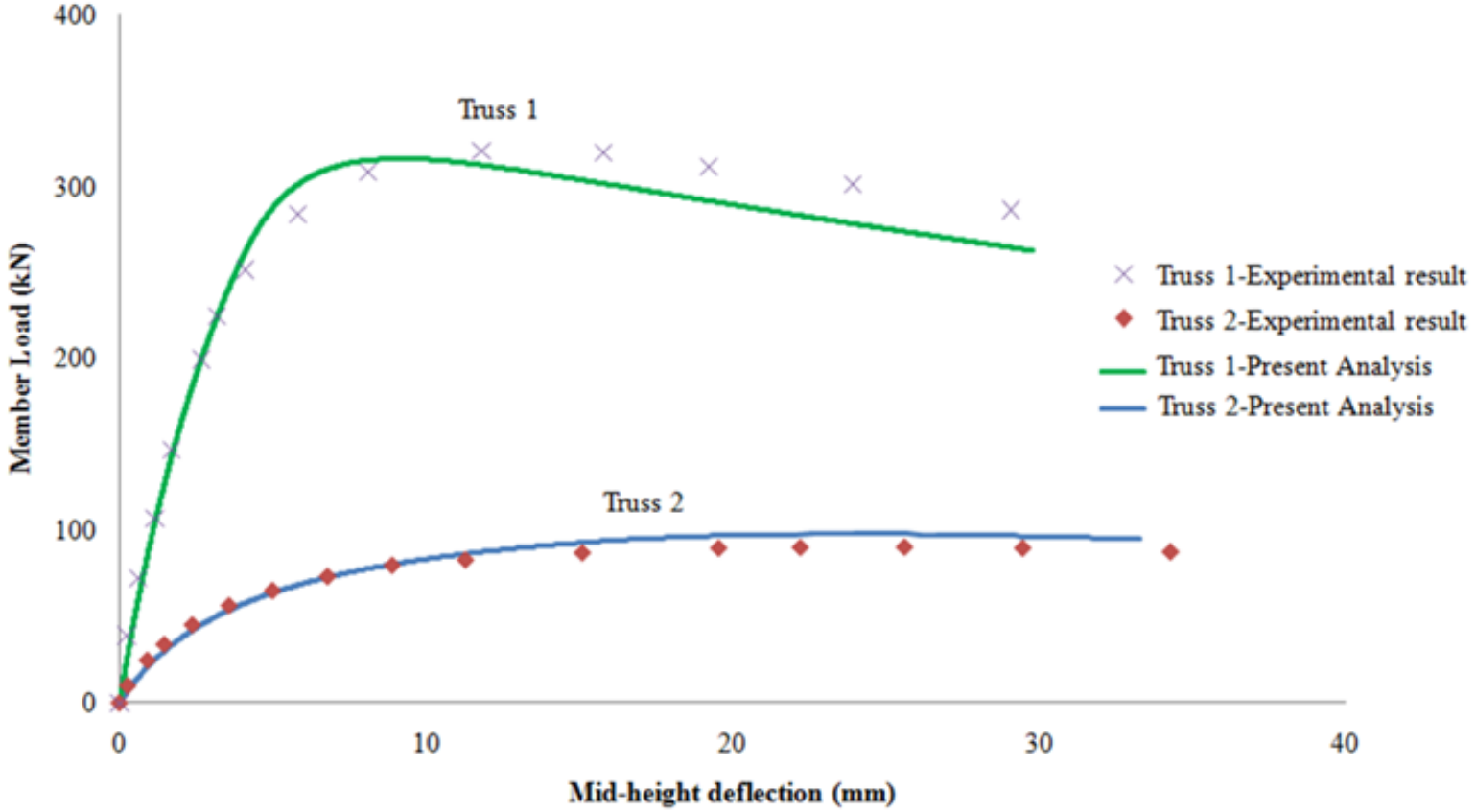

Figure 7.11 Comparison on the Test Results of the Trusses

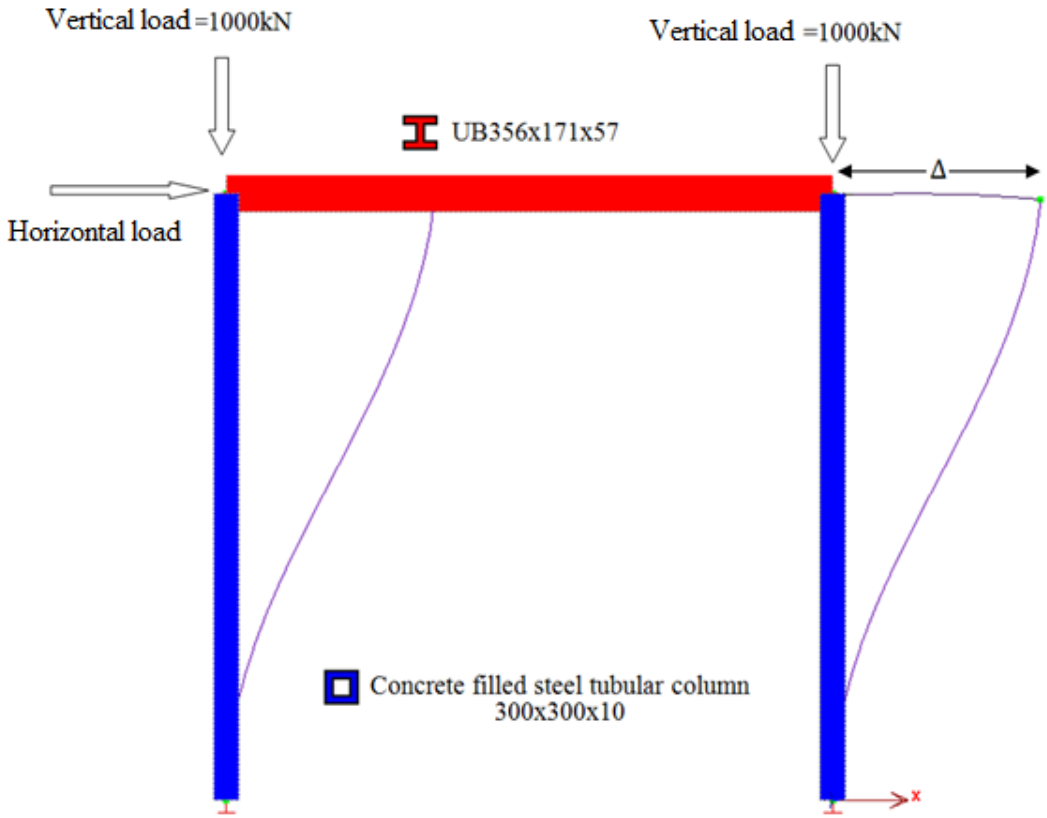

Figure 7.12 Layout and Deformed Shape of the Portal Frame

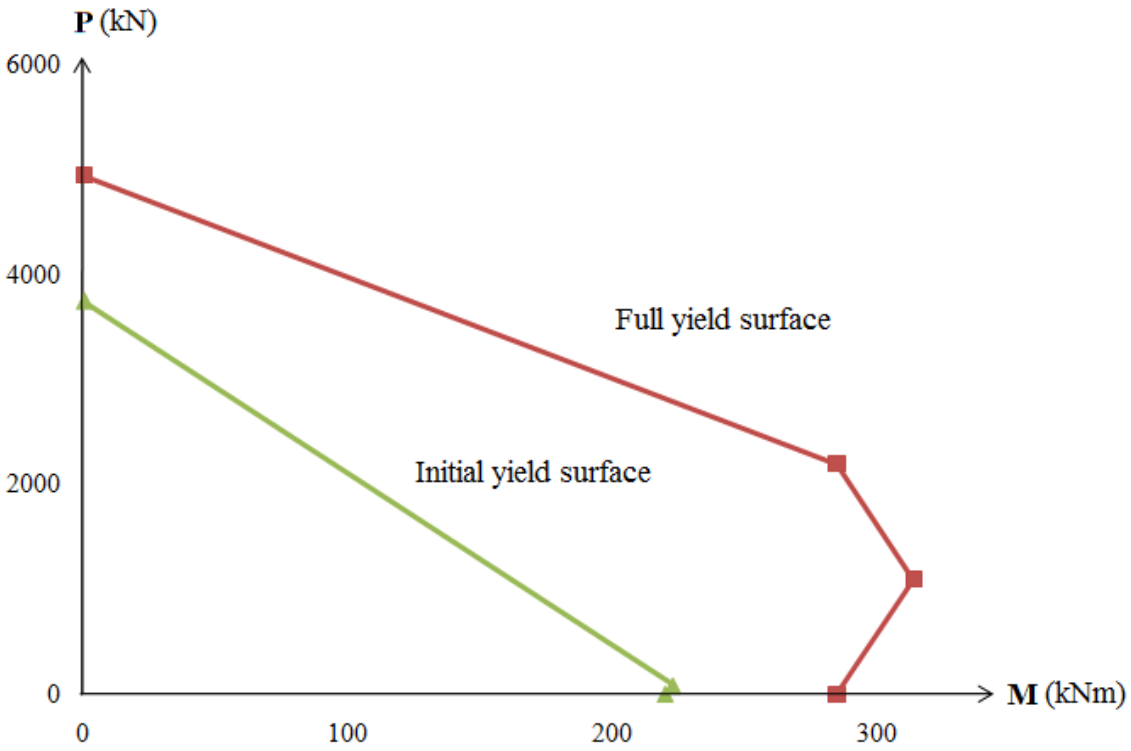

Figure 7.13 Initial and Full Yield Surfaces of the CFS Tubular Column

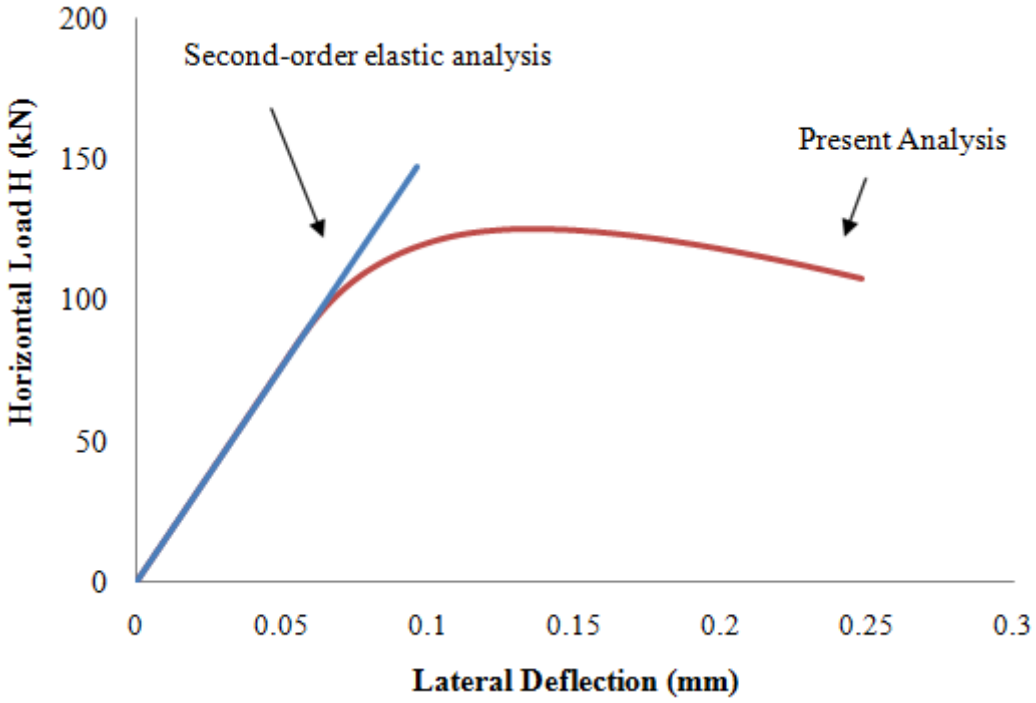

Figure 7.14 Load against Lateral Deflection Curves of the Portal Frame

Tables

Table 7.1 Properties and the Comparison Results of Concrete-filled Steel Tubular Columns

Specimen	Length	eccentricity	B	D	t	f_s	f_c	Test results	Predict load	Ratio
	mm	mm	mm	mm	mm	N/mm^2	N/mm^2	kN	kN	
Bridge (1976)										
C1	2130	38	203.7	203.9	9.96	291	30.2	1956	1938.7	0.99
C7	3050	38	152.5	152.3	6.48	254	35.0	680	723.5	1.06
C8	3050	64	152.5	152.3	6.48	254	35.0	513	548.6	1.07
Neogi et al. (1969)										
M5	3330	47.6	169.2	169.2	7.2	312	27.2	652.6	635.9	0.97

Table 7.2 Properties and the Comparison Results of Concrete-encased Steel Tubular Columns

Specimen	Length	eccentricity	B	D	Steel section	f_s	f_c	Test results	Predict load	Ratio
	mm	mm	mm	mm		N/mm^2	N/mm^2	kN	kN	
SE1	2130	0	178	203	4x3@10	292.3	25.4	1214.4	1143.5	0.95
SE2	2130	10	178	203	4x3@10	292.3	29.5	938.6	855.19	0.91
SE3	2130	20	178	203	4x3@10	292.3	27.0	573.8	586.60	1.02

Table 7.3 Properties and the Comparison Results of Composite Trusses

Specimen	B	D	t	f_y	f_c	Test results	Predict load	Ratio
	mm	mm	mm	N/mm^2	N/mm^2	kN	kN	
Truss1	50.00	30.08	2.96	399.17	89.87	90.00	97.90	1.09
Truss2	60.20	60.20	3.10	404.11	41.16	323.09	315.96	0.98

CHAPTER 8

CONCLUSIONS AND RECOMMENDATIONS

8.1 Conclusions for Present Study

This thesis presents four years research works on refining the second-order analysis and design methods to make it accurate and practical so as to replace the traditional first-order linear analysis and design method for light weight and steel-concrete composite structures. The proposed second-order analysis and design method is a simple and accurate design tool, which includes the nonlinearities in analysis in a simple and direct manner fulfilling code requirements. The accuracy of the proposed refined second-order analysis and design method for light-weight and steel-concrete composite members has been verified in not only isolated members, but also in structural frames. The originality of the reported research lies on putting code formulae and requirements to the analysis program for advanced analysis and design of composite and special structures. Verification against test results and other methods confirms the practicality of the proposed technique for possible replacement of the effective length method used in the past century.

The following conclusions can be made from the results of this study:

a) The success of a nonlinear analysis lies upon the rate of convergence and its accuracy. Therefore, the use of an efficient and accurate element is essential in nonlinear analysis. The PEP element can fulfill these requirements as only one element per member is sufficient for modeling member local and frame global imperfections. The comparison on the load-deflection curves of shallow dome between the test and analysis confirms the accuracy of PEP element in nonlinear analysis and also demonstrates the capability to trace the snap-through buckling by using the combined arc-length and the minimum residual displacement method.

b) The codified first-order analysis and design methods for design of steel structures have been described and the specific considerations for design of angle members have been emphasized. Due to the monosymmetric or asymmetric cross-section property of the angle members and additional moment from eccentric connection, design process becomes more complicated than the double symmetric sections. In general, simplification or interaction equations are provided in different design codes and the conservative predictions are generally obtained. Moreover, the method cannot rationally consider the effect of end moments on web members connected on the same or on the alternate sides of a truss. Because of the unreliability and inaccuracy in using the first-order analysis and design method, the second-order analysis and design method capable of including the local and global imperfections and residual stresses has been proposed for design of angle members so that the actual structural behavior can be reflected. The different web arrangements and the eccentric connection can be simulated and the effects can be included directly in analysis. The comparison on test and analysis results on angle trusses further

confirms the validity of the proposed second-order analysis and design method for practical applications.

c) Experimental tests have been carried out on both isolated steel and CFS columns under pinned or fixed end condition to compare the beneficial effects in both strength and ductility due to the in-filled concrete. Based on the understanding on the behavior of isolated columns, the experimental investigation has been extended to study the behavior of structural systems. Trusses consisted of steel and CFS tubular members were tested and the end movement and rotation of the members were restrained by adjacent connecting members. These end condition of the members connecting to other members in a truss is complicated but more realistic. The comparisons on the behaviors of isolated columns and members in the trusses imply that the end condition of the members is between the pinned and fixed end conditions. Therefore, assuming pinned or fixed end condition for these members either over or under designs a real structure.

d) The codified linear methods in design of steel-concrete composite columns have been presented. The accuracy of commonly used design codes in predicting the capacities of isolated columns and members in the trusses has been compared. The uncertainties and inconvenience in estimation of effective length factor and moment amplification factors have been demonstrated. Based on the disadvantages of this traditional method mentioned above, the second-order analysis and design method has herein been proposed to replace the traditional design method. The proposed method for design of composite members is more rational and accurate for reflection of structural behavior. The individual member design is replaced by the section

capacity check allowing for nonlinear effects and this leads to a considerable simplification on design of composite members. The favorable comparisons on the predicted resistances by proposed method on composite isolated members and the columns of a portal frame with results from Eurocode 4 (2004) indicate that the proposed method is consistent with the codified design output and can be used for practical structural design. Without loss of generality, the proposed method can be extended to design of complex and large composite structures for which the reliability of the effective length method is in doubt.

e) The consideration of material nonlinearity in advanced analysis is important for prediction the inelastic behavior of composite beam-columns. Therefore, a practical and codified method of design based on the second-order inelastic analysis has been proposed in this research project. Both the geometric and material nonlinearities are taken into account in analysis so that the result can be used directly for design without modifications. The use of plastic hinge in inelastic analysis is a simpler and more practical method to include the material nonlinearity because the complicated and time consuming process in plastic zone method in discretizing the cross-section and along the member length is avoided. The gradual material yield is able to be simulated in present refined-plastic hinge method whereas the traditional elastic-perfectly plastic analysis over-predicts the resistance of the structures as gradual yield in a cross-section cannot be considered. The plastic hinges simulated by the zero-length pseudo-spring can be formed at one or both ends of the element, and the plasticity of the cross-section is assumed to be lumped at the element ends. The determination of the initial and full yield surfaces, which are used to initiate the reduction of spring stiffness and indicate full plasticity, of the composite cross-

sections based on the cross-section analysis has been described. Numerical examples have been given on both the isolated composite columns and members in the structural system to demonstrate the use of the proposed inelastic analysis method in prediction of both the ultimate capacity and load-deflection relationship, and the accurate predictions against experiments confirm its validity.

8.2 Recommendations for Further Work

This thesis has presented the second-order analysis and design method for light weight structures with experimental verifications, and the advanced analysis and design method has also been extended from bare steel structures to steel-concrete composite structures. Both second-order elastic and inelastic analysis methods have been formulated and can be applied to practical design. For further research works, the following recommendations are suggested:

a) In present inelastic analysis method for composite beam-columns, the code provided and relative simple stress-strain relations have been used for steel and concrete. Further research can be conducted to use more realistic models. And the concrete cracking in compression is ignored in the presented method. Therefore, the predicted member capacity is greater than actually failure load in some cases because the cracking of concrete reduces the member stiffness. Therefore, the study on cracking surface for use in conjunction with the initial and full yield surfaces to reduce the stiffness can be carried out in the future.

b) Use of the refined plastic-hinge method in inelastic analysis for three common composite cross-sections including CFS circular and rectangular tubular sections and CES section has been proposed with experimental verifications in this thesis. However, due to the demand of high strength and ductility mega columns and fulfillment of architect's requirements, the use of composite columns with arbitrary cross-sections is increasing. The proposed second-order inelastic analysis method can be extended and applied to arbitrary cross-sections with appropriate modifications in further research works. Experimental studies on composite columns with arbitrary cross-sections by using the high strength materials can be conducted to study its behavior for providing the guidelines on design, and verification of the accuracy of the proposed inelastic analysis used in composite columns with arbitrary cross-sections.

c) The proposed refined plastic hinge method lumps the cross-section plastification at two ends of the member. However, the most critical point may locate at the middle instead of two ends of the member in some cases. Division of the member into two elements is required to allow for the formation of the plastic hinge at the middle of the member. The process to divide the member into two elements is sometimes tedious and inconvenience although only the critical members are needed for such division. Some researchers studied the use of an additional hinge at mid-span or arbitrary location along the member which, however, is considered to be too complicated in formulation and for practical uses. Therefore, a simple and accurate method allowing for the formation of the plastic hinge at an arbitrary location along the element can be studied in further research works.

d) While the second-order analysis and design method for light weight and steel-concrete composite structures has been proposed in this thesis, the method can be extended to other structural forms such as the reinforced concrete structures to provide a generalized and consistent design to structures made of any materials.

REFERENCES

ACI 318 (2008). Building code requirements for structural concrete and commentary. ACI Committee 318, American Concrete Institute. Michigan.

AISC (2010). Specification for structural steel buildings. American Institute of Steel Construction, ANSI/AISC 360-10, Chicago.

Al-Mashary, F. and Chen, W. F. (1991). "Simplified Second-Order Inelastic Analysis for Steel Frames." The Structural Engineer **69**(23): 395-399.

Al-Rodan, A. K. (2004). "Comparison between BS5400 and EC4 for Concrete-Filled Steel Tubular Columns." Advances in Structural Engineering **7**(2): 159-168.

Alvarenga, A. R. and Silveira, R. A. M. (2009). "Second-order plastic-zone analysis of steel frames Part I: Numerical formulation and examples of validation." Latin American Journal of Solids and Structures **6**(2): 131-152.

AS4100 (1998). AS4100-1998 Australian Standard. Steel structures. Sydney, Australia.

AS5100 (2004). AS5100.6-2004 Bridge design, Part 6: Steel and composite construction. Sydney, Australia.

Bathe, K. J. and Bolourchi, S. (1979). "Large deflection analysis of three dimensional beam structures." International Journal for Numerical Methods in Engineering **14**(7): 961-986.

Batoz, J. L. and Dhatt, G. (1979). "Incremental displacement algorithms for nonlinear problems." International Journal for Numerical Methods in Engineering **14**(8): 1262–1267.

Bridge, R. and Webb, J. (1993). "Thin Walled Circular Concrete Filled Steel Tubular Columns." Proceedings of the 2nd Int. Engineering Foundation Conf. of Composite Construction, Potosi, Mo.: 634–649.

Bridge, R. Q. (1976). "Concrete Filled Steel Tubular Columns." Civil Engineering Transactions **18**(2): 127-133.

Bridge, R. Q., O'Shea, M. D., Gardner, P., Grigson, R. and Tyrell, J. (1995). "Local buckling of square thin-walled steel tubes with concrete infill." Proceedings of the International Conference on Structural Stability and Design, Sydney, 1995: 307–314.

BS5400 (2005). Steel, concrete and composite bridges – Part 5: Code of practice for the design of composite bridges, BS5400. London.

BS5950 (2000). Structural use of steelwork in building – Part 1: Code of practice for design – Rolled and welded sections, BS5950. London.

Chan, S. L. (1988). "Geometric and Material Non-Linear Analysis of Beam-Columns and Frames Using the Minimum Residual Displacement Method." International Journal for Numerical Methods in Engineering **26**(12): 2657-2669.

Chan, S. L. (2001). "Non-linear behavior and design of steel structures." Journal of Constructional Steel Research **57**(12): 1217-1231.

Chan, S. L. and Cho, S. H. (2002). "Design of steel frames using calibrated design curves for buckling strength of hot-rolled members." Proceedings of Advances in Steel Structures. Elsevier: 1193–1199.

Chan, S. L. and Cho, S. H. (2008). "Second-order analysis and design of angle trusses - Part I: Elastic analysis and design." Engineering Structures **30**(3): 616-625.

Chan, S. L. and Chui, P. P. T. (1997). "A generalized design-based elastoplastic analysis of steel frames by section assemblage concept." Engineering Structures **19**(8): 628-636.

Chan, S. L. and Chui, P. P. T. (2000). "Nonlinear Static and Cyclic Analysis of Steel Frames with Semi-rigid Connections." Elsevier Science.

Chan, S. L. and Gu, J. X. (2000). "Exact tangent stiffness for imperfect beam-column members." Journal of Structural Engineering, ASCE **126**(9): 1094-1102.

Chan, S. L., Liu, Y. P. and Zhou, Z. H. (2005). "Limitation of effective length method and codified second-order analysis and design." Steel and Composite Structures **5**(2-3): 181-192.

Chan, S. L. and Zhou, Z. H. (1994). "Pointwise equilibrating polynomial element for nonlinear analysis of frames." Journal of Structural Engineering, ASCE **120**(6): 1703-1717.

Chan, S. L. and Zhou, Z. H. (1995). "Second-order elastic analysis of frames using single imperfect element per member." Journal of Structural Engineering, ASCE **121**(6): 939-945.

Chan, S. L. and Zhou, Z. H. (1998). "On the development of a robust element for second-order 'Nonlinear integrated design and analysis (NIDA)'." Journal of Constructional Steel Research **47**(1-2): 169-190.

Chan, S. L. and Zhou, Z. H. (2000). "Non-linear integrated design and analysis of skeletal structures by 1 element per member." Engineering Structures **22**(3): 246-257.

Chan, S. L. and Zhou, Z. H. (2004). "Elastoplastic and large deflection analysis of steel frames by one element per member. II. Three hinges along member." Journal of Structural Engineering, ASCE **130**(4): 545-553.

Chan, S. L., Zhou, Z. H., Chen, W. F., Peng, J. L. and Pan, A. D. (1995). "Stability analysis of semirigid steel scaffolding." Engineering Structures **17**(8): 568-574.

Chen, W. F. (2000). "Structural stability: from theory to practice." Engineering Structures **22**(2): 116-122.

Chen, W. F. and Chan, S. L. (1995). "Second-Order Inelastic Analysis of Steel Frames Using Element with Midspan and End Springs." Journal of Structural Engineering **121**(3): 530-541.

Chen, W. F. and Kim, S. E. (1997). "LRFD steel design using advanced analysis." CRC, Boca Raton, Fla.

Chen, W.F., Kim, S.E. and Choi, S.H. (2001). "Practical second-order inelastic analysis for three-dimensional steel frames." Steel Structures **1**: 213-223

Chen, W. F. and Lui, E. M. (1987). "Effects of Joint Flexibility on the Behavior of Steel Frames." Computers & Structures **26**(5): 719-732.

Chen, W. F. and Lui, E. M. (1991). "Stability Design of Steel Frames." CRC Press, Inc.

Chitawadagi, M. V. and Narasimhan, M. C. (2009). "Strength deformation behaviour of circular concrete filled steel tubes subjected to pure bending." Journal of Constructional Steel Research **65**(8-9): 1836-1845.

Cho, S. H. and Chan, S. L. (2005). "Practical second-order analysis and design of single angle trusses by an equivalent imperfection approach." Steel and Composite Structures **5**(6): 443-458.

Connor, J. J., Logcher, R. D. and Chan, S. C. (1968). "Nonlinear analysis of elastic framed structures." Journal of Structural Division, ASCE **94:**1525-1547.

CoPHK (2005). Code of Practice for Structural Use of Steel 2005. Hong Kong SAR Government.

Crisfield, M. A. (1981). "A fast incremental/iterative solution procedure that handles snap-through." Computers & Structures **13**(1-3): 55-62.

Crisfield, M. A. (1983). "An arc-length method including line searches and accelerations." International Journal for Numerical Methods in Engineering **19**(9): 1269-1289.

De Nardin, S. and El Debs, A. L. H. C. (2007). "Axial load behaviour of concrete-filled steel tubular columns." Proceedings of the Institution of Civil Engineers-Structures and Buildings **160**(1): 13-22.

Defreitas, J. A. T. and Ribeiro, A. C. B. S. (1992). "Large Displacement Elastoplastic Analysis of Space-Trusses." Computers & Structures **44**(5): 1007-1016.

Duan, L. and Chen, W. F. (1989). "Design Interaction-Equation for Steel Beam-Columns." Journal of Structural Engineering, ASCE **115**(5): 1225-1243.

Elchalakani, M., Zhao, X. L. and Grzebieta, R. H. (2001). "Concrete-filled circular steel tubes subjected to pure bending." Journal of Constructional Steel Research **57**(11): 1141-1168.

Ellobody, E. and Young, B. (2006). "Nonlinear analysis of concrete-filled steel SHS and RHS columns." Thin-Walled Structures **44**(8): 919-930.

Ellobody, E., Young, B. and Lam, D. (2006). "Behaviour of normal and high strength concrete-filled compact steel tube circular stub columns." Journal of Constructional Steel Research **62**(7): 706-715.

Ellobody, E., Young, B. and Lam, D. (2011). "Eccentrically loaded concrete encased steel composite columns." Thin-Walled Structures **49**(1): 53-65.

Eltawil, S., Sanzpicon, C. F. and Deierlein, G. G. (1995). "Evaluation of ACI-318 and AISC (LRFD) Strength Provisions for Composite Beam-Columns." Journal of Constructional Steel Research **34**(1): 103-123.

Eurocode 2 (2004). Eurocode 2: Design of concrete structures- Part 1-1: General rules and rules for buildings. BSI.

Eurocode 3 (2005). Eurocode 3: Design of steel structures - Part 1-1: General rules and rules for buildings. BSI.

Eurocode 4 (2004). Eurocode 4: Design of composite steel and concrete structures- Part 1-1: General rules and rules for buildings. BSI.

Furlong, R. W. (1967). "Strength of steel-encased concrete-filled beam-columns." Journal of Structural Division, ASCE **93**(5): 113-24.

Gardner, N. J. and Jacobson, E. R. (1967). "Structural Behavior of Concrete Filled Steel Tubes." ACI Journal **64**(7): 404-413.

Ge, H. B. and Usami, T. (1992). "Strength of Concrete-Filled Thin-Walled Steel Box Columns - Experiment." Journal of Structural Engineering, ASCE **118**(11): 3036-3054.

Gho, W. M. and Liu, D. L. (2004). "Flexural behaviour of high-strength rectangular concrete-filled steel hollow sections." Journal of Constructional Steel Research **60**(11): 1681-1696.

Gu, J. X. and Chan, S. L. (2005). "Second-order analysis and design of steel structures allowing for member and frame imperfections." International Journal for Numerical Methods in Engineering **62**(5): 601-615.

Guralnick, S. A. and He, J. X. (1992). "A Finite-Element Method for the Incremental Collapse Analysis of Elastic Perfectly Plastic Framed Structures." Computers & Structures **45**(3): 571-581.

Hajjar, J. F. and Gourley, B. C. (1996). "Representation of concrete-filled steel tube cross-section strength." Journal of Structural Engineering, ASCE **122**(11): 1327-1336.

Han, L. H. (2000). "Tests on Concrete Filled Steel Tubular Columns with High Slenderness Ratio." Advances in Structural Engineering **3**(4): 337-344.

Han, L. H. (2004). "Flexural behaviour of concrete-filled steel tubes." Journal of Constructional Steel Research **60**(2): 313-337.

Han, L. H., Lu, H., Yao, G. H. and Liao, F. Y. (2006). "Further study on the flexural behaviour of concrete-filled steel tubes." Journal of Constructional Steel Research **62**(6): 554-565.

Han, L. H., Wang, W. D. and Zhao, X. L. (2008). "Behaviour of steel beam to concrete-filled SHS column frames: Finite element model and verifications." Engineering Structures **30**(6): 1647-1658.

Han, L. H., Yao, G. H. and Zhao, X. L. (2004). "Behavior and calculation on concrete-filled steel CHS (circular hollow section) beam-columns." Steel & Composite Structures **4**(3): 169-188.

Hu, H. T., Huang, C. S. and Chen, Z. L. (2005). "Finite element analysis of CFT columns subjected to an axial compressive force and bending moment in combination." Journal of Constructional Steel Research **61**(12): 1692-1712.

Hu, H. T., Huang, C. S., Wu, M. H. and Wu, Y. M. (2003). "Nonlinear analysis of axially loaded concrete-filled tube columns with confinement effect." Journal of Structural Engineering, ASCE **129**(10): 1322-1329.

Hunaiti, Y. M. and Fattah, B. A. (1994). "Design Considerations of Partially Encased Composite Columns." Proceedings of the Institution of Civil Engineers-Structures and Buildings **104**(1): 75-82.

Iu, C. K. (2008). "Inelastic finite element analysis of composite beams on the basis of the plastic hinge approach." Engineering Structures **30**(10): 2912-2922.

Iu, C. K. and Bradford, M. A. (2010). "Second-order elastic finite element analysis of steel structures using a single element per member." Engineering Structures **32**(9): 2606-2616.

Iu, C. K., Bradford, M. A. and Chen, W. F. (2009). "Second-order inelastic analysis of composite framed structures based on the refined plastic hinge method." Engineering Structures **31**(3): 799-813.

Izzuddin, B. A. (1996). "Quartic formulation for elastic beam-columns subject to thermal effects." Journal of Engineering Mechanics, ASCE **122**(9): 861-871.

Izzuddin, B. A. and Elnashai, A. S. (1993a). "Adaptive space frame analysis: Part I, A plastic hinge approach." Proceedings of the Institution of Civil Engineers Structures and Buildings **99**(3): 303–316.

Izzuddin, B. A. and Elnashai, A. S. (1993b). "Adaptive space frame analysis: Part II, A distributed plasticity approach." Proceedings of the Institution of Civil Engineers Structures and Buildings **99**(3): 317-326.

Izzuddin, B. A. and Smith, D. L. (1996). "Large-displacement analysis of elastoplastic thin-walled frames. I. Formulation and implementation." Journal of Structural Engineering **122**(8): 905-914.

Jiang, X. M., Chen, H. and Liew, J. Y. R. (2002). "Spread-of-plasticity analysis of three-dimensional steel frames." Journal of Constructional Steel Research **58**(2): 193-212.

Johansson, M. and Gylltoft, K. (2002). "Mechanical Behavior of circular steel-concrete composite stub columns." Journal of Structural Engineering, ASCE **128**(8): 1073-1081.

Johnson, R. P. (2004). "Composite Structures of Steel and Concrete: Beams, Slabs, Columns, and Frames for Buildings." Blackwell Publishing Inc.

Johnson, R. P. and May, I. M. (1978). "Tests on restrained composite columns." The Structural Engineer **56B**(2): 21-28.

Kim, J. M., Kim, S. D. and Kwun, T.J. (1997). "A study on the unstable behavior of pin-connected single layer latticed domes considering geometric nonlinearity." Proceedings of the Seventh International Conference on Computing in Civil and Building Engineering. Seoul, Korea**:** 255-260.

Kim, S. E. and Chen, W. F. (1996a). "Practical advanced analysis for braced steel frame design." Journal of Structural Engineering **122**(11): 1266-1274.

Kim, S. E. and Chen, W. F. (1996b). "Practical advanced analysis for unbraced steel frame design." Journal of Structural Engineering **122**(11): 1259-1265.

Kim, S. E., Park, M. H. and Choi, S. H. (2001). "Direct design of three-dimensional frames using practical advanced analysis." Engineering Structures **23**(11): 1491-1502.

King, W. S. and Chen, W. F. (1994). "Practical 2nd-Order Inelastic Analysis of Semirigid Frames." Journal of Structural Engineering, ASCE **120**(7): 2156-2175.

King, W. S. and White, D. W. (1992). "Second-order inelastic analysis methods for steel-frame design." Journal of Structural Engineering **118**(2): 408-428.

Kirby, P. A. (1988). "Continuous multi-storey frames. Introduction to steelwork design to BS5950: Part 1, Chapter. 15. " The Steel construction Institute, 1988.

Kitipomchai, S., Al-Bermani, F. G. and Chan, S. L. (1990). "Elasto-plastic finite element models for angle steel frames." Journal of Structural Engineering, ASCE **116**(10): 2567-2581.

Lakshmi, B. and Shanmugam, N. E. (2002). "Nonlinear analysis of in-filled steel-column composite columns." Journal of Structural Engineering **128**(7): 922-933.

Landesmann, A. (2010). "Plastic-hinge approach for inelastic analysis of steel-concrete framed structures." Journal of Constructional Steel Research **66**(3): 323-334.

Liang, Q. Q. (2008). "Nonlinear analysis of short concrete-filled steel tubular beam-columns under axial load and biaxial bending." Journal of Constructional Steel Research **64**(3): 295-304.

Liew, J. Y. R. (2011). "Ultra-high strength composite columns for high rise buildings." Proceedings of the third international symposium on innovative design of steel structures. Hong Kong: 21-40.

Liew, J. Y. R., Chen, H. and Shanmugam, N. E. (1999). "Stability functions for second-order inelastic analysis of space frames." Light-Weight Steel and Aluminium Structures: 19-26.

Liew, J. Y. R., Chen, H., Shanmugam, N. E. and Chen, W. F. (2000a). "Improved nonlinear plastic hinge analysis of space frame structures." Engineering Structures **22**(10): 1324-1338.

Liew, J. Y. R., Chen, W. F. and Chen, H. (2000b). "Advanced inelastic analysis of frame structures." Journal of Constructional Steel Research **55**(1-3): 245-265.

Liew, J. Y. R., Punniyakotty, N. M. and Shanmugam, N. E. (1997). "Advanced analysis and design of spatial structures." Journal of Constructional Steel Research **42**(1): 21-48.

Liew, J. Y. R. and Tang, L. K. (2000). "Advanced plastic hinge analysis for the design of tubular space frames." Engineering Structures **22**(7): 769-783.

Liew, J. Y. R., White, D. W. and Chen, W. F. (1993a). "Second-order refined plastic-hinge analysis for frame design. Part I." Journal of Structural Engineering **119**(11): 3196-3216.

Liew, J. Y. R., White, D. W. and Chen, W. F. (1993b). "Second-order refined plastic-hinge analysis for frame design. Part II." Journal of Structural Engineering **119**(11): 3217-3237.

Liu, S. W., Liu, Y. P. and Chan, S. L. (2010). "Pushover analysis by 1 element per member for performance-based seismic design." International Journal of Structural Stability and Dynamics **10**(1): 111-126.

Lu, F. W., Li, S. P., Li, D. W. and Sun, G. (2007). "Flexural behavior of concrete filled non-uni-thickness walled rectangular steel tube." Journal of Constructional Steel Research **63**(8): 1051-1057.

Lu, Y. Q. and Kennedy, D. J. L. (1994). "The Flexural Behavior of Concrete-Filled Hollow Structural Sections." Canadian Journal of Civil Engineering **21**(1): 111-130.

Machowski, A. and Tylek, I. (2008). "Conceptions of Equivalent Imperfections in Analysis of Steel Frames." Advanced Steel Construction **4**(1): 13-25.

Matsui, C., Tsuda, K. and EI Din, H. Z. (1993). "Stability Design of Slender Concrete Filled Steel Square Tubular Columns." Proceedings of the Fourth East Asia-Pacific Conference on Structural Engineering and Construction: 317-322

Matsui, C., Tsuda, K. and Ishibashi, Y. (1995). "Slender Concrete Filled Steel Tubular Columns under Combined Compression and Bending." Proceedings of the Fourth Pacific Structural Steel Conference, Vol. 3, Steel–Concrete Composite Structures: 29–36.

McGuire, W. and Ziemian, R. D. (1989). "Discussion of Second-Order Elastic Analysis for Frame Design." Journal of Structural Engineering, ASCE **115**(2): 501-502.

Meek, J. L. and Lin, W. J. (1990). "Geometric and Material nonlinear analysis of thin-walled beam-columns." Journal of Structural Engineering **116**(6): 1473-1490.

Meek, J. L. and Tang, H. S. (1984). "Geometrically nonlinear analysis of space frames by an incremental iterative technique." Computer Methods in Applied Mechanics and Engineering **47**: 261-282.

Morino, S. (1998). "Recent developments in hybrid structures in Japan—research, design and construction." Engineering Structures **20**(4-6): 336-346.

Morris, N. F. (1991). "Effect of Imperfections on Lattice Shells." Journal of Structural Engineering, ASCE **117**(6): 1796-1814.

Munoz, P. R. and Hsu, C. T. T. (1997). "Behavior of biaxially loaded concrete-encased composite columns." Journal of Structural Engineering, ASCE **123**(9): 1163-1171.

Neogi, P. K., Sen, H. K. and Chapman, J. C. (1969). "Concrete-filled tubular steel columns under eccentric loading." The Structural Engineer **47**(5): 187-195.

O'Shea, M. D. and Bridge, R. Q. (1997). "Tests on circular thin-walled steel tubes filled with medium and high strength concrete." Research Report No. R755, School of Civil Engieering, University of Sydney, Sydney, Australia.

O'Shea, M. D. and Bridge, R. Q. (1997). "Tests on circular thin-walled steel tubes filled with very high strength concrete." Research Report No. R754, School of Civil Engieering, University of Sydney, Sydney, Australia.

Oran, C. (1973). "Tangent stiffness in plane frames." Journal of structural Engineering, ASCE **99**(6): 973-985.

Orbison, J. G., McGuire, W. and Abel, J. F. (1982). "Yield surface applications in nonlinear steel frame analysis." Computer Methods in Applied Mechanics and Engineering **33**(1-3): 557-573.

Pi, Y. L. and Trahair, N. S. (1994). "Nonlinear inelastic analysis of steel beam-columns. I: Theory." Journal of Structural Engineering **120**(7): 2041-2061.

Prion, H. G. L. and Boehme, J. (1994). "Beam-column behaviour of steel tubes filled with high strength concrete." Canadian Journal of Civil Engineering **21**(2): 207-218.

Rangan, B. V. and Joyce, M. (1992). "Strength of Eccentrically Loaded Slender Steel Tubular Columns Filled with High-Strength Concrete." ACI Structural Journal **89**(6): 676-681.

Riks, E. (1979). "Incremental Approach to the Solution of Snapping and Buckling Problems." International Journal of Solids and Structures **15**(7): 529-551.

Roderick, J. W. and Rogers, D. F. (1969). "Load carrying capacity of simple composite columns." ASCE Journal of the Structural Division **95**(ST2): 209-228.

Rothert, H., Dickel, T. and Renner, D. (1981). "Snap-through buckling of reticulated space trusses." Journal of the structural division **ST1**: 129-143.

Saw, H. S. and Liew, J. Y. R. (2000). "Assessment of current methods for the design of composite columns in buildings." Journal of Constructional Steel Research **53**(2): 121-147.

Schneider, S. P. (1998). "Axially loaded concrete-filled steel tubes." Journal of Structural Engineering, ASCE **124**(10): 1125-1138.

See, T. and McConnel, R. E. (1986). "Large Displacement Elastic Buckling of Space Structures." Journal of Structural Engineering, ASCE **112**(5): 1052-1069.

Shakir-Khalil, H. (1994). "Experimental study of concrete-filled rectangular hollow section columns." Structural Engineering Review **6**(2): 85-96.

Shakir-Khalil, H. and Mouli, M. (1990). "Further tests on concrete-filled rectangular hollow-section columns." The Structural Engineer **68**(20): 405-413.

Shakir-Khalil, H. and Zeghiche, J. (1989). "Experimental behaviour of concrete-filled rolled rectangular hollow-section columns." The Structural Engineer **67**(19): 346-353.

Shams, M. and Saadeghvaziri, M. A. (1999). "Nonlinear response of concrete-filled steel tubular columns under axial loading." ACI Structural Journal **96**(6): 1009-1017.

Shanmugam, N. E. and Lakshmi, B. (2001). "State of the art report on steel-concrete composite columns." Journal of Constructional Steel Research **57**(10): 1041-1080.

Shibata, R., Kato, S., Yamada, S. and Ueki, T. (1993). "Experimental study on the ultimate strength of single-layer reticular domes." Space Structures 4. G. A. R. Parke and C. M. Howard, Thomas Thelford Sevices Ltd. **1:** 387-395.

So, A. K. W. and Chan, S. L. (1991). "Buckling and Geometrically Nonlinear-Analysis of Frames Using One Element Member." Journal of Constructional Steel Research **20**(4): 271-289.

Srpcic, S. and Saje, M. (1986). "Large Deformations of Thin Curved Plane Beam of Constant Initial Curvature." International Journal of Mechanical Sciences **28**(5): 275-287.

Tao, Z., Uy, B., Han, L. H. and He, S. H. (2008). "Design of Concrete-filled Steel Tubular Members According to the Australian Standard AS 5100 Model and Calibration." Australian Journal of Structural Engineering **8**(3): 197-214.

Teh, L. H. (2001). "Cubic beam elements in practical analysis and design of steel frames." Engineering Structures **23**(10): 1243-1255.

Teh, L. H. and Clarke, M. J. (1999). "Plastic-zone analysis of 3D steel frames using beam elements." Journal of Structural Engineering, ASCE **125**(11): 1328-1337.

Tikka, T. K. and Mirza, S. A. (2006). "Nonlinear equation for flexural stiffness of slender composite columns in major axis bending." Journal of Structural Engineering, ASCE **132**(3): 387-399.

Tomii, M., Matsui, C. and Sakino, K. (1973). "Concrete filled steel tube structures." Tokyo Reg. Conf., IABSE, ASCE Tall Buildings Conference: 55-71.

Tomii, M., Yoshimura, K. and Morishita, Y. (1977). "Experimental studies on concrete filled steel tubular stub columns under concentric loading." Proceedings of the international colloquium on stability of structures under static and dynamic loads: 718–741.

Trahair, N. S. and Chan, S. L. (2003). "Out-of-plane advanced analysis of steel structures." Engineering Structures **25**(13): 1627-1637.

Trahair, N. S., Usami, T. and Galambos, T. V. (1969). "Eccentrically loaded single angle columns." Research report no. 11. St. Louis (Missouri, USA), Structural Division, Civil and Environment Engineering Department, School

of Engineering and Applied Science, Washington University, St. Louis, Missouri, USA.

Tsuda, K., Matsui, C. and Mino, E. (1996). "Strength and Behavior of Slender Concrete Filled Steel Tubular Columns." Proceedings of the Fifth International Colloquium on Structural Stability, Brasil, Strucutral Stability Research Council: 489-500

Uy, B. (1996). "Strength and ductility of fabricated steel-concrete filled." Proceedings of the Engineering Foundation Conference on Composite Construction: Composite Construction III, Irsee, Germany (1996): 616–629.

Uy, B. (2000). "Strength of concrete filled steel box columns incorporating local buckling." Journal of Structural Engineering, ASCE **126**(3): 341-352.

Uy, B. (2001). "Strength of short concrete filled high strength steel box columns." Journal of Constructional Steel Research **57**(2): 113-134.

Uy, B. (2003). "High-strength steel–concrete composite columns for buildings." Proceedings of the ICE - Structures and Buildings **156**(1): 3-14.

Uy, B. (2011). "Recent Australian innovations in the application, design and research of constructional steel." Proceedings of the third international symposium on innovative design of steel structures. Hong Kong**:** 71-87.

Uy, B. and Bardford, M. A. (1995). "Local buckling of thin steel plates in composite construction : experimental and theoretical study." Proceedings of the institution of civil engineers, Structures and building. **110:** 426-440.

Vesey, D. G., Kwan, K. K. and Xu, L. (2005). "Case studies in steel and composite design." Steel and Composite Structures **5**(2-3): 247-258.

Wang, L. K., Ha, J. P. and Li, Z. (2008). "Study on Plastic-Zone Models for Advanced Analysis of Steel Frame." Proceedings of the Tenth International Symposium on Structural Engineering for Young Experts, Vols. I and II: 406-412.

Wang, Y. C. (1999). "Tests on slender composite columns." Journal of Constructional Steel Research **49**(1): 25-41.

Wen, R. K. and Suhendro, B. (1991). "Nonlinear Curved-Beam Element for Arch Structures." Journal of Structural Engineering, ASCE **117**(11): 3496-3515.

Weng, C. C. and Yen, S. I. (2002). "Comparisons of concrete-encased composite column strength provisions of ACI code and AISC specification." Engineering Structures **24**(1): 59-72.

Yang, H., Lam, D. and Gardner, L. (2008). "Testing and analysis of concrete-filled elliptical hollow sections." Engineering Structures **30**(12): 3771-3781.

Yau, C. Y. and Chan, S. L. (1994). "Inelastic and Stability Analysis of Flexibly Connected Steel Frames by Springs-in-Series Model." Journal of Structural Engineering **120**(10): 2803-3104.

Zeghiche, J. and Chaoui, K. (2005). "An experimental behaviour of concrete-filled steel tubular columns." Journal of Constructional Steel Research **61**(1): 53-66.

Zhao, H. L., Huang, W. M. and Zhao, C. Q. (1993). "A method to calculate the critical loads of single layer shallow lattice domes with initial imperfections." Space Structures 4. G. A. R. Parke and C. M. Howard, Thomas Thelford Sevices Ltd. **1:** 127-135.

Zhao, X. L. and Packer, J. A. (2009). "Tests and design of concrete-filled elliptical hollow section stub columns." Thin-Walled Structures **47**(6-7): 617-628.

Zhou, Z. H. and Chan, S. L. (2004). "Elastoplastic and large deflection analysis of steel frames by one element per member. I: One hinge along member." Journal of Structural Engineering, ASCE **130**(4): 538-544.

Ziemian, R. D., Mcguire, W. and Deierlein, G. G. (1992). "Inelastic Limit States Design Part.1: Planar Frame Studies." Journal of Structural Engineering, ASCE **118**(9): 2532-2549.

Ziemian, R. D., Mcguire, W. and Dierlein, G. G. (1992). "Inelastic Limit States Design Part.2: 3-Dimensional Frame Study." Journal of Structural Engineering, ASCE **118**(9): 2550-2568.